

RAPID DEVOLATILIZATION AND HYDROGASIFICATION OF PULVERIZED COAL

by

Donald B. Anthony

B. S., University of Toledo
(1970)

S. M., Massachusetts Institute of Technology
(1971)

Submitted in Partial Fulfillment
of the Requirements for the
Degree of Doctor of Science

at the

MASSACHUSETTS INSTITUTE OF TECHNOLOGY

January, 1974

Signature of Author

~~_____~~
Department of Chemical Engineering

Certified by

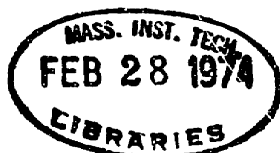
~~_____~~
H. D. Hottel, Thesis Supervisor

~~_____~~
H. P. Meissner, Thesis Supervisor

~~_____~~
J. B. Howard, Thesis Supervisor

Accepted by

~~_____~~
G. C. Williams, Chairman,
Departmental Committee on Graduate Theses



ABSTRACT

RAPID DEVOLATILIZATION AND HYDROGASIFICATION OF PULVERIZED COAL

by Donald B. Anthony

Submitted to the Department of Chemical Engineering in
January, 1974, in partial fulfillment of the
requirements for the degree of Doctor of Science.

Data on the rapid devolatilization and hydrogasification of pulverized coal has been obtained through the use of an electrical strip furnace. Correlations were advanced that successfully modelled the rates and yields of rapid coal conversion. Mechanisms have been postulated and shown to be consistent with the results of previous studies.

Weight loss measurements were acquired from a lignite and a bituminous coal as a function of residence time (0.05-20 secs), temperature (400-1100°C), heating rate (10^2 - 10^4 °C/sec), hydrogen pressures (to 100 atm) and particle size (50-1000 μ). The reactions were too fast to be studied isothermally, even at the highest rates of heating, and non-isothermal methods of data analysis were used.

The general reaction scheme was concluded to consist of a primary thermal decomposition forming volatiles and initiating a sequence of secondary reactions leading to char. A statistical distribution of activation energies (30-67 kcal/mole) was used to correlate the kinetics and yields of the primary decomposition. The effect of secondary reactions was described by a selectivity expression derived from a model hypothesizing competition between char formation reactions, diffusional escape of volatiles, and hydrogenation reactions.

From a commercial design standpoint, several experimental findings were identified as especially significant: 1) potential "rapid-rate" material was found to be a unique function of temperature, i.e., total yield is not appreciably influenced by time-temperature history; 2) bituminous coal yields were observed to depend on total pressure as well as the partial pressure of hydrogen; and 3) larger particle sizes contributed to substantial loss of yield in hydrogen. These findings and the proposed mechanisms permitted clarification of several areas of disagreement and uncertainty in the literature.

Thesis Supervisors:

Hoyt C. Hottel
Professor of Chemical Engineering

Herman P. Meissner
Professor of Chemical Engineering

Jack B. Howard
Associate Professor of Chemical Engineering

Department of Chemical Engineering
Massachusetts Institute of Technology
Cambridge, Massachusetts 02139
January, 1974

Professor David B. Ralston
Secretary of the Faculty
Massachusetts Institute of Technology
Cambridge, Massachusetts 02139

Dear Professor Ralston:

In accordance with the regulations of the Faculty, I herewith submit a thesis, entitled "Rapid Devolatilization and Hydrogasification of Pulverized Coal," in partial fulfillment of the requirements for the degree of Doctor of Science in Chemical Engineering at the Massachusetts Institute of Technology.

Respectfully submitted,

Donald B. Anthony

ACKNOWLEDGEMENTS

I wish to express my deepest appreciation to each of my three supervisors for their valuable support and continued encouragement. Professor J. B. Howard has acted as my advisor ever since I began study at M. I. T. and has assisted me through many difficult times. He first introduced me to the topic and subsequently gave generously of his time and effort to enable me to complete the thesis. Professor H. P. Meissner spent many hours critically examining the findings and my analysis of them and served as a much needed and appreciated "devil's advocate." Professor H. C. Hottel's contributions were instrumental in surmounting a number of the subtle problems, both experimental and theoretical, encountered in the course of the work.

I am extremely grateful to Charles Portal for his valuable laboratory assistance during the critical early stages of the project. Philip C. Lewellen is to be acknowledged for developing the considerable experimental data base for lignite and writing the computer programs for analysis of the data. His initiative in these undertakings added immensely to the content of the final thesis.

I also wish to recognize the experimental contributions of several student colleagues: David Tan, Hugh P. Lavery, John A. Wilkins, Charles Johnson and Allan Cohen. Discussions with Dr. Benno L. Wersborg, John H. Pohl, and Donald Aldrich of the Fuels Laboratory were most helpful in expanding my awareness of closely related fields.

Stanley R. Mitchell is to be thanked for his many technical suggestions and especially for his efforts in the preparation of the final manuscript. Technical assistance was also received from Art Clifford, Al Merrill, Charles Foshey and Paul Bletzer.

Personal financial support from the A.D. Little and Procter and Gamble fellowships is gratefully acknowledged. The M.I.T. Environmental Laboratory is to be thanked for making available funds to purchase equipment and supplies. The Institute of Gas Technology kindly supplied me with the coal samples used in the investigation. I would also like to mention the Gordon Research Conferences whose financial aid offered me the unique opportunity of attending the 1973 Coal Science Conference and meeting, on an informal basis, the principle researchers in the field.

To my parents I owe an immeasurable debt of gratitude. Their confidence and support has sustained me throughout my schooling. Finally, my wife, Darla, for whom my praise is endless, was the greatest source of encouragement. Not only did she spend her evenings and weekends typing the draft and manuscript, but she also provided me the love and devotion which were, perhaps, the most valued aids of all.

TO

DARLA SUE

TABLE OF CONTENTS

	Page
1. Summary	1
1.1 Introduction	1
1.1.1 Background	1
1.1.2 Literature Review	3
1.1.3 Objectives	5
1.2 Apparatus and Procedure	6
1.3 Results and Discussion	8
1.3.1 Devolatilization	8
1.3.2 Hydrogenation	21
1.3.3 Effect of Particle Size	25
1.4 Comparison of Results with Previous Investigations	27
1.4.1 Devolatilization	27
1.4.2 Hydrogenation	29
1.5 Application of Results	31
1.6 Conclusions	32
1.7 Recommendations	33
2. Introduction	35
2.1 Background	36
2.2 Literature Review	43
2.2.1 Existence of Rapid-Rate Carbon	44
2.2.2 Modeling the Kinetics of Rapid-Rate Carbon	50
2.2.3 Devolatilization	58
2.2.4 Effect of Particle Size	69
2.2.5 Conclusions	72
2.3 Objectives	74
3. Apparatus and Procedure	77
3.1 Selection of Apparatus	77
3.2 Apparatus Description	78
3.3 Procedure	86
3.4 Coal Type	87

4. Results	89
4.1 Devolatilization	89
4.2 Hydrogasification	100
4.3 Supplemental Results	108
5. Discussion of Results and Development of a Model	112
5.1 Decomposition Model	112
5.2 Secondary Reaction Model	125
5.3 Hydrogenation Model	130
5.4 Effect of Particle Size	133
6. Comparison of Results with Previous Investigations	137
6.1 Decomposition Model	137
6.2 Secondary Reaction Model	152
6.3 Hydrogenation	161
6.4 Effect of Particle Size	171
7. Application of Results	176
8. Conclusions	181
9. Recommendations	187
10. Appendix	190
10.1 Notes on Thermodynamics and Coal	190
10.1.1 Thermodynamic Advantage of Fresh Coal	190
10.1.2 Kinetics of Methane Cracking	192
10.1.3 Heat of Reaction for Hydrogasification of Fresh Coal	193
10.1.4 Thermodynamic Analysis of Coal Structure	194
10.1.5 Ultimate Analyses	195
10.2 Summary of Data	197
10.3 Sample Calculations	248
10.3.1 Apparatus	248
10.3.2 Experimental Data	254
10.3.3 Computer Routines	259
10.4 Nomenclature	270
10.5 Literature Citations	272
10.6 Biographical Note	279

LIST OF FIGURES

Number		Page
1-1	Weight Loss with Time for Lignite in 1.0 atm Helium	9
1-2	Yield versus Final Temperature for Lignite in 1.0 atm Helium	10
1-3	Weight Loss with Time for Lignite under Extremely Rapid Heating Conditions	11
1-4	Effect of Total Pressure on Bituminous Coal Yields	13
1-5	Comparison of Decomposition Model with Lignite Data at Different Heating Rates	16
1-6	Comparison of Lignite Yields with Decomposition Model	17
1-7	Comparison of Calculated with Experimental Weight Losses for Lignite	18
1-8	Comparison of Calculated with Experimental Weight Losses for Bituminous Coal at 1000 psig.	19
1-9	Yield versus Final Temperature for Bituminous Coal in Hydrogen and in Helium	22
1-10	Effect of Hydrogen Partial Pressure on Bituminous Coal Yields	23
1-11	Effect of Particle Size on Bituminous Coal Yields	26
1-12	Comparison of Decomposition Rate Constants	28
1-13	Comparison of Hydrogasification Rate Constants	30
2-1	"Typical" Coal Gasification Process	38
2-2	Weight Loss with Time Data from Feldkirchner and Linden	44
2-3	Weight Loss with Time Data from Hiteshue, <u>et al.</u>	46
2-4	Comparison of Char Reactivities from Moseley and Paterson	47
2-5	Hydrogasification Conversion as a Function of Hydrogen Pressure	49
2-6	Weight Loss with Time Data from Johnson	51
2-7	Effect of Temperature on Hydrogasification Rate	57
2-8	Effect of Pressure on Hydrogasification Rate	57
2-9	Arrhenius Plot of Coal Decomposition Rate Constants	64

3-1	Overall Apparatus Schematic	79
3-2	Stage Details	81
3-3	Dual Heating Circuit	83
3-4	Time-Temperature Histories at 1.0 atm Pressure	84
3-5	Time-Temperature History at High Pressure	85
4-1	Weight Loss with Time for Lignite in 1.0 atm Helium	90
4-2	Yield versus Final Temperature for Lignite in 1.0 atm Helium	91
4-3	Weight Loss with Time for Lignite under Extremely Rapid Heating Conditions	93
4-4	Weight Loss with Time under 1000 psig Helium	94
4-5	Weight Loss with Time for Bituminous Coal	95
4-6	Weight Loss with Time for Bituminous Coal under Rapid Heating Conditions	96
4-7	Weight Loss with Time for Bituminous Coal under 1000 psig Helium	97
4-8	Yield versus Final Temperature for Bituminous Coal	98
4-9	Effect of Total Pressure on Yield	99
4-10	Comparison of Hydrogen and Helium as Environments for Lignite Weight Loss versus Time	101
4-11	Weight Loss with Time for Lignite in Hydrogen and in Helium, Rapid Heating to 1000°C	102
4-12	Yield versus Final Temperature for Lignite in Hydrogen and in Helium	103
4-13	Lignite Yield as a Function of Hydrogen Pressure	104
4-14	Weight Loss with Time for Bituminous Coal in 1000 psig Hydrogen and Helium	105
4-15	Yield versus Final Temperature for Bituminous Coal in Hydrogen and in Helium	106
4-16	Effect of Hydrogen Partial Pressure on Bituminous Coal Yield	107
4-17	Effect of Particle Size on Bituminous Coal Yield	109
5-1	Weight Loss with Time Data for Lignite at Different Heating Rates	113
5-2	Yield versus Final Temperature for Lignite	114
5-3	Comparison of Decomposition Model with Lignite Data at Different Heating Rates	120

5-4	Comparison of Lignite Yields with Decomposition Model	121
5-5	Comparison of Calculated with Experimental Weight Losses for Lignite	122
5-6	Comparison of Calculated with Experimental Weight Losses for Bituminous Coal at 1000 psig	124
5-7	Secondary Reaction Model Compared with Bituminous Coal Data	129
5-8	Secondary Reaction Model Applied to Hydrogenation Results	132
5-9	Modified Secondary Reaction Model	134
5-10	"Effective" Hydrogen Pressure as a Function of Particle Size	135
6-1	Experimental First Order Rate Constants for Bituminous Coal	138
6-2	Experimental First Order Rate Constants for Lignite	139
6-3	Comparison of Coal Decomposition Rate Constants	142
6-4	Devolatilization Yields as a Function of Temperature	144
6-5	Comparison of Activation Energy Distributions	148
6-6	Pseudo-Effect of Heating Rate on Bituminous Coal yields	157
6-7	Effect of Sample Size on Bituminous Coal Yields	158
6-8	Comparison of Hydrogasification Rate Constants	162
6-9	Yield as a Function of Hydrogen Pressure	164
6-10	Bituminous Coal Yields versus Hydrogen Pressure Below 100 atm	166
6-11	Lignite Yields versus Hydrogen Pressure Below 100 atm	167
6-12	Test of Equation 2-20 with Experimental Data	169
6-13	Effect of Temperature on Hydrogasification and Devolatilization Yields	172
6-14	Effect of Particle Size on Yield	175
7-1	Hydrane Hydrogasification Section	177
10-1	Methane Equilibrium in Gasification Systems	191
10-2	Equilibrium Constant as a Function of Conversion	191

LIST OF TABLES

Number		Page
2-1	Development Efforts in Coal Gasification	41
2-2	Constants from Zahradnik and Glenn Model	59
2-3	Coal Types in Figure 2-9	65
3-1	Proximate Analyses for Coals Used in Experimental Work	88
6-1	Experimental First Order Rate Constants for This Study	141
6-2	Effect of Pre-Exponential Factor on Statistical Distribution Parameters	150
6-3	Comparison of Experimental Yields with Proximate Volatiles	153
6-4	Low Temperature Yields	155
6-5	Particle Sizes Used in Previous Investigations	173

1. SUMMARY

1.1 INTRODUCTION

1.1.1 Background

The energy crisis now confronting this country has focused attention on the fact that we are no longer able to depend on traditional sources of supply. The natural gas situation is especially serious in that artificially low prices have accelerated demand for this remarkably clean-burning fuel. New pricing policies on the part of the Federal Government could offer some relief, but alternative sources of supply will still be required. Converting a portion of our large domestic coal reserves into a synthetic pipeline gas is viewed as both feasible and imperative. Unfortunately, there are no existing commercial-scale facilities to accomplish the task. Much of the envisioned technology is new and even established features of the processes are untried on the scale that will be demanded. Further research and development is essential on both practical and fundamental levels.

The first such installation will probably manufacture a high-BTU gas by generating a synthesis gas of CO and H₂ through steam gasification of a devolatilized coal char and then catalytically upgrade this synthesis gas to pure methane. Economic assessments, however, indicate that if methane were formed in the gasifier from either the coal's volatile matter or from direct hydrogenation, it would be much less costly than catalytic formation. Several

fascinating processes emerge when the following experimental observations are considered:

- 1) Volatile matter in the coal may comprise 40% or more of the coal by weight, representing a significant source of high heating value gas. Further, there are indications that the amount of volatile matter can be increased significantly by heating under properly controlled conditions.
- 2) Freshly devolatilizing coal is more reactive than pretreated coal. Fresh is probably defined on a time scale of seconds or less and more reactive may mean several orders of magnitude in terms of rate.
- 3) The carbon in freshly devolatilized coal may also possess excess free energies. The equilibrium constant for the hydrogasification reaction ($C + 2H_2 = CH_4$) may be larger by a factor of 10 or more.

Capitalizing on these alleged advantages requires, however, that the extent to which they occur be ascertained quantitatively such that they may be compared to the increased costs and difficulties of accomodating raw coal. Many raw coals have a strong tendency to cake or agglomerate upon heating. The current level of understanding on the coal-hydrogen reaction is briefly reviewed in the next few paragraphs.

1.1.2 Literature Review

It is generally conceded that Dent (1944) in Great Britain first recognized the augmented reactivity of raw coal relative to coke. Most of the work following Dent's identified an initial rapid-rate period in the hydrogasification of coal characterized as a hydrogenation of the volatile constituents. This conclusion was supported by the correlation of these "rapid-rate" yields with proximate volatile content of the coals. However, in early 1958 Schroeder (1962) filed a patent application claiming hydrogenation yields from rapid heating of raw coal significantly exceeding proximate volatile content. The proposition that rapid-heating had contributed significantly to improvement of yields prompted a suggestion in a Bureau of Mines paper (Hiteshue, et al., 1964) for a novel reactor design scheme that would permit even faster rates of heating and better gas-solid contacting efficiency. Essentially the idea consisted of dispersing entrained coal particles at the top of a large diameter tube and allowing the particles to fall through the reaction zone. Moseley and Paterson (1967) used the technique and demonstrated nearly complete conversion of raw coal at about 500 atm of pure hydrogen. But an economic study at West Virginia University (Wen, 1972) concluded that a system pressure of 1000 psig (69 atm) was more likely from a standpoint of commercial feasibility.

The Moseley and Paterson study is admittedly inapplicable at pressures below 100 atm, but considerable disagreement prevails among the available alternative models and the data are much too incomplete to permit selection. It is well-known that this initial high reactivity

is short-lived but there are no data to show conversion of fresh coals with residence time for very short residence times. It has also been claimed that heating rate has no effect on yield (Pyrzioch, et al., 1972) and may even retard hydrogasification (Von Fredersdorff and Elliott, 1963). Further, no studies have been done to establish the effect of particle size.

The role of devolatilization with respect to hydrogasification constitutes the gravest omission in the studies to date. Volatile evolution from fresh coal is a significant source of total yield and most investigators theorize it also determines the reactivity to hydrogen of the remaining carbon. Quantitatively, the first effect is allowed for in terms of an integration constant and the second effect materializes as an elusive "active species or site". Very little may be said of the independence of the rates of hydrogasification and devolatilization.

In order to approach the problem of introducing devolatilization into the mechanism, the independent body of literature on coal pyrolysis was reviewed with the following conclusions. Despite considerable research, the kinetics and mechanism of rapid devolatilization of pulverized coal are not well-understood. Most investigators agree that the actual phenomena are very complex and most likely cannot be modeled exactly. A number of attempts have been made to correlate rates with a first order expression (Van Krevelen, et al., 1951; Boyer, 1952; Howard and Essenhigh, 1967; and Badzioch and Hawksley, 1970). Typically such correlations have been valid only for the specific condition of the experiment from which they were obtained with the result that reported values of the rate constant vary by several

orders of magnitude.

The best evidence indicates that devolatilization is essentially complete for pulverized coal ($< 200\mu$ diameter) at reasonably high temperatures in fractions of a second. Yields are known to be both dependent on the temperature of devolatilization and the method by which the devolatilization was accomplished reinforcing the concept of a complex array of reactions participating in the actual decomposition. An example of the latter instance are the results of Eddinger, et al., (1966) and Badzioch and Hawksley where entrained flow devolatilization of pulverized coal gave yields considerably in excess of the standard proximate analysis procedure. The onset of physical limitations arises somewhere in the particle size range of 200-3000 μ (Essenhigh, 1963; and Juntgen, et al., 1969). Only limited efforts have been made to synthesize a general mechanistic picture in accord with these diverse findings. Part of the problem arises from the great difficulty in obtaining consistent data under well-defined yet wide-ranging conditions.

1.1.3 Objectives

The objectives of this investigation were:

- 1 -- To determine the rate and extent of the rapid coal-hydrogen reaction under conditions of commercial interest.
- 2 -- To elucidate the role of the devolatilization process in the above reaction.

Specifically, the work was to establish the dependence of conversion

(weight loss) on important process variables, including residence time, temperature, time-temperature history (heating rate), hydrogen pressure, particle size and to a limited extent coal type. Secondly, the inter-relationship of the devolatilization mechanism and the subsequent hydrogen attack was to be explored in order to characterize this behavior. The strategy of investigation was directed toward progression from the simple to the complex. Experimentally, techniques were developed in an orderly sequence beginning with a low heating rate atmospheric pressure system, then incorporating the rapid-heating capability and finally enclosing the unit in a high pressure vessel. Not only did this method avoid early commitment to an untested concept but also provided useful data during the critical initial planning stages. Likewise, the strategy of modeling results began with very simple correlations and these were sophisticated as the data required it.

1.2 APPARATUS AND PROCEDURE

The principle factor in the selection and design of the experimental apparatus was that it be capable of providing data at commercially significant conditions of temperature, pressure and heating rate. An electrical strip furnace was used to heat finely ground coal particles quickly to a desired final temperature, maintain that temperature for the duration of the run and then rapidly quench the sample. Approximately 5-10 mg of coal were sandwiched in a folded strip of stainless steel screen. The screen was suspended between relatively massive brass electrodes and electrically heated to temperature. The heating element

and electrodes were enclosed in a high pressure vessel capable of operating at 3000 psig. The vessel could be evacuated or charged with hydrogen or inert gas such as helium. The external heating circuit was comprised of two branches, the first controlled the heating rate ($65^{\circ}\text{C}/\text{sec}$ to $12,000^{\circ}\text{C}/\text{sec}$) and the second maintained the final temperature (400 to 1100°C). The power supply consisted of two 12 volt lead-acid storage batteries connected in series to the circuits via a heavy duty relay. Variable resistors controlled current levels in each circuit branch. The actual time-temperature history of each run was recorded by a fast response thermocouple also placed between the folds of the screen.

The procedure involved weighing the screen and coal sample before and after heating and computing the fractional weight loss. The balance was accurate to ± 0.01 mg giving an experimental precision of 0.1-0.2% of the coal sample weight. The advantages of the device were several: 1) relatively inexpensive design for high pressure studies, 2) direct determination of solid conversion, 3) constant and precisely controlled atmospheres, 4) direct measurement of sample temperatures, and 5) capability to vary heating rate independent of final temperature. However, it would be remiss to disregard the shortcomings: 1) sample weight was not monitored continuously and a number of runs were necessary for rate determination; 2) quantitative product analyses could not be obtained from the small product concentrations; and 3) residence times were limited to a maximum of 20 secs.

Two different types of coal were used in the course of this investigation. One was a high volatile Pittsburgh Seam bituminous coal and the other was a dried lignite from Montana. Proximate analyses for both are given below:

	Pittsburgh Seam Bituminous	Montana Lignite
	(As-Received Basis)	
Moisture	1.65%	7.26%
Volatile Matter	39.81%	37.40%
Fixed Carbon	46.34%	43.63%
Ash	12.20%	11.71%

1.3 RESULTS AND DISCUSSION

1.3.1 Devolatilization

Upon heating in helium both types of coal were found to evolve volatile matter very quickly with much of the weight loss occurring before the sample reached final temperature. For example, weight loss with time data for Montana lignite in 1.0 atm helium are shown in Figure 1-1. Weight loss ceases after several seconds at final temperature with approximately 41% weight loss at 1000°C and 31% at 700°C. This apparent dependency on final temperature is amplified in Figure 1-2 where final weight losses or yields (residence time at final temperature 5 secs) are seen to increase with increasing temperature until around 900-950°C. No additional weight loss was observed at higher temperatures. It should be noted that these yields for lignite at all temperatures are smaller than the weight loss (44.66%) given by proximate analysis (sample held at 950°C for 7 min). Even with very rapid initial heating of the sample (nominal heating rates of 3000 and 10,000°C/sec) most of the volatiles are expelled during the heat-up with the final yield unaffected by the rate of heating (see Figure 1-3).

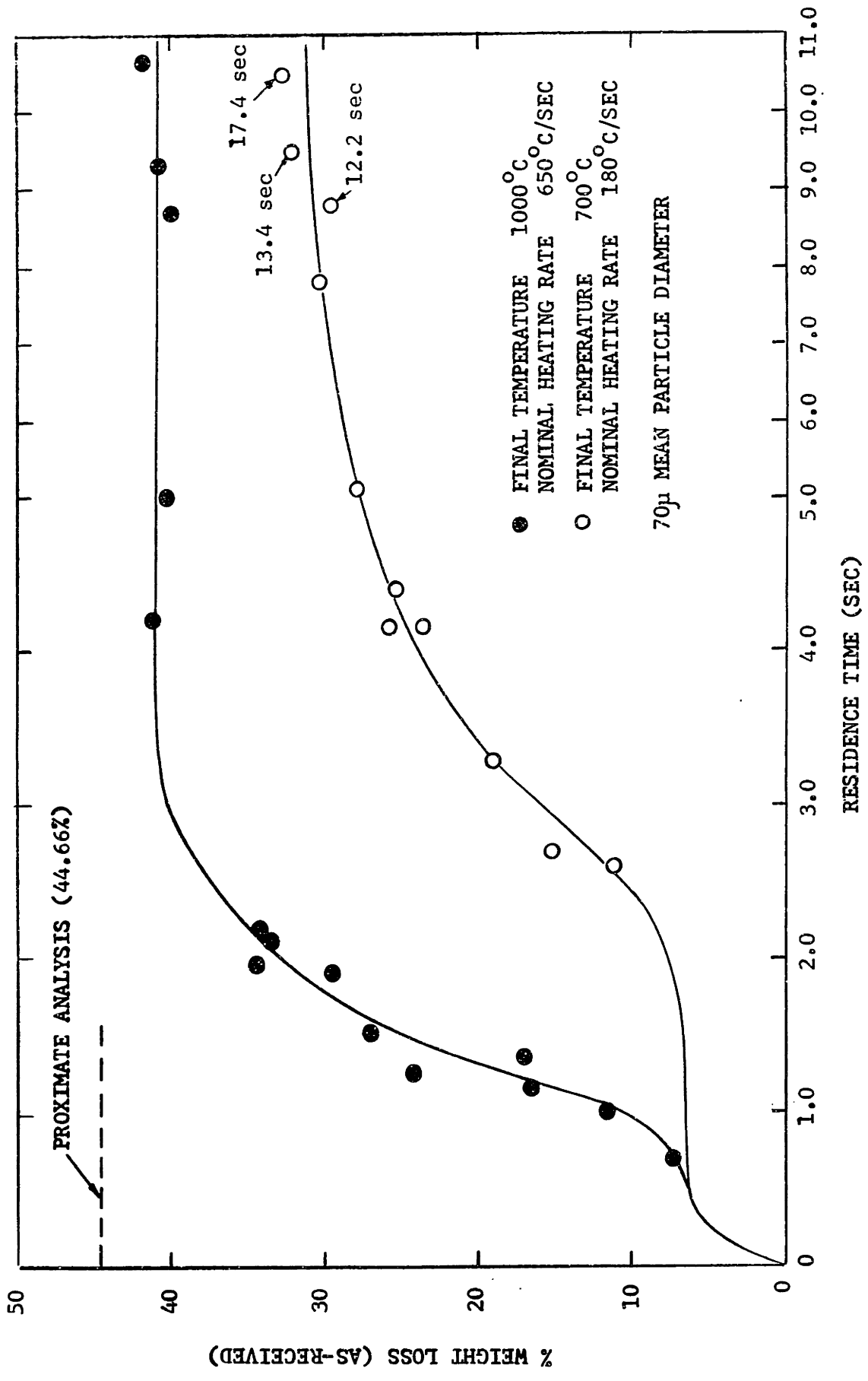


FIGURE 1-1 WEIGHT LOSS WITH TIME FOR LIGNITE IN 1.0 ATM HELIUM

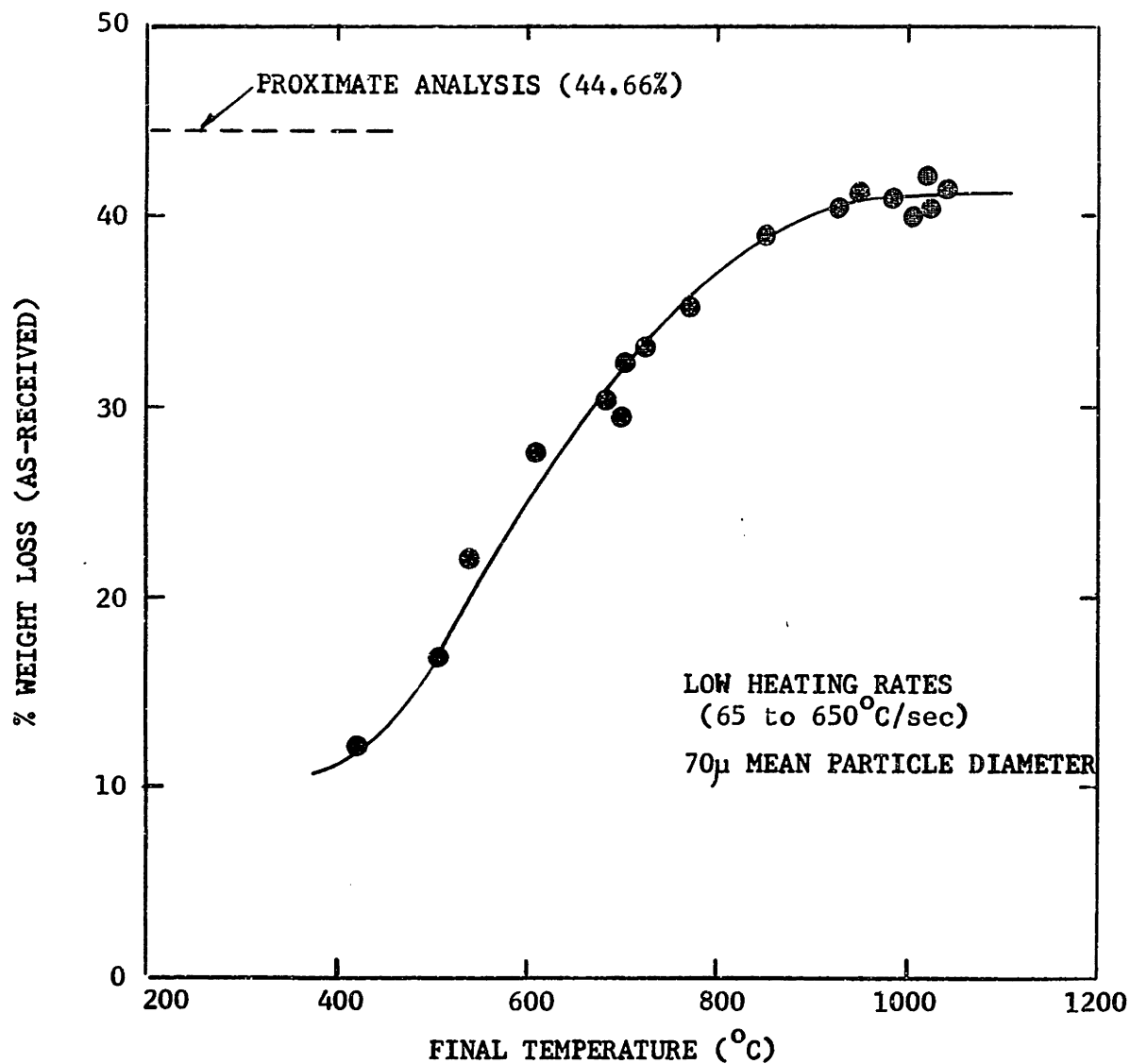


FIGURE 1-2 YIELD VERSUS FINAL TEMPERATURE FOR LIGNITE
IN 1.0 ATM HELIUM

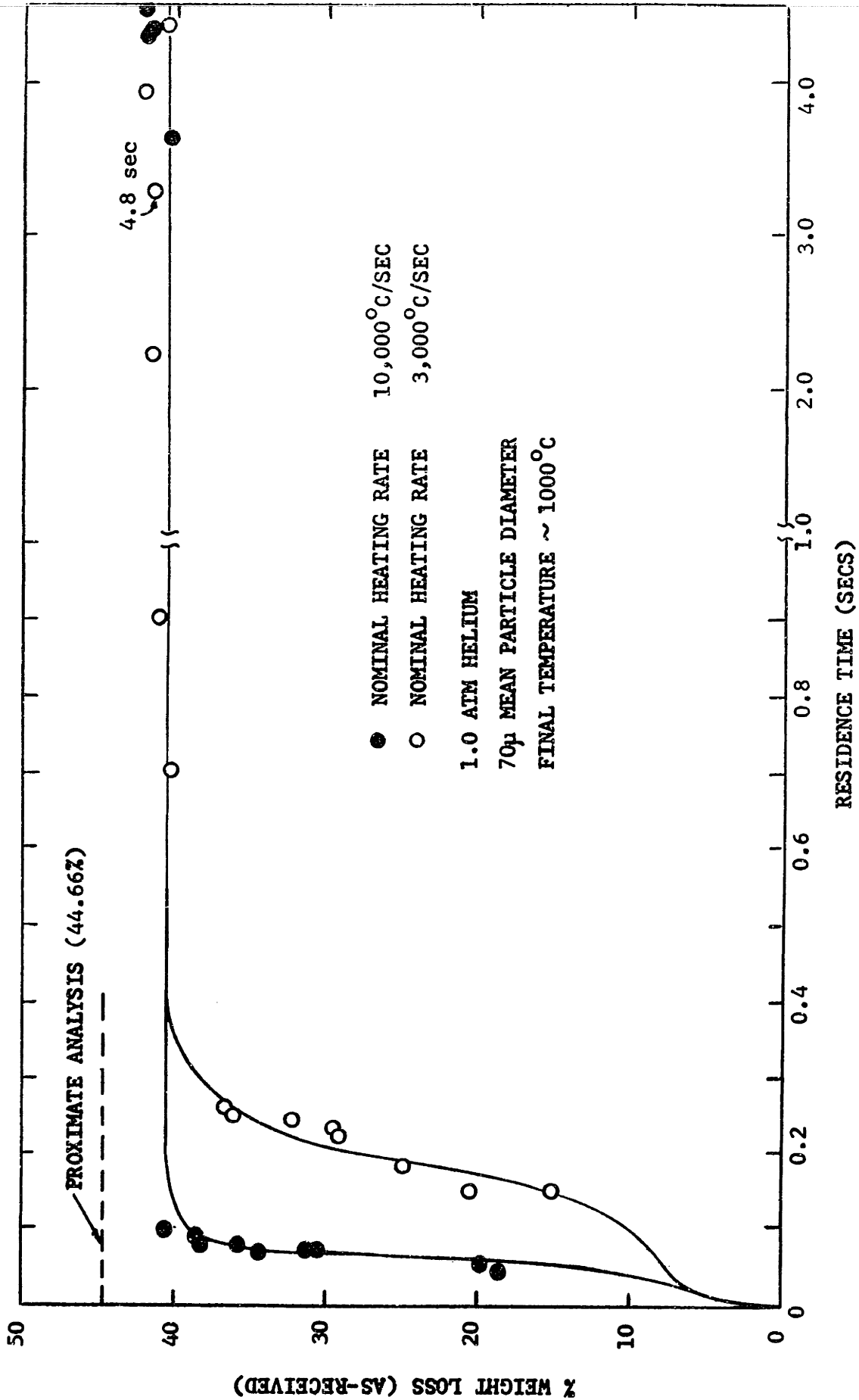


FIGURE 1-3 WEIGHT LOSS WITH TIME FOR LIGNITE UNDER EXTREMELY RAPID HEATING CONDITIONS

At a fixed pressure of inerts, bituminous coal yields as with lignite increased with increasing temperature. However, while total pressure of inerts had no effect on lignite yields, increasing pressure significantly decreased yields from bituminous coal as the data indicate in Figure 1-4. It is also possible to discern from Figure 1-4 that a higher rate of heating increased the yield at 1.0 atm by about 2 percentage points whereas the effect of heating rate was inconsequential at both high and low pressure extremes. Contrary to the results with lignite, yields from bituminous coal exceeded the proximate analysis value (41.46%) at all pressures below about 5 atm. Tar condensation was observed with bituminous coal but not with lignite. Though not apparent in Figure 1-4 the amount of tar deposited in the reactor followed the same trend as yield decreasing with increasing pressure and essentially disappearing at about 1000 psig helium.

To develop a model for devolatilization a number of possible avenues were explored:

1) Single Irreversible Decomposition Reaction

The fact that yield was dependent on final temperature invalidates any such simple reaction as well as simple heat and mass transfer models.

2) Equilibrium Limitations

Unfortunately, the reactions are not reversible.

3) Competitive Reactions

This is an appealing possibility since complex organic materials could easily have a number of potential reaction paths leading to differing amounts of volatiles and char. If such paths were influenced to different extents by temperature the resultant dependency of yield on final temperature might be explained. However, a simple experiment

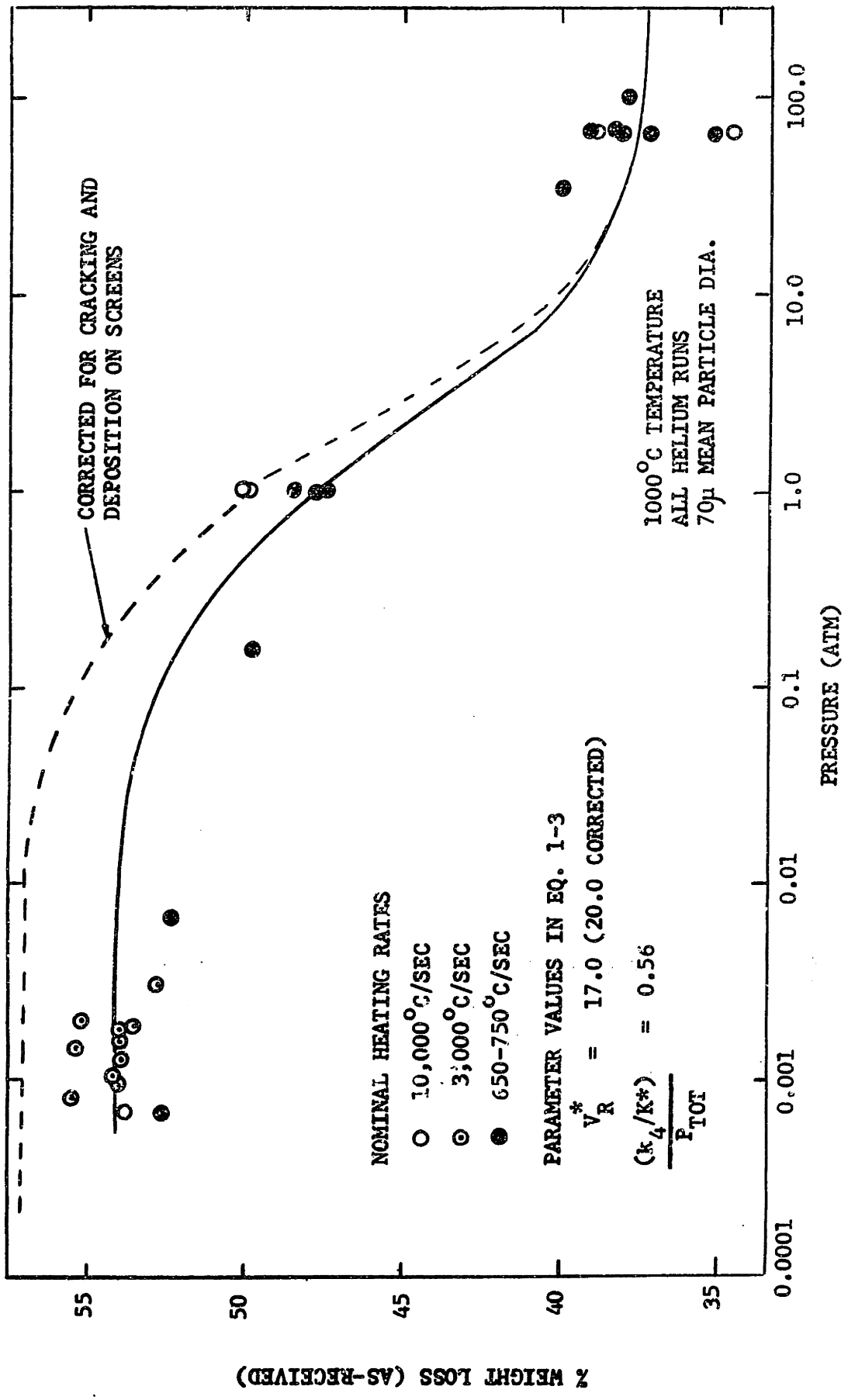


FIGURE 1-4 EFFECT OF TOTAL PRESSURE ON BITUMINOUS COAL YIELDS

was devised to test this alternative. The residual char from a long residence time low temperature run was reheated to a higher temperature. The total weight loss was the same as achieved with one step heating. This state function relationship of yield to temperature clearly contradicts the competitive reaction model.

4) Multiple Reaction Model

Such a concept assumes many different reactions occurring in coal during devolatilization. If these reactions take place at different temperatures and there are a sufficient number of them, the continuous behavior of yield with temperature in Figure 1-2 might be simulated. If no alternative reactions paths are allowed, time-temperature history would have no effect on yield provided the same final temperature and sufficient residence time are allowed. This model thus appears to meet the basic criteria for lignite though it is definitely incomplete for explaining the peculiarities of bituminous coal. Reserving comment on the bituminous coal until later, such a model is tested first on the lignite data.

If the thermal decomposition of coal is pictured as consisting of a large number of simultaneous, independent chemical reactions, the rate of one such reaction might be written

$$\frac{dV_i}{dt} = k_i (V_i^* - V) \quad (1-1)$$

where V is the mass of volatiles produced at time t ; V^* is the mass of volatiles produced as $t \rightarrow \infty$, i.e. yield; and k is the rate constant usually assumed to be an Arrhenius expression, $k = k_0 \exp(E/RT)$ where k_0 is the pre-exponential factor and E is the activation energy. The subscript i denotes one individual reaction. If sufficient reactions

are present it is possible to derive an expression for overall conversion in terms of a distribution of activation energies, $f(E)$, (Pitt, 1962):

$$\frac{V^* - V}{V^*} = \int_0^{\infty} \left[\exp\left(-\int_0^t k dt\right) \right] f(E) dE \quad (1-2)$$

The nature of the distribution is unknown but for purposes of mathematical tractability it was assumed Gaussian. Experimental data for lignite devolatilization from Figures 1-1, 1-2, and 1-3 were used in a non-linear least squares fitting routine to estimate parameter values in Equation 1-2. To simplify the integration the limits of the integral were changed to $E \pm 2\sigma$ which would include 95.5% of the reaction set. The "best fit" values for lignite and bituminous coal (determined only at 1000 psig) are:

	Lignite	Bituminous Coal (1000 psig)
k_0 (sec ⁻¹)	1.07×10^{10}	2.91×10^9
E_0 (kcal/mole)	48.7	36.9
σ (kcal/mole)	9.4	4.2
V^* (fraction of orig. coal)	0.406	0.372

E_0 is the mean activation energy in the Gaussian distribution and σ is the standard deviation. It was assumed that k_0 was the same for all reactions in a given type of coal. The calculated curves from the above parameters are shown with the experimental data for lignite in Figures 1-5 and 1-6. The agreement is good and the overall degree of fit is illustrated in scatter plots (Figure 1-7 and 1-8) where all the relevant data for lignite and bituminous coal are compared to calculated values.

It must be emphasized that Equation 1-2 is likely not a true fundamental picture of coal decomposition but rather a simple correlative

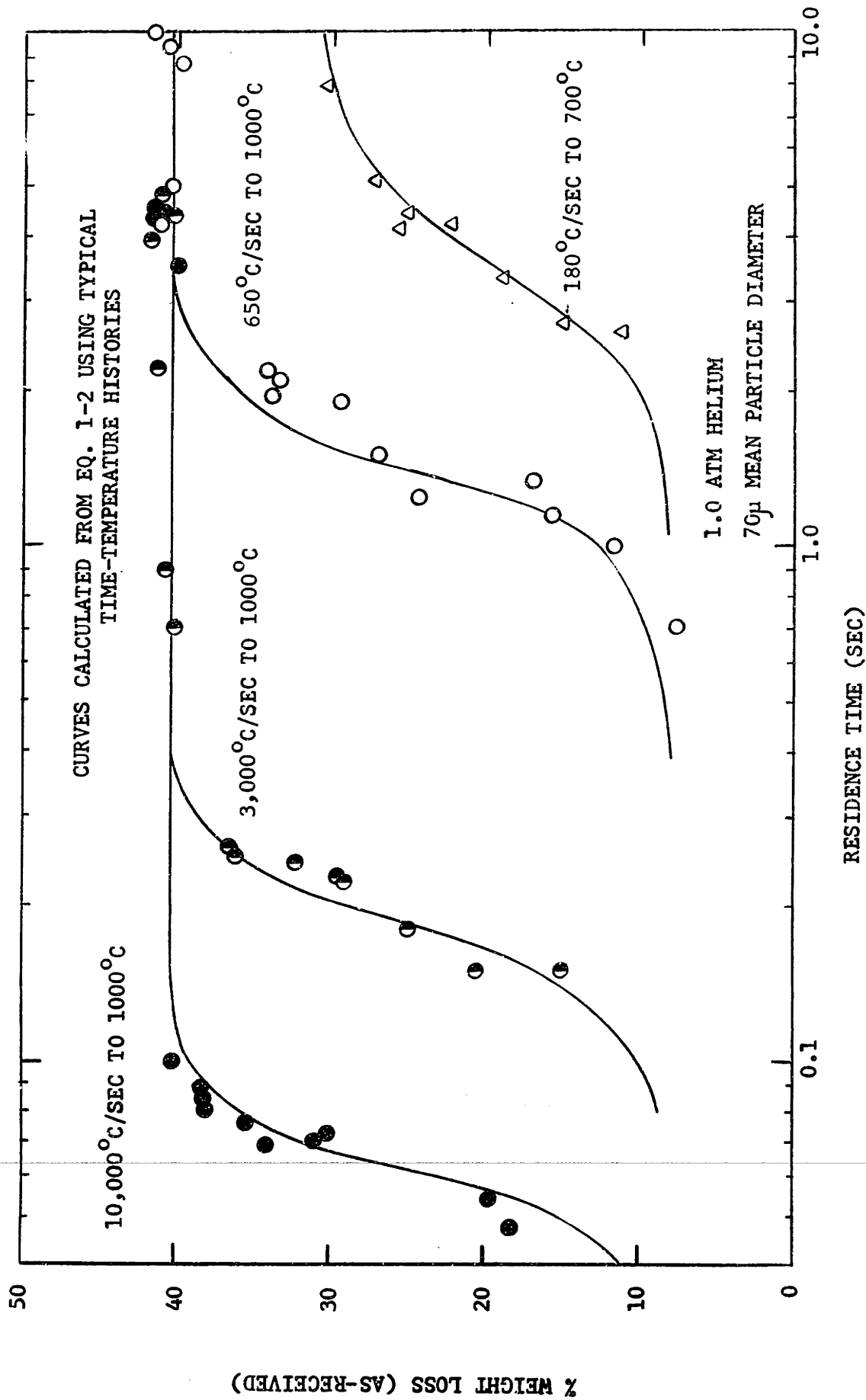


FIGURE 1-5 COMPARISON OF DECOMPOSITION MODEL WITH LIGNITE DATA AT
DIFFERENT HEATING RATES

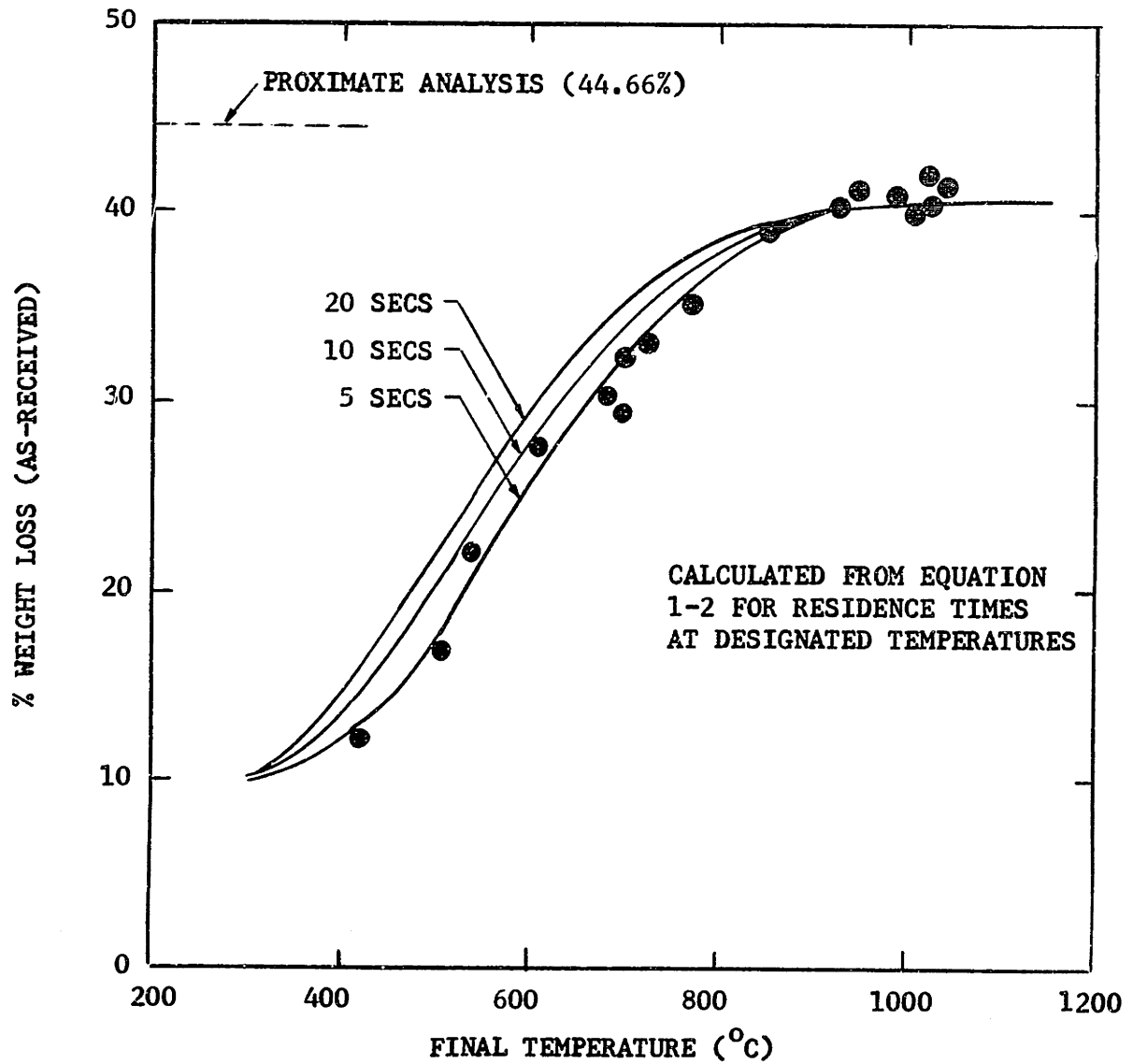


FIGURE 1-6 COMPARISON OF LIGNITE YIELDS WITH
DECOMPOSITION MODEL

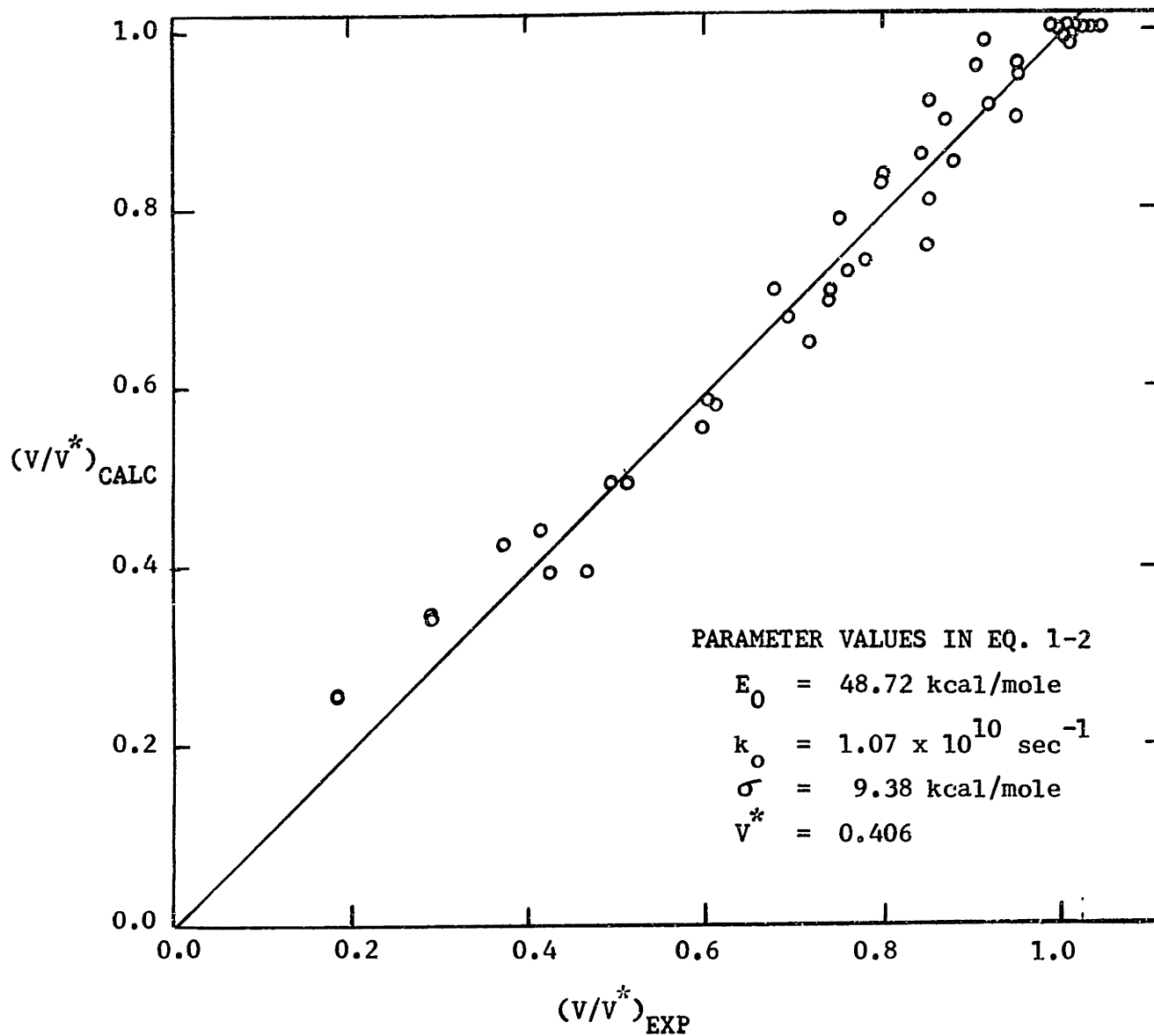


FIGURE 1-7 COMPARISON OF CALCULATED WITH EXPERIMENTAL
WEIGHT LOSSES FOR LIGNITE

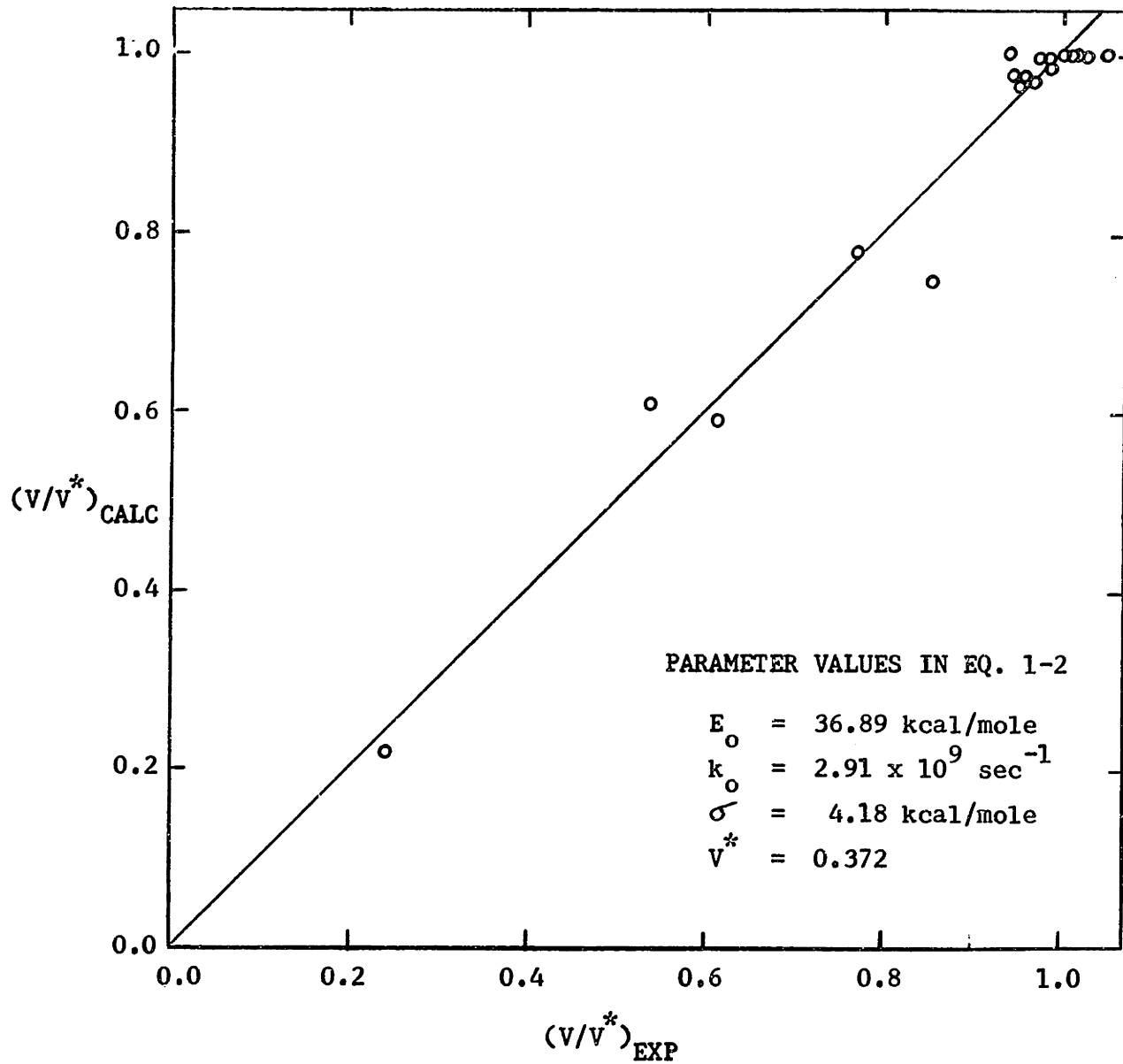


FIGURE 1-8 COMPARISON OF CALCULATED WITH EXPERIMENTAL
WEIGHT LOSSES FOR BITUMINOUS COAL AT 1000 PSIG

tool. The tool is especially valuable, though, because it contains certain characteristics that may be compared with more fundamental information. The range of activation energies, 30-67 kcal/mole for lignite and 29-45 kcal/mole for bituminous are certainly consistent with typical values for chemical reaction especially for organic decompositions.

5) Secondary Reaction Model

Despite the power of Equation 1-2 it offers no explanation for the significant influence of total pressure on the yield on bituminous coal devolatilization as illustrated in Figure 1-4. It is well-known that many volatile products are extremely reactive, thus it is not difficult to perceive reaction products of these species depositing on hot coal surfaces diminishing actual yield. If the residence time of these particular species is the controlling factor for yield, then conditions that reduce this residence time presumably would enhance yield. Hypothesizing a competition between deposition reactions of vapor phase volatiles and their diffusional escape away from the coal particle a selectivity expression for yield was derived

$$V_R = \frac{V_R^*}{1 + k_4/K^*} \quad (1-3)$$

where V_R and V_R^* are the "reactive" volatiles produced and potentially available, respectively; k_4 is the rate constant for deposition reaction and K^* is the overall mass transfer coefficient. The subscript R denotes that only a fraction of the volatile species participate in these secondary reactions. If it is further assumed that K^* is inversely proportional to pressure (proportional to

diffusivity) a trend illustrated by the curve in Figure 1-4 is obtained. For this bituminous coal, the "reactive" volatiles comprised about 35% of total potential volatile matter. Equation 1-3 is a very simple approach to the complex problem of simultaneous diffusion and secondary reaction of volatiles but it does give good agreement with the broad effects of pressure. One clue to the nature of the "reactive" species is the decreasing yield of tar with increasing pressure. The argument that tar is simply an intermediate in a series of reactions leading to char is well-supported by this data.

1.3.2 Hydrogenation

Comparison of yield with final temperature curves for both coals in atmospheres of hydrogen and helium establish the occurrence of significant hydrogasification. Data for bituminous coal are shown in Figure 1-9. The hydrogenation step is slower and occurs roughly in sequence with devolatilization. Yields from lignite are a function only of the hydrogen partial pressure but hydrogenation of bituminous coal also depends on total pressure. As shown in Figure 1-10 the presence of inerts ($P_{\text{tot}} = 1000$ psig) significantly diminishes yield at low hydrogen pressures. An interesting consequence of the pure hydrogen curve if compared to Figure 1-4 is that yield exhibits a minimum in the pressure range of 1-10 atm.

A very probable effect of hydrogen at least in the case of bituminous coal would be to stabilize the reactive species sufficiently to allow them to escape without further reaction. Accordingly,

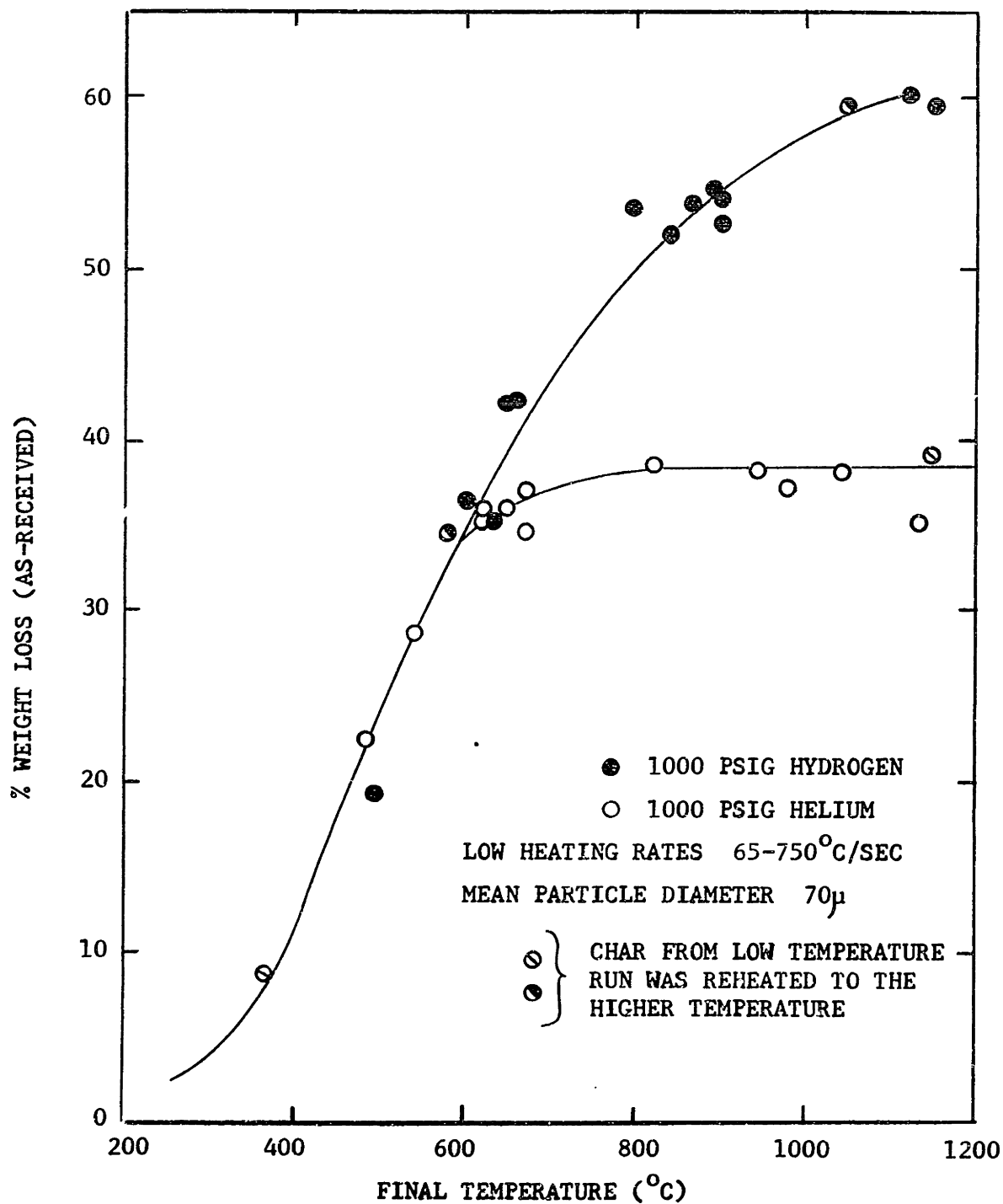


FIGURE 1-9 YIELD VERSUS FINAL TEMPERATURE FOR
 BITUMINOUS COAL IN HYDROGEN AND IN HELIUM

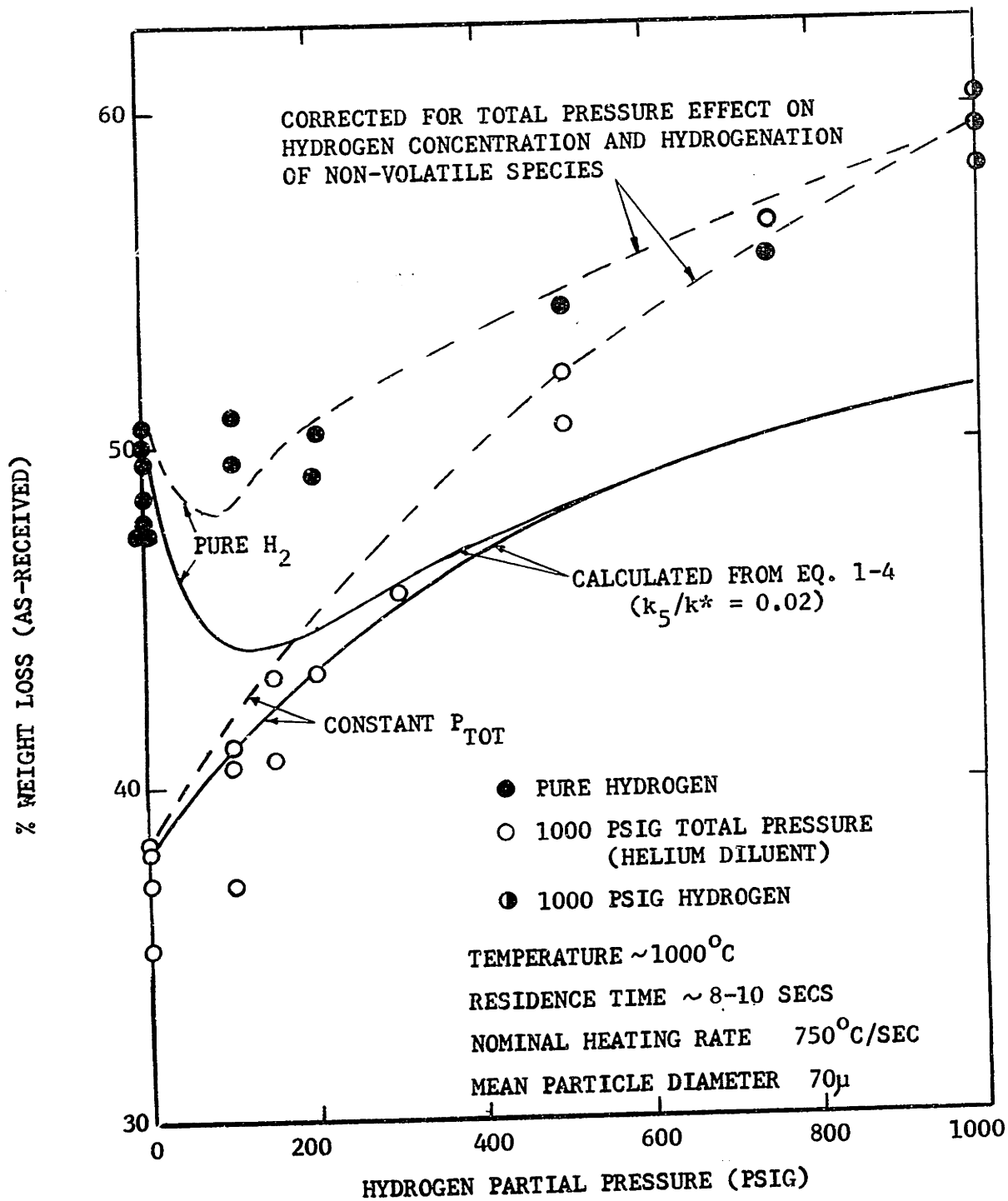


FIGURE 1-10 EFFECT OF HYDROGEN PARTIAL PRESSURE ON BITUMINOUS COAL YIELD

progressive disappearance of the tar is observed with increasing hydrogen pressure. Equation 1-3 can be rederived with an additional term to account for reaction with hydrogen (assumed first order with respect to volatile concentration and hydrogen pressure):

$$V_R = V_R^* \frac{K^* + k_5 P_{H_2}}{K^* + k_5 P_{H_2} + k_4} \quad (1-4)$$

with k_5 being the hydrogenation rate constant and P_{H_2} the partial pressure of hydrogen. Estimating a value for k_5 the correlation is tried in Figure 1-10 but the results are not exceptionally good. Not unexpected the single additional constant is insufficient to accurately represent yields in pure hydrogen plus gas mixtures. A good fit at low pressures ($P_{tot} = \text{constant}$) underpredicts yields at higher hydrogen concentrations as well as in pure hydrogen. Outright rejection of the model, however, would be premature. Broad trends are still characteristic especially the occurrence of a minimum yield in pure hydrogen. Two possible explanations are likely: 1) diffusional limitations at high total pressures would tend to decrease the differences in yields at low hydrogen partial pressures as observed (further support for this position is given later), and 2) hydrogen may react with portions of the coal not volatile in inert gas. Clearly this latter case is present in lignite hydrogenation where tarry intermediates do not exist. If these corrections are included in Equation 1-4, the fit is considerably improved as evidenced in Figure 1-10.

At this point it becomes possible to generalize on the rapid-rate phenomena. Upon heating the coal undergoes a primary thermal decomposition with different bonds rupturing at different temperatures.

The rupturing bonds form volatiles and initiate a sequence of char-forming reactions. Intermediates in the char-forming sequence are short-lived (up to one second at 1000°C) and can react with hydrogen to form additional volatile matter. In the case of bituminous coal some of these intermediates can escape as tar in inert atmospheres if residence times are short.

1.3.3 Effect of Particle Size

Data in Figure 1-11 show that hydrogenation yields were substantially reduced as particle size is increased whereas devolatilization yields in 1.0 atm helium show much less diminution with increasing particle size. It is possible to obtain from crossplotting Figures 1-10 and 1-11 "effective" hydrogen pressures based on a standard particle size of 70 μ for the yields and these were found to be inversely proportional to particle size. Unfortunately, the data at very small particle sizes (< 70 μ) were insufficiently precise to state definitely where the effectiveness factor is unity. This does provide though, substantial support to the argument for a hydrogen diffusion complication in Equation 1-4. It is apparent that one major problem in achieving high yields will be getting sufficient hydrogen in contact with the reactive species before they polymerize and crack.

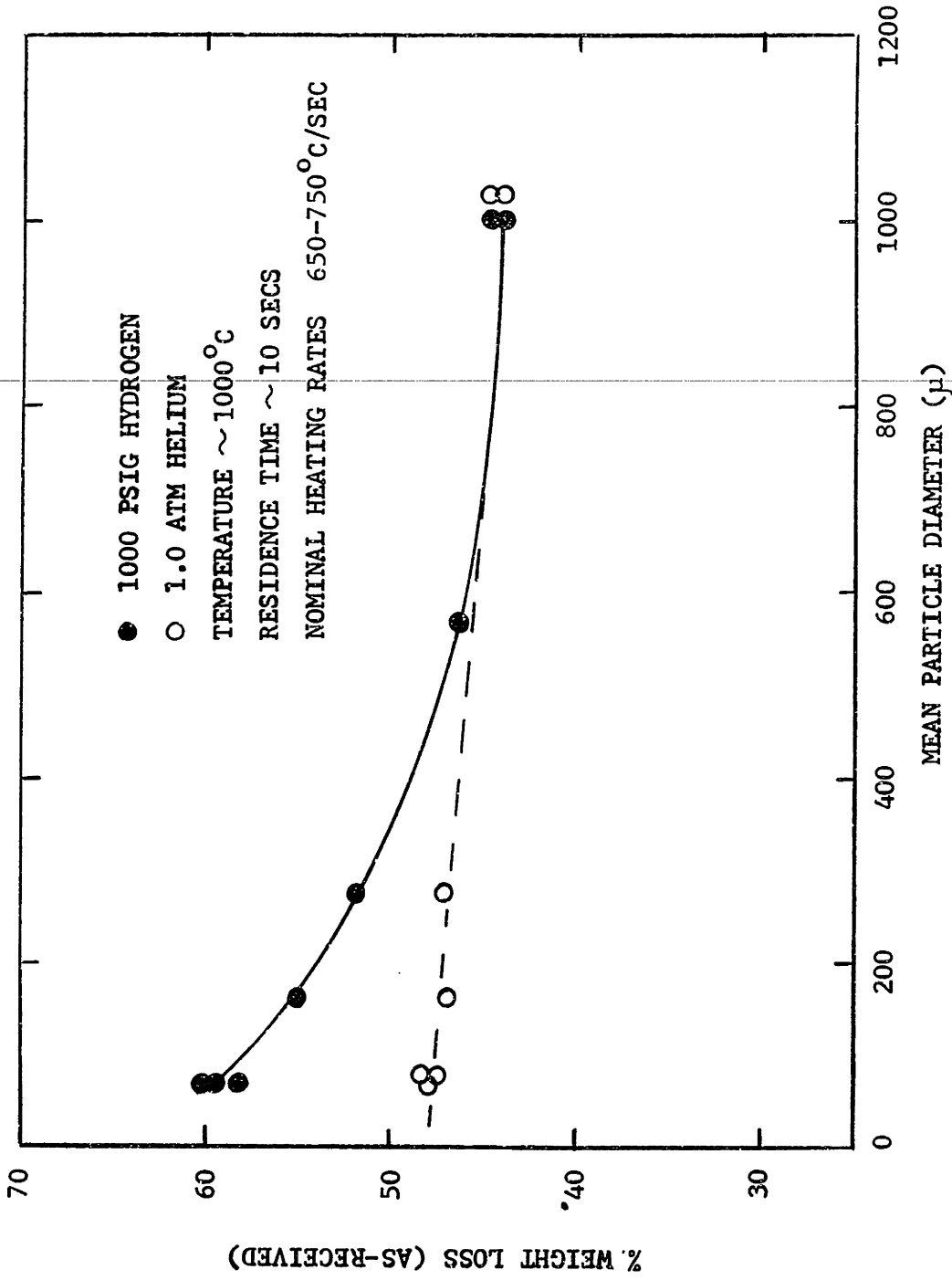


FIGURE 1-11 EFFECT OF PARTICLE SIZE ON BITUMINOUS COAL YIELDS

1.4 COMPARISON OF RESULTS WITH PREVIOUS INVESTIGATIONS

1.4.1 Devolatilization

A traditional means of correlating pyrolysis rate data is the first order decomposition model, i.e. the use of Equation 1-1 to describe the overall process. While the findings of this study clearly reject so simple a picture, it does remain a convenient basis for comparing results of different studies. For narrowly defined conditions it was possible to correlate the weight loss data from this study with a first order model and to obtain reasonable fits. Figure 1-12 compares two of these curves with values reported in the literature. While there exists a great deal of discrepancy in the range of values the results of this study are clearly in line with the general trend. An especially interesting characteristic of the statistically distributed activation energy model is that it offers a plausible explanation for the low activation energies (~ 10 kcal/mole) found in first order correlations. These low activations energies have caused considerable concern as to their mechanistic significance but from the findings of the present study are believed to be a mathematical consequence of attempting to force a complex reaction system into a simple model.

It has also been argued that rapid devolatilization can result in yields significantly greater than that indicated by proximate analysis. Clearly the secondary reaction model indicates such yields are possible but the mechanism is definitely a competition between diffusional escape and deposition reactions. While heating rate has a

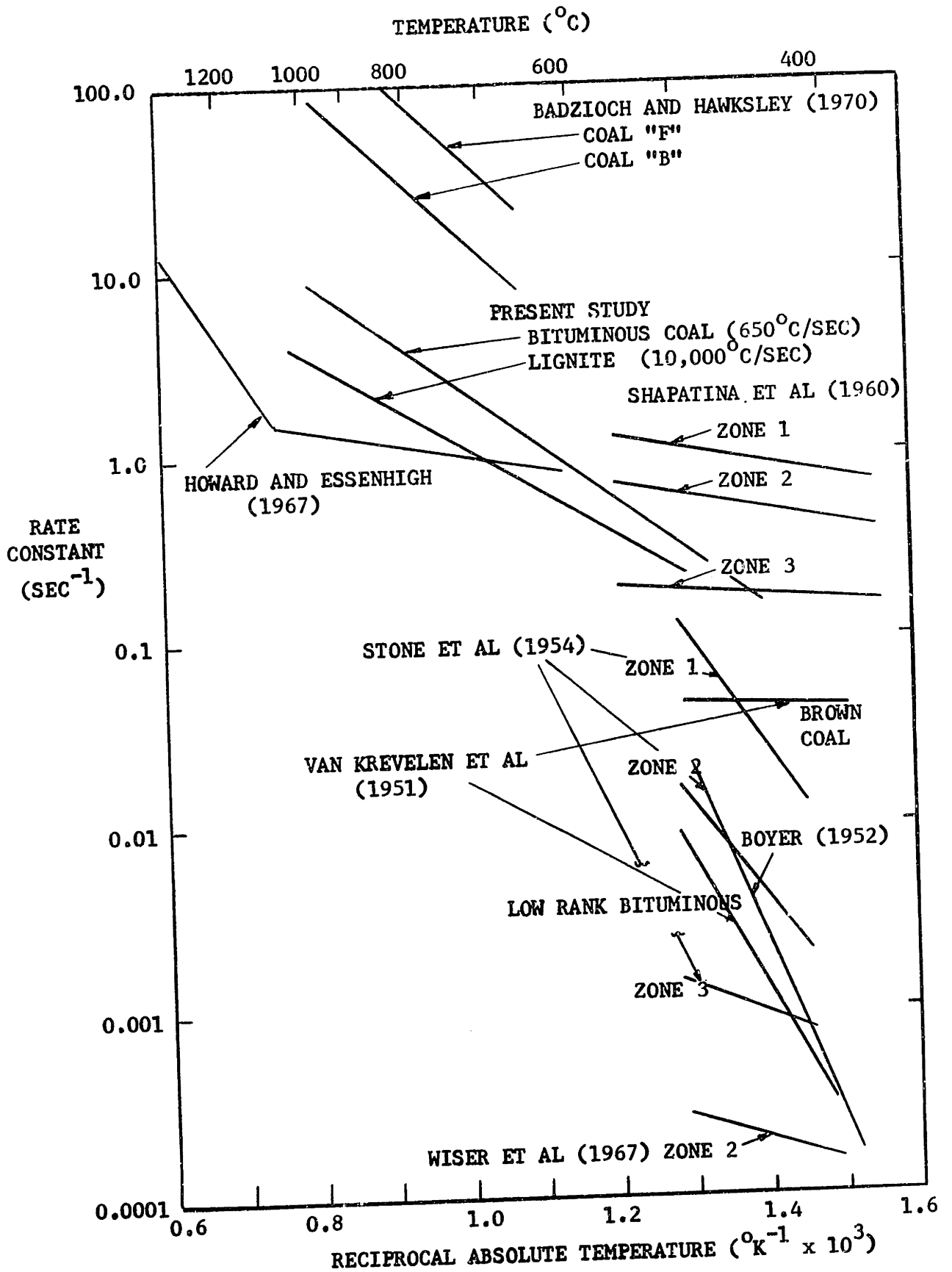


FIGURE 1-12 COMPARISON OF DECOMPOSITION RATE CONSTANTS

small effect, the principle result of most rapid heating experiments is to disperse the coal particles and thus to decrease the amount of available hot surface for deposition. Mazumdar and Chatterjee (1973) and Gray et al., (1973) have also recently reported that the dimensions of the coke charge in low heating rate experiments were quite significant in determining yields.

1.4.2 Hydrogenation

As with devolatilization the only existing basis for comparison of rate data is a power law rate expression. The form typically used in hydrogasification studies is as follows:

$$dV/dt = kP_{H_2} (V^* - V) \quad (1-5)$$

Again little faith is placed in a model that is valid only for specific conditions, but the general order of magnitude of rates observed in the results of this study and those of other investigators is quite encouraging. Figure 1-13 compares calculated rate constants for the available literature data. The agreement between Feldmann et al., (1972) and the present study for Pittsburgh Seam bituminous coal at 1000 psig is especially good and lends considerable confidence to the application of these thesis results to larger scale continuous systems.

Another major conflict in the literature is the dependence of yield on hydrogen pressure, primarily in the low pressure range (< 100 atm). Experiments conducted in disperse phase reactors show very little change in yield for pressures from 0 to 1000 psig whereas

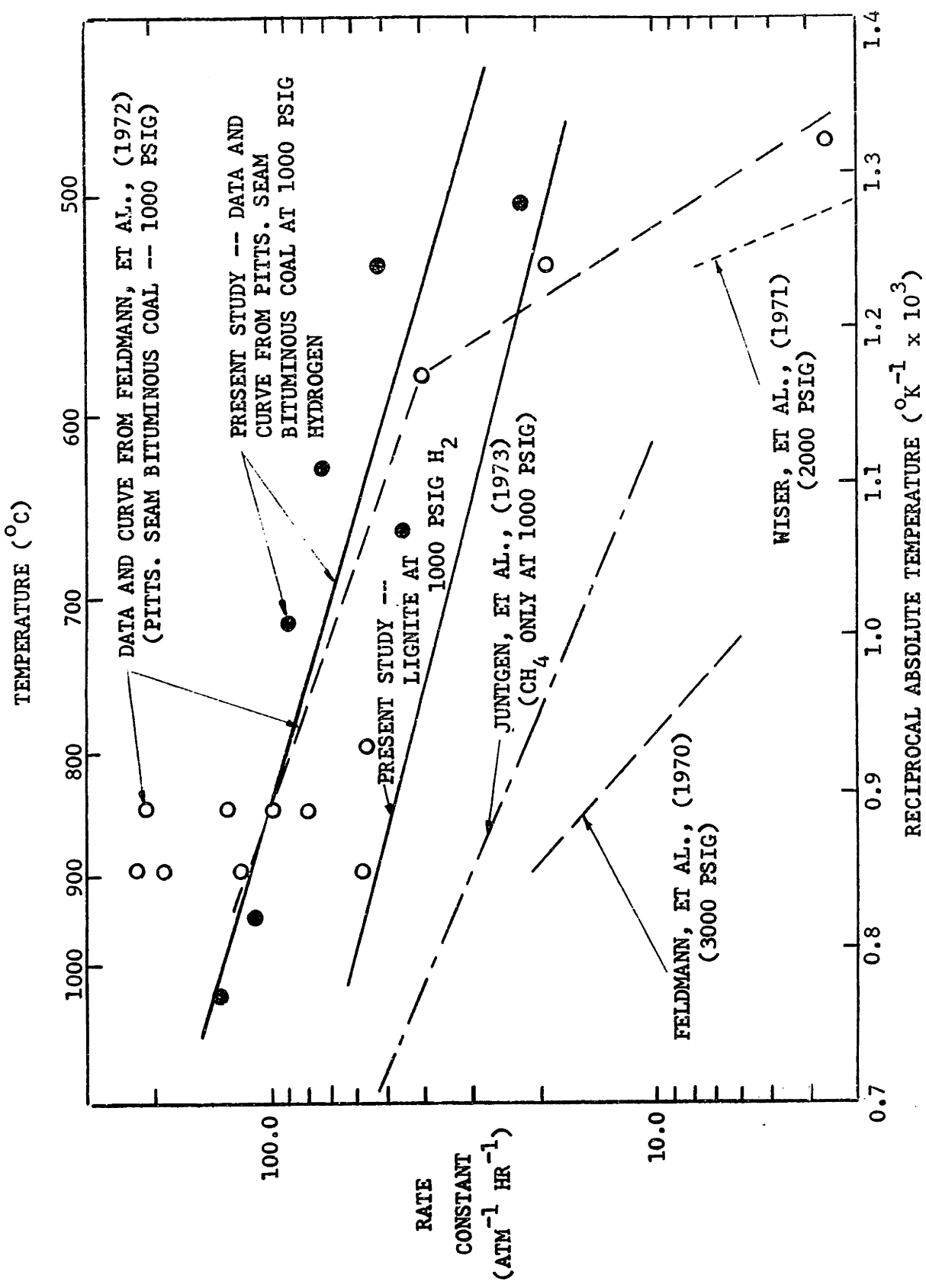


FIGURE 1-13 COMPARISON OF HYDROGASIFICATION RATE CONSTANTS

experiments conducted in packed beds show a very strong dependence on hydrogen pressure. This seemingly paradoxical behavior is believed to arise from the loss of potential volatiles through secondary reactions in the bed much the same as high total pressures in Figure 1-10 caused deposition at low hydrogen concentrations. Most important, however, is to recognize the occurrence of such secondary reactions in terms of scaling from dissimilar bench-scale apparatus to plant-scale systems.

1.5 APPLICATION OF RESULTS

The impetus for this investigation was the need for more fundamental data on the devolatilization and hydrogasification of coal at conditions of commercial interest. Accordingly, models were constructed consistent with the findings in this laboratory as well as those reported in the literature. Key design parameters were isolated and the important mechanisms elucidated. Correlation methods evolved that should be valuable in future bench-scale and pilot-plant work.

Among the present gasification schemes under serious consideration, only the Bureau of Mines Hydrane process envisions hydrogen-rich conversion of fresh coal. The hydrogasification section is to be comprised of two stages with the initial stage lower in temperature and hydrogen concentration. From the data in Figure 1-9 it is concluded that this initial hydrogen-lean stage could be operated at temperatures up to around 600°C without loss of reactivity toward hydrogen. The hydrogen-rich second stage would then presumably be maintained at a high temperature to maximize total conversion. The data of the present

study also indicate that conversions approximately twice as high as those estimated by the Bureau of Mines (Feldmann, et al., 1972) will be likely, thus permitting substantial reduction in reactor size. Further improvements in yield would be possible if particle sizes were reduced from the planned 150-300 μ to less than 100 μ , assuming difficulties with gas-solid disengagement can be overcome.

1.6 CONCLUSIONS

1. The electrical strip furnace has been demonstrated to be an effective tool for study of extremely fast reactions in coal at high temperatures and pressures.
2. The specific findings are:
 - a. The rate of coal conversion is very fast with weight loss virtually ceasing within a second after reaching final temperature in both hydrogen and helium.
 - b. Yields in both hydrogen and helium increases with increasing temperature.
 - c. Heating rate (650-10,000^oC/sec) has no effect on lignite yields and only increases bituminous coal yields by two percentage points.
 - d. Total inert pressure has no effect on lignite yields but increasing pressure from 0 to 1000 psig does reduce bituminous coal yields from 48% to 37%. Increasing hydrogen pressure increases yields for both coals.
 - e. Larger particle sizes decrease hydrogenation yields from bituminous coal significantly but shows only a small decrease in devolatilization yields.
3. The general reaction scheme for coal is concluded to consist of a primary thermal decomposition forming volatiles and initiating a sequence of secondary reactions leading to char. Unique in the

case of bituminous coal, intermediates in this char-forming sequence can appear as tar if residence times are short. Primary decomposition is modeled as though it is an infinite set of simultaneous first order decomposition reactions with a statistical distribution of activation energies ranging from approximately 30 to 67 kcal/mole. The effect of secondary reactions is correlated by a selectivity expression derived from a model hypothesizing a competition between char formation and diffusional escape of volatiles.

4. Hydrogen can interrupt this sequence of secondary reactions and increase the volatile yield. Modeling difficulties are experienced probably due to diffusional complications and the unknown nature of the secondary reactions.
5. The data agrees well with previously reported experimental trends and the model offers reasonable explanations for some of the observed "anomalies".
 - a. When simple power law rate models are used to correlate both the devolatilization and the hydrogenation data, the computed rate constants agree very well with literature values.
 - b. The interesting claim of rapid heating induced excess yields is put into perspective in terms of secondary reactions. Pressure and sample dimensions are found to be more critical in determining yields, but it is emphasized that coal type played an important role.
 - c. Discovery of the total pressure effect on bituminous coal hydrogasification clarifies the previous experimental trends in the region of commercially significant pressures (less than 100 atm).

1.7 RECOMMENDATIONS

The recommendations are grouped into three general categories:

1. Further work is recommended in acquisition of useful data for design and evaluation of process flowsheets including detailed product analysis, study of ultrafine particles and the influence of potential catalysts.
2. Additional fundamental work is needed in developing useful models particularly in terms of identifying the composition of primary volatiles and understanding the diffusional properties of a physically changing coal particle.
3. Finally it is suggested that the electrical strip furnace be used in studies of oil shale and refuse conversion to pipeline gas, general studies of gas-solid reactions, and classification of other types of coal.

2. INTRODUCTION

The current world oil situation has awakened this nation to the inescapable fact that domestic energy supply and demand are no longer in balance. Quite simply, the United States has found itself increasing the rate of energy consumption faster than the available supply has been augmented. The problem, serious in general, is especially acute in the natural gas market. Environmental constraints curtailing the use of certain traditional sources of supply (as in the case of high-sulfur coals) have boosted demand for clean-burning fuel. Unfortunately, the resultant depletion of gas reserves has been further accelerated by the Federal Power Commission's maintenance of excessively low prices. The facts are that the working inventory of natural gas, ratio of proven reserves to annual production, has fallen from 19.7 years in 1962 to 15.6 years in 1967 and to 10.7 years in 1972, and the prospects are not bright for the future (Linden, 1973; and West, 1973).

While improvements in the gas pricing structure will undoubtedly stimulate much needed gas exploration efforts, it seems clear that the demand for this relatively clean fuel will more than justify developing alternative sources of pipeline gas. In the very near future imported LNG and SNG from hydrocarbon liquids appear as potential substitutes, but this country's anticipated unwillingness to base such a critical sector of the economy on unstable foreign sources and the rising price of petroleum feedstock will limit their inroads. Production of synthetic pipeline gas from coal thus emerges as one of the most attractive sources of supply in the long run. The logic of the scheme is appealing; direct conversion of an undesirable but extremely

abundant resource to a clean-burning and very scarce gaseous fuel. The prospects for gas from coal are tremendous. It is quite evident that exploitation of this alternative will be limited more by our ability to provide sufficient quantities of such gas at economical prices rather than by demand for the gas itself. Crude estimates of supply and demand elasticities for natural gas suggest that a mere 1% reduction in final gas price by some process improvement would yield, say in 1985, an additional \$350 million market for synthetic pipeline gas. It would seem that sufficient incentives for such work are present.

2.1 BACKGROUND

The technology for generating fuel gases from coal is not new. In fact, the first commercial use of gaseous fuel was based on a coal process developed by Murdock in 1792 (Shreve, 1967). The discovery of large natural gas reserves forced coal gas schemes into virtual obsolescence. Only recently have economic pressures in the natural gas market stimulated renewed interest in gas from coal. The emphasis is now focused on developing a comparable high-BTU substitute for natural gas.¹

Basically, it would be most desirable to simply react coal and water to form methane and carbon dioxide:



$$H_{25}O_C = +3.6 \text{ kcal/mole}$$

¹ Early coal gas (containing significant amounts of H₂ and CO) had less than 50% the heating value of natural gas. However, there is also currently a major interest in low and intermediate-BTU gas for industrial use and power generation.

However, thermodynamics, in particular, the phase rule requires for description of a three component system of carbon, hydrogen, and oxygen; three degrees of freedom, for example, temperature, pressure, and H/O ratio. To completely describe the six constituents deserving of consideration (C, CO, CO₂, H₂, H₂O, and CH₄) three independent equilibria must be specified. The following were chosen:

1. Hydrogasification



$$\text{H}_{25^\circ\text{C}} = -17.9 \text{ kcal/mole}$$

2. Steam Gasification



$$\text{H}_{25^\circ\text{C}} = +31.4 \text{ kcal/mole}$$

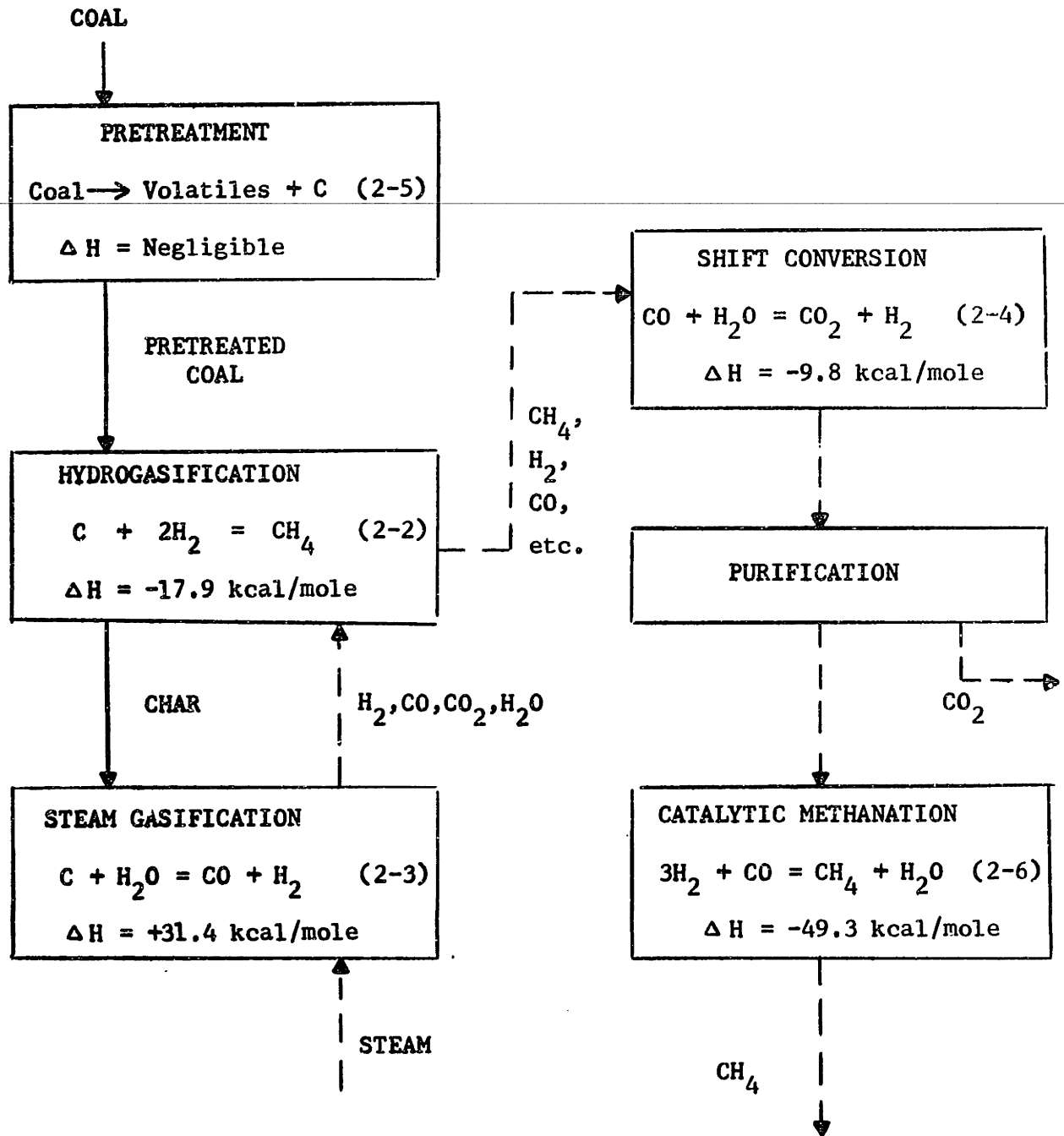
3. Water-Gas Shift



$$\text{H}_{25^\circ\text{C}} = -9.8 \text{ kcal/mole}$$

The sum of these three equations yields Equation 2-1. Simultaneous solution of these equations show Equation 2-1 favorable to methane formation only at low temperatures where the kinetics are too slow for commercial application. To circumvent this thermodynamic dilemma, several process schemes have been suggested.

To facilitate discussion of coal gasification processes, a "typical" process has been sketched schematically in Figure 2-1. The essential components of the diagram in coal-flow sequence are: 1) a pretreatment stage to eliminate caking and agglomeration (typically involves partial devolatilization, i.e. Reaction 2-5), 2) a hydrogasification step where pretreated coal is reacted under high pressures with hydrogen to form

**Notes:**

1. Only major reactions are listed for each stage.
2. Heats of reaction are based on 25°C. Negative sign denotes exothermic.

FIGURE 2-1 "TYPICAL" COAL GASIFICATION PROCESS

methane (Reaction 2-2) and, 3) steam gasification (Reaction 2-3) to produce the hydrogen needed for Reaction 2-2. The gases from the hydrogasification stage are then upgraded to the final product gas (essentially pure methane). The H_2/CO ratio is first improved by catalytic shift conversion (Reaction 2-4); CO_2 and other impurities (especially H_2S) are removed in the purification section; and finally, the remaining H_2 and CO are reacted over catalyst to form methane (Reaction 2-6). The laws of thermodynamics are significant in process consideration in two major respects. First, in terms of energy requirements steam gasification is extremely endothermic. Among the proposed techniques of energy supply now under consideration are the addition of O_2 to react with part of the char, close-coupling of steam gasification with hydrogasification to take advantage of the latter's exothermicity, electrical heating of the bed and transfer of hot inert solids to the reaction zone. Henry and Louks (1971) have discussed at length the significance on this energy-cost relationship as it pertains to overall process economics. The second influence of thermodynamics is in determining equilibrium compositions of the gases. A few general observations along this line indicate that the endothermic steam gasification reaction (2-3) is favored (thermodynamic tendency to proceed to the right) at high temperatures whereas the very important hydrogasification reaction (2-2) behaves in exactly the opposite fashion. In fact, at temperatures of kinetic interest there is a strong tendency for the methane formed from fresh coal (by Reaction 2-5) actually to decompose. This establishes the very critical need for extremely high high hydrogen pressures and relatively short residence times at high temperatures.

At present there is no commercially available process for the production of pipeline quality gas. Table 2-1 lists most of the current efforts to develop such technology. The processes have been roughly categorized into three generations of sophistication and comparative statistics of conversion, yields, and efficiencies have been provided where available. First generation processes included all schemes which have commercially proven technology for generation of synthesis gas such as Lurgi and Koppers-Totzek. Essentially, all that is required is addition of shift conversion and methanation to upgrade the synthesis gas to pipeline quality. Second generation technology describes processes which have begun or are entering pilot plant stage development but lack full-scale experience. New concepts which are still bench-scale with no immediate plans for pilot plant construction are tagged as third generation. A trend in gasification design, partially discernible from the conversion figures in Table 2-1, is to form greater amounts of methane in the gasifier via hydrogasification. The Koppers-Totzek process produces virtually no methane directly, Bigas and Synthane achieve about 20% conversion of coal to methane and Hydrane is expected to attain 40%. Most economic evaluations of coal gasification schemes indicate that catalytically formed methane (Reaction 2-6) is much less efficient and much more costly than methane from the coal's volatile matter and hydrogasification (Reactions 2-2 and 2-5). From the results of their optimization work Wen, et al., (1972) concluded:

"Thermodynamically, production of methane by direct coal-hydrogen reactions utilizing devolatilization and hydrogenolysis is more efficient than the carbon monoxide-hydrogen reaction..... It appears that, from the optimum efficiency point of view, the final methanation step should be used only to convert the final traces of the CO in the product and that as much as possible of the methane should be generated in the gasification subsystem."

TABLE 2-1

DEVELOPMENT EFFORTS IN COAL GASIFICATION

<u>Process</u>	<u>Gasifier Conversion</u>	<u>Gasifier Yield</u>	<u>Carbon Efficiency</u>	<u>Thermal Efficiency</u>	<u>Gas Price</u>
1st Generation:					
Lurgi	0.141			0.464	87.9
Koppers-Totzek	0.0015	0.00455	0.329	--	--
2nd Generation:					
IGT Hygas-Electrothermal	0.23	0.67	0.35	0.520	85.3
IGT Hygas-Oxygen	0.38	0.90	0.42	0.614	71.5
IGT Hygas-Steam-Iron	0.22	0.59	0.36	--	--
Consol. Coal CO ₂ -Acceptor	0.16	0.46	0.36	0.592	63.9*
BCR Bigas	0.22	0.51	0.44	0.681	69.6
Bureau of Mines Synthane	0.19	0.56	0.34	0.641	68.8
Kellogg Molten Carbonate	0.10	0.29	0.34	--	--
Applied Tech. Atgas	(No Data)				
Batelle/Union Carbide	(No Data)				
FMC Cogas	(No Data)				
3rd Generation:					
Bureau of Mines Hydrane	0.41	0.95	0.44	0.778	62.7

$$\text{Conversion} = \frac{\text{C in CH}_4 \text{ from Gasifier}}{\text{C in Solids Fed}}$$

$$\text{Yield} = \frac{\text{CH}_4 \text{ from Gasifier}}{\text{CH}_4 \text{ in Final Product}}$$

$$\text{C Efficiency} = \frac{\text{Conversion}}{\text{Yield}}$$

$$\text{Thermal Efficiency} = \frac{\text{H}_{\text{comb}} \text{ of Final Product}}{\text{H}_{\text{comb}} \text{ of Solids Fed}}$$

Price = ¢/MMBTU (\$4/ton coal; \$3/ton lignite*)

References: (Von Fredersdorff and Elliott, 1963; Hottel and Howard, 1971; Furman, 1972; Wen et al, 1972)

Henry and Louks (1971) also found:

"The cost of producing methane from devolatilized char is four times that of producing methane from the coal's volatile matter. To reduce the cost of methane from coal, therefore, a process must be used that will optimize the production of devolatilized methane and keep the cost of adding heat to the steam-carbon system to a minimum. Hydrogasification is one way of reducing the cost of adding heat."

In light of these economic considerations, the following experimental observations strongly suggest that raw coal as opposed to a devolatilized or pretreated char be fed directly to the gasifier.

1 -- Volatile matter in coal may comprise 40% or more of the coal by weight, representing a significant source of high heating value gas. Further, there are indications that the amount of volatile matter can be increased significantly by heating under properly controlled conditions.

2 -- Freshly devolatilizing coal is more reactive than pretreated coal. Fresh is defined on a time scale of seconds or less and more reactive may mean several orders of magnitude difference in rate.

3 -- Freshly devolatilized coal also appears to possess excess free energies. The equilibrium constant for the hydrogasification reaction may be larger by a factor of 10 or more.

Capitalizing on these alleged advantages requires that the extent to which they occur be ascertained quantitatively such that they may be evaluated with respect to the increased costs and difficulties of accomodating fresh or raw coals. The reported values of conversion for second and third generation technology in Table 1 are illuminating but there is little assurance that they are any more than speculative and will, in fact, occur in full scale operation. A wide range of new information will be necessary for more detailed calculations and evaluations. One of the important areas of research focuses on the understanding of the fundamentals of the coal-hydrogen reaction. The following section reviews past work in this area and critically appraises the current level of understanding.

2.2 LITERATURE REVIEW

2.2.1 Existence of "Rapid-Rate" Carbon

It is generally well-known that the residual "fixed carbon" in char or coke will combine with hydrogen to produce methane. The reported rates for this reaction are relatively slow, ranging from 0.6 - 3.0 %/hr¹atm H₂ at 927°C (Feldkirchner and Linden, 1963). Dent's (1944) early experimental work, however, showed that a substantial portion of the carbon in fresh coal (volatiles intact) could be more rapidly converted to methane than carbon in coke. Birch, et al., (1960, 1969) identified two distinct stages in their fluid bed hydrogasification of raw brown coal, with the second stage comparable in rate to the hydrogenation of coke. The initial stage was described as a rapid hydrogenation of volatiles, the yield of which depended only on temperature and hydrogen pressure and was found independent of residence time (for residence times greater than 6 minutes, the minimum achievable in their fluidized bed).

Feldkirchner and Linden carried out "semi-flow" rate experiments by dropping a few grams of fresh coal onto a preheated alumina bed and passing gas mixtures through it. Conversion results with time for three different coals are shown in Figure 2-2. Again, two clearly distinct rate periods are present with the first stage undoubtedly occurring during the heat-up period. Extrapolating the slow rate period to zero reaction time indicates conversions roughly equivalent to proximate volatile contents.

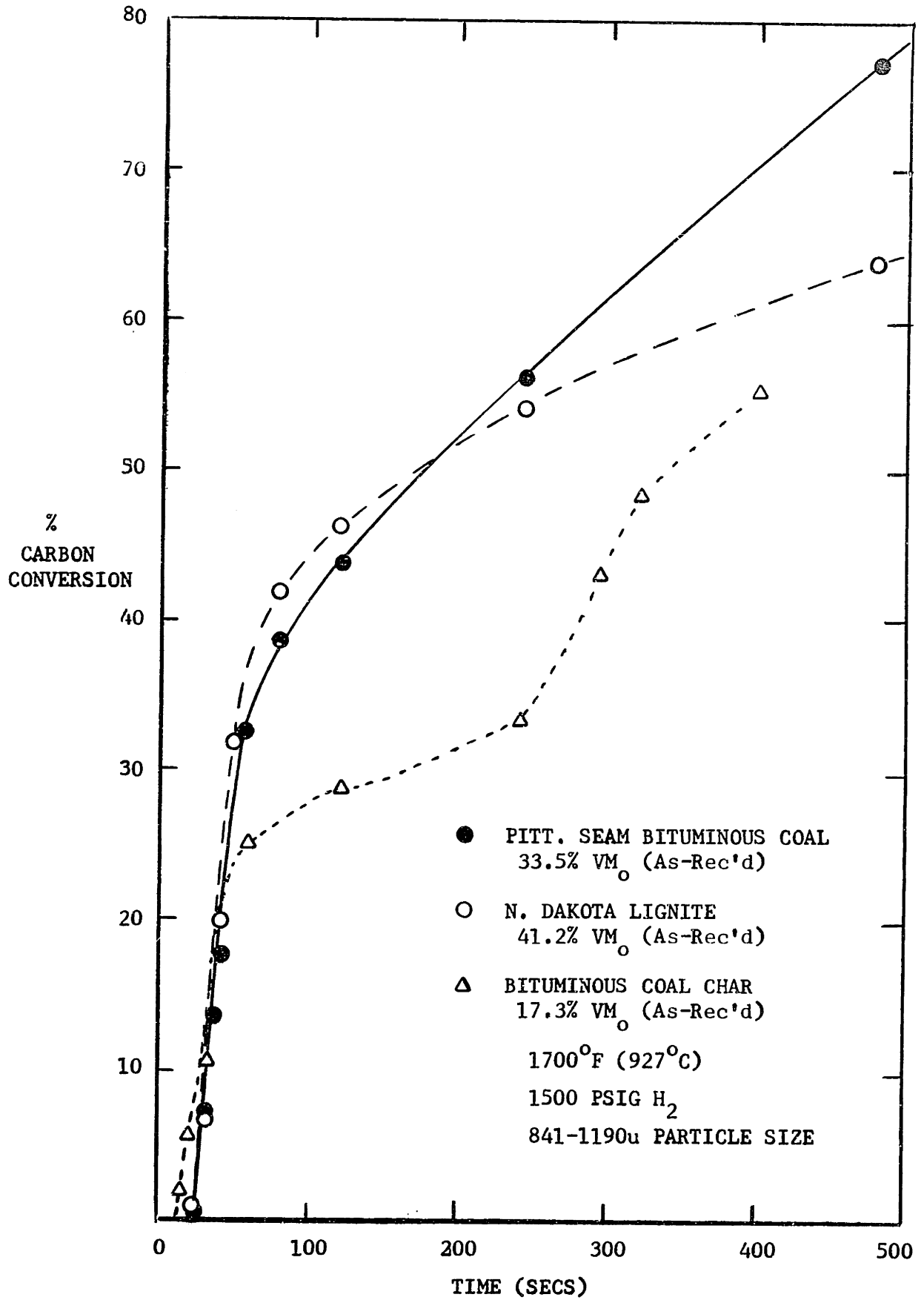


FIGURE 2-2 WEIGHT LOSS WITH TIME DATA FROM
 FELDKIRCHNER AND LINDEN (1963)

Schroeder (1962) and later Hiteshue, et al., (1962a, 1962b, 1964) passed hydrogen through a heated bed of raw coal and analyzed the resulting products. Conversions as a function of time are plotted in Figure 2-3 for bituminous coal at 800°C. Since a finite amount of time was required for heating the bed to temperature and then cooling, "zero residence time" on the graph corresponds to the time required to reach temperature followed by an immediate quench (total time of 40 secs above 300°C). The significant conversions observed at this "zero residence time" are first indicative of the extremely fast reactions taking place and secondly provide convincing evidence that a substantial portion of the coal's proximate "fixed carbon" also participates in the rapid-rate period.

Moseley and Paterson (1965a) employed a novel variation of the "semi-flow" technique by spreading coal and char powders along a tubular reactor mounted horizontally above a railway along which a series of burners were propelled followed by water jets for cooling. Heating and cooling rates of 25°C/sec were possible with a minimum of 15 secs at temperature. A comparison between the initial rates (times less than 1 min) for char and coal showed higher initial rates for coal but apparently a faster decay in this initial reactivity also occurred. A subsequent entrained flow apparatus achieved extremely high heating rates and demonstrated the effect of pretreatment (or volatile content) on the initial rate as shown in Figure 2-4. (Moseley and Paterson, 1965b). Unfortunately, the equipment was unable to accommodate raw caking coals.

The most significant evidence, to date, of "rapid-rate" carbon has been gathered from an experimental technique suggested by Hiteshue, et al., in 1964. Essentially, coal is introduced and dispersed at the top

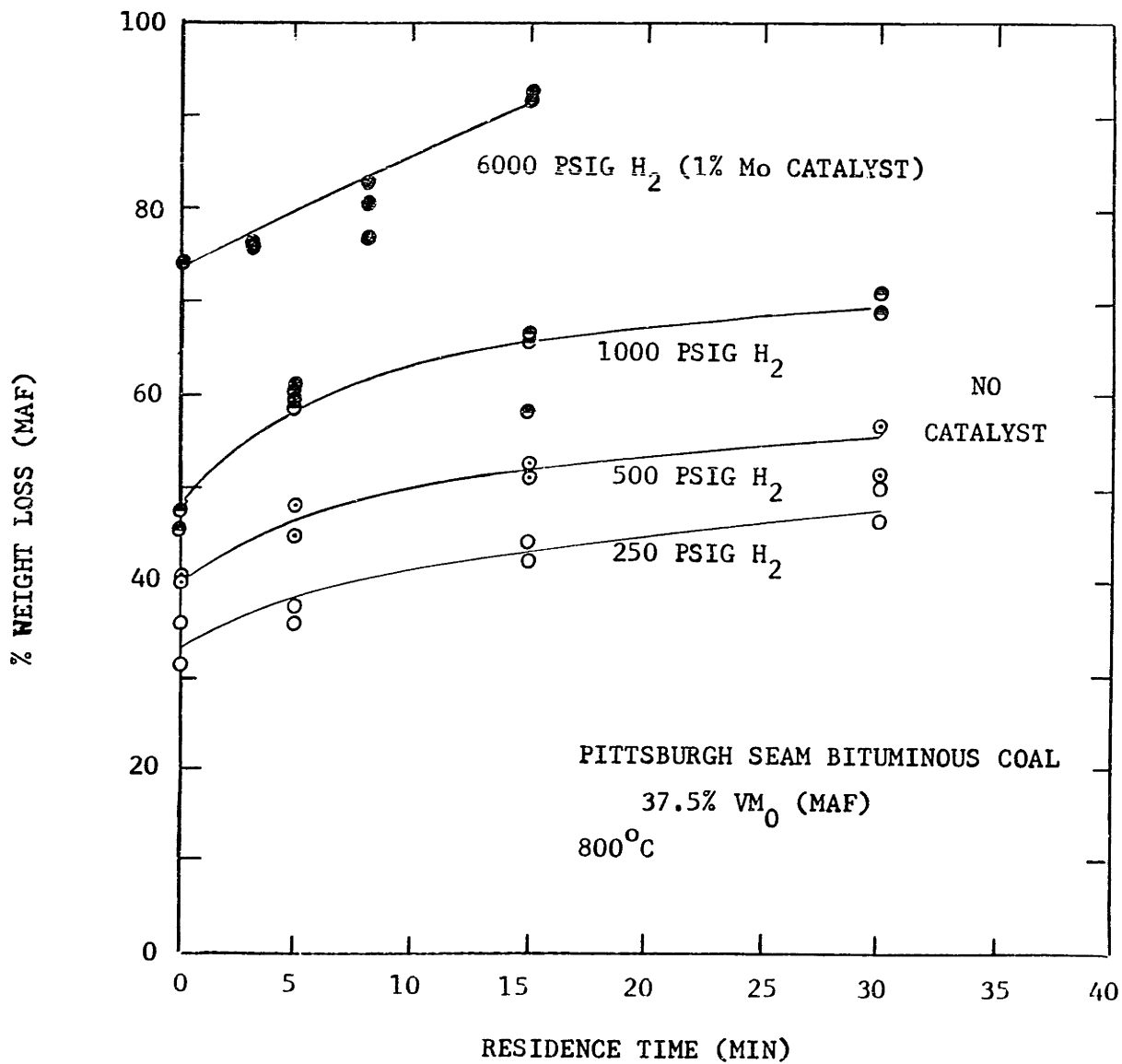


FIGURE 2-3 WEIGHT LOSS WITH DATA FROM
HITESHUE, ET AL., (1962b,1964)

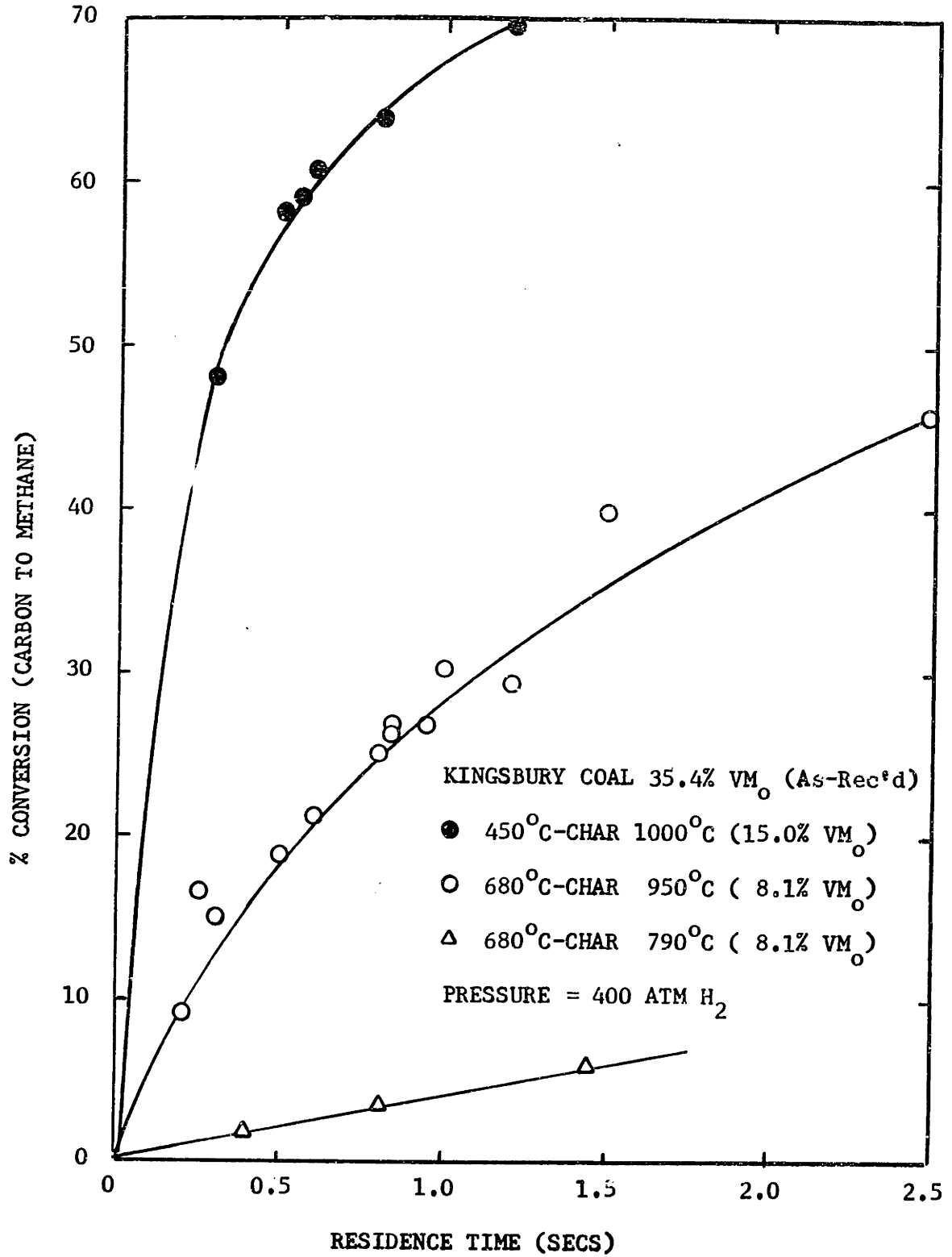


FIGURE 2-4 COMPARISON OF CHAR REACTIVITIES
FROM MOSELEY AND PATERSON (1965b)

of a large diameter reactor and allowed to pass through the heated reaction zone in free-fall (terminal velocity). Using just such a free-fall reactor, Moseley and Paterson (1967) demonstrated nearly complete conversion of coal to methane was possible under sufficient hydrogen pressure. Their data are illustrated in Figure 2-5 along with their proposed model. (Derivational details of the various models for "rapid-rate" carbon are reserved for discussion later.)

Workers at the Bureau of Mines have also used the free-fall reactor as a convenient means for achieving rapid heating of agglomerating coals (Lewis, et al., 1967). Feldmann, et al., (1970) accumulated data from an integral version of the reactor, i.e. gas composition contacting the coal changed during a run. To permit graphical analysis of the results, conversions at constant hydrogen pressure have been estimated from Feldmann's published model and plotted in Figure 2-5. The agreement with the Gas Council results is surprisingly good if one remembers: 1) different types of coal were used; 2) particle sizes used by Moseley and Paterson were 100-150 μ vs. 150-300 μ in Feldmann's work; and 3) reactor lengths were slightly different, 4½ ft for the Gas Council and 5-6 ft for the Bureau.

Zahradnik and Glenn (1971) have analyzed data from the Bituminous Coal Research Inc. continuous flow hydrogenation reactor (5 ft vertical tube). Their model was shown to fit the relatively low pressure (< 30 atm H₂) BCR data as well as reasonably predict the high pressure results of Moseley and Paterson (see Figure 2-5). With only a limited amount of information available it appears that workers at the Univ. of Utah have also achieved high yields (to 85 wt%)

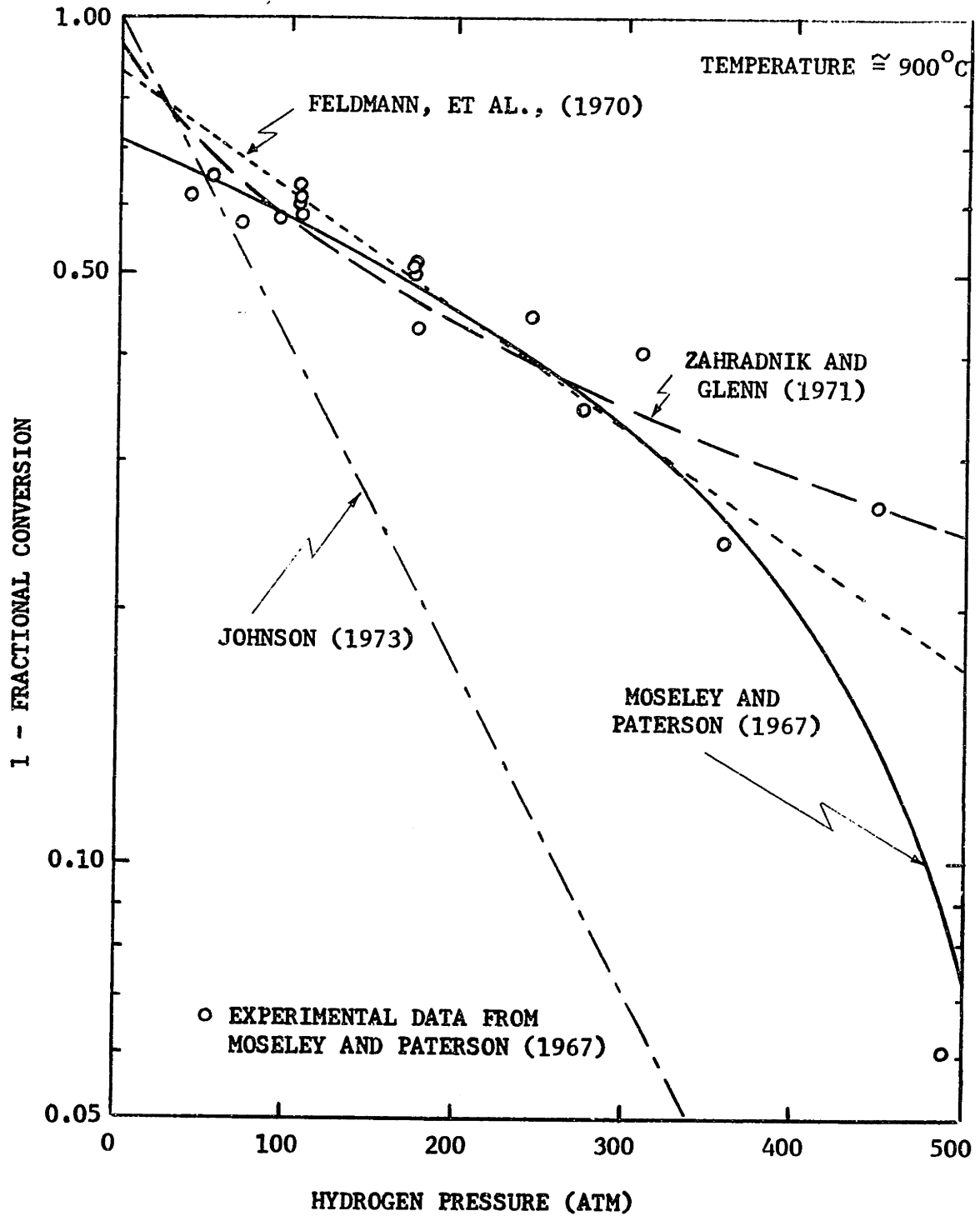


FIGURE 2-5 HYDROGASIFICATION CONVERSION AS A
FUNCTION OF HYDROGEN PRESSURE

with a free-fall reactor ($< \frac{1}{2}$ sec residence time) (Wiser, et al., 1971).

It should be added that such yields were attained at substantially less severe temperatures (ca. 500°C) with the aid of a catalyst.

Johnson (1971) has published some interesting results from his thermobalance in which the coal sample (enclosed in a wire mesh basket) is lowered into a preheated reaction zone where the weight is continuously recorded. Three distinct stages in raw coal hydrogenation are clearly evidenced in Figure 2-6.

- | | | |
|------------------------------|---|---------------------|
| 1 -- Devolatilization | } | "Rapid-Rate" Carbon |
| 2 -- Rapid Hydrogasification | | |
| 3 -- Slow Hydrogasification | | |

At this point it would be convenient to introduce, in some detail, the various empirical models which have been advanced by the investigators and then comment on how the process variables are accounted for in the models. Finally an attempt will be made to relate these empirical models to more fundamental concepts and theories on coal structure and behavior.

2.2.2 Modeling the Kinetics of "Rapid-Rate" Carbon

Models proposed thus far in the literature may be generally divided into two classes; strictly empirical correlations of data or more sophisticated models based on suspected mechanisms.

Empirical Correlations -- The principle correlative tool in this category is the general power law rate model where the rate of

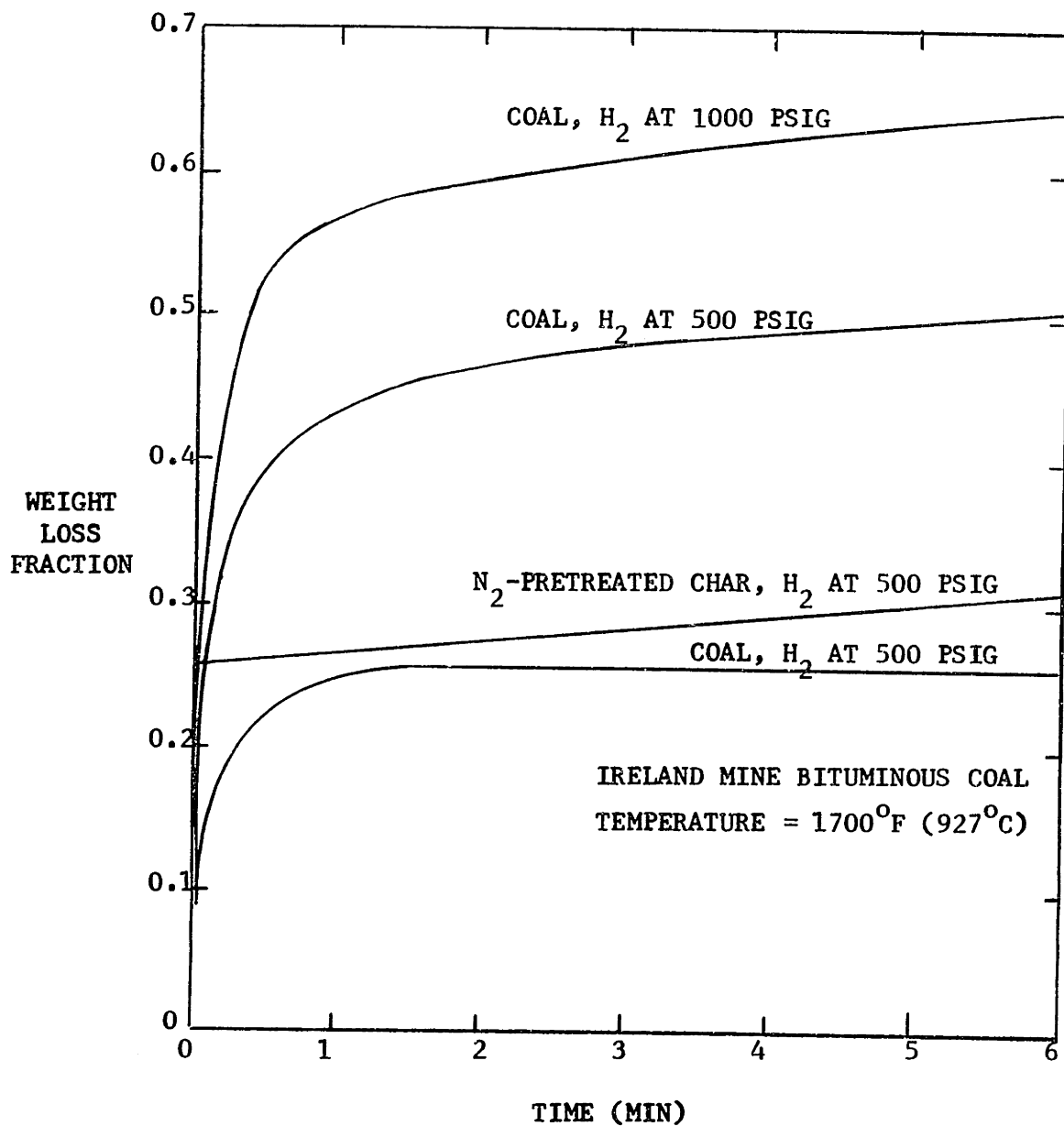


FIGURE 2-6 WEIGHT LOSS WITH TIME DATA FROM JOHNSON (1971)

conversion is found to be proportional to the concentration of each reactant (in this case hydrogen and "rapid-rate" carbon) to some power:

$$\frac{dX}{dt} = k_3 P_{H_2}^a (X^* - X)^b \quad (2-7)$$

where X = fractional conversion of "rapid-rate" carbon material,²
 X^* = total amount of "rapid-rate carbon",
 k_3 = rate constant,
 P_{H_2} = partial pressure of hydrogen, and
 a, b = constants.

Various forms of Equation 2-7 have been employed by a number of investigators to describe coal hydrogenation (Wen and Huebler, 1965; Feldmann, et al., 1970; Wiser, et al., 1971; and Juntgen, et al., 1973).

²Note: No attempt has been made to use the nomenclature of the original papers. It was felt that greater clarity could be achieved by deriving the models within a uniform framework of nomenclature such that similarities as well as dissimilarities will be obvious. Naturally, this has required certain standardizations. For instance, the term "fractional conversion" (X) was defined in several different ways in the original papers:

Moseley and Paterson (1965a) Zahradnik and Glenn (1971) Juntgen <u>et al.</u> , (1973)	$X = \frac{\text{Grams of Carbon as Methane}}{\text{Grams of Original Carbon}}$
(Moseley and Paterson also reported total carbon conversion and weight loss).	
Wen and Huebler (1965) Feldmann, <u>et al.</u> , (1970)	$X = \frac{\text{Grams of Carbon Gasified}}{\text{Grams of Original Carbon}}$
Wiser, <u>et al.</u> , (1971)	$X = \frac{\text{Grams of Coal Gasified}}{\text{Grams of Original Coal}}$
Johnson (1973)	$X = \frac{\text{Grams of Fixed Carbon Gasified}}{\text{Grams of Fixed Carbon}}$

Such fine distinctions are not made in the text since it remains unestablished which definition provides the best measure of conversion.

In each paper the constants a and b have been set equal to one though Wen stipulates this reaction rate must go to zero near equilibrium and replaces the term P_{H_2} with $P_{H_2} - P_{H_2}^*$, the difference between the actual hydrogen pressure and the hydrogen pressure at equilibrium. The equilibrium data used by Wen, however, indicates this relationship is valid only for reaction with char residue.

The major shortcoming of Equation 2-7, though, is that for any practical use, it is necessary to be able to predict the amount of potential rapid-rate carbon as a function of pertinent parameters. Integrating Equation 2-7 one obtains

$$X = X^* (1 - e^{-k_3 P_{H_2} t}) \quad (2-8)$$

Wen and Wiser agree that X^* is a function of temperature but offer no correlations. Feldmann, et al., contend that it is also dependent on hydrogen pressure but again the reader is left without the functionality. Further, the effect of variables unaltered in these experiments remains unknown.

Active Species Model -- To explain the rapid decay in coal's initial reactivity toward hydrogen as well as temperature and pressure effects on yield, Moseley and Paterson (1965a) pictured coal thermally decomposing to yield volatiles plus active sites. These active sites would then react either by hydrogenation to form methane or by thermal cross-linking to form inactive char structure (which subsequently reacted very slowly with hydrogen to produce methane). The mechanism further assumed rapid methanation resulted in no net consumption of active sites. The rate of methane formation was written as

$$\frac{dX}{dt} = k_3 P_{H_2} C^* \quad (2-9)$$

where C^* is the concentration of active sites present. Assuming that active sites disappeared by a first order decomposition, an expression for C^* may be written

$$C^* = C_o^* \exp(-k_2 t) \quad (2-10)$$

substituting into Equation 9,

$$\frac{dX}{dt} = k_3 P_{H_2} C_o^* \exp(-k_2 t) \quad (2-11)$$

and integrating,

$$X = \frac{k_3 P_{H_2} C_o^*}{k_2} (1 - e^{-k_2 t}) \quad (2-12)$$

Treating the thermal destruction of active sites as very fast, the exponential term in Equation 2-12 becomes negligible within fractions of a second resulting in the rapid-rate yield being proportional to

hydrogen pressure

$$X = \frac{k_3 P_{H_2} C_o^*}{k_2} \quad (2-13)$$

Zahradnik and Glenn (1971) used a similar model but theorized more in terms of an active species rather than sites and consistent with such thinking modified Equation 2-10 to account for the disappearance of this active species via methanation

$$C^* = C_o^* \exp(-k_3 P_{H_2} t - k_2 t) \quad (2-14)$$

Equation 2-12 then becomes

$$X = \frac{k_3 C_o^* P_{H_2}}{k_3 P_{H_2} + k_2} (1 - \exp(-k_3 P_{H_2} t - k_2 t)) \quad (2-15)$$

or by again neglecting the exponential term after some minimum residence time

$$X = \frac{\frac{k_3}{k_2} C_o^* P_{H_2}}{1 + \frac{k_3}{k_2} P_{H_2}} \quad (2-16)$$

Johnson (1973), on the other hand, has conceptually viewed the active species as catalyzing the reaction between fixed carbon and hydrogen. With this argument, Johnson altered the form of Equation 2-9

$$\frac{dX}{dt} = k_3 P_{H_2} (1 - X)^{2/3} \exp(-aX^2) C^* \quad (2-17)$$

The conversion integral was found for the actual determined value of $a = 0.97$ to approximate:

$$\int_0^X \frac{dX}{(1 - X)^{2/3} \exp(-aX^2)} = -\ln(1 - X) \quad (2-18)$$

This, of course, implies a simpler expression for Equation 2-17

$$\frac{dX}{dt} = k_3 P_{H_2} (1-X) C^* \quad (2-19)$$

If Equation 2-10 is substituted for C^* , the integrated expression for conversion becomes

$$-\ln(1 - X) = \frac{k_3 P_{H_2} C_o^*}{k_2} (1 - e^{-k_2 t}) = \frac{k_3 P_{H_2} C_o^*}{k_2} \quad (2-20)$$

Interestingly enough, this gives a straight line in Figure 2-5 with an intercept at zero hydrogen pressure corresponding to proximate volatile content. At temperatures below 1500°F (816°C) Equation 2-20 was found

to be inadequate and a temperature dependent relationship for C_o^* was proposed by Johnson (Pyrclioch, et al., 1972):

$$C_o^*(T) = C_o^* \left(1 - \int_0^\infty f(E) \exp\left(-\int_0^t k_1 dt\right) dE \right) \quad (2-21)$$

or assuming the ratio k_3/k_2 to be temperature independent:

$$-\ln(1 - X) = \frac{k_3}{k_2} C_o^* P_{H_2} \left(1 - \int_0^\infty f(E) \exp\left(-\int_0^t k_1 dt\right) dE \right) \quad (2-22)$$

where $f(E)$ = distribution of activation energies such that $\int_0^\infty f(E) dE = 1$,

k_1 = rate constant, Arrhenius form, and

E = activation energy.

The derivation of Equation 2-21 was based on the hypothesis that the active site formation reaction was actually composed of a very large (to be mathematically precise, infinite) set of parallel reactions of differing activation energies (described by $f(E)$). Furthermore, it was assumed that the rate of active site formation was much slower than its subsequent decomposition ($k_1 \ll k_2$), as opposed to the model of Moseley and Paterson as well as Zahradnik and Glenn where the formation of active sites was fast relative to their disappearance.

Moseley and Paterson (1965a) have also introduced evidence, although unaccounted for in their model, that the number of active sites (C_o^*) is dependent on temperature but uninfluenced by pressure. In Figure 2-7 the decay in methanation rate is shown at two temperatures (815°C and 950°C). At 85 seconds the low temperature run was increased to 915°C with the resultant surge and rapid decay in rate. This shows that more active species were produced by simply raising the temperature whereas a similar step change in hydrogen pressure, Figure 2-8, produced no such surge but simply increased the residual gasification rate.

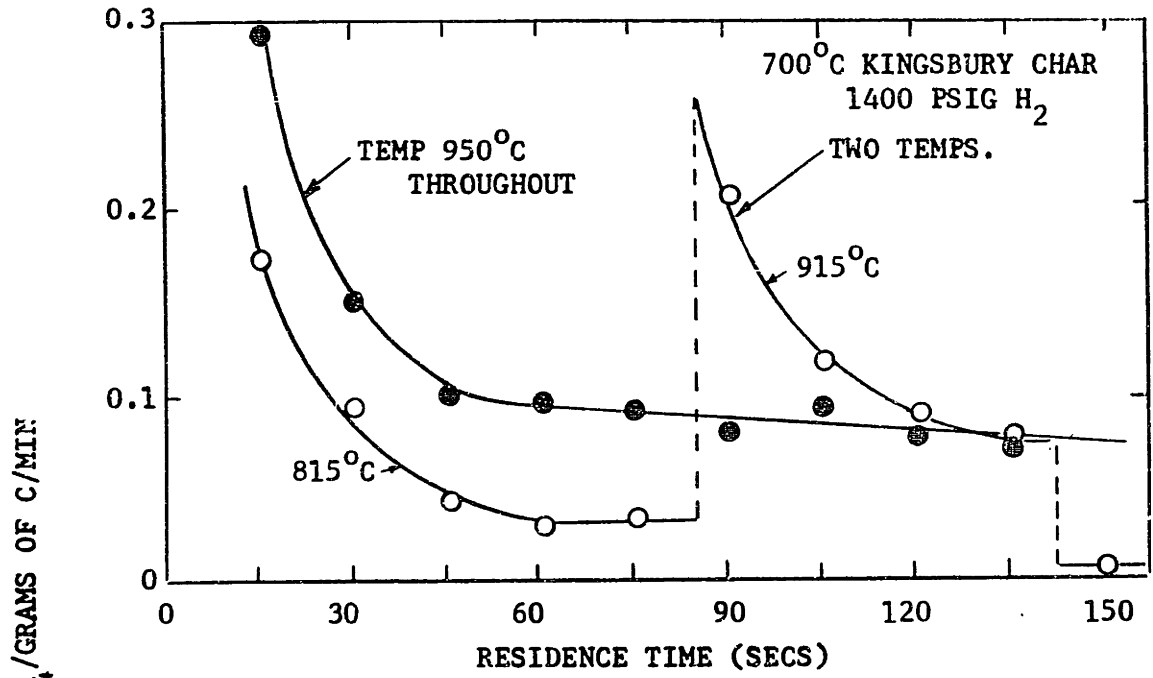


FIGURE 2-7 EFFECT OF TEMPERATURE ON HYDROGASIFICATION RATE
(MOSELEY AND PATERSON, 1965a)

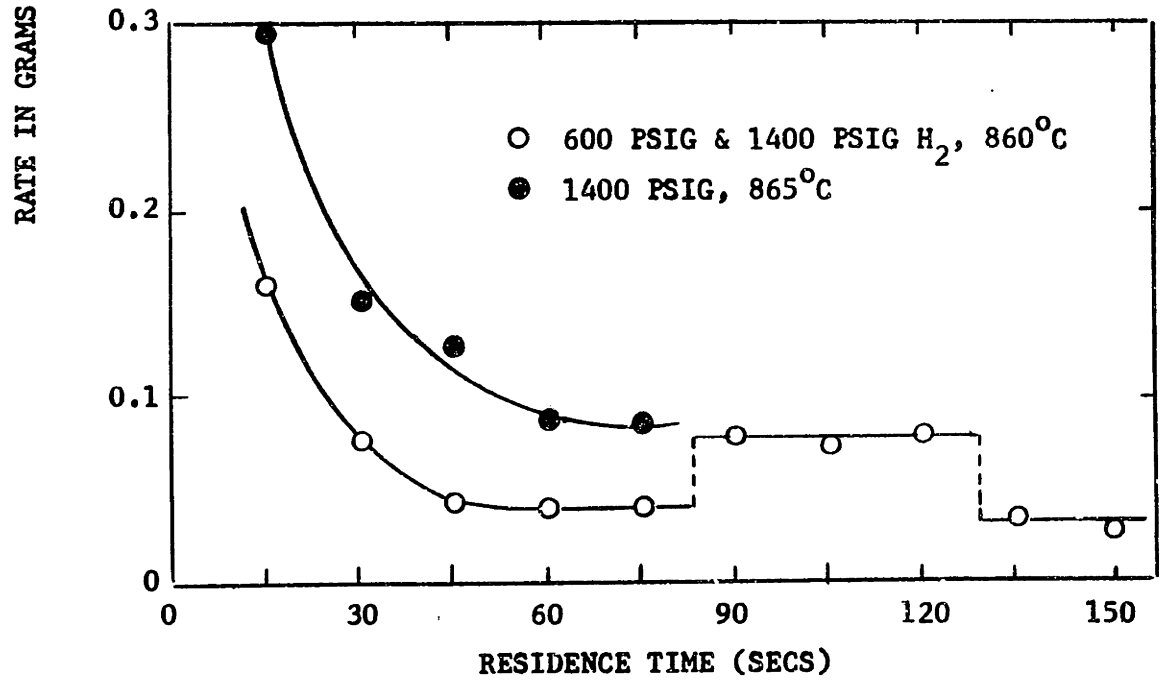


FIGURE 2-8 EFFECT OF PRESSURE ON HYDROGASIFICATION RATE
(MOSELEY AND PATERSON, 1965a)

Zahradnik and Glenn, however, argue that the methane formation step is favored at high temperatures and support this by showing a plot of $\ln(k_3 C_O^*/k_2)$ versus $1/T$ to be a straight line with a negative slope. The negative slope, in turn, is taken as proof that the methane formation step is more highly activated than thermal deactivation. Of course, this assumes C_O^* is independent of temperature which is inconsistent with surge in rate observed in Figure 2-7. It is interesting, though, to examine values of C_O^* which may be calculated from the constants reported by Zahradnik and Glenn in Table 2-2. Adding to this total active carbon the amount of carbon appearing as methane during devolatilization (constant b_1), the total potential carbon for methane approaches or exceeds unity in every case. (To be fair, revised versions of the model set $b_3 = b_2/(1-b_1)$, or fractional available carbon is defined as unity (Zahradnik and Grace, 1972; and Zahradnik, 1973)). Since a substantial quantity of the carbon in coal may volatilize as carbon oxides or heavier hydrocarbons this conclusion is questionable. The issue now arises as to the proper method for treating volatile carbon.

2.2.3 Devolatilization

Upon heating in the absence of air coal will decompose to yield a mixture of gases, liquids, and coke. There is general agreement in the literature that this devolatilization process is intricately involved with rapid hydrogasification. Two problems persist, however; 1) how to account quantitatively for the volatiles contribution to yield and, 2)

TABLE 2-2
 CONSTANTS FROM ZAHRADNIK AND GLENN (1971) MODEL

Temperature (°C)	b_1	b_2	b_3	C_o^*	Fraction of Original Carbon as Methane
950	0.08	0.0054	0.006	0.90	0.98
850	0.07	0.0033	0.0035	0.94	1.01
727	0.08	0.0016	0.00176	0.91	0.99

Nomenclature:

$$b_2 = k_3 C_o^* / k_2$$

$$b_3 = k_3 / k_2$$

$$C_o^* = b_2 / b_3$$

$$\text{Total C as CH}_4 = \frac{b_2}{b_3} + b_1$$

how to explain the volatiles role in the increased reactivity of fresh coal to hydrogen. Focusing, for the moment, on the first problem it is informative to examine the various routes chosen by past investigators. Wen and Huebler (1965) along with Birch (1969) simply refer to the initial rapid rate period as "hydrogenation of volatiles" apparently together the two phenomena of devolatilization and rapid hydrogasification. The yield of volatiles is "ignored" by Moseley and Paterson (1967) with the statement: "the carbon in the volatiles is readily hydrogenated in the presence of some hydrogen." They go on to suggest that their rate model (Equation 2-13) would not be accurate at pressures below 100 atm. Feldmann, as well as Zahradnik and Glenn, assume that devolatilization occurs instantaneously with respect to rapid hydrogasification. Feldmann incorporates a constant of integration in Equation 2-7 to account for this instantaneous volatile fraction, i.e. conversion at $t = 0$. Zahradnik and Glenn add a constant (b_1 in Table 2-2) to their final yield expression (Equation 16) signifying the contribution from "instantaneous" devolatilization. In both cases, however, these approaches are questionable. Feldmann reports values for initial yield (obtained from computer fitting of data) as 0.22 at 725°C and 0.14 at 900°C. The numbers seem inordinately low when compared to the standard proximate volatile content³ of this coal (40.9% MAF). Further, a decreasing volatile yield with increasing temperature is exactly the opposite behavior observed in pyrolysis experiments. The Zahradnik and

³The ASTM standard determination of volatile matter by proximate analysis involves lowering a crucible containing one gram of dried coal into a pre-heated furnace (950°C) for 7 minutes. The measured weight loss is the volatile matter and is expressed as a weight per cent of the original coal. The coal's original weight may be the as-received weight, moisture-free (MF) weight or moisture-ash-free (MAF) weight.

Glenn constants in Table 2-2 are also exceptionally low for a coal containing 39.3% volatile matter (as-rec'd basis), but no significant temperature dependency was observed. Again, these constants were fitted values to a yield expression and were not experimentally observed. Zahradnik and Glenn based their assumption of an extremely fast initial reaction on coal devolatilization work done in the BCURA laboratories in Great Britain (Badzioch, 1967). It is unfortunate, though, that this constitutes one of the very few references in the literature on rapid hydrogasification to the very large independent body of literature on the thermal release of volatile matter from coal. It seems appropriate at this point to pursue in some detail this available resource in attempting to provide a better understanding of the coal-hydrogen reaction.

Most authors in the field concur that the decomposition and volatile evolution of coal is a very complex process which most likely cannot be described exactly. Some success is reported, however, in approximating the rate as a first order decomposition of volatile groupings occurring uniformly throughout the particle. Characteristically, the appearance of volatiles is expressed as:

$$\frac{dV}{dt} = k(V^* - V) \quad (2-23)$$

where V = amount of volatiles evolved at time t (usually a weight per cent of the initial coal),

V^* = amount of volatiles at $t = \infty$, and

k = rate constant.

The unknown parameters, k and V^* , have been the focus of most kinetic studies.

V^* represents the effective volatile content of the coal. Badzioch and Hawksley (1970) emphasize that V^* is to be carefully distinguished from volatile matter, VM_o , as determined by standard proximate analysis. This standard is a convenient, albeit deceptive, point of reference. To be precise, proximate analysis determines the volatile yield of a sample under certain arbitrarily specified conditions (Footnote 3), which may not be amenable to theoretical modeling. To associate this yield with the potential yield of, for example, a single pulverized coal particle is probably incorrect. One argument is that escaping volatiles from particles in the relatively substantial packed bed (with respect to individual particle dimensions) of proximate analysis may undergo degradation. A thin film of carbon is readily observable on the upper surfaces of the crucible and the extent of such cracking within the bed is unknown. BCURA workers have spent considerable effort investigating the relationship (or lack thereof) between actual volatile yield and proximate volatile content of coal and char under a wide range of conditions. Gregory and Littlejohn (1965) accumulated and analyzed a large amount of literature data for retort carbonization of coals and their results indicate yields less than VM_o . Experiments with finely divided particles entrained in a preheated gas stream experiencing high rates of heating show an increase in actual yield over loss of proximate volatile matter and these results have been empirically correlated for 11 different coals with the following relation (Badzioch and Hawksley, 1970):

$$V^* = Q (1 - C) VM_o \quad (2-24)$$

Q is a proportionality factor relating total weight loss to loss of

proximate volatile matter and C is a correction factor which physically corresponds to the fraction of proximate volatile matter in the char residue. Experimental values of Q varied from 1.3 to 1.8 depending on coal type which led to values for the ratio, V^*/VM_0 , greater than one. This finding is not unique as a number of other investigators have found increased yields with rapid heating techniques (Loison and Chauvin, 1964; Jones, et al., 1964; Eddinger, et al., 1966; Rau and Robertson, 1966; and Mentser, et al., 1970).

The rate constant in Equation 2-23 is typically correlated by an Arrhenius-type expression:

$$k = k_0 e^{-E/RT} \quad (2-25)$$

where E = activation energy,

R = gas constant,

T = absolute temperature, and

k_0 = pre-exponential factor.

A collection of such values is illustrated in Figure 2-9. It was from the magnitude of the rate constants reported in the BCURA papers that Zahradnik and Glenn reached the conclusion that devolatilization was virtually instantaneous. As is apparent from Figure 2-9, however, there is little agreement on the observed rates of devolatilization with several orders of magnitude discrepancy. The BCURA values actually represent the upper limit. Some, but by no means all, of the discrepancies are explainable in a qualitative sense. These data have been limited to rate constants for high volatile coals (see Table 2-3). Even within this limitation, however, differences are expected but hopefully not to the extent observed. Other

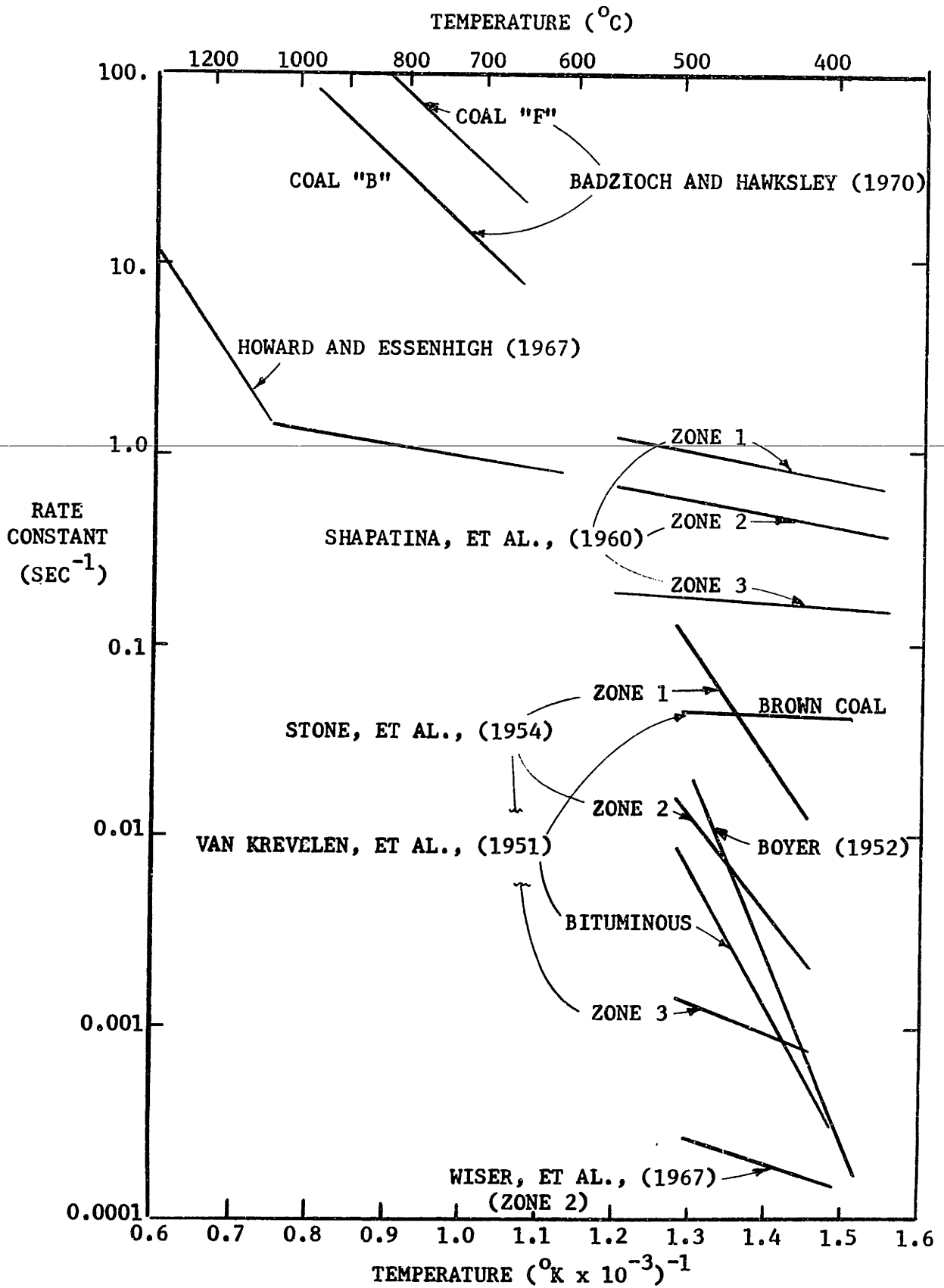


FIGURE 2-9 ARRHENIUS PLOT OF COAL DECOMPOSITION RATE CONSTANTS

TABLE 2-3
COAL TYPES IN FIGURE 2-9

<u>Investigators</u>	<u>Coal</u>	<u>VM_o (MF)</u>	<u>VM_o (MAF)</u>
Badzioch and Hawksley (1970)	"B" NCB 902	35.2	36.4
	"F" NCB 601	34.9	35.3
Boyer (1952)	St. Fontaine Bituminous	----	36.0
Howard and Essenhigh (1967)	Pittsburgh Seam Bituminous	35.91	37.35
Shapatina, <u>et al.</u> , (1960)	Moscow District Brown Coal	34.5	50.2
Stone, <u>et al.</u> , (1954)	Pittsburgh Seam Bituminous	40.7	42.2
Van Krevelen, <u>et al.</u> , (1951)	Brown Coal	----	51.0
	Low Rank Bituminous	----	39.5
Wiser, <u>et al.</u> , (1967)	Utah Bituminous	47.46	----

explanations also exist. Many authors have contended that a simple first order model affords inadequate description of their results. One approach to sophisticating Equation 2-23 has been to describe the devolatilization curve (weight loss as a function of time) as a series of several first order processes. Shapatina, et al., (1960) depict three stages (0-0.06 sec, 0.06-0.1 sec and 0.1-180 sec). Stone, Batchelor, and Johnstone (1954) also model their results in such a fashion with time intervals (typically much longer than the Soviet work) dependent on both coal type and temperature. Finally, assuming that Equation 2-23 or even a series of equations does not describe the process exactly, the very nature of the experiment could then contribute to various deviations.

Of course, the first order decomposition model represents only one approach to correlating data. Several papers have suggested that the rate curve or at least a portion of it might be explained in terms of an n^{th} order rate expression:

$$\frac{dV}{dt} = k^{\circ} (V^* - V)^n \quad (2-26)$$

Wiser, et al., (1967) showed that n values of approximately 2 gave the best fit for the first 60 minutes of weight loss (this period was followed by a first order period and that rate constant is plotted in figure 2-9. Skylar, et al., (1969) reduced any confidence in Equation 2-26 by demonstrating that values of n ranging from 2 to 8 were necessary to provide reasonable fit for nonisothermal devolatilization of different coals. Pitt (1962) correlated his weight loss curves very well with the empirical relation:

$$(V^* - V)/V^* = A - B \log(t) \quad (2-27)$$

where A and B are constants. Pitt further alleged that Equation 2-27 coincided with calculated results for a number of independent first order decompositions having a statistical distribution of activation energies (this modeling approach was undoubtedly the forerunner of Equation 2-21).

Juntgen and Van Heek (1968) have proposed that modeling attempts should focus on the individual volatile species and subsequently correlated their results with a nonisothermal variation of Equation 2-23. By replacing k with Equation 2-25 and substituting a constant heating rate, i.e. $dT/dt = m$, they obtained the following rate for volatile evolution:

$$\frac{dV_i}{dT} = \frac{k_0}{m} e^{-E/RT} (V_i^* - V_i) \quad (2-28)$$

The parameters, k_0 and E, are determined for each evolved species (i^{th} component), therefore, direct comparison of this information with total weight loss data of the previously discussed work is difficult. The higher hydrocarbons, e.g. ethane, were successfully described by a simple first order reaction but species like methane and hydrogen clearly involved more complex formation reactions and were postulated to consist of several overlapping reactions. The mathematical modeling of these complex reactions was done in a manner quite similar to Pitt's statistically distributed activation energies (Hanbaba, et al., 1968; and Juntgen and Van Heek, 1969 and 1970).

The foregoing discussion has proceeded on the assumption that the rate-controlling mechanism was a decomposition reaction. Not all of the published results are in agreement with this assumption. Berkowitz (1960) investigated the pyrolysis of Alberta sub-bituminous

coals in the range of 250-524°C. In his opinion, rate was limited by diffusion. Studies at higher temperatures modified the conclusion to postulate movement of carbon lamellae as rate-determining (Berkowitz and Den Hertog, 1962). The conclusions were strongly influenced by the low activation energies obtained from the use of Equation 2-23.

Zielinski (1967) collated data from several different authors and promptly discounted any attempts to model devolatilization as a first order decomposition. He concluded from an analysis of the literature data that heating rate was the controlling factor.

Lacking an accepted theory for the rate of devolatilization, any discussion of its role in determining the reactivity of coal to hydrogen must necessarily be qualitative. One argument theorizes that volatile constituents actually comprise the reactive fraction; thus, devolatilization itself deactivates the coal. This line of reasoning was supported primarily in the older papers (Birch, et al., 1960; Von Fredersdorff and Elliott, 1963; and Wen, et al., 1967). This is viewed as inadequate because of reported rapid-rate hydrogenation yields in excess of proximate volatile matter. However, devolatilization results with rapid heating suggest that such "excess" yields are possible. Unfortunately, few results are available to compare devolatilization with hydrogasification under similar conditions. Johnson's data in Figure 2-6 imply that something more than simple devolatilization is occurring. The second argument assumes devolatilization initiates a series of reactions culminating in residual char or coke. Certain intermediate species are extremely reactive toward hydrogen. This concept is obviously supported in models by Moseley and Paterson and Zahradnik and Glenn but it seems that both models are based on the assumption that a true

gas-solid reaction is occurring. In contrast, Graff and Squires (1972) argue that rapid heating will "vaporize" up to 75% of the coal's initial mass. The light species thus formed are so reactive, however, that unless hydrogenated and cooled quickly, they will polymerize to tar, then crack forming coke and gas.

2.2.4 Effect of Particle Size

Very little experimental evidence has been accumulated on this particular subject. Moseley and Paterson (1967), based on qualitative experiments, report a "definite tendency for conversion to rise with smaller particles". Moseley and Paterson found their experimental technique unsuited for extensive studies of particle size. Several other models have introduced a particle size effect but without any experimental verification. Johnson shows rate proportional to $(1-X)^{2/3}$ implying a shrinking core behavior. Zahradnik and Glenn originally derived their model by assuming the methanation step (Equation 2-9) to be described as;

$$\frac{dX}{dt} = k_3 P_{H_2} C^*{}^{2/3} \quad (2-29)$$

also a shrinking core postulation. However, the final expression for yield in both cases was independent of the two-thirds formulation reducing the argument to a mere point of academics.

Studies of coal devolatilization and the effect of particle size are also limited but do provide some clues as to the significance of this parameter.

Chemical reaction control in a porous particle stipulates the rate of volatile evolution independent of particle dimensions. Badzioch and Hawksley tried coal particles of 20 μ and 60 μ diameters and observed no effect on rate. Similarly, Howard (1967) reported the absence of any influence for particle diameters from 0 to 200 μ . Also, weight loss curves prepared by Wisler, Hill and Kertamus (1967) were unaltered for samples of 60-74 μ versus 246-417 μ . It is, however, not unreasonable to assume that further increases in particle size would ultimately modify these conclusions. There is widespread acknowledgement that heat and/or mass transfer limitations at some critical particle size at transition and the nature of the rate-limiting mechanism, though, are unestablished. Several possible effects are hypothesized:

External Heat Transfer --- Increasing size will alter the particle's heating rate. For pure conductive transport to a sphere of uniform temperature, the heat transfer coefficient is inversely proportional to the diameter. The controlling mechanism for volatile release is still a volumetric chemical reaction, however, the reaction temperature history will vary with particle size. Badzioch (1967) has performed calculations of this type which suggest the effect will become appreciable for spheres of approximately 100 μ in diameter. It should be emphasized that conclusions, derived from calculation, regarding the actual point of transition depend exclusively on the chosen values of reaction rate.

Internal Heat Transfer -- Alternative systems with significantly higher external heat transfer coefficients (fluid beds, turbulent flow, radiation from flames) will produce temperature gradients internal to

the particle. Peters (1960) provided the following empirical equation to explain the apparent zero order reaction observed for particles 250-2000 μ :

$$\frac{dV}{dt} = 0.03(T_A - 330)d^{-0.26} \quad (2-30)$$

with T_A = ambient temperature, $^{\circ}\text{C}$,

d = particle diameter, mm.

The results are interpreted as representing the propagation of an evaporation front ($T \sim 330^{\circ}\text{C}$) through the particle. The driving force for volatile release is the overall temperature gradient. Koch, Juntgen, and Peters (1969) discussed extension of these findings for prediction of the transition region between a first order volume reaction (independent of particle size -- Equation 2-28) and a heat transfer controlled region (zero order reaction, function of particle size). A calculated critical particle size was given as a function of heating rate:

Linear Heating Rate	Calculated Critical Particle Size
100 $^{\circ}\text{C}/\text{sec}$	2000 μ
1000 "	500 μ
10,000 "	200 μ

These numerical values were estimated from the original curve for purposes of illustration.

Mass Transfer -- Approaching the problem from a different point of view, Essenhigh (1963) postulated the mechanism of devolatilization for larger particles (295-4760 μ) as diffusion through the porous char. Modeling a single particle as containing a shrinking spherical liquid core he obtained the relation for devolatilization time:

$$t_V = k'' V d^2 / P_0 = K_V d^2 \quad (2-31)$$

with P_0 = permeability of porous char, and

k'' , K_V = constants.

Experimental data confirmed this "square-law" hypothesis and a mean value for K_V of 0.9 sec/mm^2 was determined in studies of 10 different British coals. These findings are contrary to Peter's data where devolatilization time is reportedly related to particle diameter to the 0.26 power. Direct comparison of rates is difficult because Essenhigh did not specify the temperature functionality of K_V which Peters found to be linear.

Empirical verification of the "square-law" relationship does not directly distinguish between heat and mass transfer control. Transient molecular transport are usually solved in terms of the dimensionless Fourier group, $\alpha t/r^2$ (α = mass or thermal diffusivity and r = radius). For any particular solution one may expect the time to be proportional to the radius or diameter squared. The 0.26 power relationship observed by Peters is not well-founded in simple theoretical solutions but then simple solutions are not necessarily expected.

2.2.5 Conclusions from Literature Survey

Hydrogasification -- The evidence appears to establish that rapid heating of fresh pulverized coal in the presence of hydrogen will result in rapid and substantial conversion to methane. It is also well-known that this initial high reactivity is short-lived under reaction conditions. The data, however, are much too incomplete to permit selection from the available models. There are no data to show conversion of fresh coals with residence time at very short residence times. The effects of heating rate and particle size cannot be predicted with any

quantitative assurance. In fact, the only variables explored in reasonable depth are hydrogen pressure and temperature and there still remains disagreement over their respective influences.

The role of devolatilization with respect to hydrogasification constitutes the gravest omission in the studies to date. Volatile evolution from fresh coal is a significant source of total yield and most investigators theorize it also determines the reactivity of the remaining carbon to hydrogen. Quantitatively, the first effect is allowed for in terms of an integration constant and the second effect materializes as an elusive "active species or site." Very little may be said of the independence of the rates of hydrogasification and devolatilization.

Devolatilization -- Devolatilization is a complex process and characterizing the rate as a first order decomposition is undoubtedly an oversimplification. Assessment of its value as an approximation, however, has been impeded by considerable disagreement among the accumulated data. The limits of its applicability are still unknown. Part of the explanation may be found in the diversity and non-homogeneity of coal types studied. The apparent rapidity of the reaction also complicates experimental studies resulting in data obtained under conditions that are not readily amenable to even a simple model.

The best evidence indicates that devolatilization of pulverized coal ($< 200\mu$) is essentially complete at reasonably high temperatures in fractions of a second. The effect of temperature is discerned as an exponential activation energy. Yields appear altered to some extent by both the final temperature level and the time-temperature history reinforcing the concept of a complex array of reactions participating

in the actual decomposition. The onset of physical transport limitations arises somewhere in the particle size range of 200-2000 μ . Numerical values of various descriptive parameters, though, remain applicable only to given sets of conditions and the particular peculiarities of the apparatus.

These reviews have, for the most part, bypasses discussion of the chemical reactions occurring within the coal's molecular structure. While fully recognizing the value of such an approach to ultimate understanding, this particular effort focused on eliciting from the available body of literature values of pertinent rate parameters for models suitable for engineering design. The resultant difficulty accentuates the formidable task of proposing and establishing models of greater complexity.

2.3 OBJECTIVES

The principle objectives of this study were:

- 1 - To determine quantitatively the rate and extent of the rapid coal-hydrogen reaction under conditions of commercial interest.
- 2 - To elucidate the role of the devolatilization process in the reaction.

Specifically, the work was designed to establish the dependence of conversion (weight loss) on important process variables, including residence time, temperature, time-temperature history (heating rate), hydrogen pressure, particle size, and to a limited extent coal type.

Secondly, the interrelationship of the devolatilization mechanism and the subsequent hydrogen attack was to be explored in order to characterize this behavior.

Hopefully, the study would yield answers to the following process consideration questions:

-- How and to what extent does close-coupling devolatilization and hydrogasification accelerate the latter reaction? In Office of Coal Research computer studies, Wen (1972) has assumed a rate increase factor of 100 for fresh over pretreated coals.

-- Can higher heating rates increase yields? Several studies conducted at high heating rates suggested that pyrolysis yields as much as 80% in excess of standard practice were possible. On the other hand, some investigators report no influence of heating rate on hydrogasification yields (Pyrclach, et al., 1972) and it has also been suggested that higher heating rates may actually retard hydrogasification (Von Fredersdorff and Elliott, 1963).

-- How significant are heat and mass transfer effects?

These questions are of obvious interest in process development. Despite numerous studies the phenomena are not well understood and controversy prevails. For example, pulverized coal is suggested for process use on the grounds that small particles: 1) expose greater surface area (per unit mass) to hydrogen attack during initial devolatilization, 2) heat more rapidly thus possibly augmenting yield, and 3) tend to minimize any physical transport limitations (high effectiveness factors). The "supposed" advantages would be gained at

the expense of increased costs of comminution and handling. The justification for pursuing the issue seems well-established.

The strategy of investigation was roughly divided into five major steps.

1. Review literature on devolatilization and hydrogasification reactions to assess limits on the available body of knowledge and to appraise potential experimental techniques.
2. Select experimental system and conduct preliminary experiments to verify feasibility.
3. Study devolatilization under vacuum or atmospheric pressure.
4. Study hydrogasification (and devolatilization) under high hydrogen pressures.
5. Concurrent with steps 3 and 4, test the validity of proposed models.

3. APPARATUS AND PROCEDURE

3.1 SELECTION OF APPARATUS

To provide data that will be useful in the design of actual gasification systems, it is important that the range of conditions studied experimentally be comparable to those expected in full-scale operation. From a review of proposed designs (Hottel and Howard, 1971), it is anticipated that under commercial conditions the initial rapid reactions will take place at temperatures of 500-1000°C, heating rates up to 10⁴ °C/sec, and hydrogen pressures as high as 1500 psig. (On the latter point Wen, et al., (1972) conclude that a total operating pressure of 1000 psig (69 atm) is most likely optimum since the system can be tied directly to pipeline distribution systems).

Experimentally, such an environment is difficult to simulate in small scale. Captive sample techniques, where a fixed quantity of coal is heated in the presence of hydrogen, have been employed by several investigators (Feldkirchner and Linden, 1963; Hiteshue, et al., 1962a; Moseley and Paterson, 1965a; and Feldkirchner and Johnson, 1968). While this approach is experimentally simple, it does restrict achievable heating rates to perhaps 100°C/sec at the most. Schemes in which the coal is fed continuously to a flow reactor more closely approximate full-scale conditions but the complexity and cost of the apparatus are greatly increased. The methods used include fluidized beds (Birch, et al., 1960), entrained flow reactors (Moseley and Paterson, 1965b; and Glenn, et al., 1967), and free-fall reactors (Moseley and Paterson, 1967; and Lewis, et al., 1967). To retain the simplicity and precision of the captive

sample technique and still simulate severe conditions, a more flexible means of heating the coal was required.

The chosen technique involves electrical heating of a thin strip of stainless steel screen upon which rested a small amount of coal. Cech (1950) has reviewed most of the early work with a "hot microscope stage" or electrical strip furnace and Finch and Taylor (1969) showed that a relatively simple DC timing circuit with batteries was capable of attaining heating rates of 10^3 to 10^4 °C/sec. Variations of this approach have been used for studies of coal pyrolysis in vacuum and under nitrogen (Loison and Chauvin, 1964; Rau and Robertson, 1966; Juntgen and Van Heek, 1968; and Mentser, et al., 1970). The technique was never used under high pressure conditions. Furthermore, all of these devices operated with a single heating circuit permitting only a rapid heat-up or a fairly slow heat-up with extended time at the final temperature whereas the device used here and described below utilizes a dual heating circuit allowing both rapid heat-up as well as extended time at a given temperature.

3.2 APPARATUS DESCRIPTION

As shown in Figure 3-1, the electrically heated stage is enclosed in a high pressure vessel. The vessel can be evacuated or charged with hydrogen or inert gas such as helium. The vessel itself is fabricated entirely from 316SS and designed for a 3000 psig working pressure. All cutting and welding was done by the Middlesex Welding Co., Cambridge, Mass. Since the vessel was not heated during the experiment, the

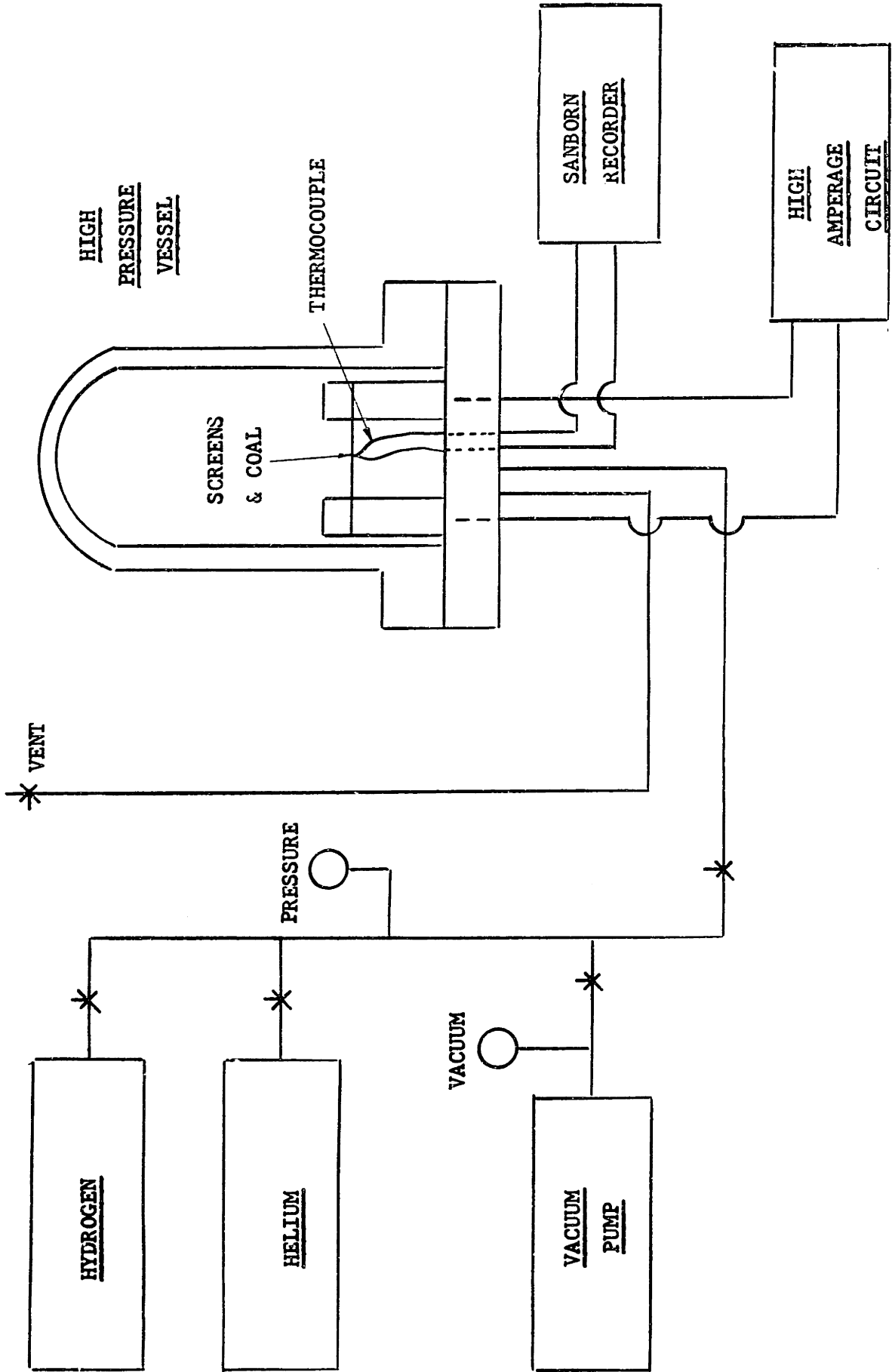


FIGURE 3-1 OVERALL APPARATUS SCHEMATIC

allowable stress of the material was substantially increased permitting less costly construction. For example, standard 1500 lb flanges have an allowable operating pressure of 3600 psig at room temperature. Tubing is all 1/4" SS (std. wall) with SS Swagelok fittings. The chamber is vented to the outside by means of a remotely activated solenoid valve (Skinner V52HD23002). For safety a 1/2" Fike rupture disc with vacuum support was installed in the vent line (2900 psig burst at 72°F ± 5% tolerance). Additional safety precautions included draping the reactor during the run with a bomb blanket (Davis Aircraft Products, Long Island, New York) as well as shielding the entire setup with 1 1/8" free-swinging wood panel.

Details of the stage are illustrated in Figure 3-2. Conax high pressure connectors were used to pass the electrical leads for the heating element (EG-125-A-CU-N) and the thermocouple (TG-24-4A-N) into the chamber. The terminals were cut and machined from a single length of solid brass rod (1 3/8" x 5"). A 325 mesh SS screen (4.5 x 5.0 cm) is formed into a "sandwich" heating element and connected across the terminals. Stainless steel screen was chosen for the sample support for several reasons: 1) screens have less mass than a solid strip, 2) screens permit easy escape of volatiles even with a "sandwich" arrangement, and 3) stainless has a high electrical resistance (minimizing current requirements) and a high tolerance against temperature and corrosion. Since the screen weight changed slightly under reaction conditions, all of the screens are pre-fired in the actual gas environment to prevent further weight change. An insulated baffle is positioned directly under the screen to minimize convection currents and stabilize the screen temperature especially at high pressures.

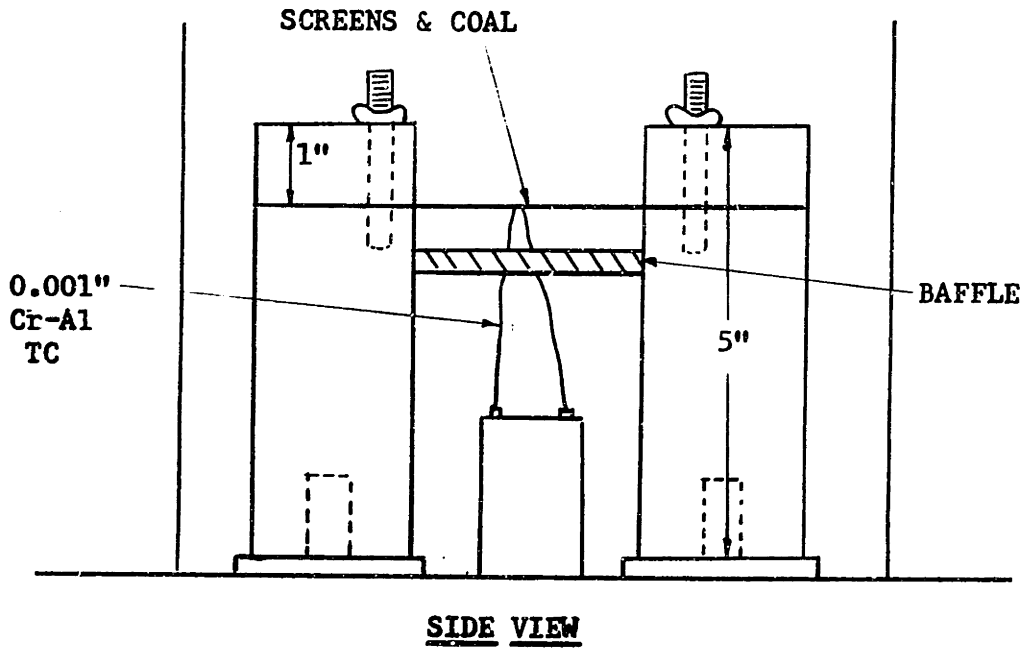
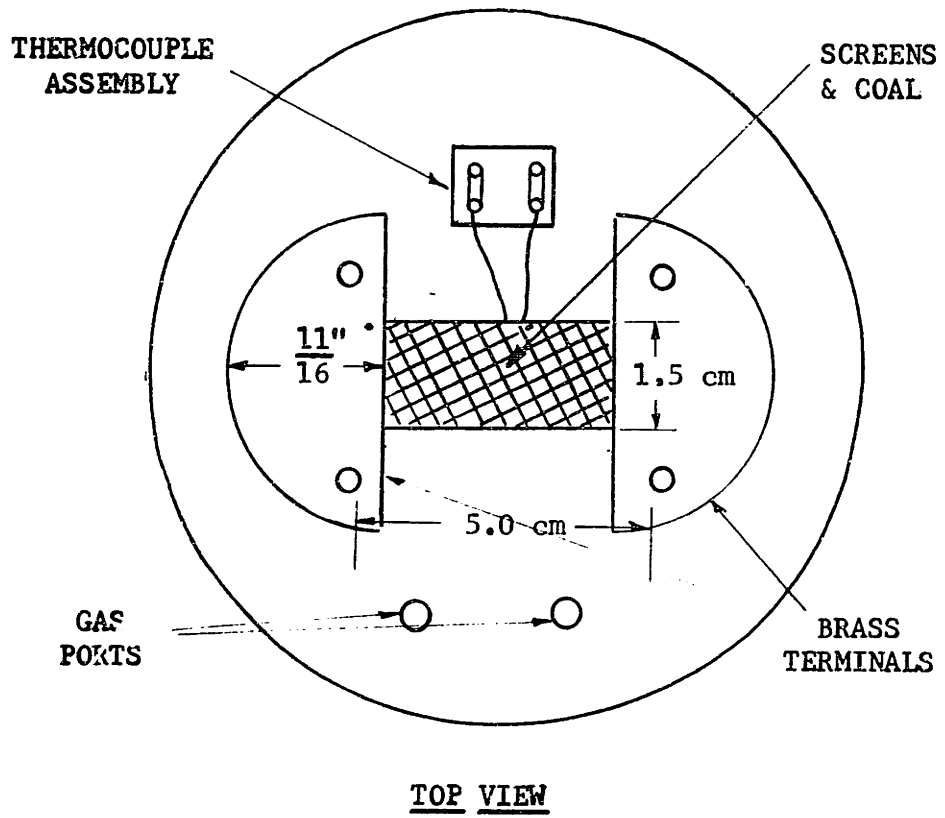


FIGURE 3-2 STAGE DETAILS

The first branch of the dual heating circuit controls the heating rate ($65\text{--}12,000^{\circ}\text{C}/\text{sec}$) and the second maintains the final temperature ($400\text{--}1100^{\circ}\text{C}$). The major components of the circuit are sketched in Figure 3-3. The power supply consists of two 12 volt lead-acid batteries connected in series to the circuits via a power relay (Potter and Brumfield PRL1AY). The current in each branch is controlled by 1000 watt (3 ohm) variable resistors. At the beginning of a run, the preset timer (Singer TDAF-1S) is activated, closing the relay on the heat-up circuit. At the end of the heat-up period the timer switches the relay to the lower current circuit which maintains the final temperature until run termination.

A 0.025 mm chromel-alumel thermocouple is placed between the screens to determine the time-temperature history of each run which is recorded on a Sarnborn 380 recorder. Typical time-temperature histories are reproduced in Figures 3-4 and 3-5. At low pressures (Figure 3-4) maintenance of a steady final temperature of 1000°C is shown for nominal heating rates of $650^{\circ}\text{C}/\text{sec}$ and $10,000^{\circ}\text{C}/\text{sec}$. At high pressures (Figure 3-5) approximately 150% more power is required to maintain the same temperature and a noticeably less stable temperature trace results with fluctuations of $\pm 20^{\circ}\text{C}$. The explanation lies in the fact that at low pressures radiation accounts for nearly all of the heat transfer (over 90%) but at higher pressures natural convection also becomes a significant transport mechanism thus demanding greater energy input for the same steady-state temperature and giving rise to less stable temperature profiles.

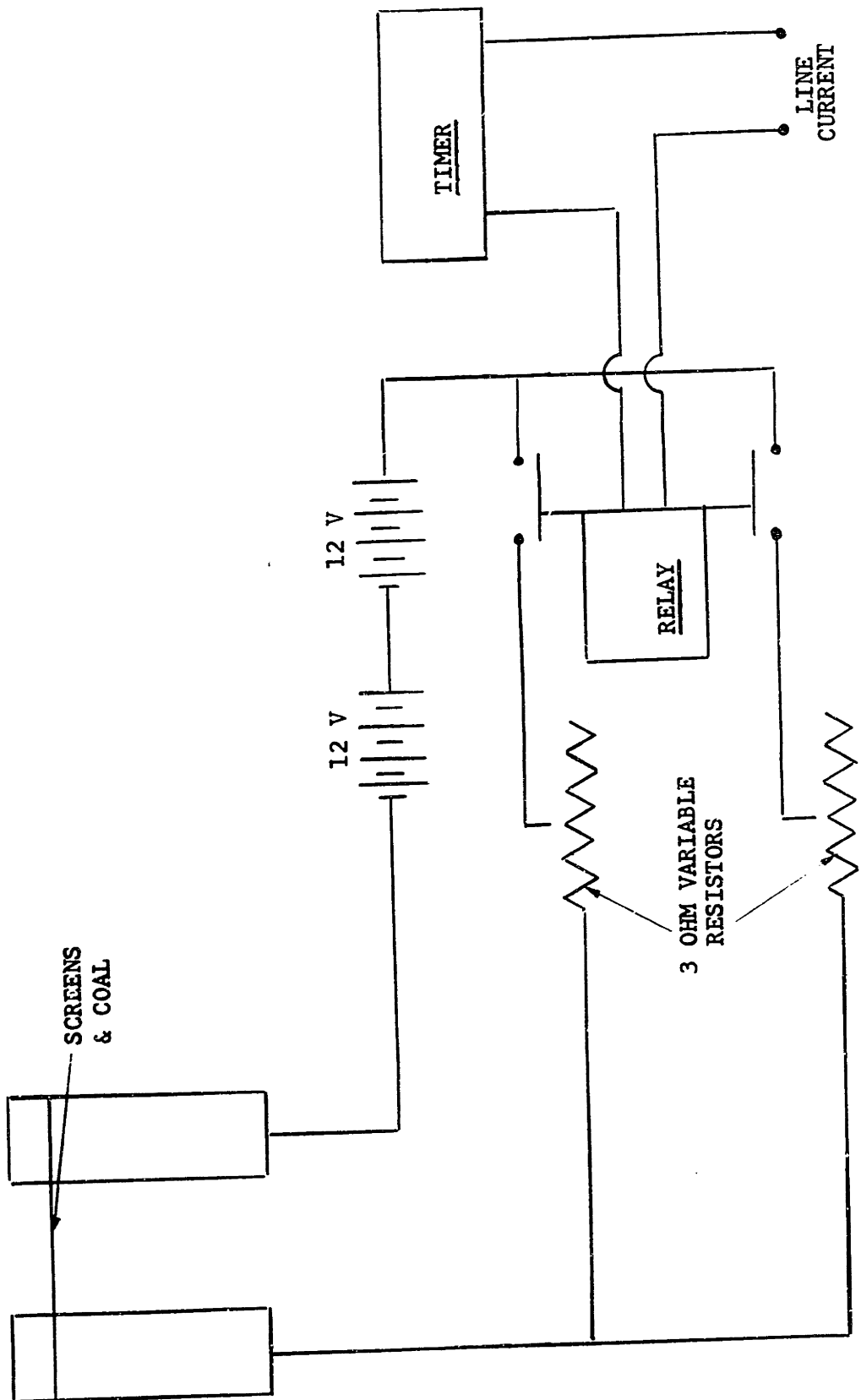


FIGURE 3-3 DUAL HEATING CIRCUIT

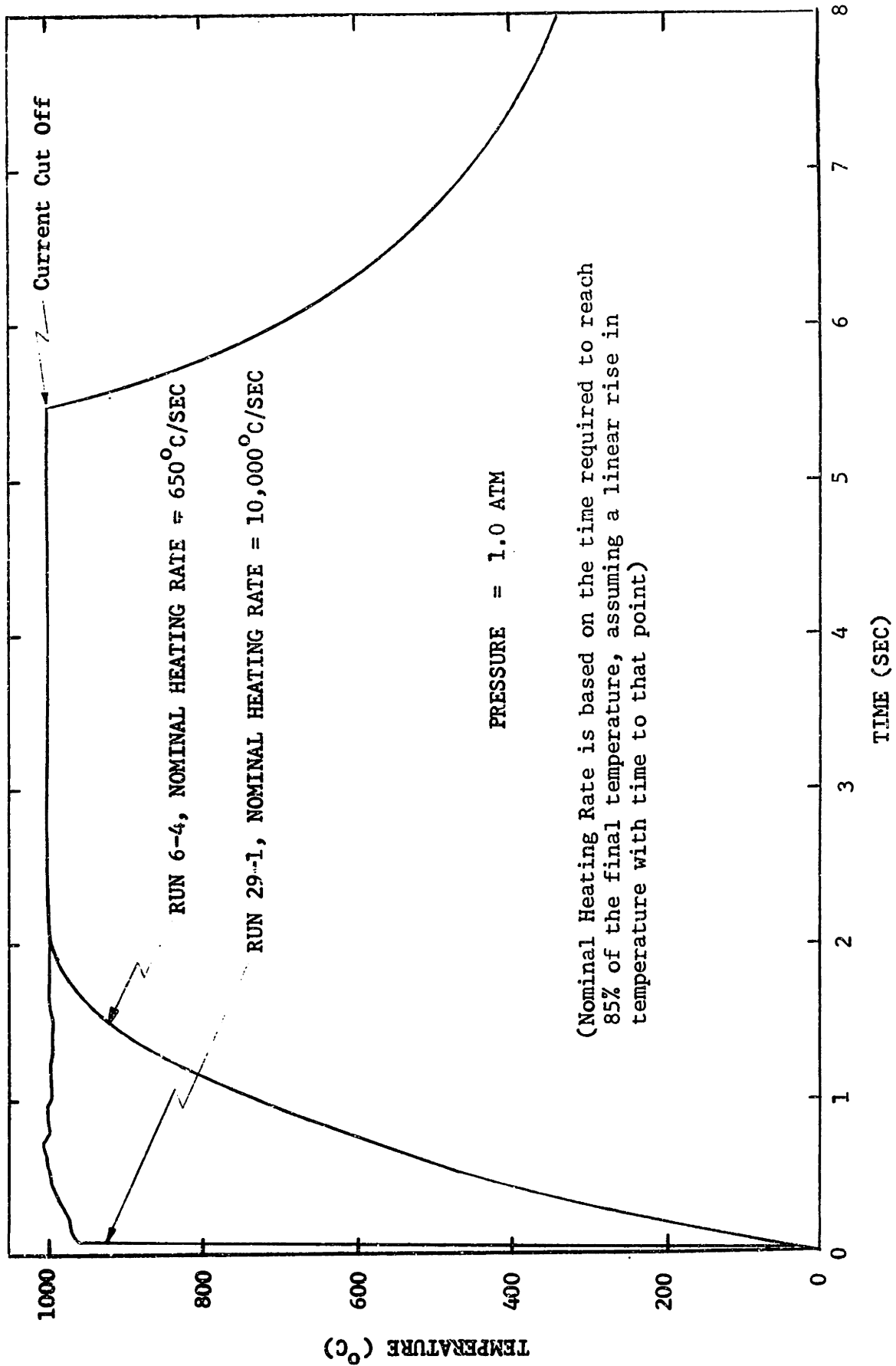


FIGURE 3-4 TIME-TEMPERATURE HISTORIES AT ONE ATMOSPHERE PRESSURE

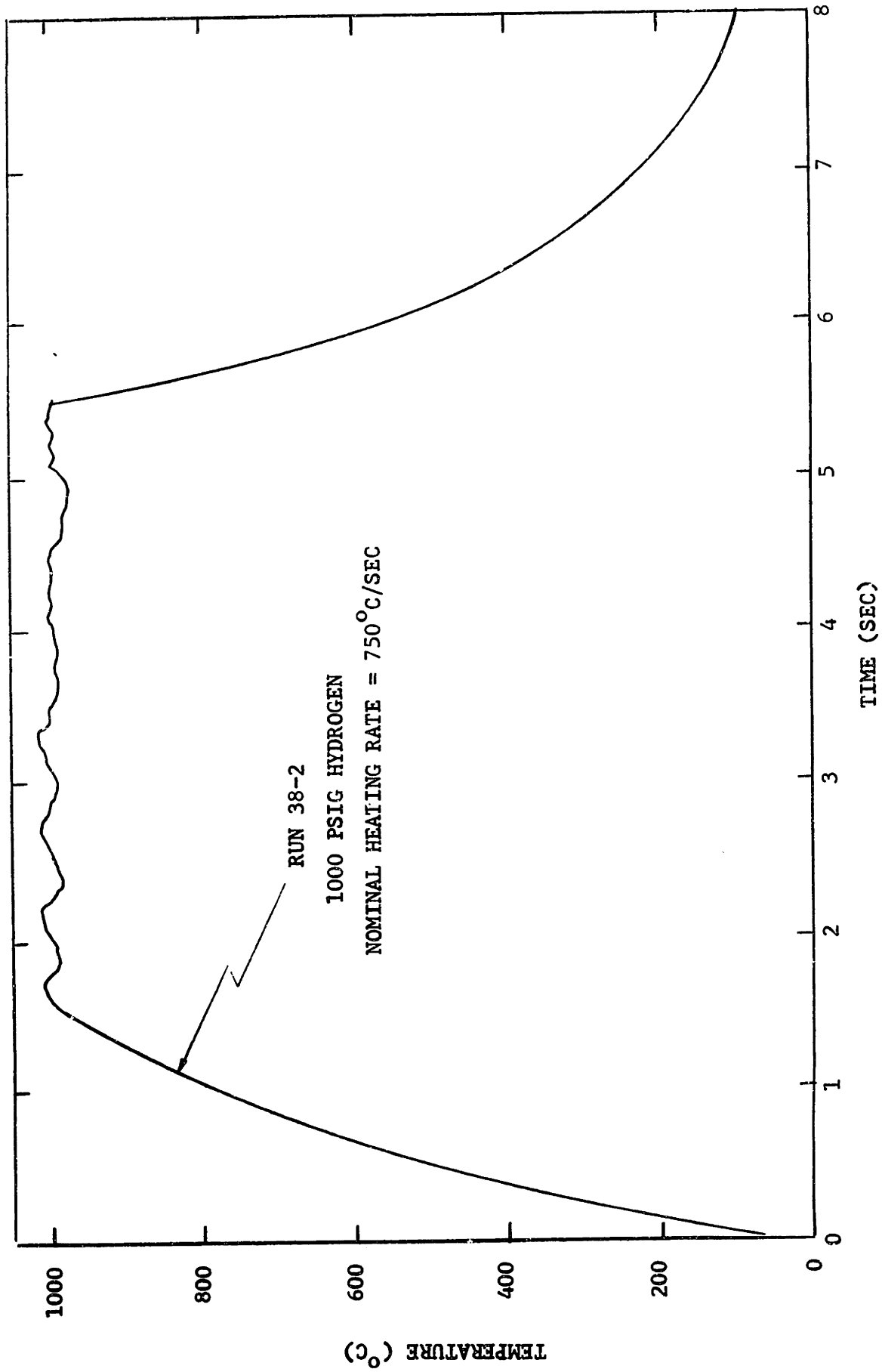


FIGURE 3-5 TIME-TEMPERATURE HISTORY AT HIGH PRESSURE

3.3 PROCEDURE

Approximately 5-10 mg of ground coal are carefully spread in the center of a pre-weighed screen (roughly 1/2 g) which is then folded twice forming a 1.5 x 5.0 cm strip. The screen plus coal is weighed on a Mettler H20 semi-micro analytical balance, and placed across the terminals. The coal and char samples are transferred from the apparatus to the balance in a culture dish filled with dessicant to avoid moisture pick-up. The thermocouple is then positioned between the folds of the screen. The vessel is evacuated and flushed several times with the test gas to eliminate trace oxygen contamination. After the run the screen plus char is weighed to determine weight loss (conversion). The balance is accurate to ± 0.01 mg giving an experimental precision of 0.1-0.2% of the coal weight.

The advantages of this device are several: 1) relatively inexpensive design for high pressure studies; 2) direct determination of solid conversion; 3) constant and precisely controlled atmospheres since the total mass of gas present is extremely large compared to the mass released by reaction (about 1000 times greater at 1000 psig H_2); 4) direct measurement of sample temperature (the collapse of thermal gradients between the screens is extremely fast thus making the temperature of the screens, coal, and thermocouple bead essentially identical at all times); 5) variation of heating rate independent of final temperature. However, it would be remiss to disregard the shortcomings: 1) sample weight is not monitored continuously and a number of runs are necessary for rate determination; 2) quantitative product analyses cannot be obtained from the small product concentrations; and 3) residence times are limited to a maximum of 20 secs.

3.4 COAL TYPE

Two different types of coal were used in the course of this investigation. Both were obtained through the courtesy of the Institute of Gas Technology, Chicago, Illinois. One is a high volatile Pittsburgh Seam (No. 8) bituminous coal, typical of eastern U.S. coals, from the Ireland Mine (Consolidation Coal Co.); the other is a dried lignite from the Savage Mine (Knife River Coal Mining Co.) in Montana. Table 3-1 contains proximate analyses for both samples.

TABLE 3-1
 PROXIMATE ANALYSES FOR COALS USED IN EXPERIMENTAL WORK

Pittsburgh Seam Bituminous

	<u>As-Received</u>	<u>MF</u>	<u>MAF</u>
Moisture	1.65	--	--
Volatile Matter	39.81	40.48	46.21
Fixed Carbon	46.34	47.12	53.79
Ash	12.20	12.40	--

Montana Lignite

	<u>As-Received</u>	<u>MF</u>	<u>MAF</u>
Moisture	7.26	--	--
Volatile Matter	37.40	40.33	46.15
Fixed Carbon	43.63	47.04	53.85
Ash	11.71	12.63	--

4. RESULTS

The purpose of this section is to present the experimental results of the investigation. The significance and implications of these findings will be dealt with in the subsequent chapter devoted to discussion and modeling.

4.1 DEVOLATILIZATION

Figure 4-1 shows weight loss with time for Montana lignite at two different final temperatures, 700°C and 1000°C, in 1.0 atm helium. In both cases much of the weight loss occurs during the heat-up period with weight loss ceasing after several seconds at final temperature⁴. It is significant, however, that the total amount of weight loss increases with higher final temperature. This dependency is amplified in Figure 4-2 where these final weight losses or yields (yield defined as weight loss observed for long residence times at final temperatures, usually greater than 5 seconds) are correlated with temperature showing increasing yield with increasing temperature until approximately 900-950°C. It should be noted that these yields are all smaller than the weight loss (44.66%) given by the A.S.T.M. Proximate Analysis Procedure (sample held at 950°C

⁴Residence time is defined as the time in which current is flowing through the screens.

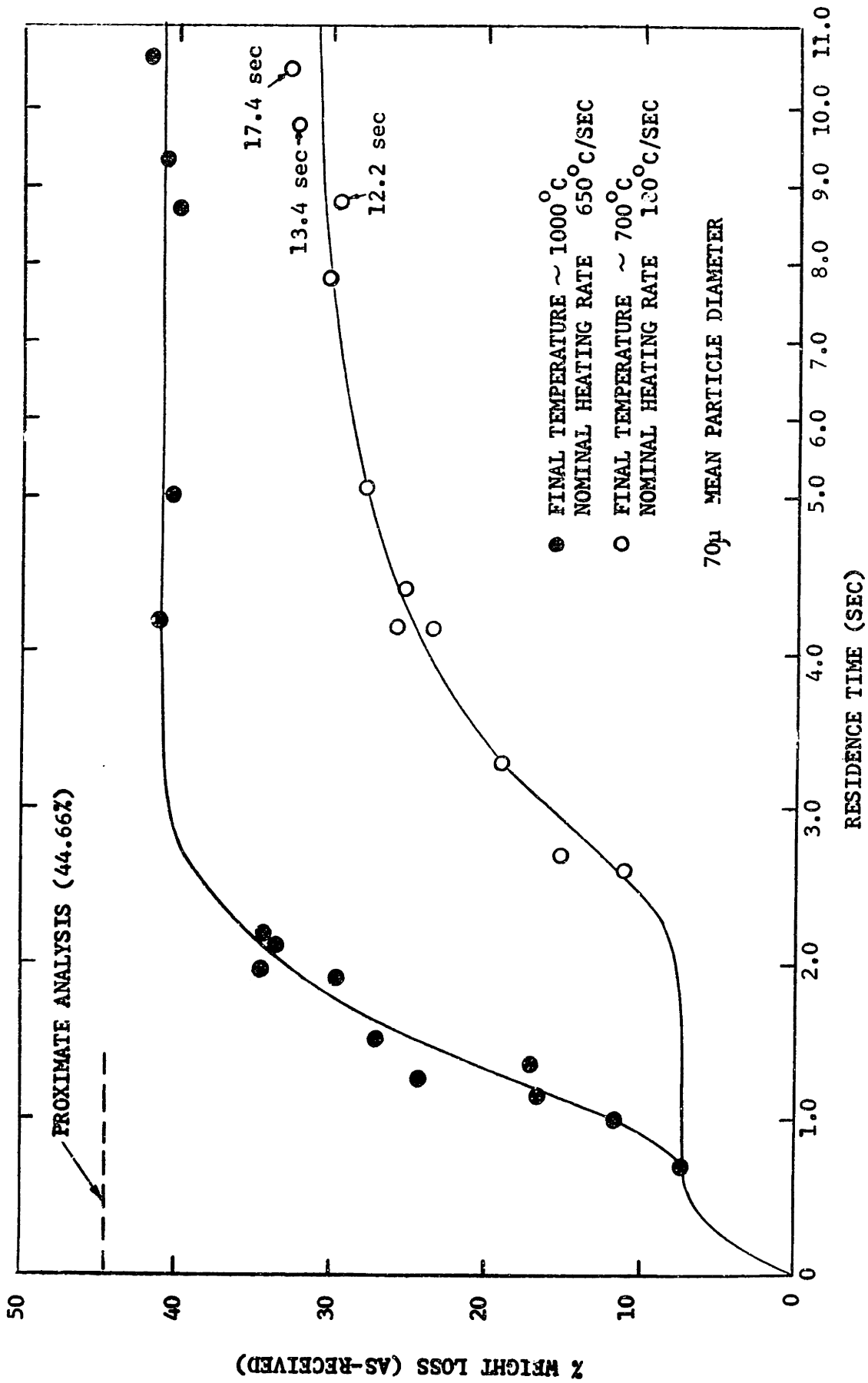


FIGURE 4-1 WEIGHT LOSS WITH TIME FOR LIGNITE IN 1.0 ATM. HELIUM

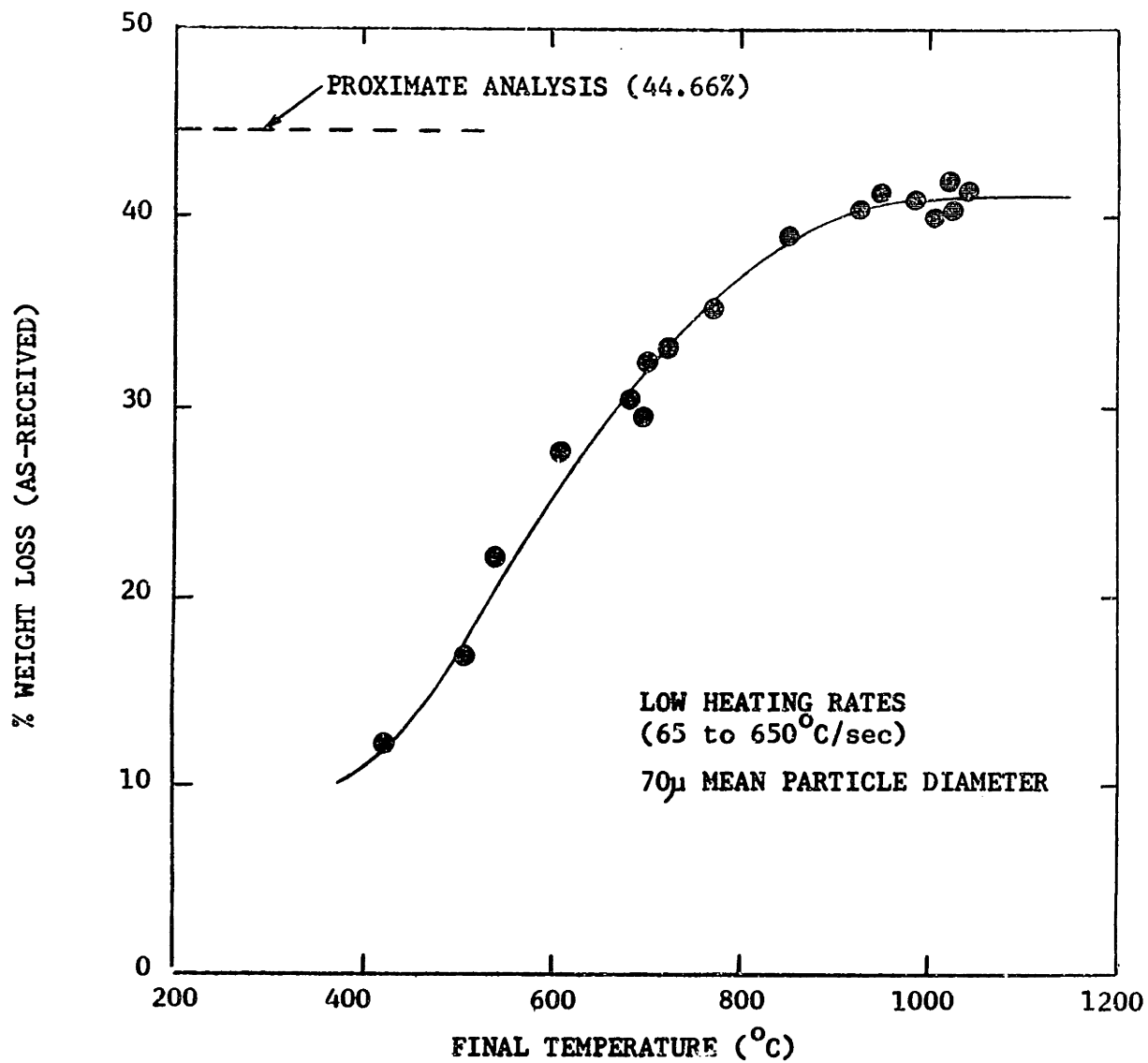


FIGURE 4-2 YIELD VERSUS FINAL TEMPERATURE FOR LIGNITE
IN 1.0 ATM HELIUM

for 7 minutes). Very rapid heating of the sample (to $10,000^{\circ}$ C/sec) gives results shown in Figure 4-3. Again, nearly all of the weight loss occurs during heating and the final yield appears independent of heating rate for heating rates between $650-10,000^{\circ}$ C/sec. Similar data are plotted in Figure 4-4 for runs at 1000 psig (69 atm) helium pressure. The results are virtually identical with runs made under atmospheric conditions.

Data on weight loss with time for Pittsburgh bituminous coal are illustrated in Figure 4-5; the general trends are quite similar to the behavior of lignite. Under rapid heating (Figure 4-6) the results are again similar to lignite except that the final yield is approximately 2 percentage points higher than for the low heating rate (50% weight loss versus 48%). Increasing the total pressure to 1000 psig helium decreases the final yield to around 38% as shown in Figure 4-7. Experiments with very rapid heating at 1000 psig show no dependency of yield on heating rate. As with lignite, bituminous coal yields depend on final temperature. This dependence is shown in Figure 4-8. Yield from standard proximate analysis is seen to fall somewhere between the low and high pressure results. The influence of pressure is further examined in Figure 4-9 where data have been accumulated over a wide range of total pressure (0.5mm Hg to 1500/psig). The weight loss of lignite is essentially independent of total pressure whereas bituminous coal yields increase significantly with decreasing pressure in the range of 0.01 to 100 atm.

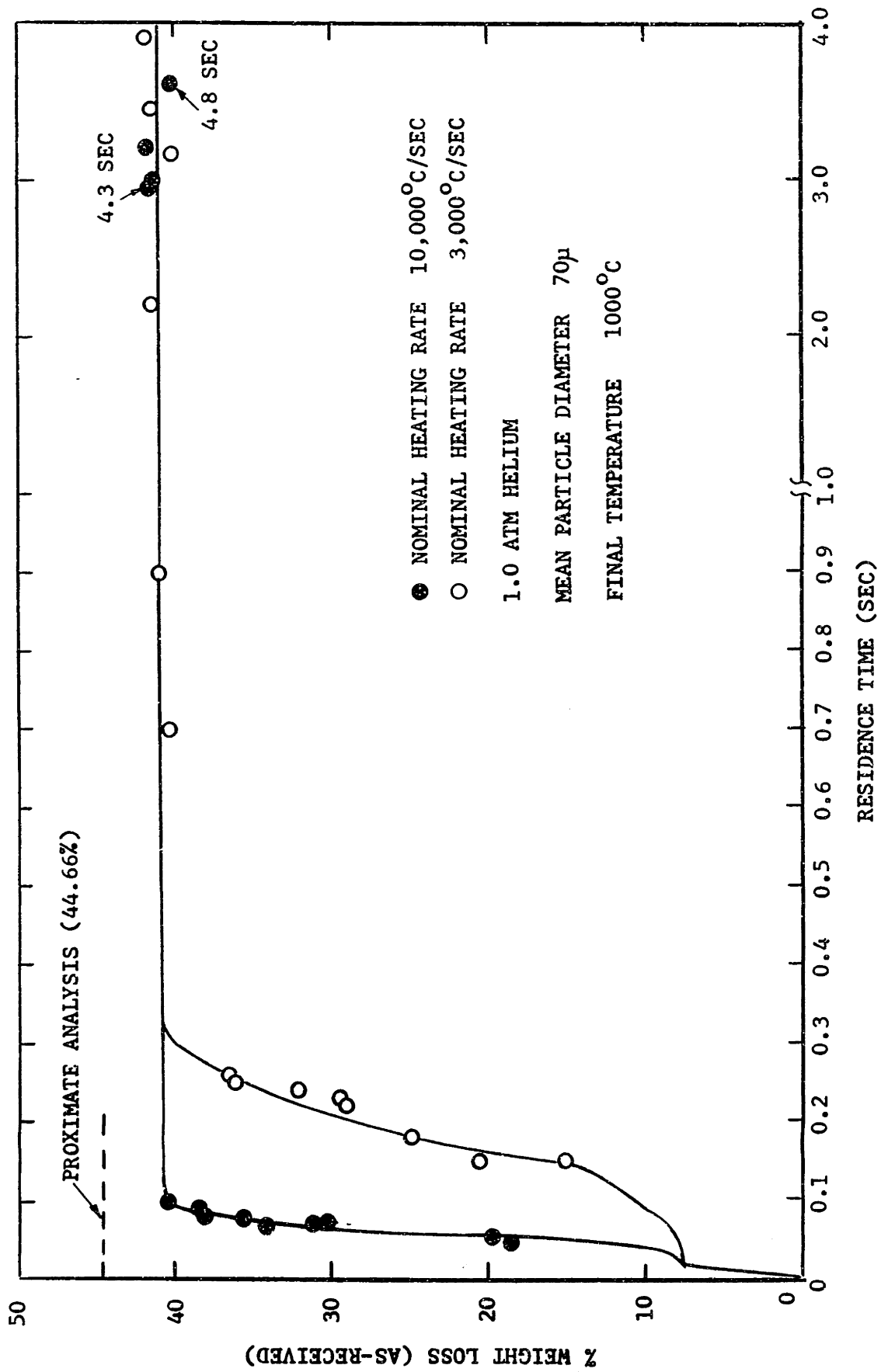


FIGURE 4-3 WEIGHT LOSS WITH TIME FOR LIGNITE UNDER EXTREMELY RAPID HEATING CONDITIONS

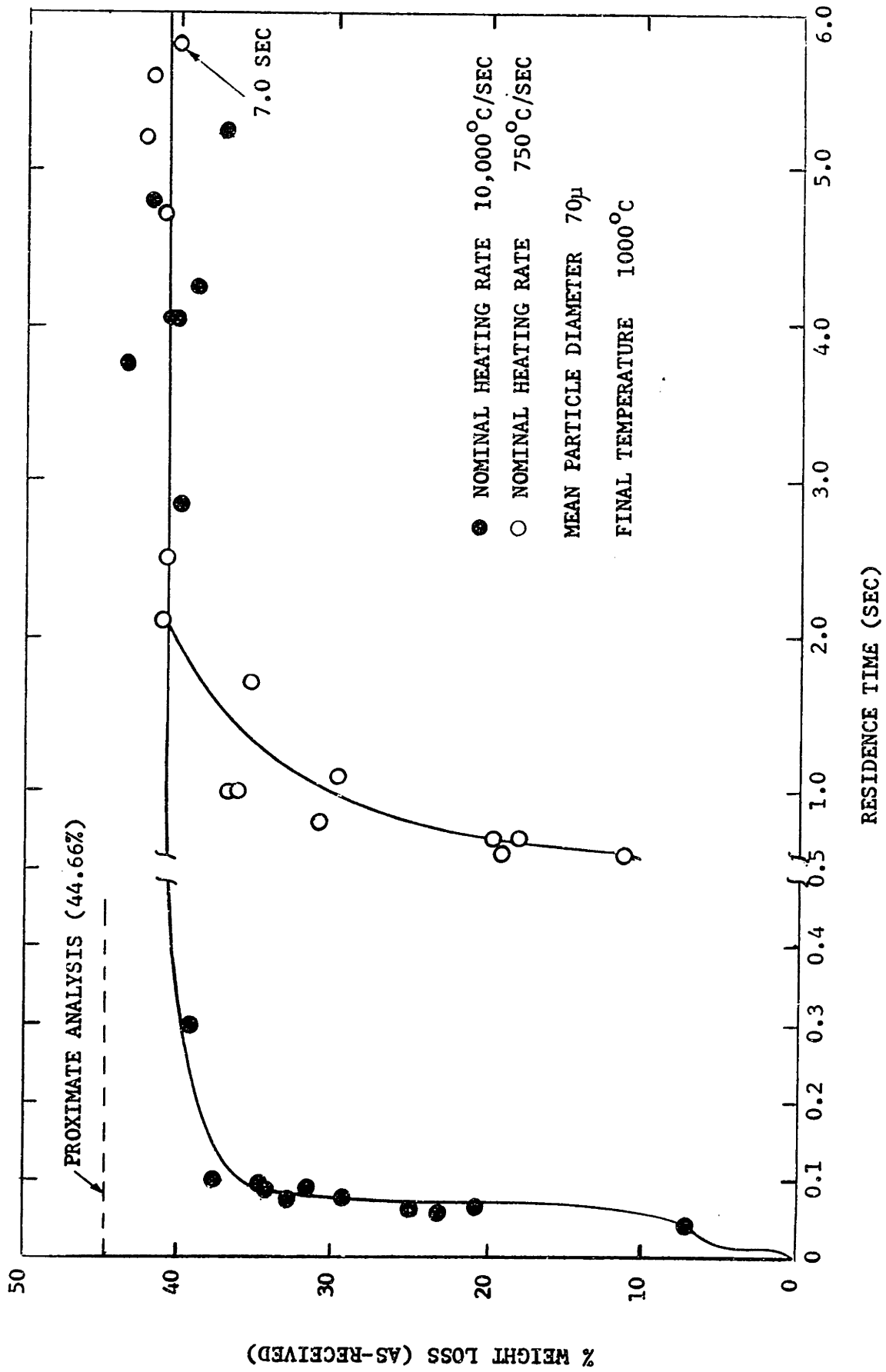


FIGURE 4-4 WEIGHT LOSS WITH TIME FOR LIGNITE UNDER 1000 PSIG HELIUM

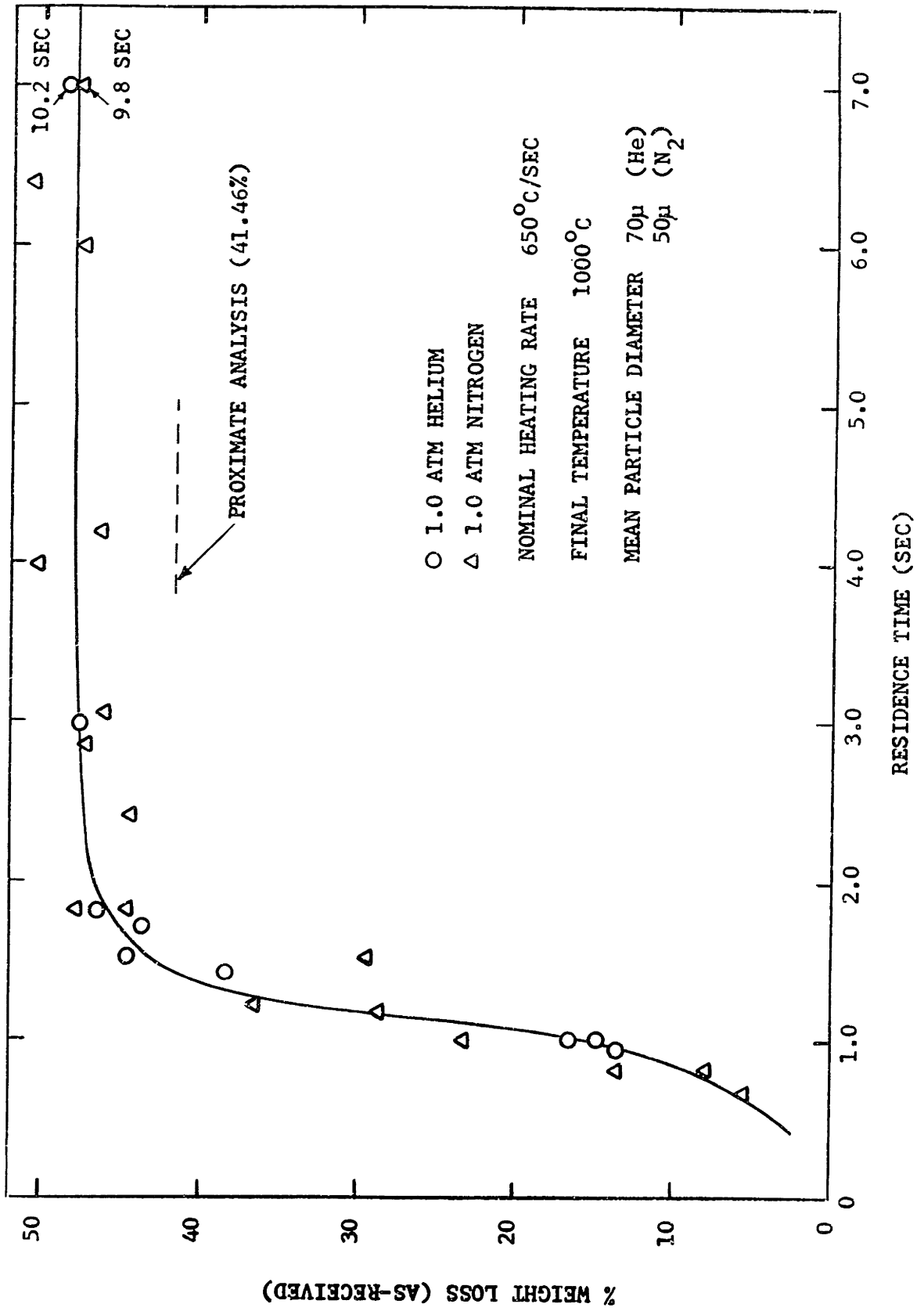


FIGURE 4-5 WEIGHT LOSS WITH TIME FOR BITUMINOUS COAL

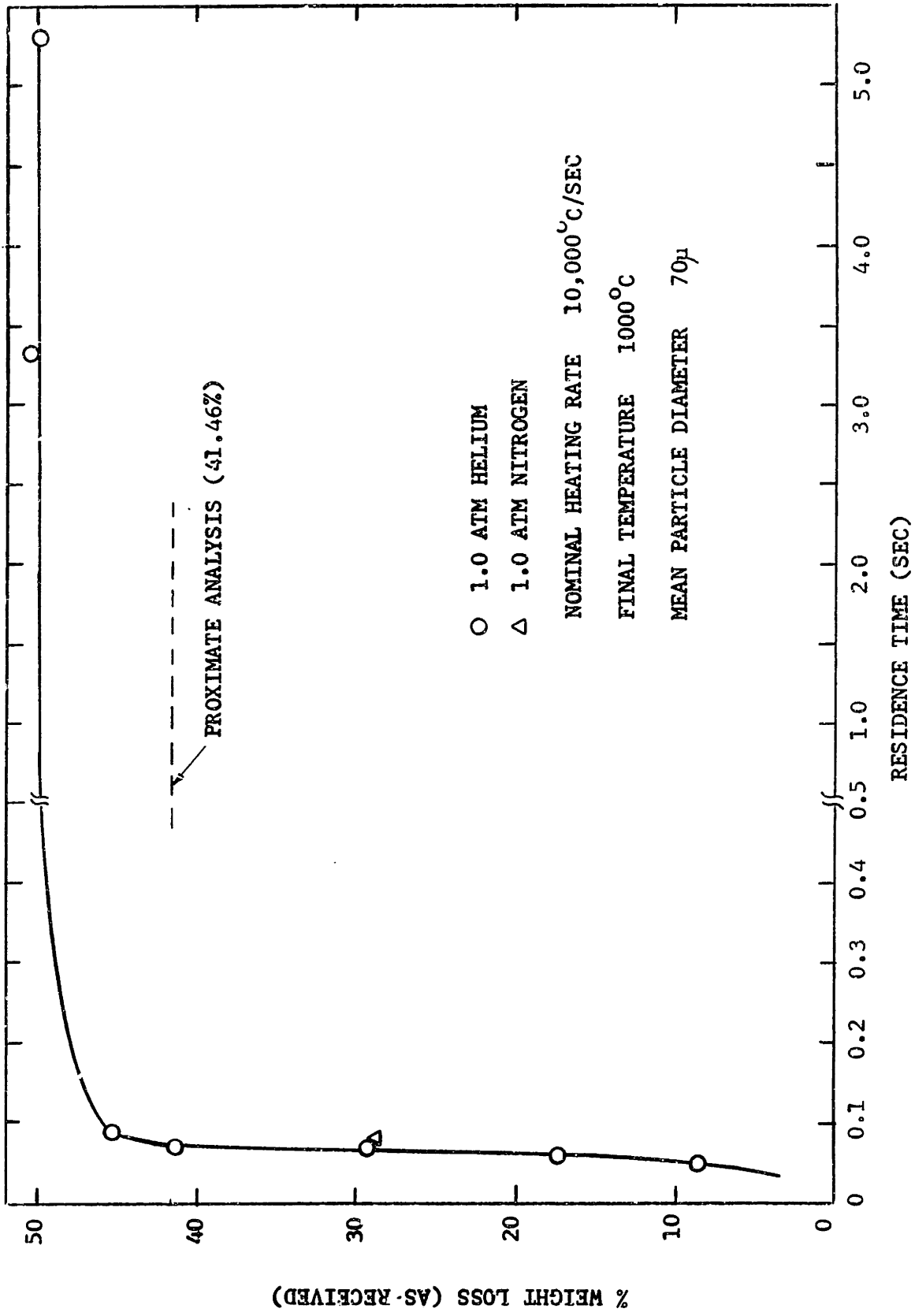


FIGURE 4-6 WEIGHT LOSS WITH TIME FOR BITUMINOUS COAL UNDER RAPID HEATING CONDITIONS

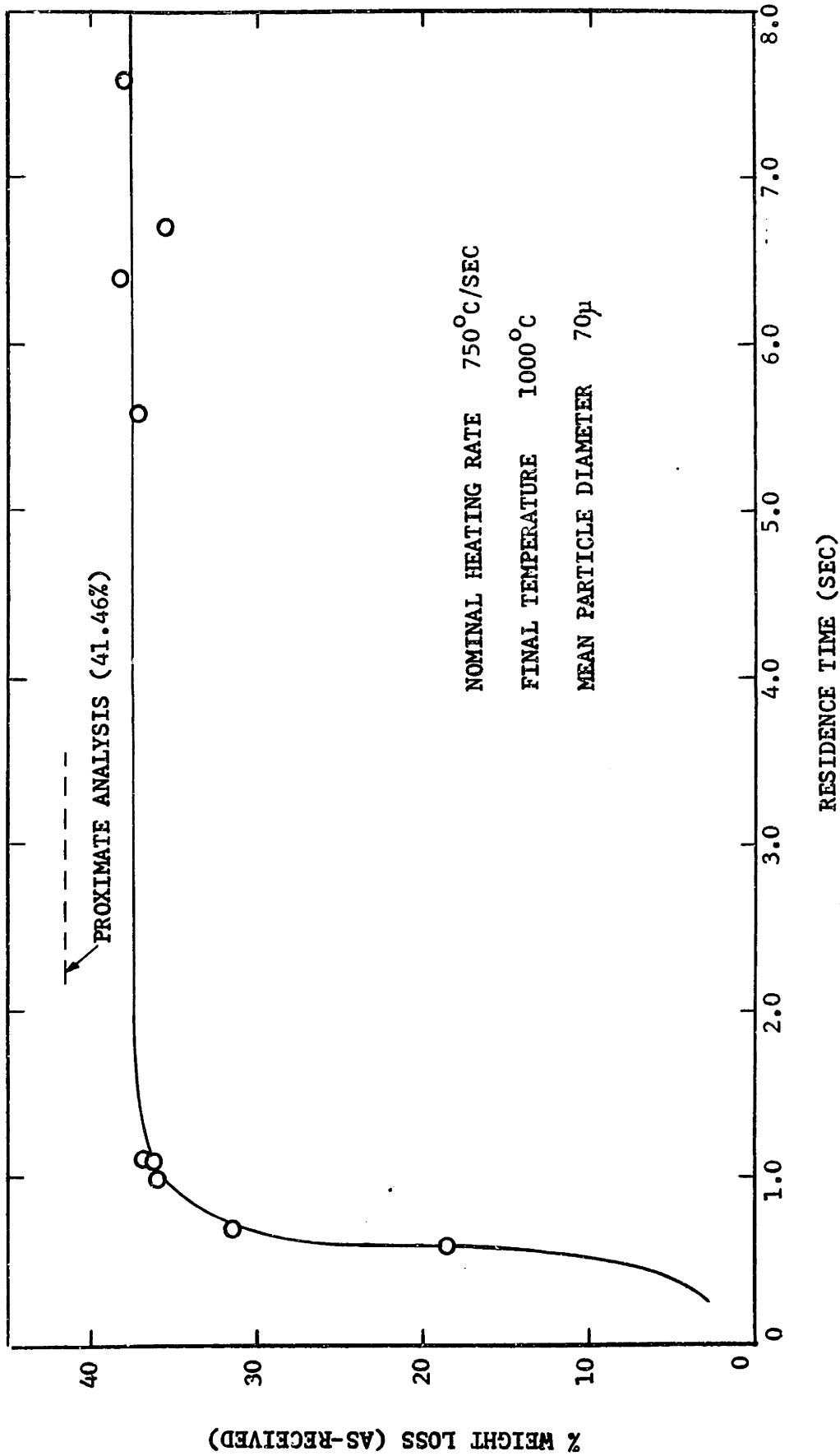


FIGURE 4-7 WEIGHT LOSS WITH TIME FOR BITUMINOUS COAL UNDER 1000PSIG HELIUM

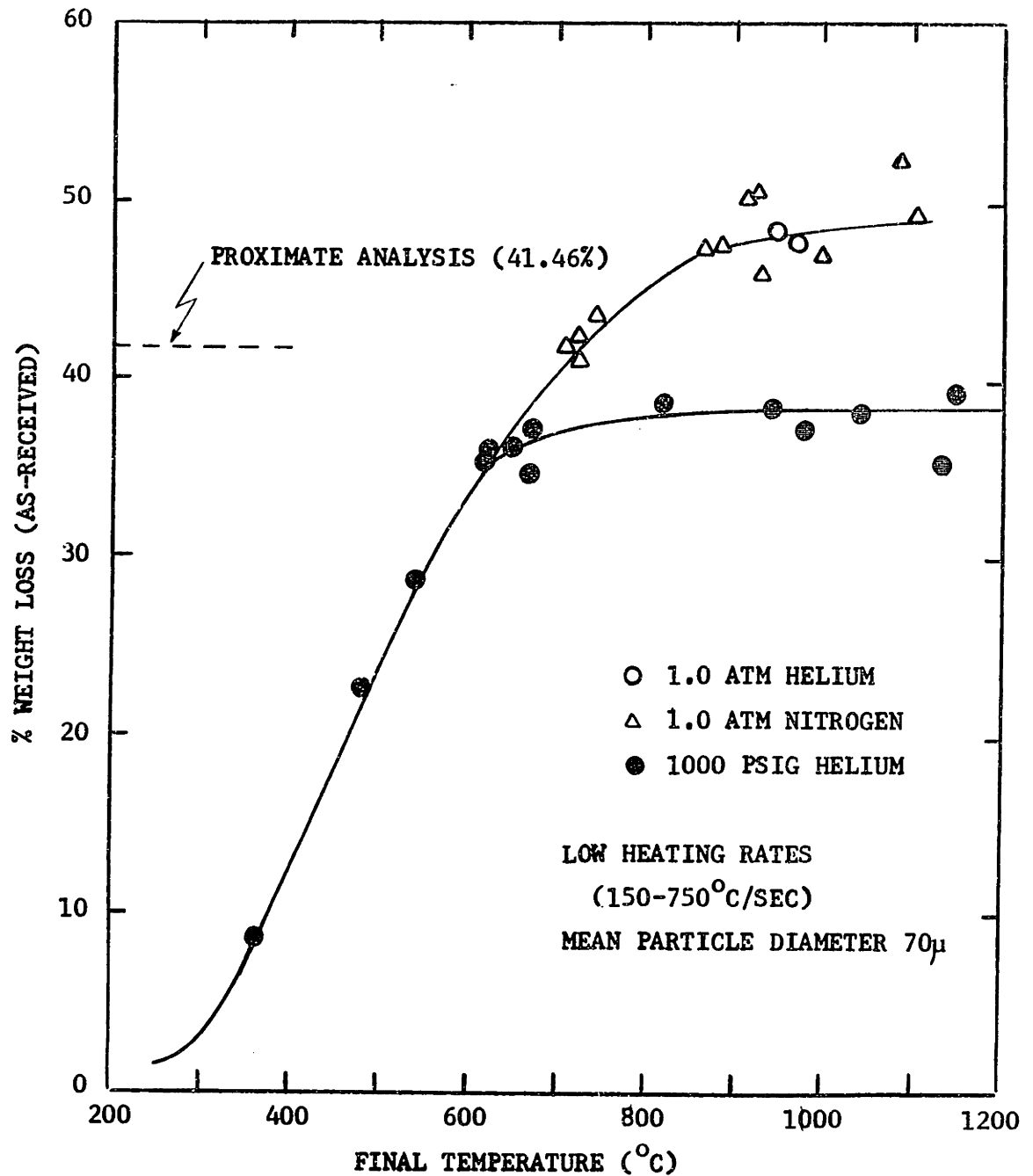


FIGURE 4-8 YIELD VERSUS FINAL TEMPERATURE FOR BITUMINOUS COAL

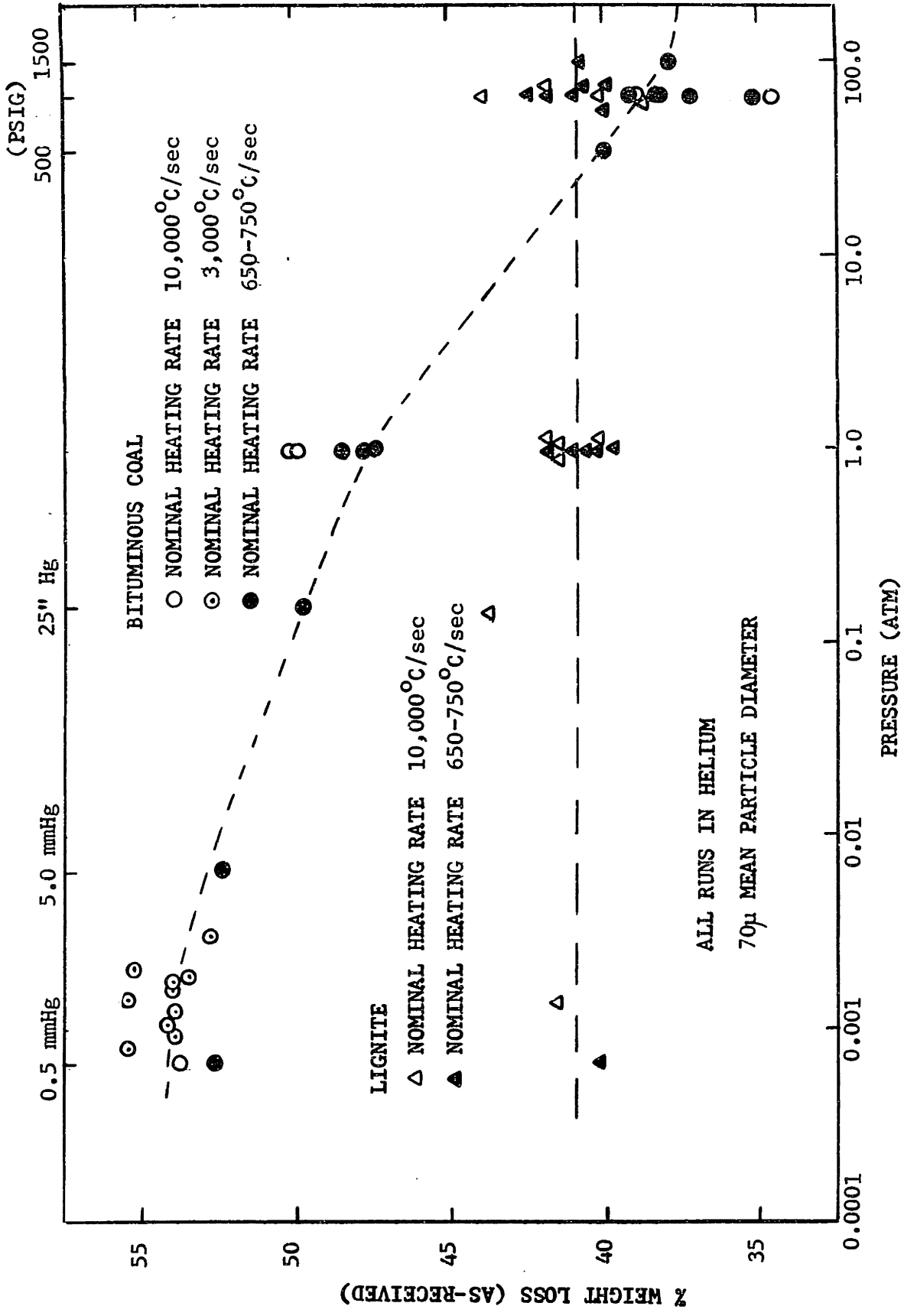


FIGURE 4-9 EFFECT OF TOTAL PRESSURE ON YIELD

4.2 HYDROGASIFICATION

The effect, on lignite weight loss at 100 psig gas pressure, of substituting hydrogen for helium is shown in Figure 4-10. The two curves, for hydrogen and helium, begin to diverge at a weight loss of 30-35% ($3/4$ sec), ultimately yielding about 17 percentage points more weight loss in hydrogen. Figure 4-11 depicts results under very rapid heating conditions which likewise show increasing yields with increasing hydrogen pressure. It is also evident from the curves in Figure 4-11 that hydrogenation may be subdivided into at least two stages, the first complete in 0.1 second, the second slower stage extending over several tenths of a second. Final temperature has a significant influence on hydrogenation yields similar to devolatilization. This comparison is made in Figure 4-12. The overall effect of hydrogen pressure in increasing yields is illustrated in Figure 4-13.

A weight loss with time curve for bituminous coal under 1000 psig hydrogen is compared to a similar curve in helium in Figure 4-14. The curves are identical to approximately one second after which they diverge resulting in significantly higher yield in hydrogen. The temperature dependency of these yields is established in Figure 4-15. It's interesting to note that for final temperatures below 600°C, the presence of hydrogen produces no additional weight loss. Figure 4-16 characterizes yields as a function of the hydrogen partial pressure. Since devolatilization yields are dependent on total pressure, data are shown for conditions of pure hydrogen and a constant total pressure of 1000 psig. The curves appear to converge between 600-800 psig of hydrogen pressure. Heating rate was found to have no

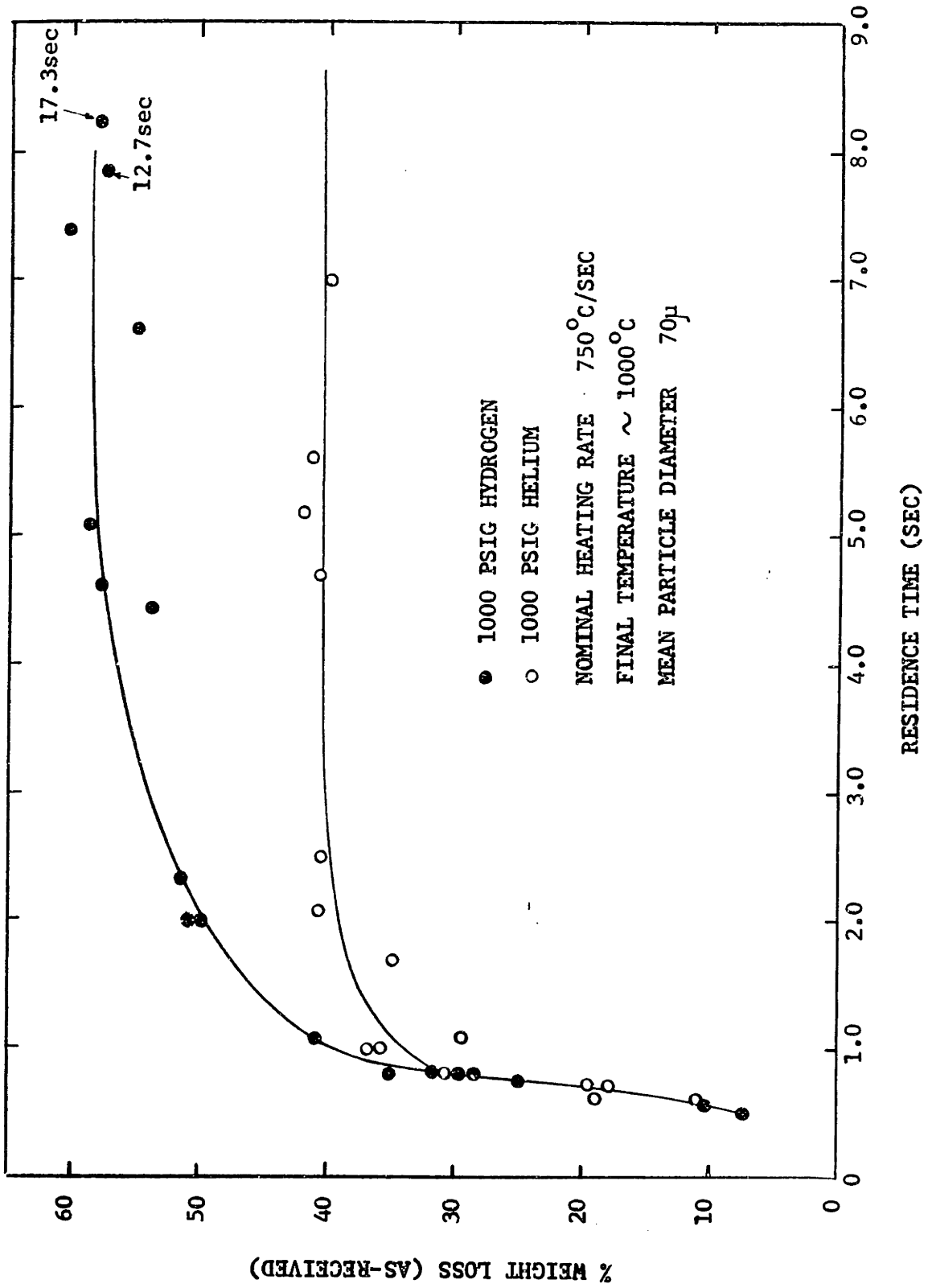


FIGURE 4-10 COMPARISON OF HYDROGEN AND HELIUM AS ENVIRONMENTS FOR LIGNITE WEIGHT LOSS VERSUS TIME

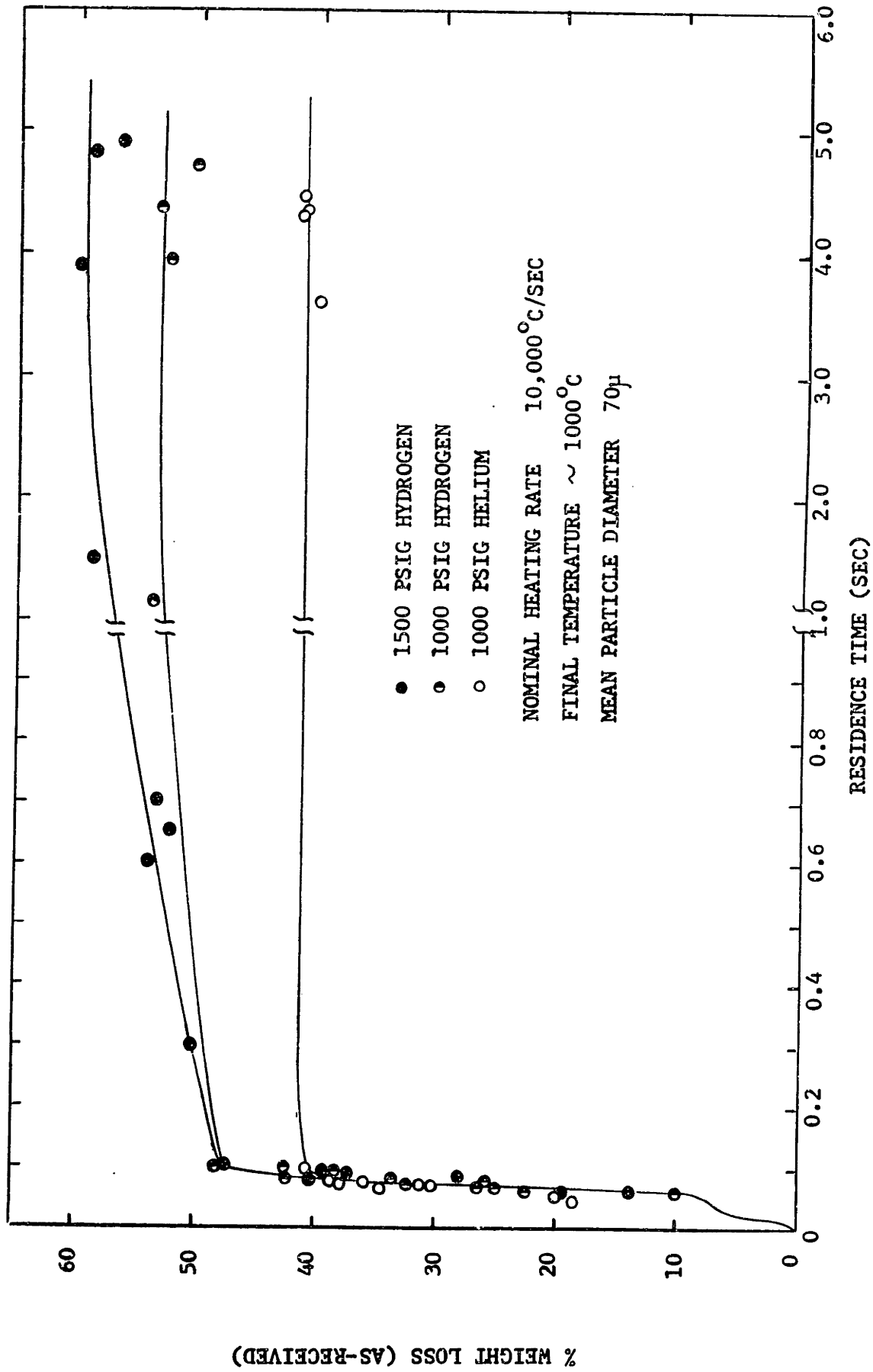


FIGURE 4-11 WEIGHT LOSS WITH TIME FOR LIGNITE IN HYDROGEN AND IN HELIUM,
 RAPID HEATING TO 1000°C

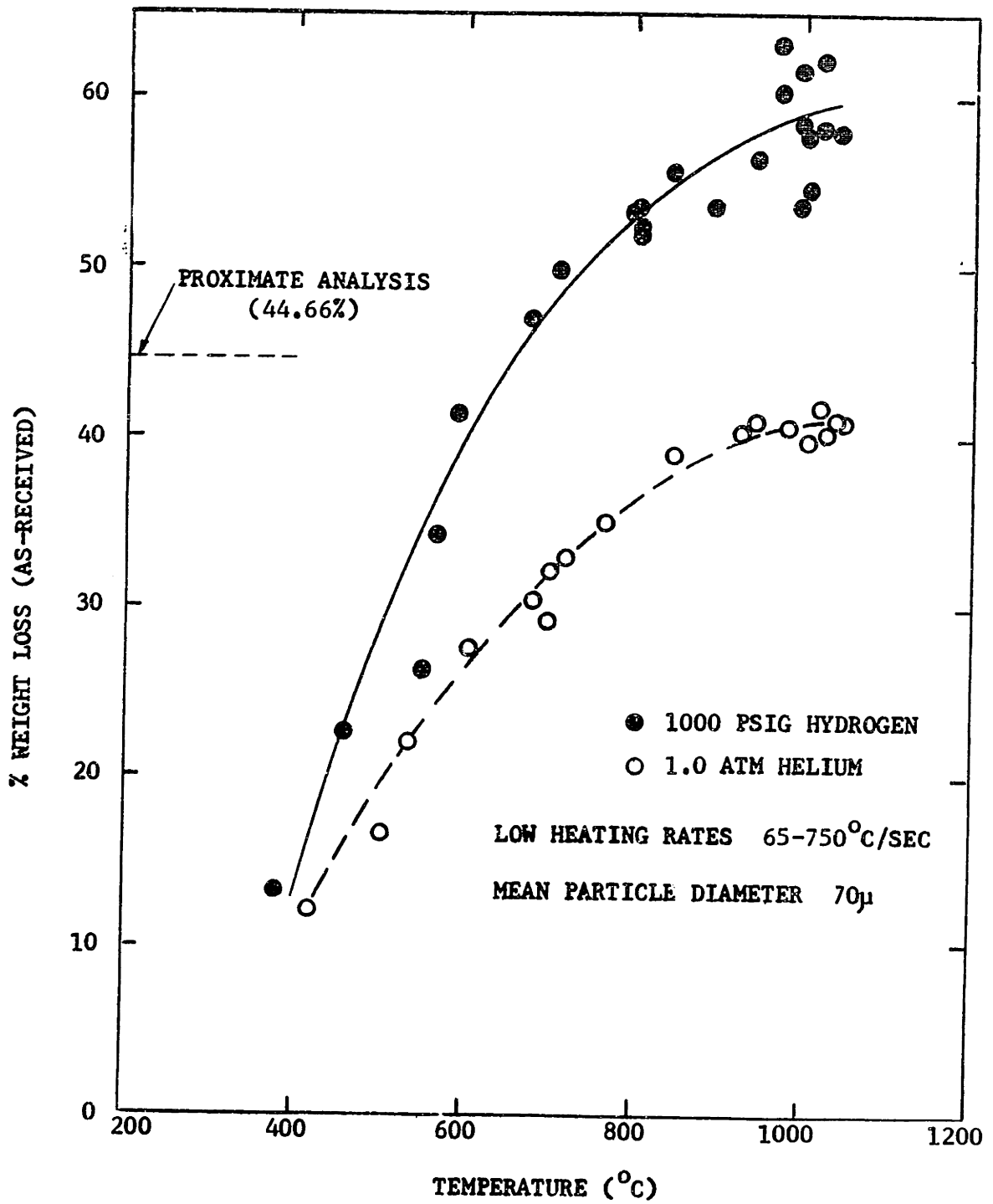


FIGURE 4-12 YIELD VERSUS FINAL TEMPERATURE FOR
LIGNITE IN HYDROGEN AND IN HELIUM

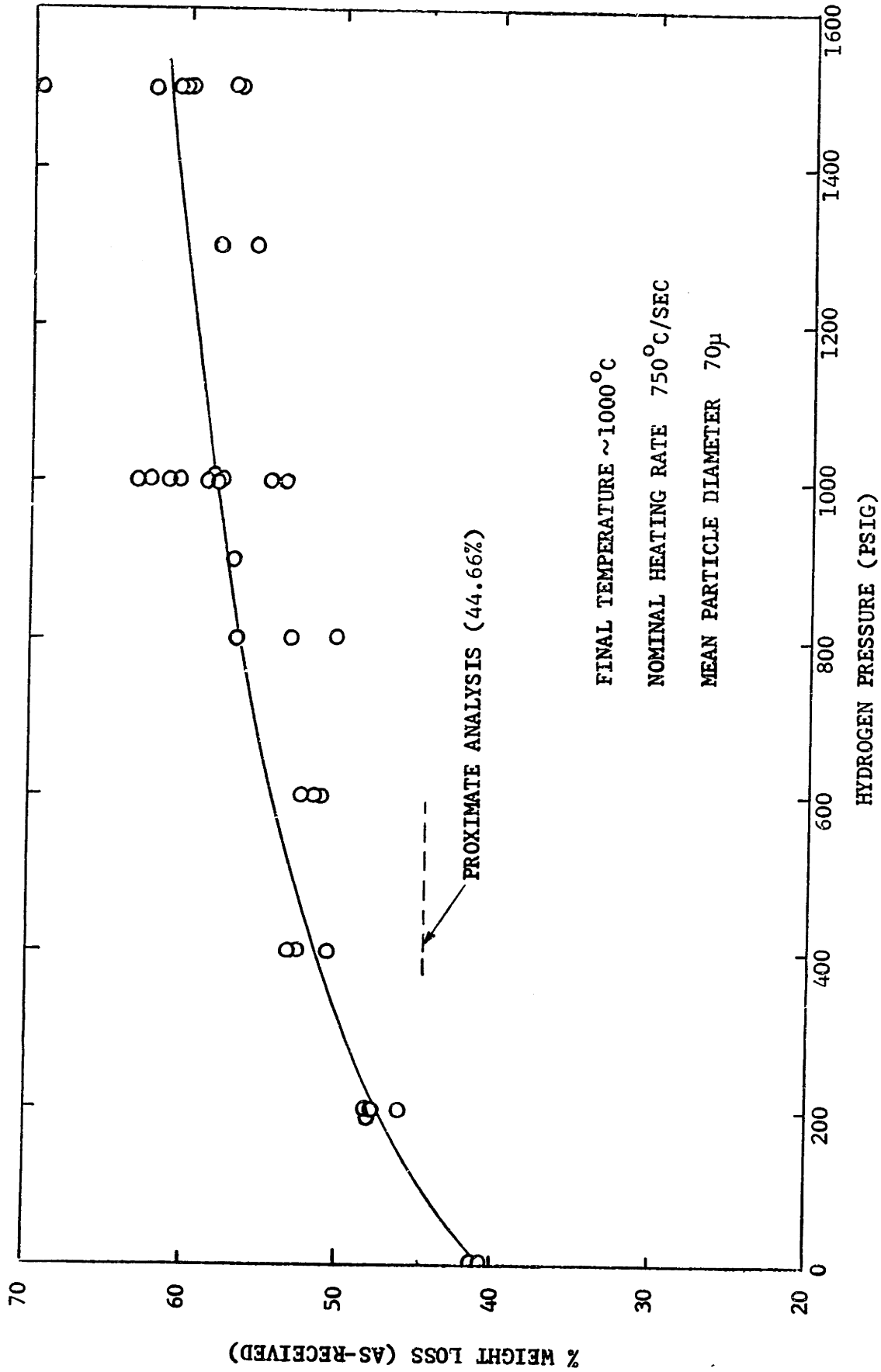


FIGURE 4-13 LIGNITE YIELD AS A FUNCTION OF HYDROGEN PRESSURE

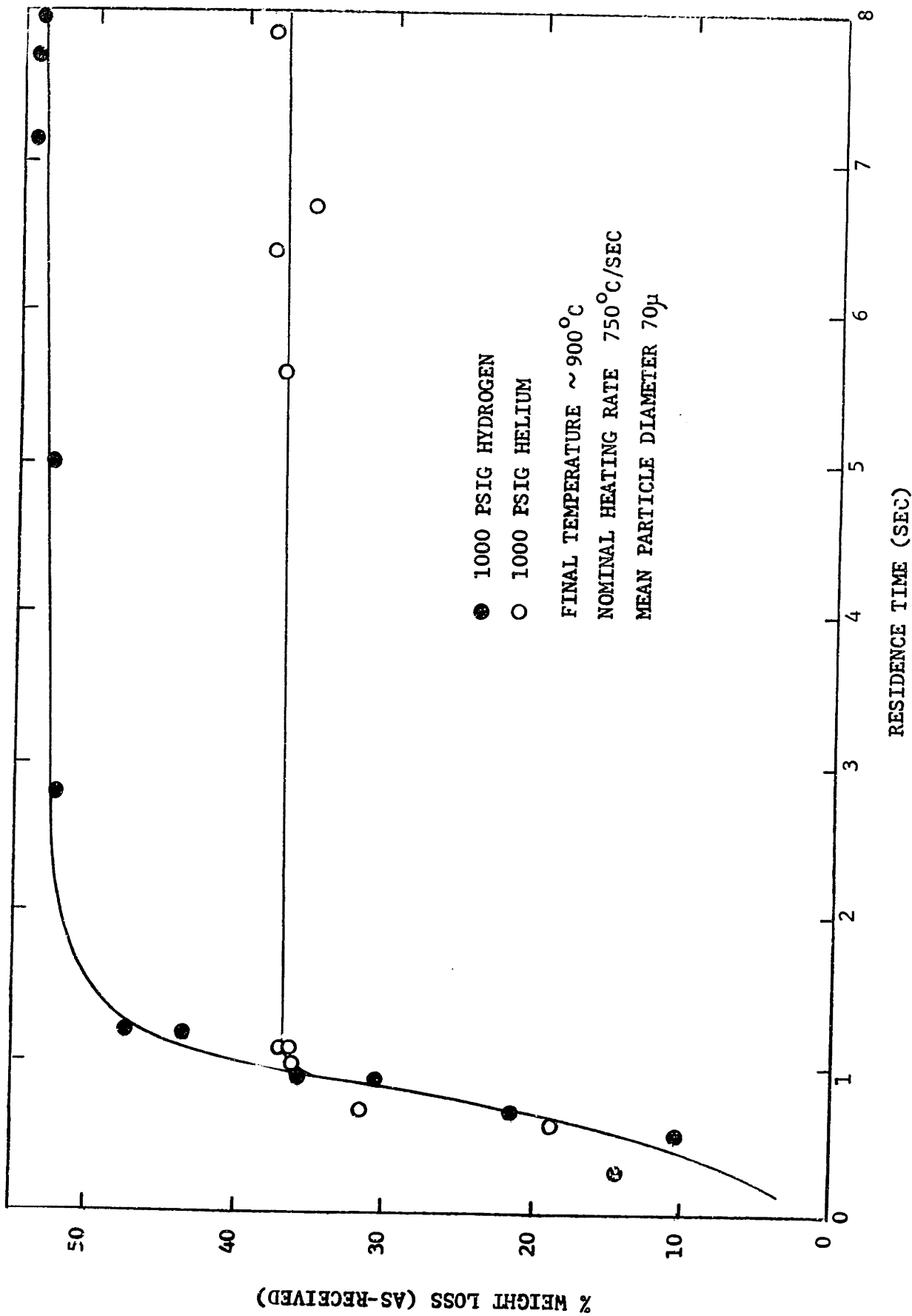


FIGURE 4-14 WEIGHT LOSS WITH TIME FOR BITUMINOUS COAL IN 1000PSIG HYDROGEN AND HELIUM

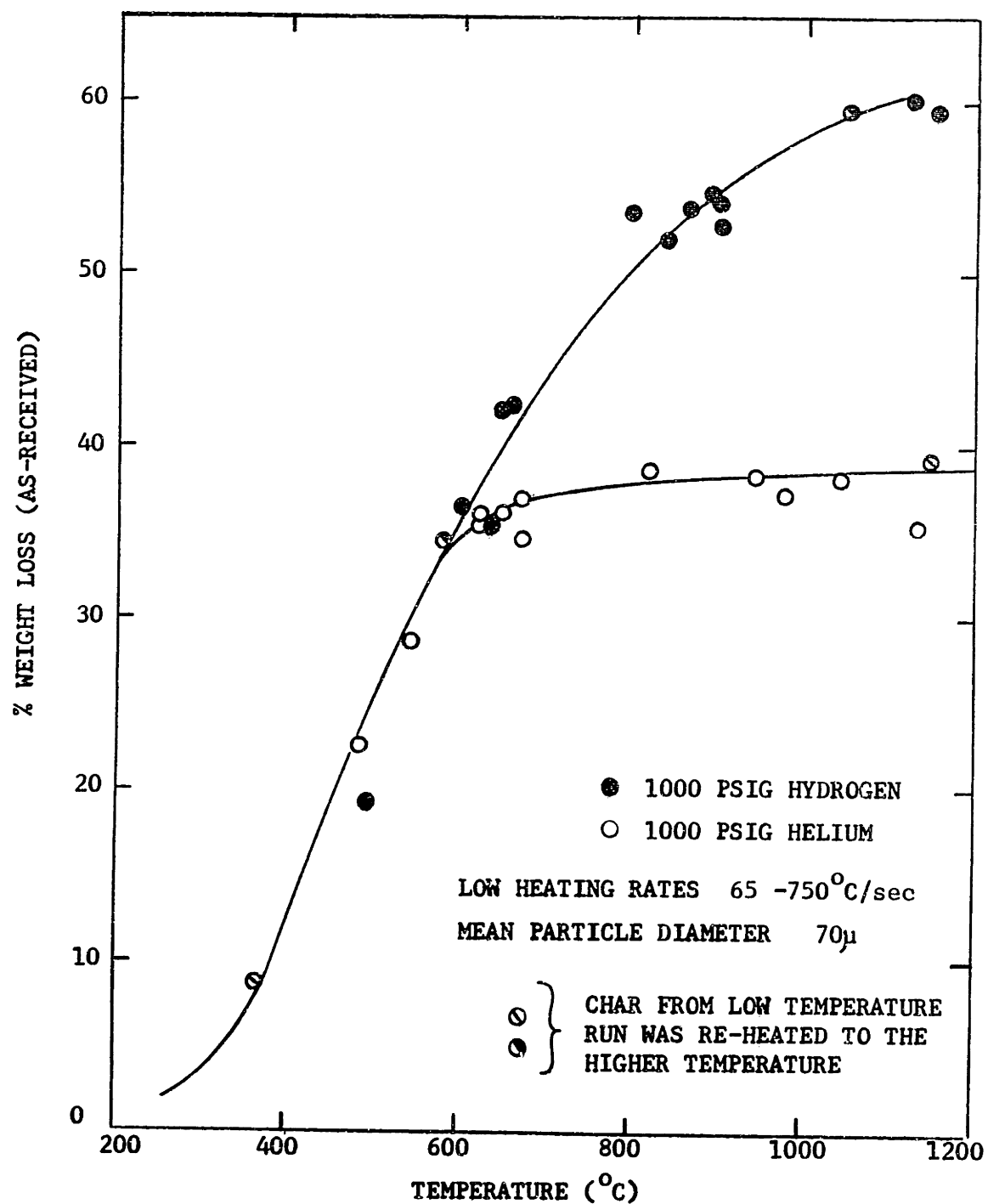


FIGURE 4-15 YIELD VERSUS FINAL TEMPERATURE FOR
 BITUMINOUS COAL IN HYDROGEN AND IN HELIUM

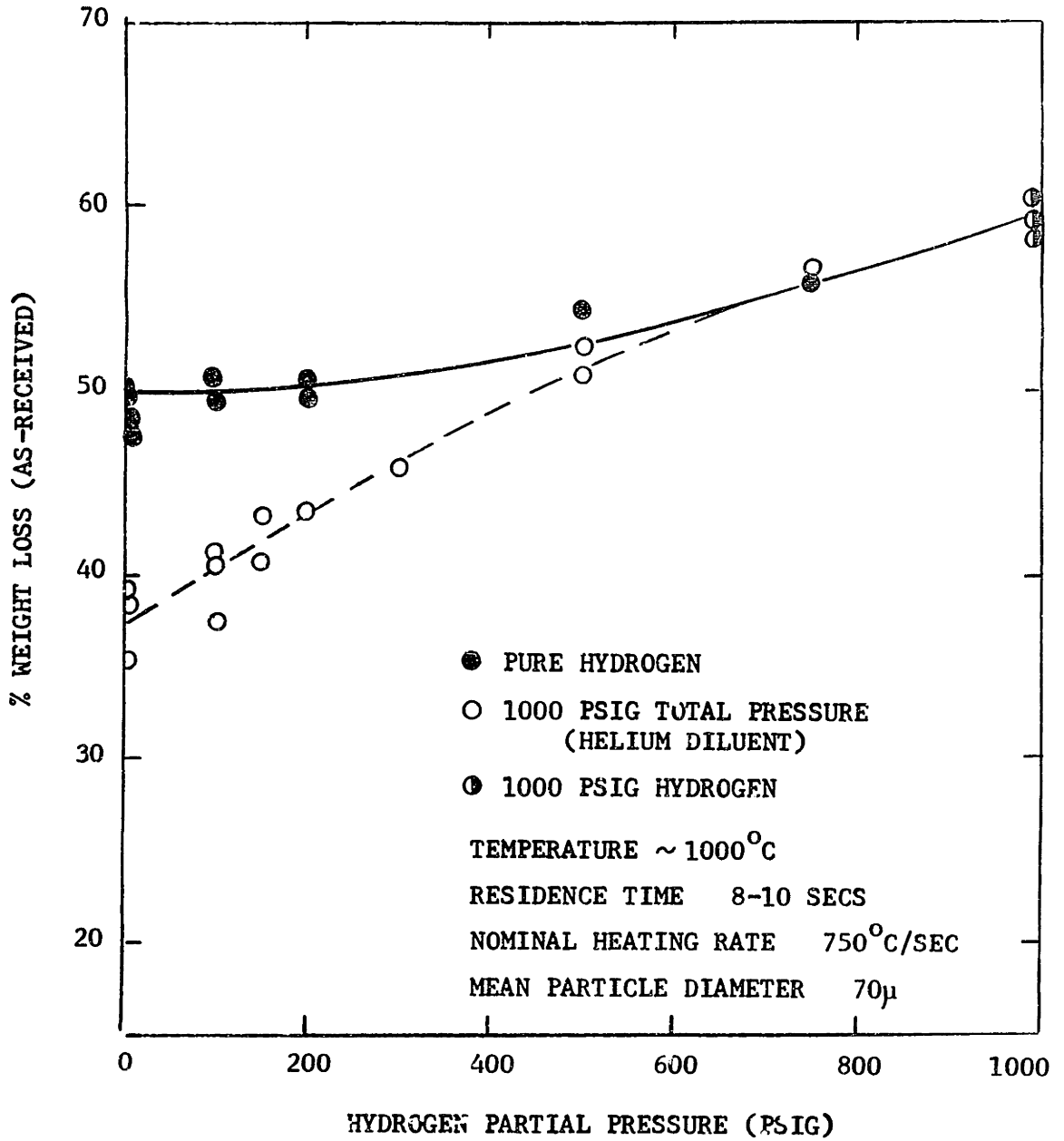


FIGURE 4-16 EFFECT OF HYDROGEN PARTIAL PRESSURE ON BITUMINOUS COAL YIELDS

effect on bituminous coal yields at 1000 psig. Larger particle sizes resulted in significantly lower yields for bituminous coal in hydrogen as plotted in Figure 4-17. In contrast, particle size has little, if any, influence on simple devolatilization in helium at 1.0 atm.

4.3 SUPPLEMENTAL RESULTS

While the preceding results constitute the bulk of the accumulated experimental evidence, the findings were supplemented by the acquisition, both incidental and deliberate, of valuable additional information. Under non-pressure conditions it was possible to observe the devolatilization process visually. Upon heating, particles of bituminous coal would simultaneously melt, swell, and fuse appearing virtually to "boil" on the screens. A very cloudy, yellowish stream of volatiles was seen to rise from the sample. The lignite particles did not fuse or swell during heating and the volatile stream was much less cloudy and white instead of yellow. In experiments with bituminous coal, deposits of a yellow-brown tarry material were observed on the baffle as well as on the terminals and walls of the vessel. The amount of tar deposited decreased with increasing pressure of either hydrogen or helium and essentially disappeared at about 1000 psig. Increasing the heating rate at one atmosphere and under vacuum appeared to augment the yield of tar. In a semi-quantitative attempt to measure the tar yields, Lavery (1973), determined the weight change of the foil covered baffle and found about 15% tar (based on original coal mass) at 1.0 atm hydrogen verses

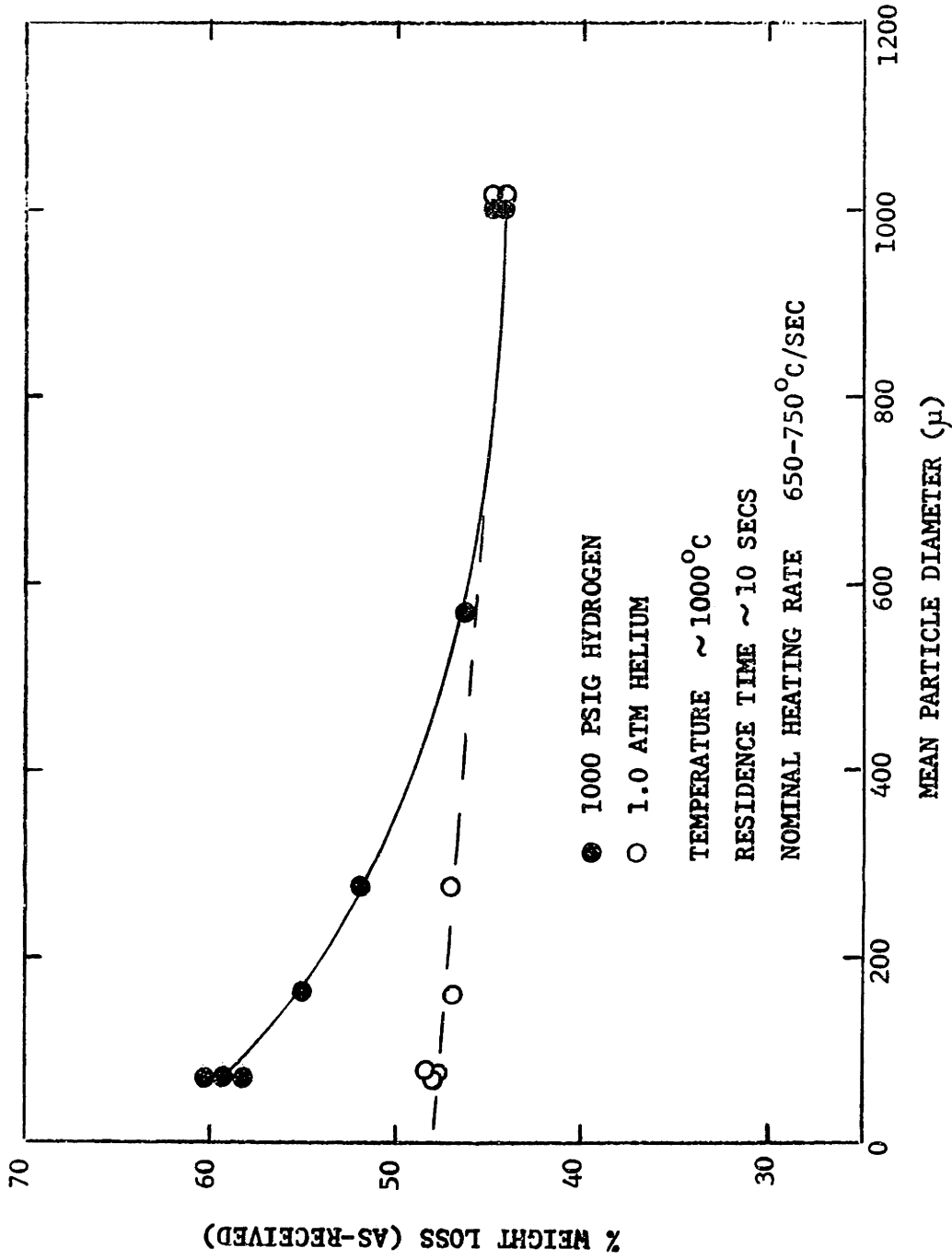


FIGURE 4-17 EFFECT OF PARTICLE SIZE ON BITUMINOUS COAL YIELDS

about 1% at 1000psig hydrogen. No tar deposits were observed on experiments with lignite. Under certain experimental conditions, the screens themselves were darkened, apparently by deposits of cracking volatiles. At one atmosphere pressure with bituminous coal the screens were noticeably blackened; however, the gain in screen weight was measured to be less than 1% of the original coal mass. Under high vacuum and very rapid heating conditions, the weight gain of the screens was estimated at between 2-3% of the original coal mass. At high pressures the screens were essentially clean. With lignite significant darkening of the screens occurred only under extremely high vacuum and with rapid heating conditions. Similar to bituminous coal, the maximum weight gain of the screens amounted to about 2-3% of the original coal mass.

The results of two interesting experiments on bituminous coal are shown in Figure 4-15. In the first case the char residue from the devolatilization run at 370°C (marked triangle) was reheated to over 1100°C. The total weight loss from both runs as a per cent of the original coal mass was also plotted in Figure 4-15 (similarly marked triangle), showing perfect agreement with samples heated directly to their final temperature. Similarly, the char residue from a hydrogenation run at 580°C was cooled and reheated to 1050°C and its total yield also agreed with the results of one-step heating.

Bituminous coal chars from several one atmosphere devolatilization runs at 1000°C were analyzed by standard proximate analysis procedures and found to contain 4.5-7.0% volatile matter (based on original coal). Since the samples were much smaller than required by the A.S.T.M. standard (10-20 mg vs. 1.0 gram), and because of the very low

volatile content of the chars, the values are less accurate than standard determinations. However, it is clear that such residual material would go undetected in runs of 10-20 seconds duration since the rate would be on the order of 1%/min.

5. DISCUSSION OF RESULTS AND DEVELOPMENT OF A MODEL

The intent of this discussion is to elucidate the mechanisms indicated by the results and simultaneously develop descriptive and useful models. There is no lack of available models adequate to describe both the devolatilization and hydrogenation of coal under particular conditions. The difficulty arises when it is demanded that the model successfully describe behavior over a wide range of conditions.

5.1 DECOMPOSITION MODEL

Since the major portion of observed weight loss may be directly attributed to devolatilization, that specific phenomenon will be discussed first. Possible mechanisms and models can be efficiently screened by drawing from the data certain characteristics that the model must possess. Those which fail this simple criteria can be discarded from consideration.

In the case of lignite, the rate of weight loss quickly falls to zero after the sample has reached final temperature (see Figures 4-1,-3,-4; combined in Figure 5-1). In Figure 5-2 the total yield increases continuously with final temperature but is unaffected by time-temperature history (see Figure 5-1). This latter point is strongly emphasized by the experiment which demonstrates that the excess yield of high temperature runs versus low temperature runs is recoverable by simply heating the low temperature char to a higher

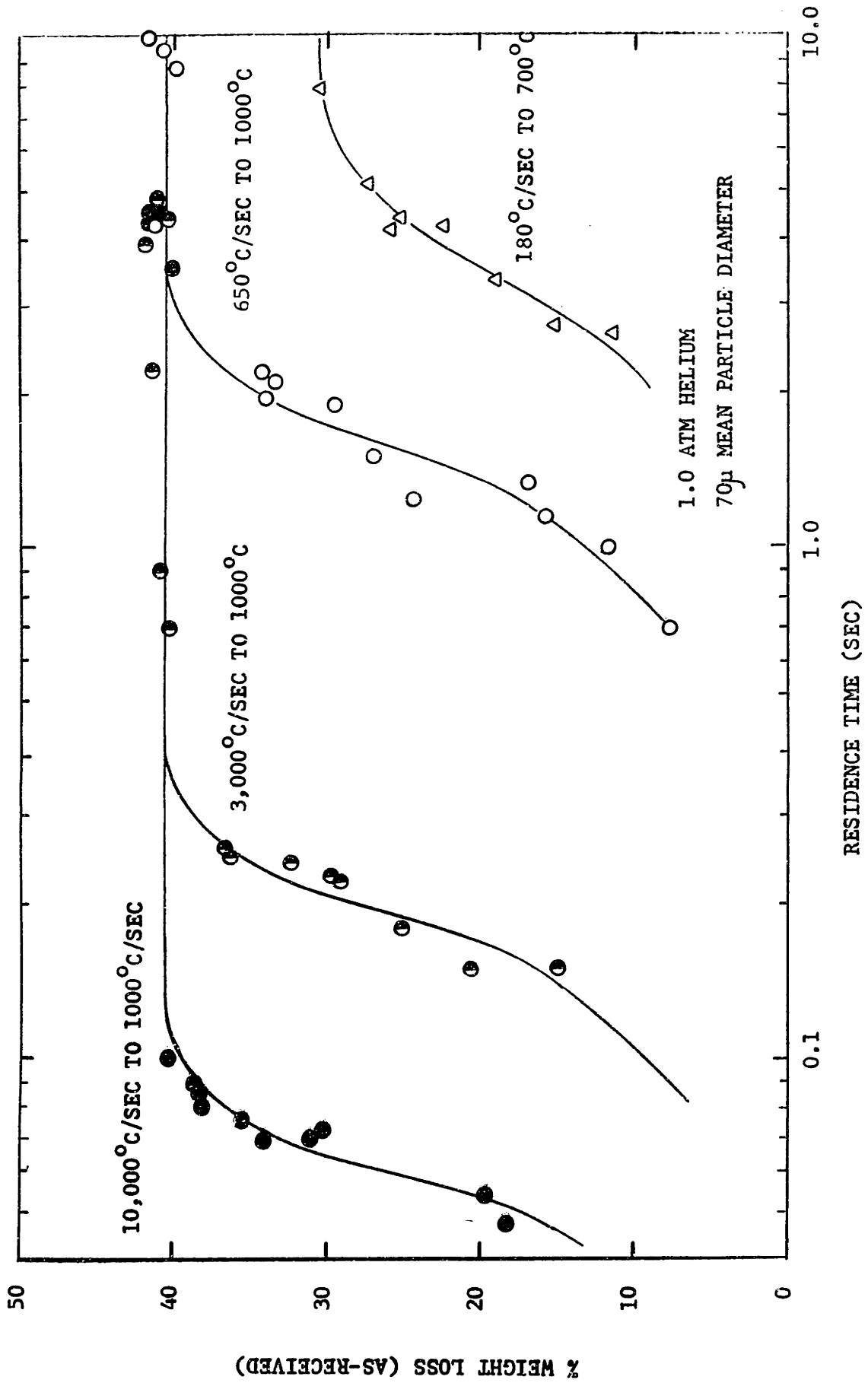


FIGURE 5-1 WEIGHT LOSS WITH TIME DATA FOR LIGNITE AT DIFFERENT HEATING RATES

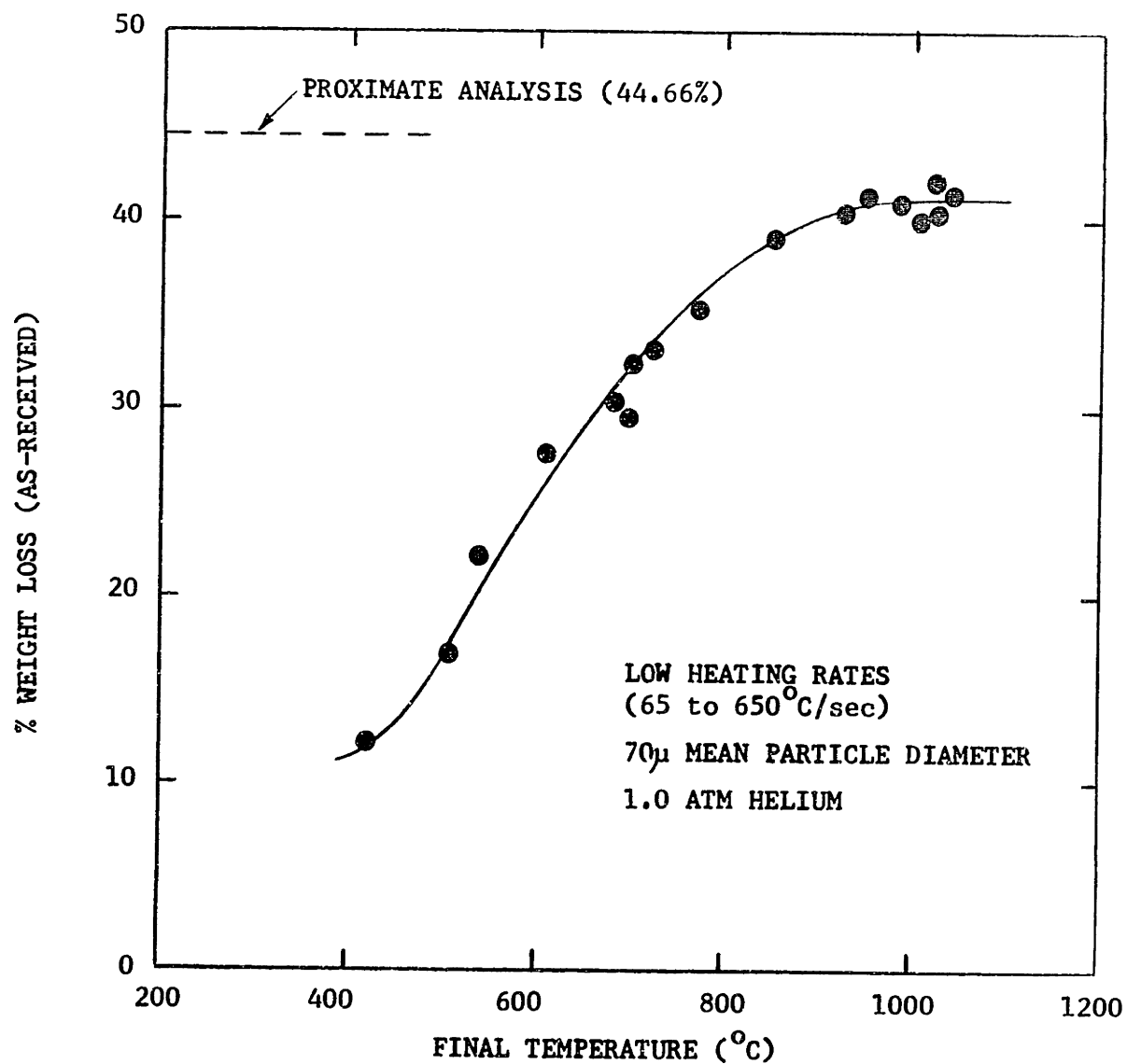


FIGURE 5-2 YIELD VERSUS FINAL TEMPERATURE FOR LIGNITE

temperature. Finally, total pressure is seen to have no effect. In general, similar comments may be made with respect to bituminous coal except that total pressure does significantly affect yield (refer to Figure 4-9). The rate of heating also has a small effect in the range of moderate pressures (0.1 to 10 atm).

To develop a model for devolatilization a number of possible avenues were explored:

1) Single Irreversible Decomposition Reaction

The fact that yield was dependent on final temperature invalidates any such simple reaction as well as simple heat and mass transfer models.

2) Equilibrium Limitations

Unfortunately, the reaction are not reversible.

3) Competitive Reactions

This is an appealing possibility since complex organic materials could easily have a number of potential reaction paths in competition each leading to differing amounts of volatiles and char. If such paths were influenced to different extents by temperature the resultant dependency of yield on final temperature might be explained. However, a simple experiment was devised to test this alternative. The residual char from a long residence time low temperature run was reheated to a higher temperature. The total weight loss was the same as achieved with one step heating. This state function relationship of yield to temperature clearly contradicts the competitive reaction model.

4) Multiple Reaction Model

Such a concept assumes many different reactions occurring in coal during devolatilization. If these reactions take place at

different temperatures and there are a sufficient number of them, the continuous behavior of yield with temperature in Figure 5-2 might be simulated. If no alternative reaction paths are allowed, time-temperature history would have no effect on yield provided the same final temperature and sufficient residence time are allowed. This model appears to meet the basic criterion for lignite though it is definitely incomplete for explaining the peculiarities of bituminous coal. Reserving comment on the bituminous coal until later, such a model is tested first on the lignite data.

Consider the thermal decomposition of a coal molecule as consisting of a large number of independent chemical reactions. Due to differences in chemical bond strength throughout the molecule, the temperature at which the various bonds rupture will vary markedly. The thermal decomposition of a single organic species can typically be described as a simple first order irreversible reaction, i.e., rate is proportional to the amount of unreacted material remaining. If such a rate expression is applied to a particular reaction within the coal structure, the rate of volatile evolution is given in the form of Equation 2-23:

$$\frac{dV_i}{dt} = k_i(V_i^* - V_i) \quad (5-1)$$

where k is usually an Arrhenius expression (Equation 2-25).

The subscript "i" in Equation 5-1 denotes that it is valid for one particular reaction. The amount of volatiles as yet unreleased by reaction is obtained by integration of Equation 5-1:

$$V_i^* - V_i = V_i^* \exp\left(-\int_0^t k_i dt\right) \quad (5-2)$$

The time integral is retained since the rate constant is a function of the time-temperature history. The dilemma is that for even simple expressions like Equations 5-1 and 5-2, parameter values for k_0 , E , and V_i^* cannot be predicted a priori and must be estimated for experimental data. This problem is multiplied by the number of reactions postulated. For the correlation of overall weight loss data a far simpler model is necessary. One simplification is possible if the major difference between k_i 's is in the temperature coefficient, E , and furthermore that sufficient reactions are present such that E may be expressed as a continuous distribution. Under these conditions V_i^* becomes differential fraction of the total volatile content, V^* , and may be written

$$\frac{dV^*}{dE} = V^* f(E) \quad (5-3)$$

such that

$$\int_0^{\infty} f(E) dE = 1 \quad (5-4)$$

The total amount of unreacted volatile material is obtained by summing up the contribution from each reaction or integrating Equation 5-2 for all values of E

$$V^* - V = \int_0^{\infty} V^* \exp\left(-\int_0^t k dt\right) f(E) dE \quad (5-5)$$

The dropping of the subscript "i" denotes reference to the overall reaction. The nature of the distribution, $f(E)$, is unknown but for purposes of mathematical tractability let's assume the distribution is Gaussian. Equation 5-5 becomes, with recognition of the negligible numerical difference in altering the lower integration limit from 0 to $-\infty$,

$$V^* - V = \int_{-\infty}^{\infty} V^* \exp\left(-\int_0^t k dt\right) \frac{\exp\left[-\frac{(E-E_0)^2}{2\sigma^2}\right]}{\sigma \sqrt{2\pi}} dE \quad (5-6)$$

with E_0 = mean activation energy and σ = standard deviation. It should be noticed that evaluation of Equation 5-6 requires estimation of only one additional parameter beyond that required for description of a single reaction (Equation 5-2). Yet Equation 5-6 constitutes an infinite set of parallel reactions. The additional parameter arises from separation of the single activation energy, E , into a distribution represented by E_0 and σ .⁵

Experimental data for lignite devolatilization from Figures 4-1, 4-2, and 4-3 were used in a non-linear least squares fitting routine to estimate parameter values for Equation 5-6. To simplify the integration the limits of the integral were changed to $E_0 \pm 2\sigma$ which would include 95.5% of the reaction set. The "best-fit" values were found to be:

$$\begin{aligned} k_0 &= 1.07 \times 10^{10} \text{ sec}^{-1} \\ E_0 &= 48.72 \text{ Kcal/mole} \\ \sigma &= 9.38 \text{ Kcal/mole} \\ V^* &= 0.4063 \text{ (fraction of original coal mass,} \\ &\quad \text{as-received basis)} \end{aligned}$$

⁵In isothermal situations where k is not a function of time, Equation 5-6 may be written in dimensionless form:

$$\frac{V^* - V}{V^*} = f\left(k_0 t, \frac{E_0}{RT}, \text{ and } \frac{\sigma}{E_0}\right) \quad (5-6a)$$

$$\frac{V^* - V}{V^*} = \int_{-\infty}^{\infty} \frac{\exp\left[-k_0 t e^{-\frac{E_0 Z}{RT}}\right] \exp\left[-\frac{(Z-1)^2}{2(\sigma/E_0)^2}\right]}{(\sigma/E_0) \sqrt{2\pi}} dz \quad (5-6b)$$

where $Z = E/E_0$

Figures 5-1 and 5-2 are reproduced in Figures 5-3 and 5-4 comparing the calculated curves with the actual experimental data. The agreement in each case is good. However, discrepancies are present since the actual recorded time-temperature history for each data point may deviate somewhat from the typical time-temperature history used in the calculation. Figure 5-5 is a better indicator of fit by directly comparing calculated and experimental values for the actual time-temperature histories. In this correlation the 45° line is indicative of perfect fit. Statistically, the goodness of fit has been calculated in two ways, first, by estimating confidence limits for the data and secondly by estimation confidence limits for the correlation itself.

Case 1 (Confidence Limits on Data)

$$\text{Standard Deviation} = \pm S = \pm \sqrt{\frac{\text{SSE}}{n-d.f.}} = \pm 1.73\%$$

(wt.% based on original mass of coal)

$$95\% \text{ Confidence Limits} = \pm 2S = \pm 3.46\%$$

Case 2 (Confidence Limits on Correlation)

$$\text{Standard Deviation} = \pm S' = \pm \sqrt{\frac{\text{SSE}}{n(n-d.f.)}} = \pm 0.25\%$$

$$95\% \text{ Confidence Limits} = \pm 2S' = \pm 0.50\%$$

Case 1 is the region which includes 95% of the data, while Case 2 is the region in which it is 95% probable that the experimental mean is located.

Equation 5-6 has also been used to correlate bituminous coal devolatilization results at 1000 psig He where yields were found independent of total pressure and heating rate satisfying the mechanistic criteria of the model. It would also have been possible to use data at extremely high vacuum since here too the mechanistic

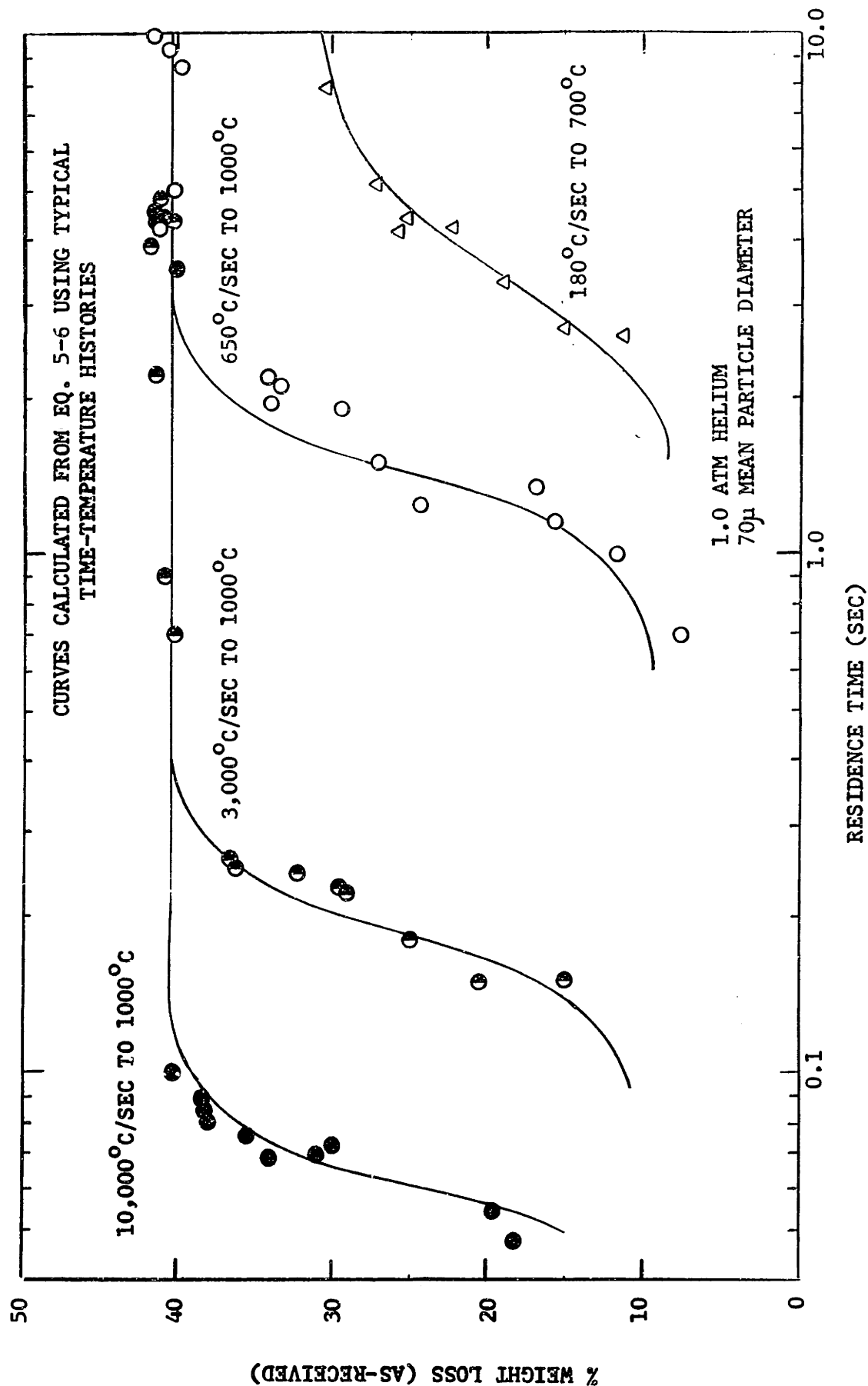


FIGURE 5-3 COMPARISON OF DECOMPOSITION MODEL WITH LIGNITE DATA AT
DIFFERENT HEATING RATES

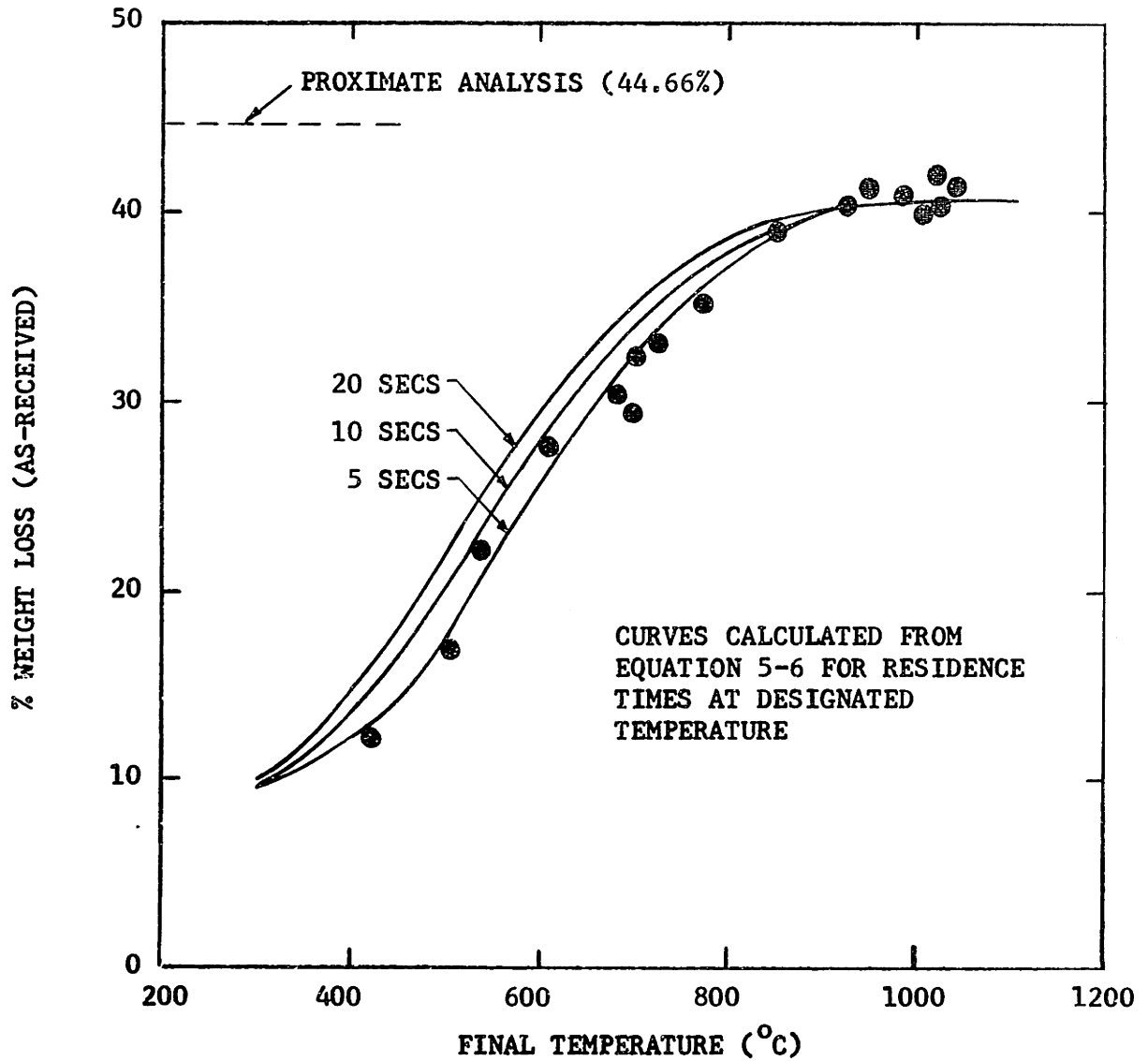


FIGURE 5-4 COMPARISON OF LIGNITE YIELDS WITH
DECOMPOSITION MODEL

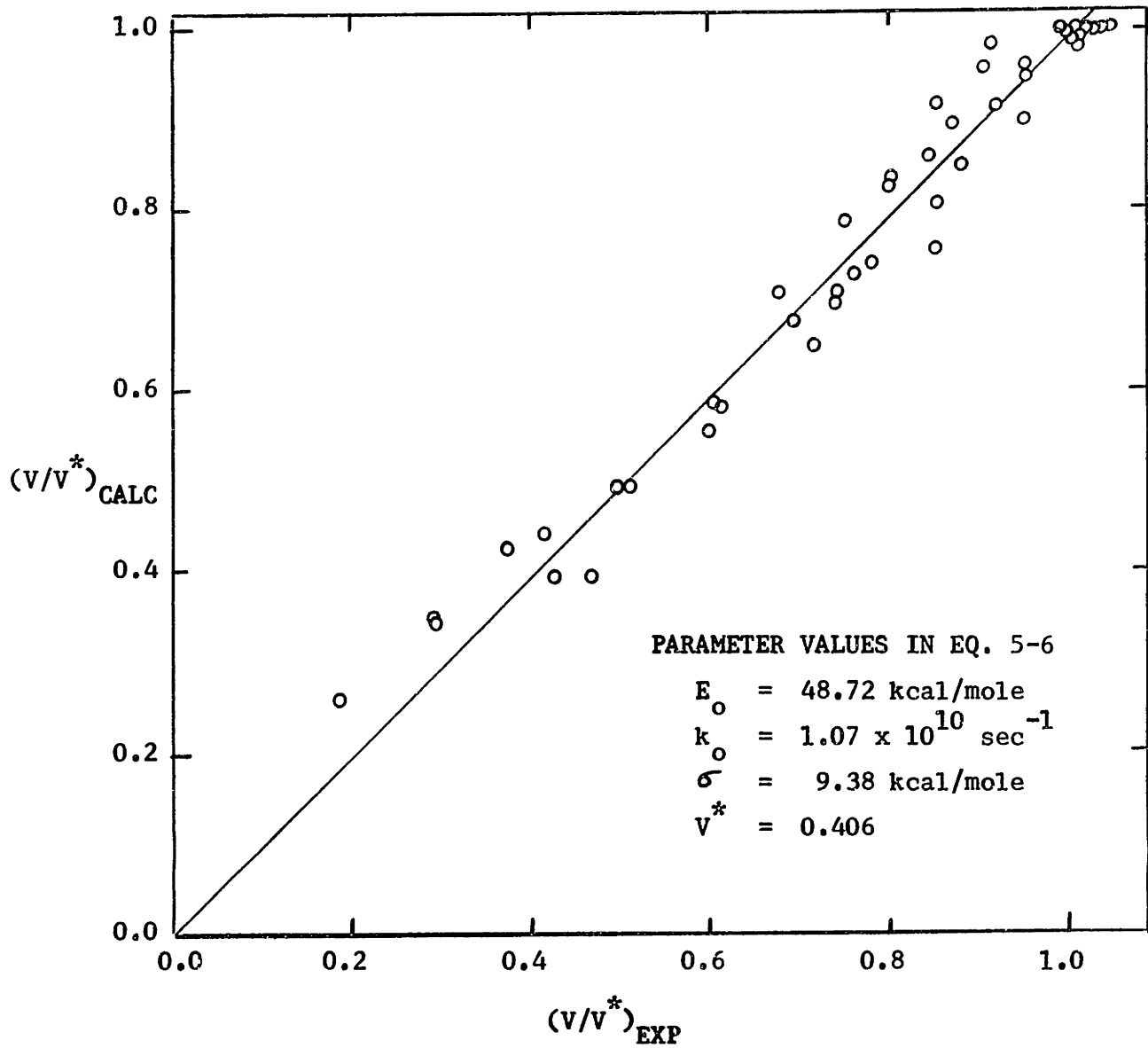


FIGURE 5-5 COMPARISON OF CALCULATED WITH EXPERIMENTAL
 WEIGHT LOSSES FOR LIGNITE

criteria of pressure and heating rate independency were satisfied. However, the apparatus was ill-suited for obtaining accurate data under high vacuum since substantial cracking and carbon deposition on the screen was observed. Further, it was felt that results at high pressure would be more meaningful in terms of interpreting the interrelationship of devolatilization and hydrogasification. Summary values of the fitted parameters and associated error for both coals are listed below.

	Lignite	Bituminous
k_0 (sec^{-1})	1.07×10^{10}	2.91×10^9
E_0 (kcal/mole)	48.72	36.89
σ (kcal/mole)	9.38	4.18
V^* (fraction of orig. coal)	0.4063	0.3718
S (Case 1)	$\pm 1.73\%$	$\pm 1.85\%$
S' (Case 2)	$\pm 0.25\%$	$\pm 0.42\%$

Data from Figures 4-7 and 4-8 are compared with calculated results in Figure 5-6. Again, the fit is good.

A number of interesting observations are possible with this model. First, it must be emphasized that Equation 5-6 is likely not a true fundamental picture of coal decomposition but rather a simple correlative tool. The tool is especially valuable, though, because it contains certain characteristics that may be compared with more fundamental information. The range of activation energies, 30-67 kcal/mole for lignite and 29-45 kcal/mole for bituminous, are certainly consistent with typical values for chemical reaction especially for organic decompositions. The range for the bituminous coal is located precisely at the lower limit of the lignite range.

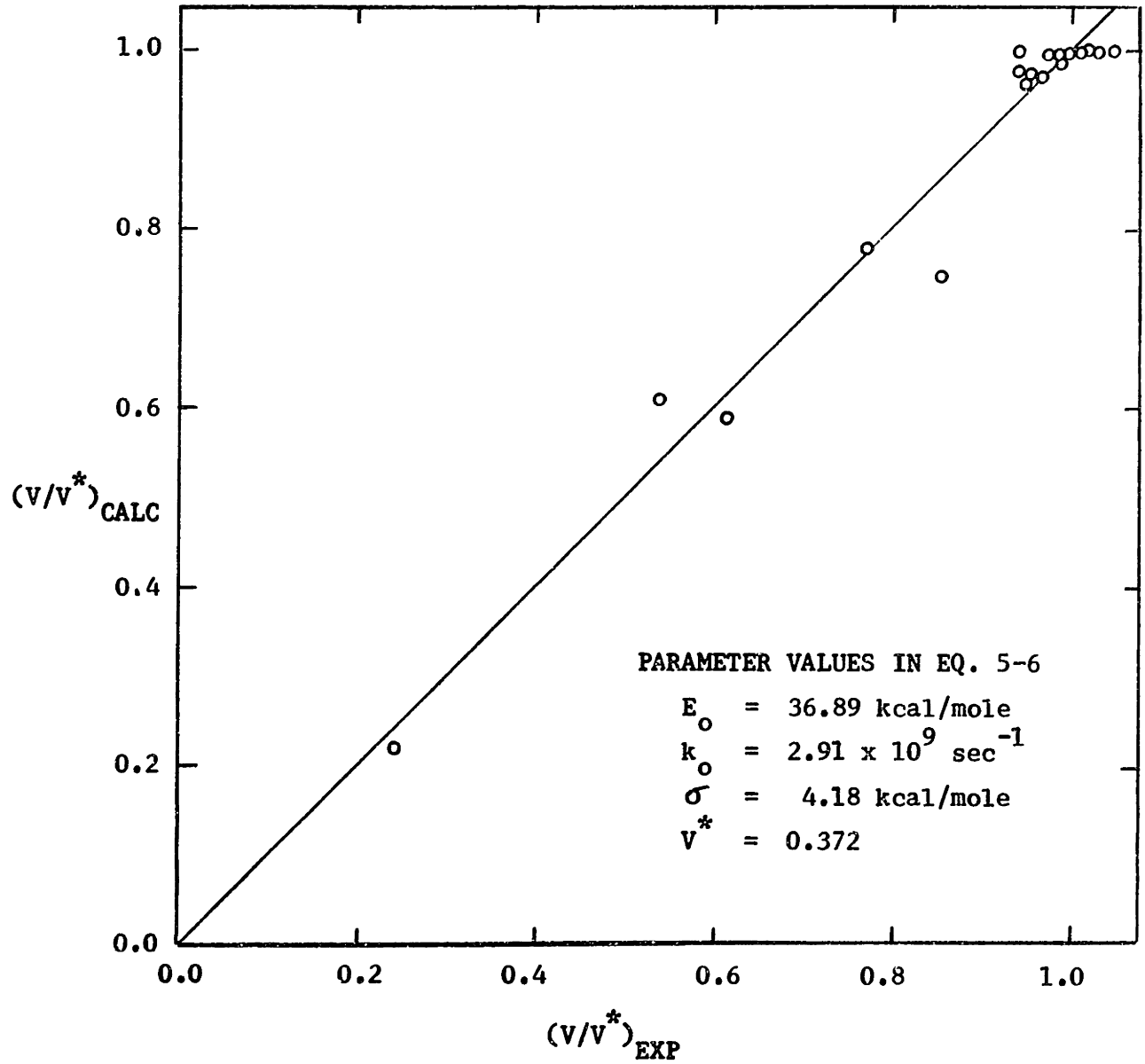


FIGURE 5-6 COMPARISON OF CALCULATED WITH EXPERIMENTAL
WEIGHT LOSSES FOR BITUMINOUS COAL AT 1000 PSIG

Figures 4-8 and 5-2 validate this since the temperature at which the yield becomes independent of temperature is about 200°C lower for bituminous coal (~700°C) than lignite (~900°C). If these additional reactions for bituminous coal were included in the statistical model, their estimated activation energies would be accordingly higher more in line with the distribution found for lignite.

5.2 SECONDARY REACTION MODEL

Despite the power of Equation 5-6 it offers no explanation for the significant influence of total pressure on the yield of bituminous coal devolatilization as illustrated in Figure 4-9. It is well-known that many volatile products are extremely reactive, probably even more so during the initial stages of decomposition where free radical species likely exist. Thus, it is not difficult to perceive of many of these species polymerizing and cracking on the hot coal surfaces diminishing actual yield. If the residence time of these particular species is the controlling factor for yield, then conditions that reduce this residence time presumably would enhance yield. Quite possibly the observed influence of total gas pressure is directly involved in the diffusional escape of such reactive volatiles.

To test this argument the following material balance for vapor phase "reactive" volatiles species present in the coal particle's void fraction is suggested:

$$Q - K^*C - k_4C = \frac{dC}{dt} \quad (5-7)$$

- where
- Q = Formation generation rate of "reactive volatiles,
mass of volatiles/time per unit mass of original coal
 - C = Void fraction vapor phase concentration of "reactive"
volatiles, mass per unit mass of original coal
 - K^* = Overall mass transfer coefficient, time^{-1}
 - k_4 = Rate constant for deposition reaction, time^{-1}

The picture given by Equation 5-7 envisions a coal particle possessing a fixed internal void space of uniform composition and temperature. Species enter this space via the thermal decomposition reaction, Q , which is independent of concentration. The species are assumed to leave this designated volume either by mass transfer away from the particle (rate proportional to concentration difference with the bulk gas phase concentration taken as zero) or by secondary reaction resulting in solid deposition (approximated by a first order gas phase reaction). It is also advantageous to neglect the accumulation term, dc/dt , by making a pseudo-steady state approximation, tantamount to saying that the density of "reactive" volatiles in the vapor phase is much less than in the solid phase. This reduces Equation 5-7 to

$$Q - K^*C - k_4C = 0 \quad (5-8)$$

or

$$C = Q/(K^* + k_4) \quad (5-9)$$

Experimentally, it is possible only to measure the net weight loss of the coal or in terms of Equation 5-8, the amount of material transferred away by the second term thus permitting the overall material to be written

$$\frac{dV_R}{dt} = K^*C = Q/(1 + \frac{k_4}{K^*}) \quad (5-10)$$

with V_R = weight loss of "reactive" volatiles per unit mass of coal.

If the form of Q is assumed to be an isothermal first order decomposition reaction⁶, $Q = k_1 V_R^* \exp(-k_1 t)$, then Equation 5-10 may be integrated over time

$$\int_0^{V_R} dV_R = \left[\frac{1}{1 + \frac{k_4}{K^*}} \right] \int_0^t k_1 V_R^* e^{-k_1 t} dt \quad (5-11)$$

$$V_R = \left[\frac{1}{1 + \frac{k_4}{K^*}} \right] V_R^* (1 - e^{-k_1 t}) \quad (5-12)$$

As $t \rightarrow \infty$, the exponential term becomes negligible resulting in a selectivity expression for yield based on total potential yield, V_R^* :

$$V_R = \frac{V_R^*}{1 + \frac{k_4}{K^*}} \quad (5-13)$$

To understand the influence of pressure, attention should be focused on the mass transfer coefficient, K^* . Assuming that this constant is proportional to the diffusion coefficient for the volatiles, then it is possible to replace K^* with k^*/P_{tot} converting Equation 5-13 to the

⁶The insouciant use of an isothermal first order decomposition expression may at first seem in contradiction with the preceding discussion on the decomposition model. The reactions occur neither isothermally nor in accord with a first order model. The intent, however, was to provide a mathematically simple path to Equation 5-13. Use of the more valid but far more complicated Equation 5-6 for Q would have led, at long residence times and high final temperatures, to the identical expression assuming that k_4 and K^* are independent of time-temperature history. Since the relevant data in Figure 4-9 satisfy both criteria of residence time and temperature, the approach should be valid.

following form

$$V_R = \frac{V_R^*}{1 + \frac{k_4}{k^*} P_{tot}} \quad (5-14)$$

Adding to V_R the yield of non-reactive volatiles (V_{NR})

$$V_{tot} = V_{NR} + \frac{V_R^*}{1 + \frac{k_4}{k^*} P_{tot}} \quad (5-15)$$

Equation 5-15 shows asymptotic behavior at pressure extremes. Estimating values of V_{NR} and V_R^* from the experimental asymptotes in Figure 4-9 and choosing an appropriate value for k_4/k^* , total yield may be calculated as a function of total pressure. Figure 5-7 illustrates the success of the model. At vacuum conditions yields have been corrected for estimated deposits on the screens (max. +3%).

Equation 5-15 represents a very simple-minded approach to the complex problem of simultaneous diffusion and secondary reactions of volatiles. It does explain surprisingly well the broad effects of pressure but the fundamental mechanisms of diffusion and secondary reactions are concealed in the convenient ratio k_4/k^* . Heating rate is seen to have a small effect at intermediate pressures suggesting that the ratio (k_4/k^*) is not independent of time-temperature history but the effect is small. One clue to the nature of the "reactive" species is the decreasing yield of tar with increasing pressure. The argument that tar is simply an intermediate in a series of reactions leading to coke is well-supported by this data.

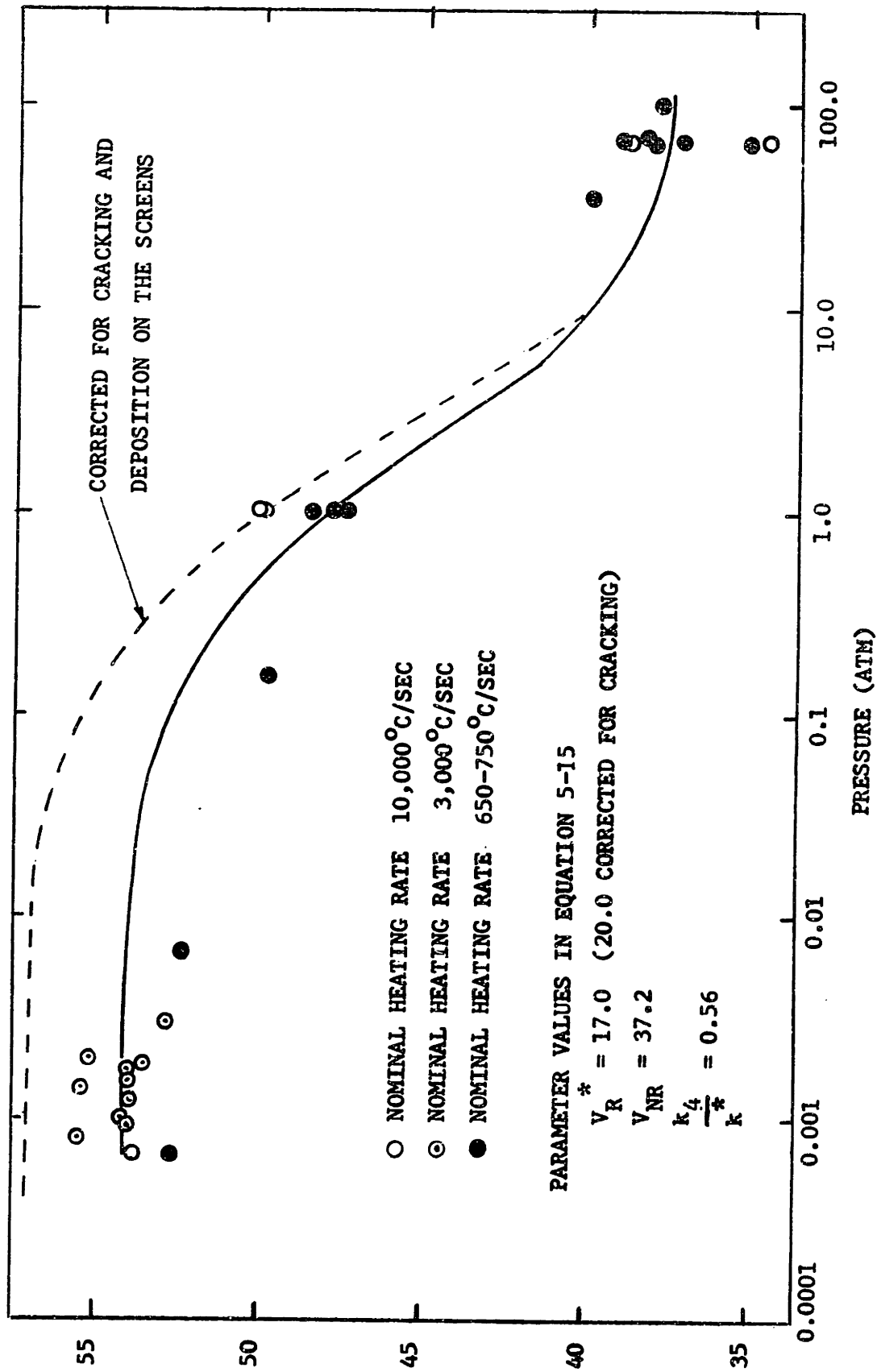


FIGURE 5-7 SECONDARY REACTION MODEL COMPARED WITH BITUMINOUS COAL DATA

5.3 HYDROGENATION MODEL

Continuing the line of argument supporting the existence of vapor-phase reactive species, a very probable effect of hydrogen would be to stabilize these species sufficiently to allow them to escape without further reaction. Accordingly, progressive disappearance of the tar is observed with increasing hydrogen pressure. Mathematically, Equation 5-8 may be modified with an additional term to account for the disappearance of reactive species by reaction with hydrogen

$$Q - K^*C - k_4C - k_5P_{H_2}C = 0 \quad (5-16)$$

k_5 is the reaction rate constant in $\text{atm}^{-1} \text{time}^{-1}$ and P_{H_2} is the partial pressure of hydrogen in atm. The hydrogenation reaction is assumed to proceed at a rate proportional to the concentration of volatiles and hydrogen. The overall material balance (Equation 5-10) must be modified to include the hydrogenated products as follows

$$\frac{dV_R}{dt} = (K^* + k_5P_{H_2})C \quad (5-17)$$

Continuing to duplicate the preceding mathematics we finally arrive at new expressions for Equations 5-13 and 5-15 respectively

$$V_R = V_R^* \left[\frac{K^* + k_5P_{H_2}}{K^* + k_5P_{H_2} + k_4} \right] \quad (5-18)$$

$$V_{\text{tot}} = V_{\text{NR}} + V_R^* \left[\frac{1 + \frac{k_5}{k^*} P_{H_2} P_{\text{tot}}}{1 + \frac{k_5}{k^*} P_{H_2} P_{\text{tot}} + \frac{k_4}{k^*} P_{\text{tot}}} \right] \quad (5-19)$$

Since estimates of V_{NR} , V_R^* , k_4/k^* were made from devolatilization data,

the only constant left to evaluate is the ratio k_5/k^* . With hydrogenation data from Figure 4-16 two values of k_5/k^* are tested in Figure 5-8. The results are interesting but not exceptionally good.

The inability of a single additional constant to explain hydrogenation prevents accurate representation of yields at both constant total pressure and in pure hydrogen. A good fit at low partial pressures of hydrogen ($P_{\text{tot}} = 69 \text{ atm}$) underpredicts yields at higher hydrogen concentrations as well as yields in pure hydrogen. The calculated minimum is more pronounced than the experimental data show.⁷ Rejection of the model, however, would be premature. Broad trends are still characteristic despite the descriptive limitations of the single rate constant k_5 . The mass transfer coefficient k^* and the deposition rate constant k_4 may change as the bulk gas phase undergoes transition from helium to hydrogen but these are expected to be small effects. More likely two other effects are responsible. First, hydrogen concentration in the particle may be limited by diffusion at high total pressures. Secondly, the hydrogen may also react with portions of the coal not volatile in inert gas. This latter point is especially satisfying when viewing the hydrogenation results with lignite (Figures 4-11 and 4-13). In Figure 4-11 two stages of hydrogenation were identified earlier. The initial rapid hydrogenation period is probably hydrogen stabilizing extremely reactive vapor phase species. (Their existence was suggested by the

⁷ Under conditions of pure hydrogen (where $P_{\text{H}_2} = P_{\text{tot}}$) Equation 5-19 goes through a minimum. Differentiating Equation 5-19 with respect to P and setting the result equal to zero, one obtains

$$P_{\text{min}} = k^*/k_5 \quad (5-20)$$

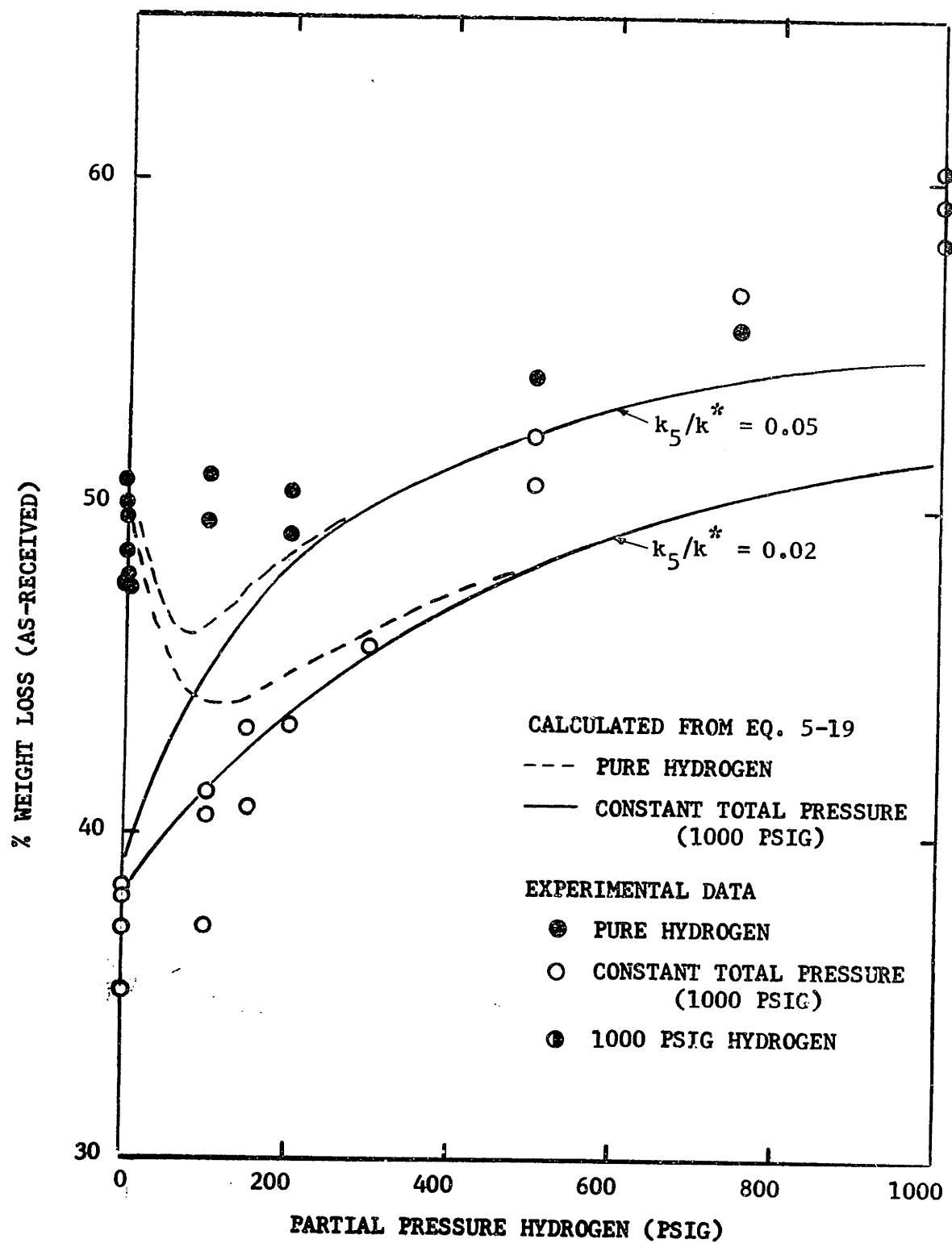


FIGURE 5-8 SECONDARY REACTION MODEL APPLIED TO HYDROGENATION RESULTS

appearance of cracking deposits on the screens at high vacuum with no change in measured weight loss). The slower second stage may be hydrogasification of the "solid" phase. Again, competitive reactions are hypothesized, hydrogenation to volatile products versus thermal stabilization to coke. If stabilization were slower in the solid phase than the gas phase, then this extended rate period would be accountable. Moseley and Paterson postulate just such a mechanism and the yield was found to be proportional to hydrogen pressure which is not inconsistent with the data in Figure 4-13. Incorporating these two effects, lower hydrogen concentrations at high total pressures and conversion of the "solid" phase, the fit can be improved markedly as indicated in Figure 5-9. Uncertainty in the data concerning the amount of this residual gasification occurring in bituminous coal limits the gain of extending this theory too far. (Calculational details are given in the Appendix.)

5.4 EFFECT OF PARTICLE SIZE

The final variable to be discussed and perhaps one of the most significant in terms of process design is particle size. Data in Figure 4-17 show that hydrogenation yields are substantially reduced as particle size is increased. Empirically, it is interesting to cross plot data from Figures 4-16 and 4-17, substituting the "effective" hydrogen pressure (from the curve at constant P_{tot}) for yield in Figure 4-17. The result is a correlation of "effective" hydrogen pressure versus particle size in Figure 5-10. The assumption is that

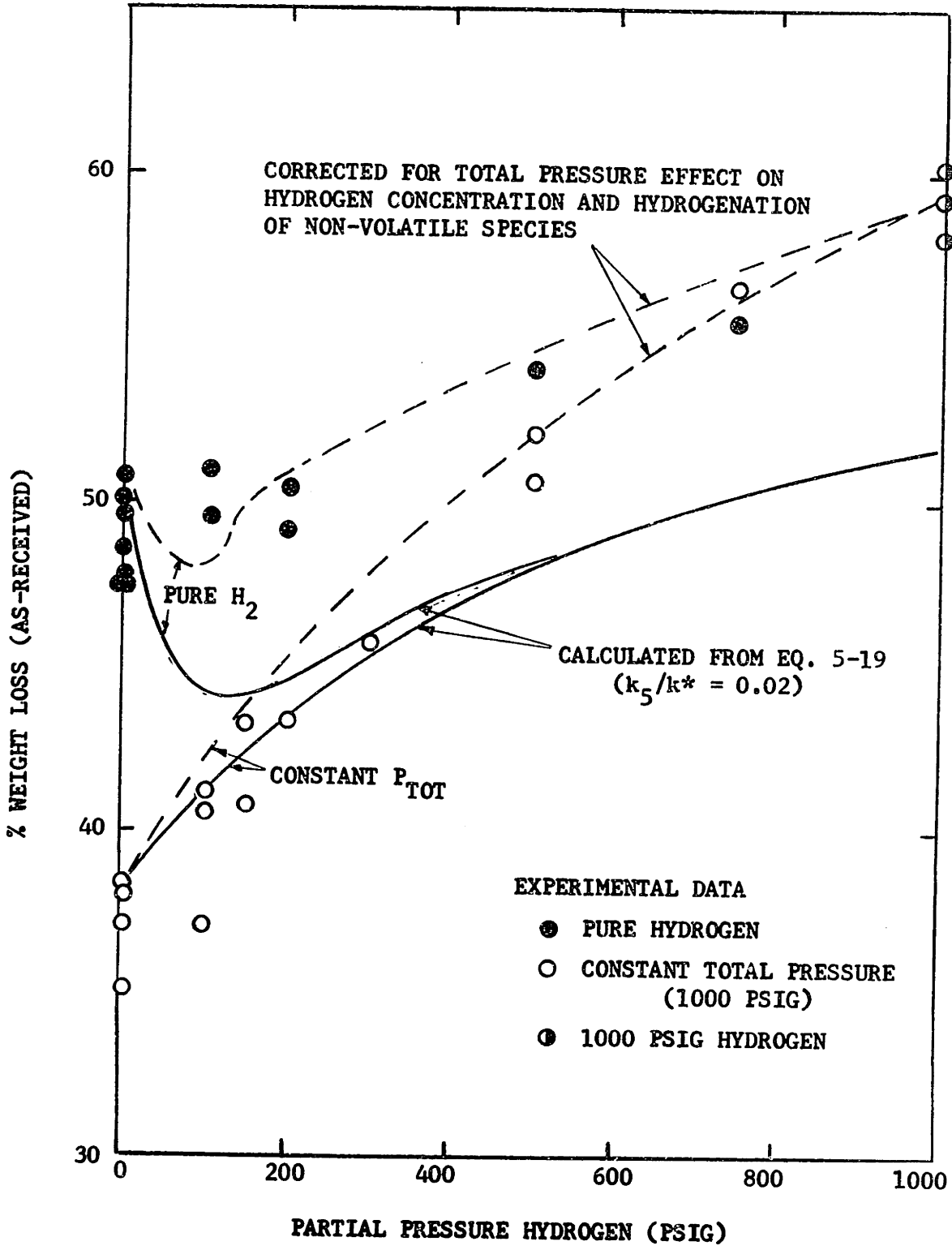


FIGURE 5-9 MODIFIED SECONDARY REACTION MODEL

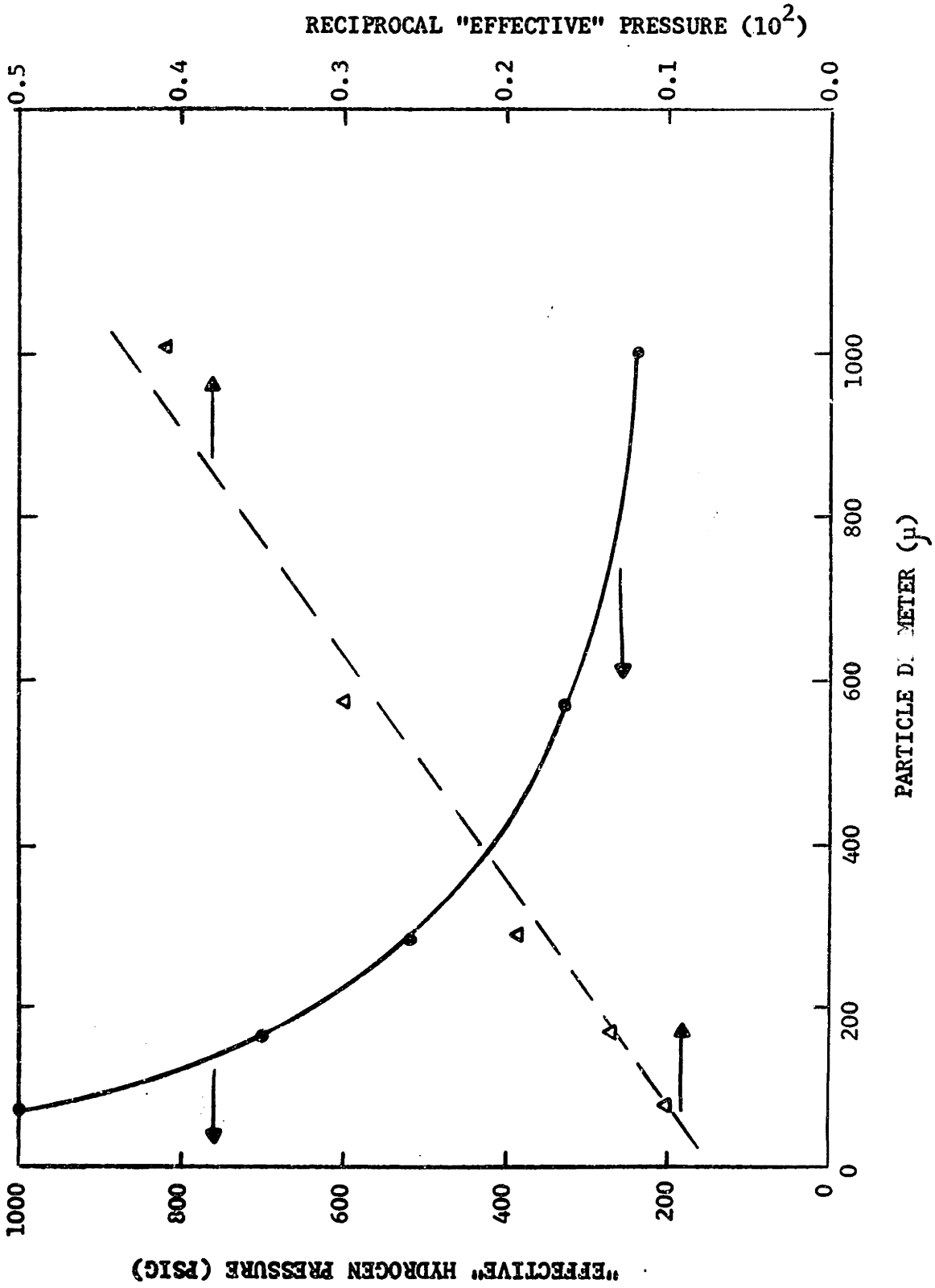


FIGURE 5-10 "EFFECTIVE" HYDROGEN PRESSURE AS A FUNCTION OF PARTICLE SIZE

particles in the 50-100 micron range actually see the full 1000 psig H₂ but the cross plot certainly casts doubt with regard to that conclusion. No effect was observed experimentally in using 100 micron particles versus 50 micron particles but the scatter in data would explain the absence of effect. It was impossible to use particles finer than 50 μ in the present apparatus to test the limits of this trend. Also in Figure 5-10 the reciprocal of the "effective" pressure is plotted against particle size showing a fairly linear correlation. This does provide substantial support for the previous argument that diffusion is affecting the hydrogen concentration. It is apparent one major problem in achieving high yields will be getting sufficient hydrogen in contact with the reactive species before they polymerize and crack.

6. COMPARISON OF RESULTS WITH PREVIOUS INVESTIGATIONS

The preceding section dealt exclusively with the findings of this specific study. Of course, the pyrolysis and hydrogenation of coal has been extensively researched and a great number of models and theory have been advanced. In this section, the intent is to first critically examine these previous models in light of the new experimental evidence and secondly to check for consistency between past experimental results and the models advanced in their study.

6.1 DECOMPOSITION MODEL

A traditional means of correlating pyrolysis rate data is the first order decomposition model; i.e. rate is proportional to unreacted volatile material remaining.

$$dV/dt = k(V^* - V) \quad (2-23)$$

While the findings of this study clearly reject so simple a picture, it does remain a convenient basis for comparing results from different workers. It was possible to take individual weight loss with time curves from this study and by assuming a constant V^* (estimated from weight loss at long times) correlate the data with a non-isothermal version of Equation 2-23. As long as the conditions were narrowly defined, it was possible to obtain reasonable fits as evidenced in Figures 6-1 and 6-2. Figures 6-1 and 6-2 are Arrhenius plots of the experimental rate constants as functions of

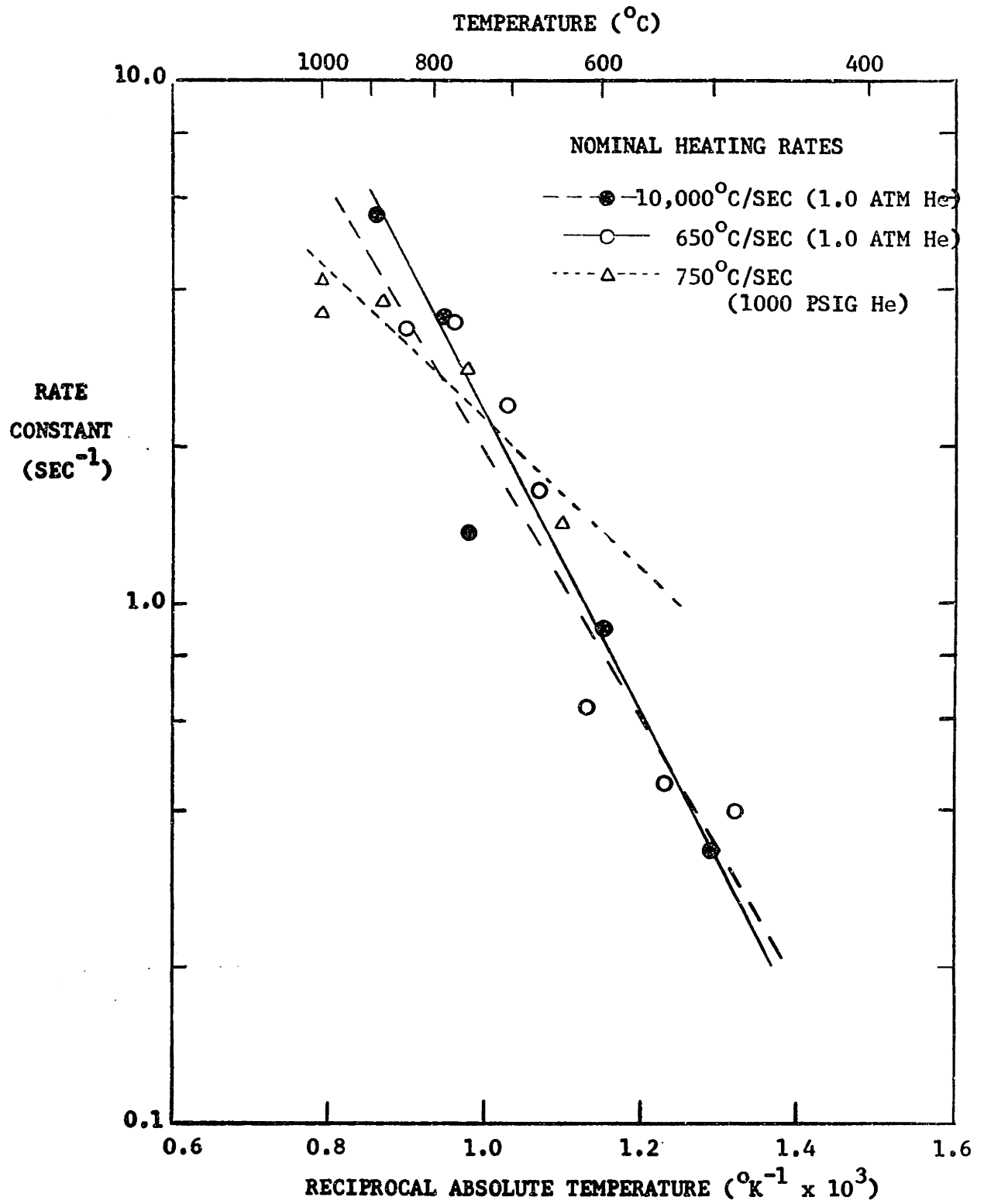


FIGURE 6-1 EXPERIMENTAL FIRST ORDER RATE CONSTANTS FOR BITUMINOUS COAL

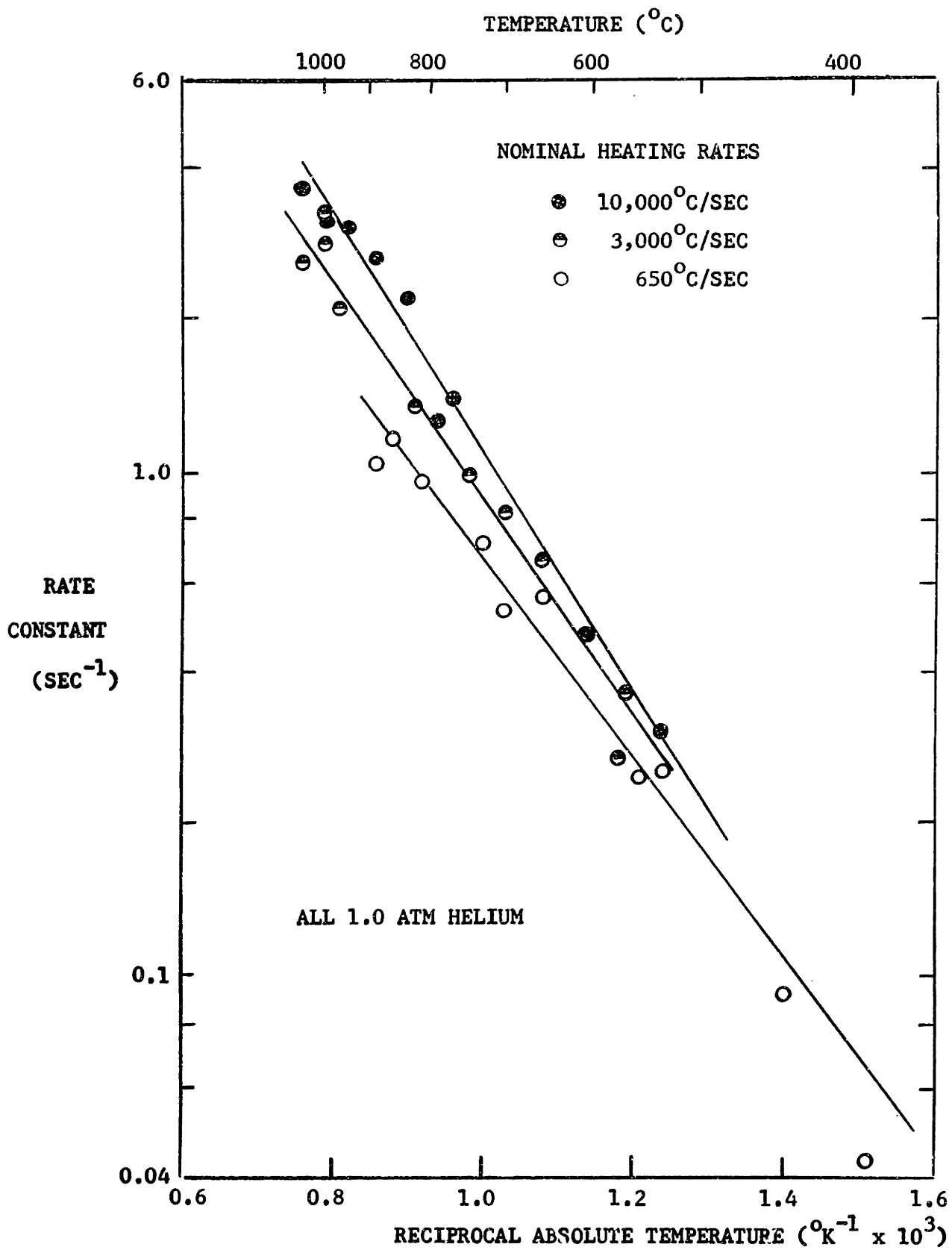


FIGURE 6-2 EXPERIMENTAL FIRST ORDER RATE CONSTANTS FOR LIGNITE

reciprocal absolute temperature.⁸ "Best fit" straight lines are drawn and the associated degree of fit are compiled in Table 6-1. The weakness of the model as a useful correlative tool is reflected in the fact that different values of k_0 and E were obtained for each particular set of conditions, though a single set of values would probably have been sufficient for the bituminous coal.

Figure 6-3 compares several of these curves with values reported in the literature. While there exists a great deal of discrepancy in the range of values the results of this study are clearly not out of line. One especially interesting comparison is between the curve reported by Badzioch and Hawksley (1967) for coal "B"

⁸The data points in Figures 6-1 and 6-2 are not taken from strictly isothermal conditions. Each point represents a finite heating and cooling period. The importance of the cooling period is indicated by the higher apparent rate constant obtained when it is neglected. These non-isothermal periods are converted into equivalent time at maximum temperature in the following manner. The equivalent time may be defined as

$$t_{eq} = \frac{\int k_0 \exp(-E/RT(t)) dt}{k_0 \exp(-E/RT^*)} \quad 6-1$$

with $T(t)$ = actual time-temperature history of the experimental run and T^* = designated temperature of the run (arbitrarily chosen as the maximum temperature). The integral sign \int signifies integration over the entire temperature cycle of a run. The experimental rate constant is then computed from the measured weight loss

$$k_{exp} = \frac{\ln(1-V/V^*)}{t_{eq}} \exp \quad 6-2$$

A standard least squares regression routine is used to select values of k_0 and E to achieve the best fit. The advantages of this approach are two-fold; it permits comparison of non-isothermal data in the customary fashion and provides for the inclusion of experimental fluctuations in temperature.

TABLE 6-1

EXPERIMENTAL FIRST ORDER RATE CONSTANTS FOR THIS STUDY

<u>Conditions</u>	<u>Activation Energy</u>	<u>Pre-Exponential Factor</u>	<u>Std. Deviation</u> (Wt. % Orig. Coal)
Bituminous Coal			
650°C/sec, 1 atm He	13.3 kcal/mole	1799. sec ⁻¹	+ 1.4 ± 3.8
10,000°C/sec, 1 atm He	11.8 kcal/mole	706. sec ⁻¹	+ 2.6 ± 5.9
750°C/sec, 1000 psig He	6.6 kcal/mole	61.9 sec ⁻¹	+ 0.7 ± 1.5
Lignite			
650°C/sec, 1 atm He	9.0 kcal/mole	60.7 sec ⁻¹	+ 0.6 ± 2.0
3,000°C/sec, 1 atm He	10.0 kcal/mole	128. sec ⁻¹	+ 0.5 ± 1.7
10,000°C/sec, 1 atm He	11.1 kcal/mole	283. sec ⁻¹	+ 0.5 ± 1.5
10,000°C/sec, 1 atm He	20.0 kcal/mole	290,000. sec ⁻¹	+ 1.2 ± 3.9

$$\sqrt{\frac{SSE}{n(n-2)}}$$

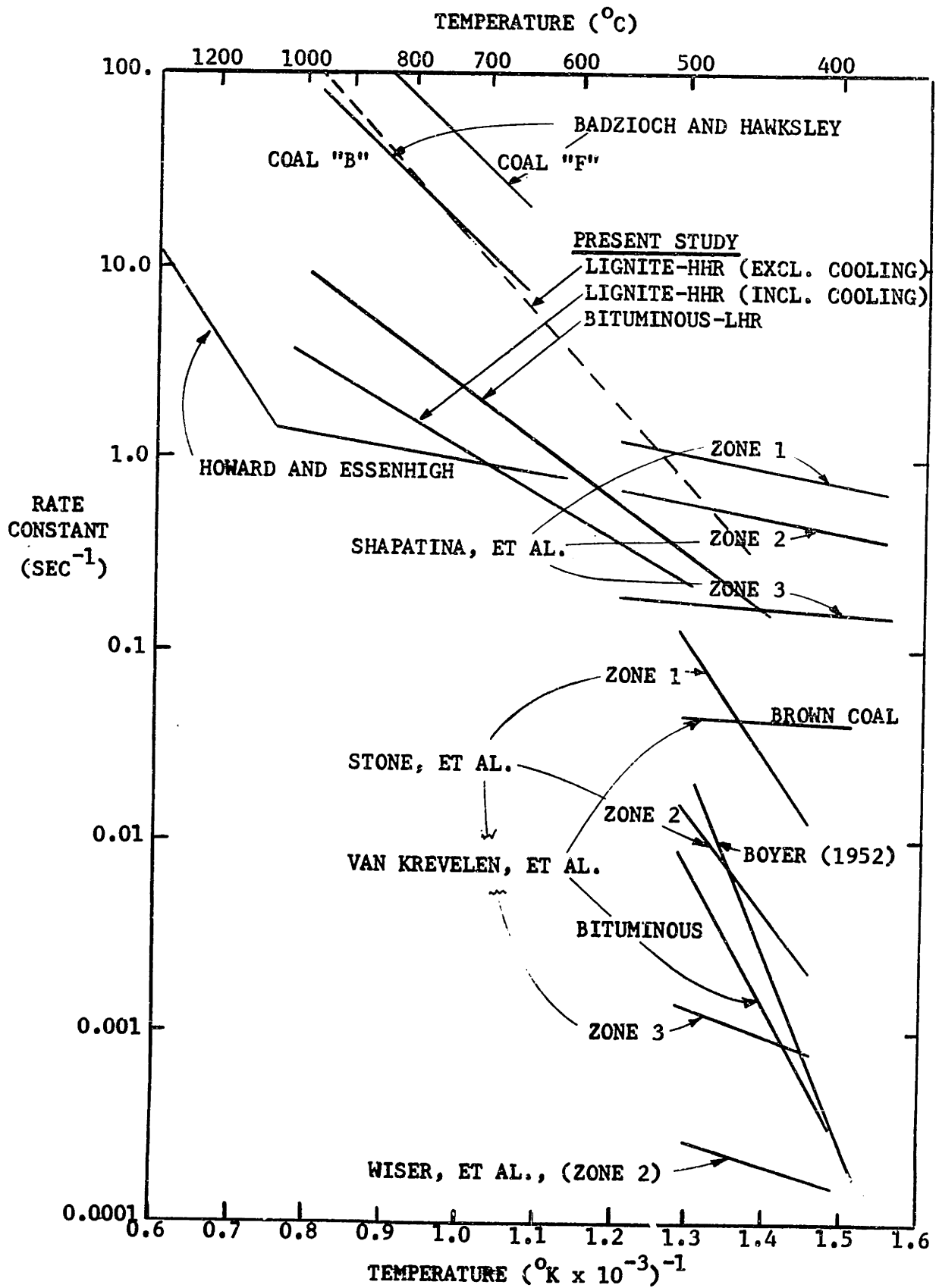


FIGURE 6-3 COMPARISON OF COAL DECOMPOSITION RATE CONSTANTS

and this study's results for lignite at high heating rate assuming the weight loss during cooling negligible. The low apparent activation energy cautions against such an assumption and this concern is confirmed by the significantly lower rate constant obtained when the cooling curve is included. However, the importance of the cooling curve is greatly diminished if we assume the true nature of the mechanism to be in accord with the statistical model where actual activation energies are quite large such that the reaction may be effectively quenched by cooling. The most important conclusion, though, is that a better model is demanded by the results.

The most compelling argument for rejection of Equation 2-23 is that yield, i.e. V^* , is a function of final temperature, a fact that is neither mechanistically consistent with nor mathematically amenable to Equation 2-23. Figure 6-4 offers a good illustration of how pyrolysis yields depend on temperature. The data of each investigator have been normalized to 100% yield at 1000°C, an observation consistent with all the previous work save that of Kimber and Gray (1967b). The various curves on the plot require some explanation. Dryden's (1957) generalized correlation is based on the slow carbonization of a large number of American and British coals. The curve shown is based on a coal having about 35-40% volatile matter (MAF). The curve is general in the sense that it will accommodate any coal by simply sliding the abscissa to the right or left ($\sim 50^\circ\text{C}$ to the left per 10% increase in VM_0). The Soviet experimental technique involved dropping coal particles through a heated chamber (residence time 0.45sec) and then catching them in a heat trap and "soaking" them for the duration of the run (Shapatina, et. al., 1960).

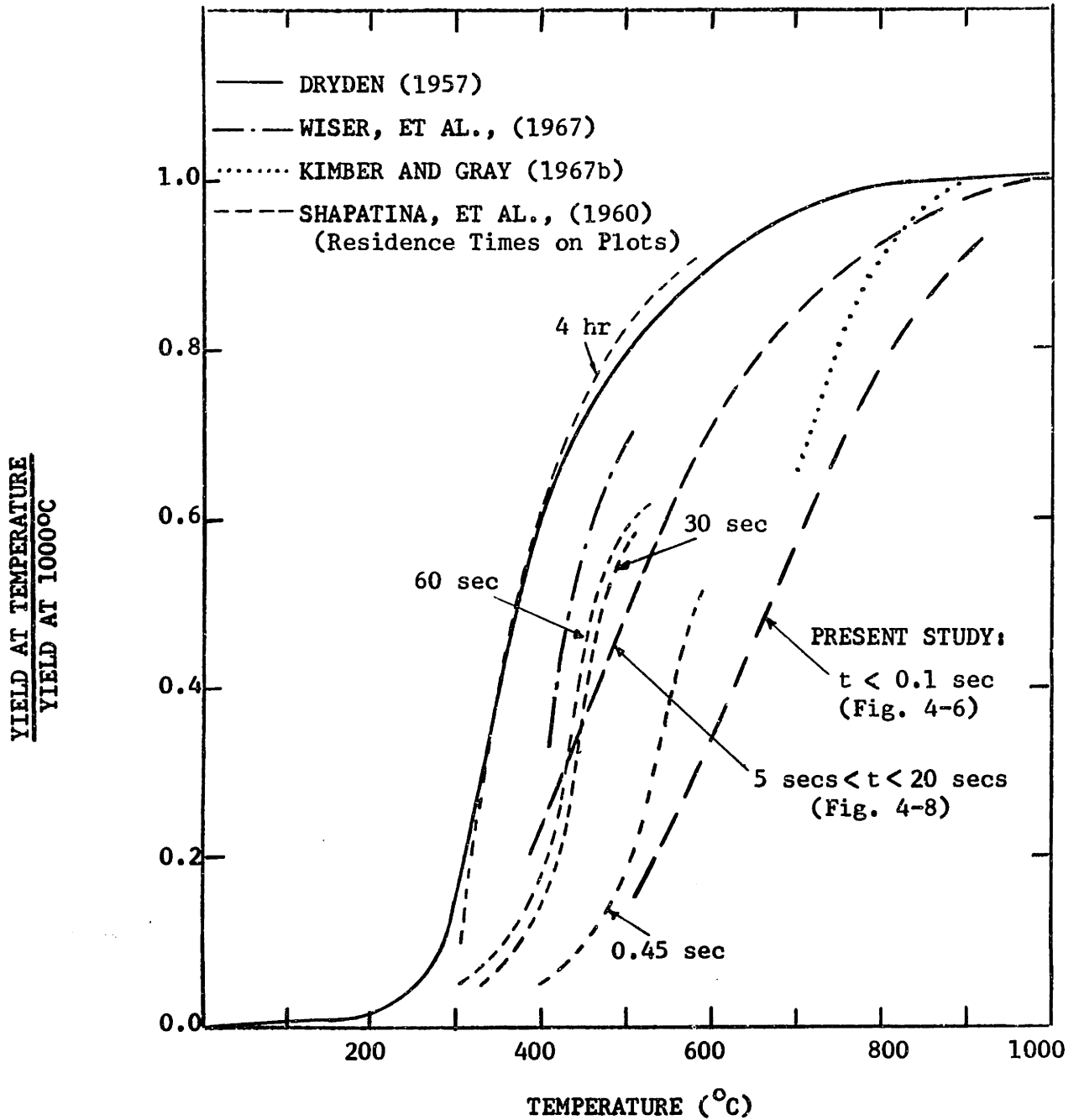


FIGURE 6-4 DEVOLATILIZATION YIELDS AS A FUNCTION OF TEMPERATURE

Particles soaked for 4 hours show a weight loss trend consistent with Dryden's prediction. At shorter residence times, 30-60 sec, the yields are less and they are diminished further if only the heat-up period of 0.45 sec is considered. The fact that the additional weight loss observed between 0.45 sec and 30 sec is roughly equivalent to the amount lost between 30 sec and 4 hours is strong evidence that there exists a very rapid initial decomposition followed by a very slow residual degasification. The BCURA results also for times much less than one second show a significant displacement from Dryden's correlation. Wiser, et. al., (1967) determined values of V^* by subtracting a final devolatilization stage he identified as a constant rate period. The yields from the present study of bituminous coal (long residence times, 5-20 secs) are in good agreement with the Soviet data at 30-60 secs. The conversions obtained from extremely rapid heating ($10,000^{\circ}\text{C}/\text{sec}$; conversion during heatup only) establish a trend similar to the Soviet yields at 0.45 sec. Since all data in Figure 6-4 were normalized to unity at 1000°C , the curves do not reflect yields in excess of proximate volatile content as observed by workers at BCURA as well as during the course of the present investigation. Dryden and Wiser used experimental techniques comparable to standard analysis methods and would not be expected to see changes in total yield at high temperatures. The Soviet workers used proximate analysis as a measuring technique and therefore would be unaware of influences of their disperse phase rapid heating.

Methods by which this temperature-dependent behavior may be modelled are not well-established. Chuckhanov theorizes that coal

decomposition takes place through a combination of parallel and consecutive reaction each of different kinetic characteristics. (Shapatina et. al, 1960). However, we have no specific details of such a model. Wiser, et. al, has treated all data isothermally, integrating first and second-order versions of Equation 2-26 and then inserting an appropriate value of V^* depending of the temperature level. Similarly, Badzioch and Hawksley (1967) correlated data with an expression derived by isothermal integration of Equation 2-23, substituting a temperature dependent function for V^* . The problem with this approach is that neither of these two investigators considered the difficult integration involved in non-isothermal cases where a finite heating period exists. Badzioch and Hawksley claimed little decomposition occurred during their extremely rapid heat-up and Wiser, et.al, simply neglected any weight losses before their sample reached desired temperature (~ 5 minutes to reach temperature). In the latter case this omission amounted to the 497°C sample being 60% devolatilized (based on V^*) before the initial reading was taken. A glance at Figure 6-4 indicates that this includes nearly all of the rapid devolatilization period and as a result any rate determinations would merely be an average over an undefined temperature history. This same difficulty has confounded nearly all investigators attempting to evaluate coal decomposition kinetics isothermally. Such information is highly questionable at best.

Pitt's (1962) recognition of this problem led him to adapt Vand's (1943) technique of accomodating a large number of independent, parallel rate processes. Essentially, this method is the statistical decomposition model described in the preceding section. Pitt applied

this model in a slightly different fashion, though, by selecting a value for k_0 and then constructing a distribution of activation energies to best fit his weight loss data. The results are not considered reliable in the initial stages of decomposition due to Pitt's inability to sample his fluidized bed at solids residence times less than 10-15 secs. For example, the initial sample of coal was 62% devolatilized at 450°C and 89% devolatilized at 650°C (based on devolatilization at 100 minutes). Furthermore, Pitt's determination of weight losses by differences in proximate volatile content of coal and char excluded the possibility of yields greater than proximate. However, it is interesting to compare the form of Pitt's distribution of activation energies with the Gaussian distribution estimated for lignite in this study (see Figure 6-5). Pitt used a Binley coal containing 46.2% (MAF) volatile matter identical to the proximate volatile contents of both coals used the present study. The graphical comparison was made using the distribution estimated from lignite since the distribution for bituminous coal was based only on high pressure data and does not contain the higher activation energies associated with those species participating in secondary reactions. In the course of this comparison it must be remembered that Pitt used a fixed value of k_0 ($1.67 \times 10^{13} \text{ sec}^{-1}$) while in the present study the value was estimated directly from the lignite data ($k_0 = 1.07 \times 10^{10} \text{ sec}^{-1}$). A partial consequence of this lower pre-exponential factor is a shift in the distribution to lower activation energies. Data from this study were refit to the statistical model this time using Pitt's assumed value of $k_0 = 1.67 \times 10^{13} \text{ sec}^{-1}$. The expected shift to a higher mean activation energy (56.28 vs 48.72 kcal/mole) is observed

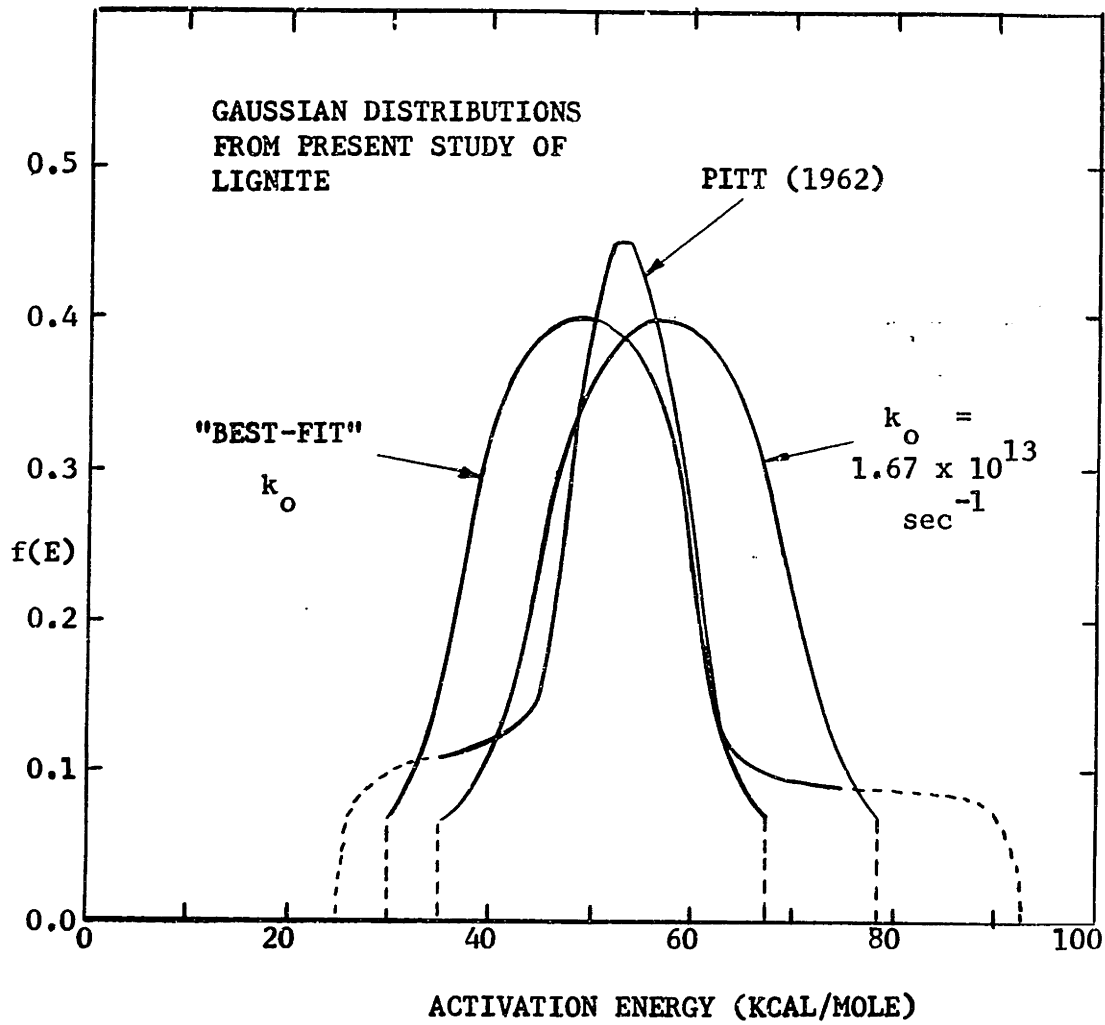


FIGURE 6-5 COMPARISON OF ACTIVATION ENERGY DISTRIBUTIONS

with the distribution width virtually unchanged ($\sigma = 10.91$ vs 9.38 kcal/mole previously). The very high values of E determined by Pitt are consistent with his much longer residence times which would include the slow residual devolatilization. Allowing these discrepancies the Gaussian distribution duplicates the shape of Pitt's constructed distribution very well.

Use of the higher value of k_0 is justified, at least to some extent, on theoretical grounds. From transition-state theory the frequency factor is calculated to have a value around 10^{13}sec^{-1} . This is roughly equivalent to the pre-exponential factor (k_0) in the Arrhenius expression if the entropy of activation does not differ too greatly from zero (Benson, 1968). Summary values of the rate parameters and associated error with the higher value of k_0 for both coals are given in Table 6-2. For lignite the change results in a negligible increase in error and while the error increase is larger for bituminous coal, it nevertheless appears, from a practical standpoint, a perfectly adequate simplification of the model.

Another interesting characteristic of the statistical distribution model is that it offers a plausible explanation for the low activation energies typically found in simple first order correlations. The observed low activation energies, typically less than 20 kcal/mole (~ 10 kcal/mole in this investigation), have caused considerable concern as to whether chemical kinetics are controlling and indeed prompted Berkowitz (1960) to reject chemical kinetics in favor of a diffusion process. The experimental technique employed in this study would cancel any rate limitations by diffusional processes and permit direct measurement of chemical kinetics. In a similar vein Juntgen and Van Heek (1970) demonstrated by calculation that a set of overlapping,

TABLE 6-2
EFFECT OF PRE-EXPONENTIAL FACTOR CHOICE ON
STATISTICAL DISTRIBUTION PARAMETERS

Lignite

k_0 (sec ⁻¹)	1.07×10^{10}	1.67×10^{13}
E_0 (kcal/mole)	48.72	56.28
σ (kcal/mole)	9.38	10.91
SSE	0.013452	0.013779
S	$\pm 1.73\%$	$\pm 1.75\%$
S'	$\pm 0.25\%$	$\pm 0.25\%$

Bituminous Coal (1000 psig)

k_0 (sec ⁻¹)	2.91×10^9	1.67×10^{13}
E_0 (kcal/mole)	36.89	50.65
σ (kcal/mole)	4.18	7.01
SSE	0.005022	0.0075881
S	$\pm 1.85\%$	$\pm 2.29\%$
S'	$\pm 0.42\%$	$\pm 0.52\%$

independent, parallel first-order reactions could be approximated by a single first-order expression having both lower activation energy and pre-exponential factor than any of the reactions in the set. This is, of course, in accord with experimental findings of the present study. Also, calculations were performed to illustrate this important phenomena. Weight loss with time curves from four hypothetical independent first-order reactions (each having a $k_0 = 2 \times 10^{10} \text{ sec}^{-1}$ and with activation energies of 47,50,53, and 56 kcal/mole, respectively) were added together and approximated successfully by a single first order expression with $k_0 = 1.6 \times 10^6$ and $E = 30.4$ kcal/mole.

The continuous behavior of yield versus temperature coupled with virtual independence of residence time strongly supports the existence of very steep energy barriers that may only be overcome with increases in temperature. Juntgen and Van Heek have focused most of their experimental work on the evolution kinetics of particular volatile species ($C_1 - C_4$). The implication was that each volatile species would represent a specific fundamental reaction within the coal structure. However, the evidence showed that the formation of the major volatiles also involved complex sets of reactions, thus forcing definition of activation energy distributions for each species. To calculate the weight loss from such a large set of equations is an extremely cumbersome task and in fact impossible since all evolving species have not been measured.

Van Krevelen, et al., (1956 and 1961) have pictured coal decomposition as a series of consecutive reactions (Coal \rightarrow Metaplast \rightarrow SemiCoke \rightarrow Coke) with primary volatiles formed in the resolidification of the metaplast and secondary gas evolved during the final coking stage.

Recognizing the inadequacy of this simple sequence in explanation of temperature-dependent yields, Chermin and Van Krevelan (1957) theorized that secondary gas evolution from semi-coke could become progressively more difficult with extent of reaction. Mathematically, this was expressed as a conversion-dependent activation energy

$$\frac{dV}{dt} = k_0 (V^* - V) e^{-(E_{\max} - a(V^* - V))/RT} \quad (6-3)$$

On reflection it is seen that Equation 6-3 will have the descriptive powers of statistically distributed activation energies. Since both models are approximations to a real situation undoubtedly involving both parallel and consecutive reactions, the choice is arbitrary though the mathematics of Equation 6-3 are decidedly less tractable in non-isothermal situations (where the exponential term is a function of both conversion and time).

6.2 SECONDARY REACTION MODEL

It has also been argued that rapid devolatilization can result in yields significantly greater than indicated by proximate analysis. The accumulated evidence is compiled in Table 6-3. A large number of American, British and French coals have been tested with the ratio of V^*/VM_0 varying from 0.75-1.36. Changes in heating rate by these investigators from 600-50,000°C/sec, however, produce very little effect as substantiated by our work with bituminous and lignite coals. A second important observation is that not all coals give yields in excess of proximate volatile content. While it is claimed by the BCURA workers that yields have been achieved as high as 80%

TABLE 6-3

COMPARISON OF EXPERIMENTAL YIELDS WITH PROXIMATE VOLATILES

<u>Investigators</u> & <u>Coals</u>	Proximate <u>Volatiles (VM₀)</u>	<u>V*</u>	<u>V*/VM₀</u>	
Loison and Chauvin (1964)	(MF)			(to 1100°C at 1500°C/sec)
Maigre Oignies	8.4	8.4	1.00	
Bergmannsgluck	18.1	23.6	1.30	
Emma	20.4	24.5	1.25	
Lens-Lieven	24.4	26.7	1.09	
Flenus de Bruay	31.0	39.6	1.18	
Wendell III	33.9	34.5	1.02	
Faulquemont	36.4	36.7	1.01	
Rau and Robertson (1966)	(MF)			(to 950°C at 600°C/sec)
Colver (MVB)	25.3	19.	0.75	
Kopperston #2 (HVAB)	31.6	36.	1.14	
Federal (Pitts HVAB)	37.7	49.	1.30	
Elkol (Wyo. Subbit.)	40.7	48.	1.17	
Orient #3 (HVB)	44.0	41.	0.93	
Mentser, <u>et al.</u> , (1973)	(MF)	(Peak Wt. Loss)		(to 1200°C at 8000°C/sec)
Pocohontas #3	16.8	18.5	1.10	
Lower Kittanning	25.3	30.8	1.22	
Pittsburgh	35.1	47.9	1.36	
Rock Springs	37.7	42.4	1.12	
Colchester	48.0	55.8	1.16	
Badzioch and Hawksley (1970)	(MAF)		Q(1-C)	(to 950°C at 20-50,000°C/sec)
NCB 203 (K)	17.7	17.7	1.00	
NCB 301a(J)	22.7	20.6	0.91	
NCB 301b(H)	25.2	26.0	1.03	
NCB 602 (E)	34.3	44.2	1.29	
NCB 401 (G)	34.4	35.1	1.02	
NCB 601 (F)	35.3	45.1	1.28	
NCB 802 (D)	36.1	47.0	1.30	
NCB 902 (B)	36.4	40.0	1.10	
NCB 802 (C)	37.8	42.8	1.13	
NCB 902 (A)	37.9	42.9	1.13	
Present Study	(As-Rec'd)			(MF) (to 1000°C)
Pitts Bituminous				
LHR--650°C/sec	41.46	47.9	1.15	1.16
HHR--10,000°C/sec	"	50.0	1.20	1.21
Montana Lignite	44.66	40.6	0.91	0.89

(value of Q in Equation 2-24) in excess proximate volatile content, intercomparisons of work necessitate use of a common basis, in this case values of V^* which diminish these claims somewhat. It should be remembered, though, that the very short residence times associated with the data in Table 6-3 are not sufficient to completely devolatilize the char. This finding is supported not only by our work but also the findings of Shapatina, et al., (1960), Badzioch (1967) and Howard (1967). Table 6-4 contains results from studies at lower temperatures (500-600°C). Both Sass (1972) and Peters (1960) found continuous coal flow schemes with rapid heating giving significantly higher yields than the standard Fisher retort method.⁹ The major change in the volatiles was observed primarily in the yields of tar. On the other hand, Soviet researchers upon changing the heating rate of a given apparatus observed essentially no change. The tar content of this Moscow brown coal was also seen to be quite small (as with our lignite). Mazumdar and Chatterjee (1973) found that the dimensions of the coke charge were quite significant in determining volatile yields. Heating rate was a contributing factor but not nearly as important as bed width.

A number of experiments were carried out at M.I.T. with a proximate analysis apparatus using crucibles of different sizes and a basket to heat up samples at rates slower than were possible with the electrical strip furnace. A pseudo-heating rate effect on

⁹The Fischer retort procedure involves slowly heating 20 to 100 grams of coal to a designated temperature (400-600°C) and holding it there until evolution of volatiles ceases. The coal is heated in a special aluminum retort with an outlet tube leading a condenser where liquid products are collected (Fischer, 1925).

TABLE 6-4
LOW TEMPERATURE YIELDS

<u>Investigators</u>	<u>Coal</u>	<u>Proximate Volatiles</u>	<u>V</u> [*]	<u>Tar</u>	<u>Gas</u>	<u>Water</u>	<u>V</u> [*] / <u>VM</u> ₀	<u>Method</u>
Sass (1972)	W. Kentucky HVB	41.0(MF)	30.7	16.3	5.0	9.4	0.75	Fischer Assay 500°C Transport Reactor at 500°C
		41.0	41.3	33.0	6.6	1.7	1.01	
Peters (1960)	Furst Leopold	31.0(MF)	29.3	11.2	10.0	8.1	0.95	Fischer Assay 600°C Fluid Bed 600°C
		31.0	33.2	18.7	7.0	7.5	1.07	
Shapatina, et al., (1960)	Moscow Brown Coal	34.5(MF)	22.5	4.6	11.9	6.0	0.65	Slow Heating 5°C/min Rapid Heating to 500°C
		34.5	21.7	4.0	8.1	9.6	0.63	

bituminous coal yields is seen from these experiments in Figure 6-6. It is termed a "pseudo-effect" since the most significant changes in yield are observed at transitions in apparatus or procedure rather than changes in heating rate although the latter does have some influence. A partial correction for the residual volatile content of the chars from short duration runs at very high heating rates is included on the plot which only serves to further emphasize the need to get volatiles away from hot surfaces. Likewise, the sample size in the standard proximate analysis apparatus can result in significant differences if the deposits formed on the crucible are accounted for in total yield. This latter effect is explored in greater detail in Figure 6-7 where the ratio of yield to proximate volatile content is plotted as a function of sample size. The cube root of total sample mass is used as a measure of path length in crucible experiments. To put results from the electrical strip furnace on a similar basis the mass of a single particle is used as more representative of sample size for the system geometry. As this "path length" is decreased a substantial increase in the yield of volatiles is observed. A smooth curve with a very steep upward trend results when the residual volatile content of the chars from short duration runs is allowed for in the data. Similar findings have been reported by Mazumdar and Chatterjee (1973) and Gray, et al., (1973) although very small sample dimensions (approaching single particles) were not studied in either investigation.

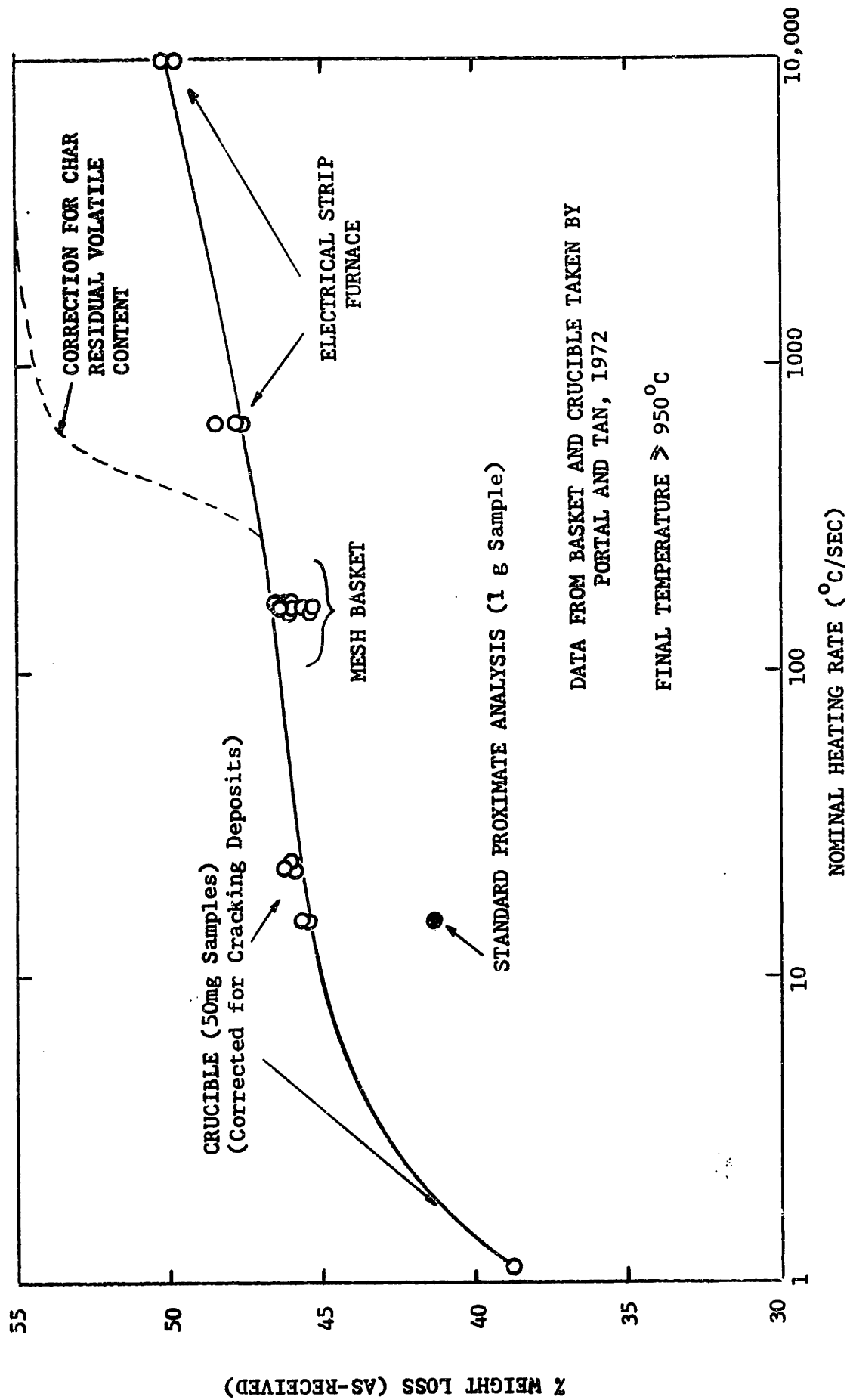


FIGURE 6-6 PSEUDO-EFFECT OF HEATING RATE ON BITUMINOUS COAL YIELDS

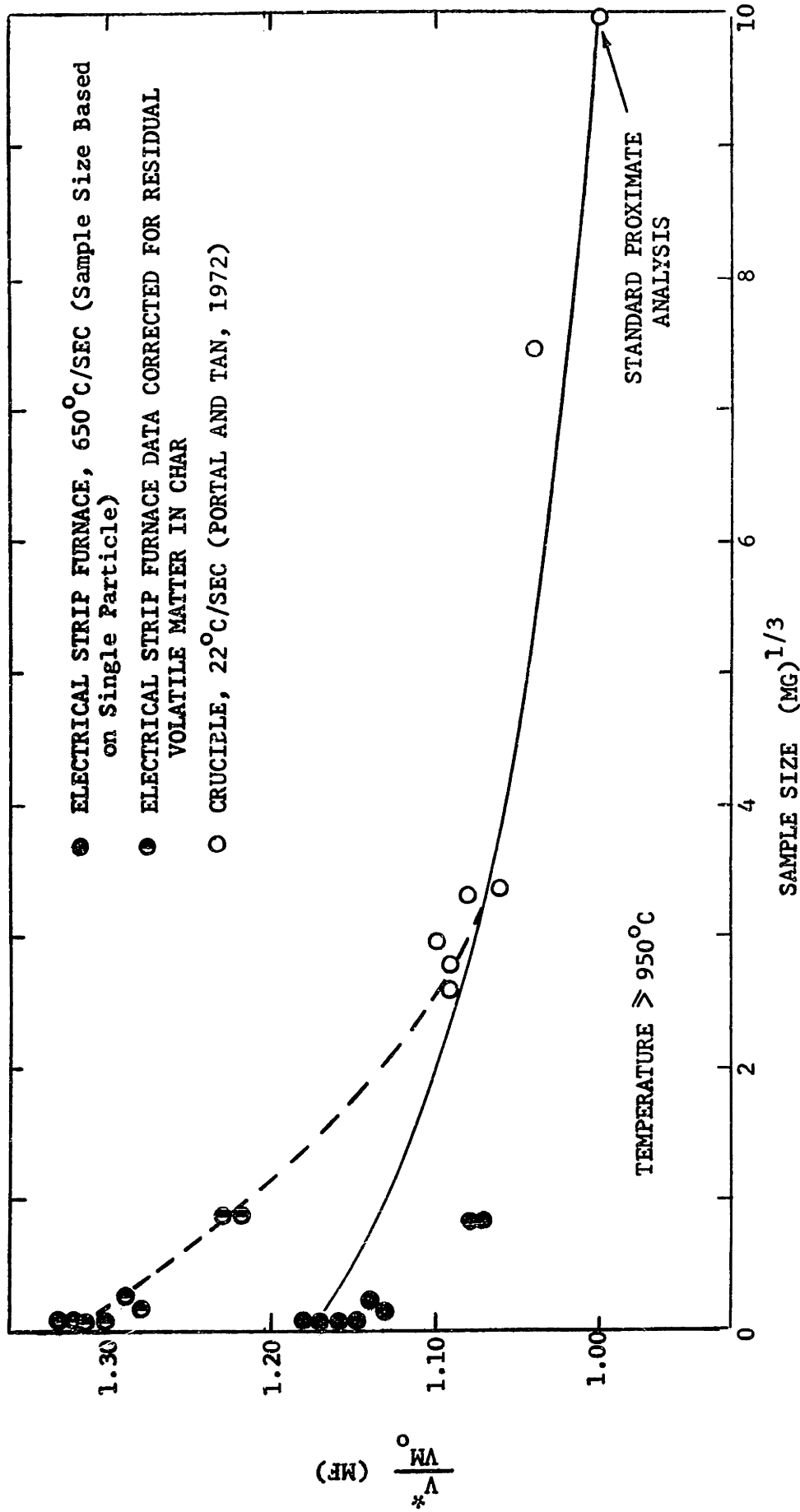


FIGURE 6-7 EFFECT OF SAMPLE SIZE ON BITUMINOUS COAL YIELDS

It is generally agreed that secondary reactions are responsible for these variations in yield, though Yellow (1965) and Van Krevelen, et al., (1956) have suggested the possibility of fragments of coal substance (metaplast) being physically carried away by rapidly escaping gases. There is also broad support for the contention that these reactions are primarily concerned with the tar fraction of the volatiles. The increasing tar/gas ratio with increasing yields coupled with the known instability of the tarry species compared to the gaseous volatiles gives considerable weight to this position. At this stage, disagreement exists over whether the primary volatiles are relatively small free radical ring structures or large condensed ring structures (essentially identical to the tar that will be ultimately evolved). ESR spectra by Bond (1968) with Den Hertog and Berkowitz's (1960) devolatilization work in the presence of a known free radical scavenger, nitric oxide, do support the existence of free radical processes but the size of the species remains undetermined. In a hydrogen deficient environment, the small species would polymerize to coke unless they could escape as tar at some intermediate stage of polymerization. The escaping tar might also undergo cracking reactions producing coke and gas. Mazumdar and Chatterjee have discounted this latter reaction since they observed no increase in gas yield as tar was lost in larger beds. However, Peter's data in Table 6-3 definitely shows an increase in gas yield under retort conditions. Presumably, both mechanisms, cracking and polymerization, are involved but their relative extents are unestablished.

Regardless of the exact nature of the secondary reactions, their extent is strongly influenced by the residence time and concentration of reactive species in contact with hot surfaces. Large packed beds and the accompanying slow rate of heating virtually insure a minimum yield of volatiles by providing sufficient surface area and residence time for the secondary reactions. Similarly, devolatilization at elevated pressures retards the diffusional escape of these reactive species increasing internal concentrations and thus the rate of secondary reactions. Consistent with the findings of this study, Belt, et al., (1971) discovered that highest yields of char were obtained from their entrained flow carbonizer at highest inert gas pressures. The above arguments are not to be taken as proof of a diffusion limited rate process. For even at a fixed rate of volatile escape (chemical reaction controlled) reduction of the overall mass transfer coefficient by increased total pressure would still increase the internal concentration of reactive species and diminish total yield. In this sense, the model proposed here must be clearly distinguished from the simple diffusion rate controlled models advanced by Essenhigh (1963) and Berkowitz (1960) which did not consider the role of secondary reactions.

6.3 HYDROGENATION

As with the devolatilization results essentially the only existing basis for comparison of hydrogenation rate data is a first order version of Equation 2-7

$$\frac{dV}{dt} = k_o e^{-E/RT} P_{H_2} (V^* - V) \quad (6-4)$$

Results with bituminous coal and lignite at 1000 psig H_2 have been correlated with this model and the best fit rate constants are plotted in Figure 6-8. Actual data for the bituminous coal are included using the equivalent time at temperature technique described previously. Activation energies are again quite low, 5.5 kcal/mole for bituminous coal and 4.8 kcal/mole for lignite. Results of Feldmann, et al., (1972) with Pittsburgh coal at 1000 psig are plotted and show exceptionally good agreement. Juntgen, et al., (1973) data for methane evolution (major hydrogenation product) and Feldmann's (1970) data at 3000 psig exhibit lower apparent rate constants. At low temperatures, Wiser et al., (1971) reports catalytic hydrogenation results which are again not too far out of line. The principle conclusion to be drawn from the plot is not that hydrogenation of coal has been successfully modelled, but rather that data obtained by the present and by other widely varying experimental techniques are nevertheless comparable in magnitude. The literature values in Figure 6-8 are not good. First, devolatilization yields are unaccounted for in Equation 6-4 causing an apparent pressure dependency on the rate constant (eg., Feldmann's results at 1000 and 3000 psig). Feldmann, at the higher pressure, did attempt to

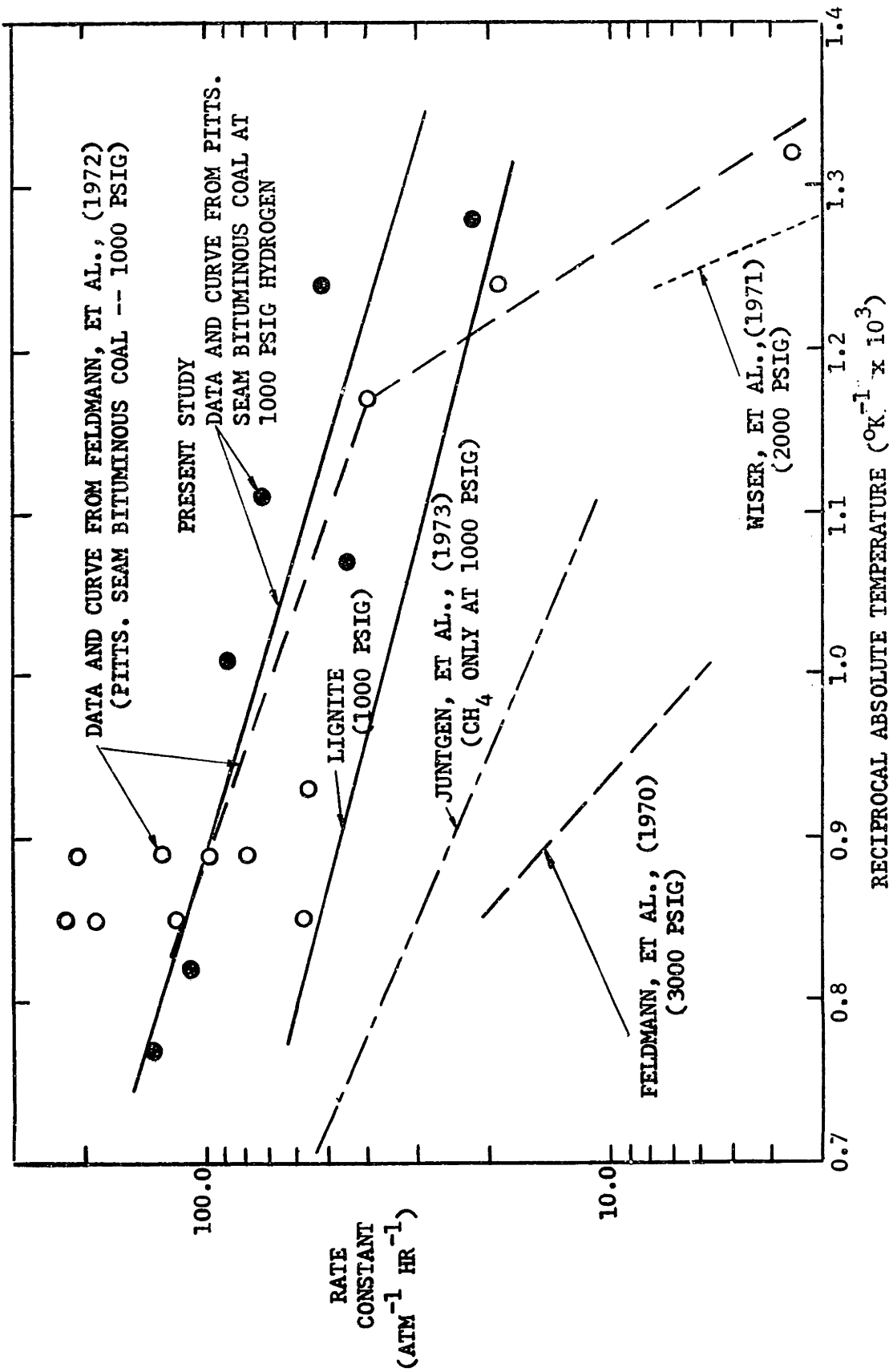


FIGURE 6-8 COMPARISON OF HYDROGASIFICATION RATE CONSTANTS

correct for devolatilization by providing an initial condition of instantaneous yield in Equation 6-4. There is no explanation, however, as to why this computed constant should decrease from 0.22 at 725°C to 0.14 at 900°C, nor why it is so very low. Such results place great doubt on the validity of such a model. The curves by Juntgen, et al., and Wiser, et al., are also questionable in terms of direct comparison since they were obtained at very low heating rates and extend over a minimum time scale of 10 minutes or more. Completely disenchantment with the model is reached upon realization that yield, V^* , is a function of hydrogen pressure, temperature and particle size.

Invoking mechanistic considerations, Moseley and Paterson first suggested a model to account for yield dependency on hydrogen pressure

$$\frac{dx}{dt} = k_3 P_{H_2} C_o^* e^{-k_2 t} \quad (2-11)$$

$$x = \frac{k_3 P_{H_2} C_o^*}{k_2} \quad (\text{at long times}) \quad (2-13)$$

The model indicates that the rate of conversion ($\frac{dx}{dt}$) is proportional to hydrogen pressure and the concentration of an exponentially decaying active species. At long times, the expression for yield is proportional to hydrogen pressure. This model and the original data are plotted in Figure 6-9. Data from Hiteshue, et al., (1962b, 1964) are also included showing general agreement except that the data bend downward sharply near the axis. The Moseley and Paterson model is extrapolated linearly to proximate volatiles content, however, the

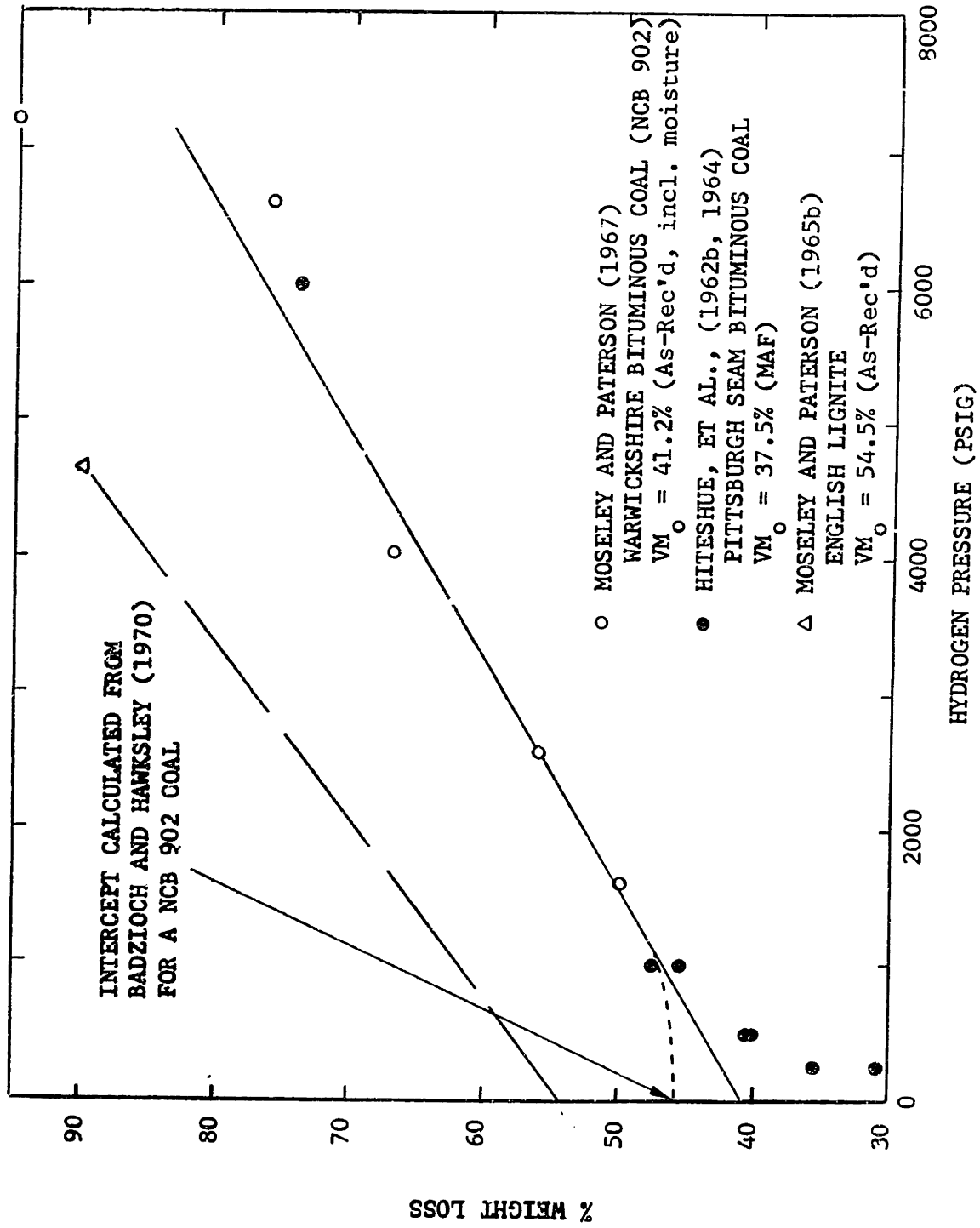


FIGURE 6-9 YIELD AS A FUNCTION OF HYDROGEN PRESSURE

results of this and several other studies using disperse phase rapid heating techniques suggest this may underestimate yield at zero hydrogen pressure. Since Badzioch and Hawksley worked with a similar British Coal (NCB 902), their experimental ratio of $V^*/VM_0 = 1.13$ has been used to calculate a more appropriate intercept (indicated by the dotted line). The trend is decidedly more in line with the present study's findings for bituminous coal in pure hydrogen. Part of the explanation for Hiteshue's steeper initial slopes is that the experiment was conducted at relatively low heating rates in a packed bed. In the absence of hydrogen the tar-forming species would probably all be lost in secondary reactions. It might be expected then that, despite the use of pure hydrogen by Hiteshue, his results would nevertheless be more analogous to data of the present study at constant total pressure which also showed a fairly steep slope at low pressures. This hypothesis is pursued in more detail in Figure 6-10 where data only in the range of 100 atm are examined. Here the calculated behavior of Moseley and Paterson's results are seen trendwise in good agreement with bituminous coal yields in pure hydrogen. Yields at constant total pressure follow a steeper slope, again paralleling Hiteshue's findings. Extrapolation of the Moseley and Paterson work with English lignite in Figure 6-11 gives a slope over this range in pressure not too different from the present work with lignite.

The yields obtained at very high pressures by Moseley and Paterson and Hiteshue are large enough to validate the conclusion that hydrogasification of the solid phase is probably occurring. Over the range of pressures studied in this investigation (to 100 atm) the amount of such conversion is probably small. The above

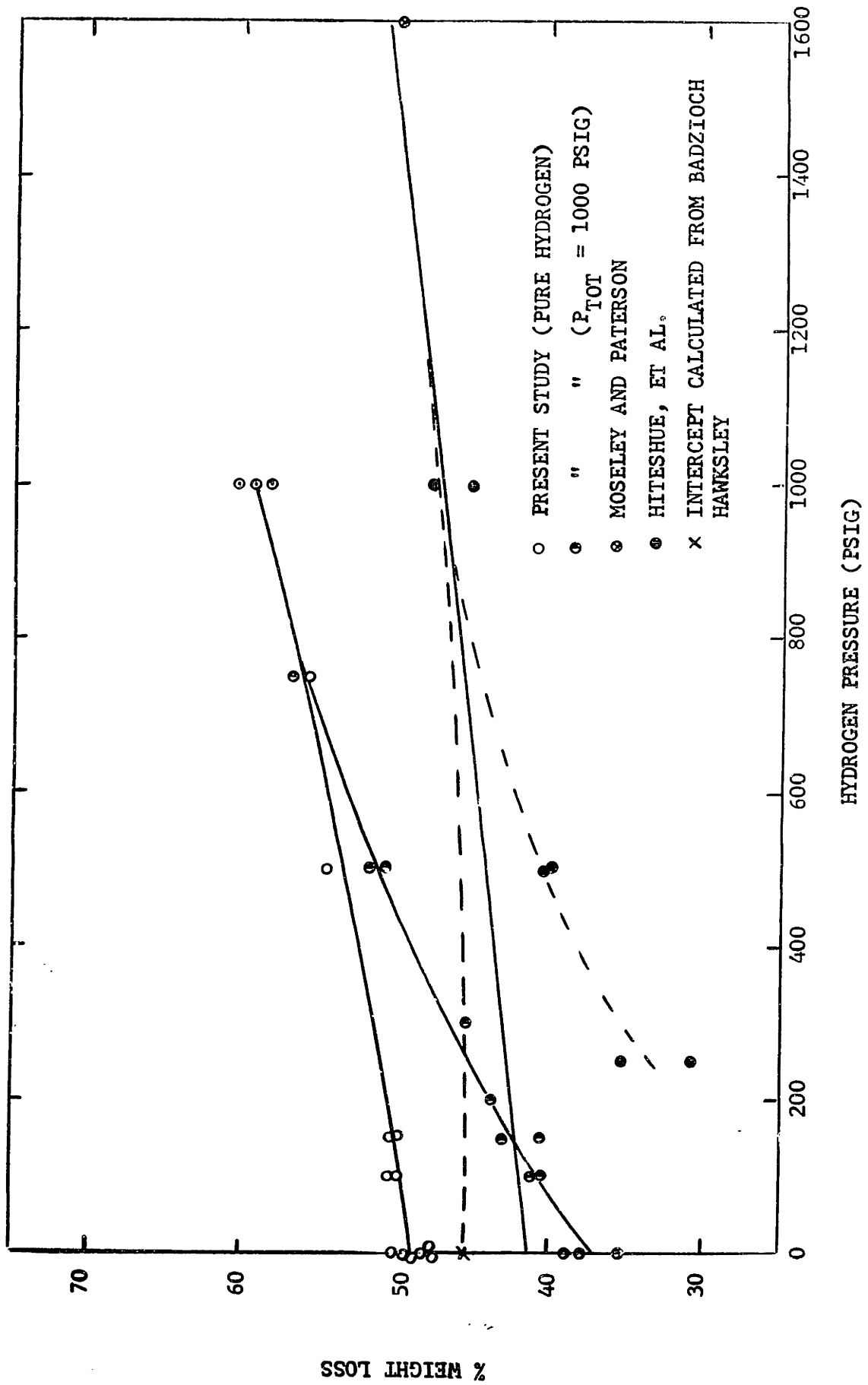


FIGURE 6-10 BITUMINOUS COAL YIELDS VERSUS HYDROGEN PRESSURE BELOW 100 ATM

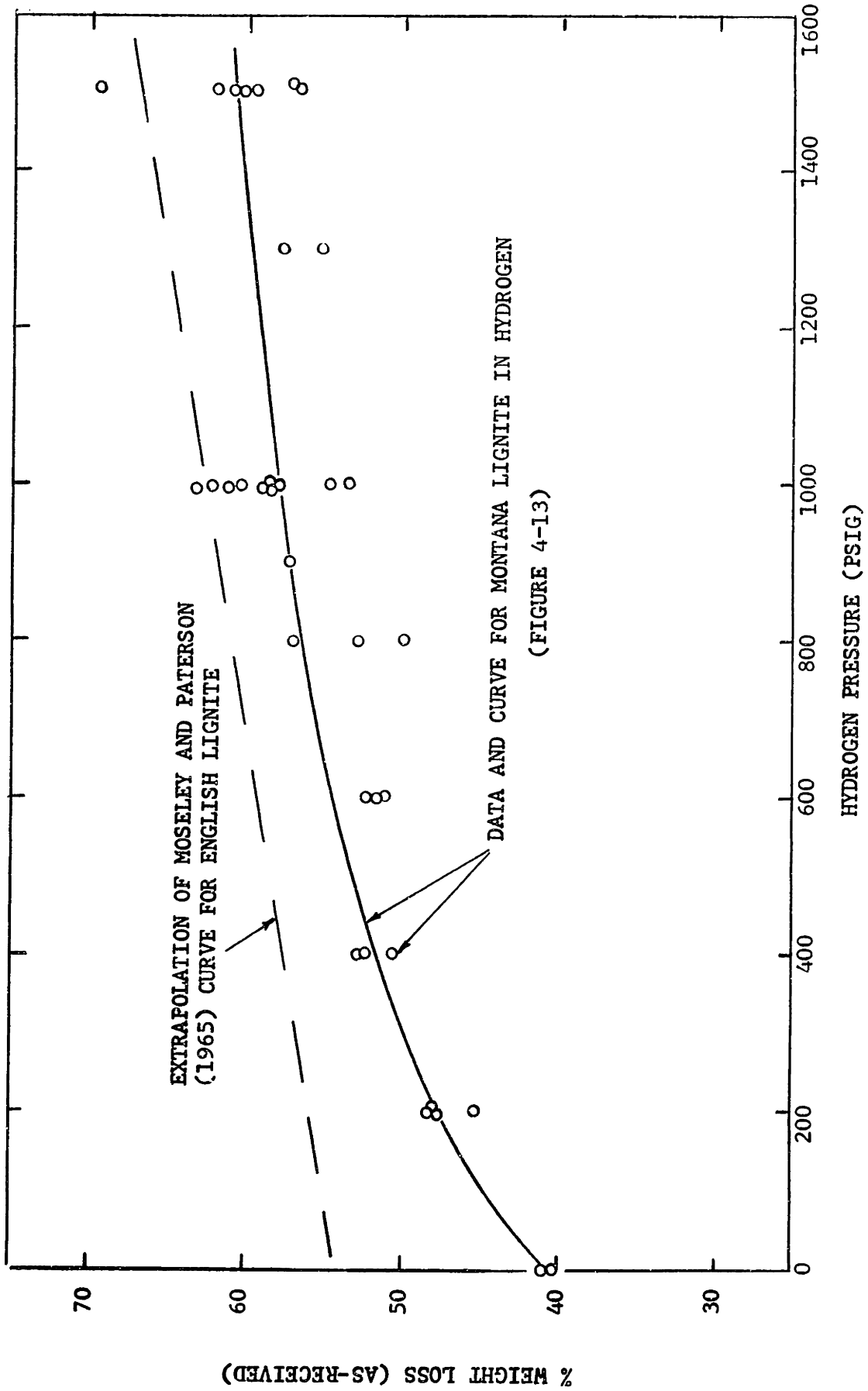


FIGURE 6-11 LIGNITE YIELDS VERSUS HYDROGEN PRESSURE BELOW 100 ATM

interpretation of Hiteshue's data is based on this study's findings at constant total pressure. The only other literature reference to this sort of behavior is the work by Belt and Roder (1972) who also found that total pressure as well as hydrogen pressure is important in determining yields. However, the small amount of experimental data in that work led to several implausible conclusions (e.g., a maximum in yield was reported with respect to hydrogen concentration at a constant total pressure) and no mechanistic explanations were offered.

Since the original work by Moseley and Paterson several modifications have been suggested. Johnson used an extremely complex variation of Equation 2-11 to include a dependency of the rate on the extent of conversion. As Johnson notes, his results indicate that a much simpler version would suffice:

$$\frac{dx}{dt} = k_3 P_{H_2} (1 - X) C^* \quad (2-19)$$

$$- \ln(1 - X) = \frac{k_3 P_{H_2} C_o^*}{k_2} \quad (2-20)$$

Johnson interprets the participation of the active species, C^* , as a catalytic agent promoting conversion of the coal's fixed carbon. In Figure 6-12, the data from Figure 6-9 are plotted in accord with Equation 2-20 ($\ln(1-X)$ vs P_{H_2}). Due to the uncertainty in the data, no strong disagreement is observed. However, the slope is markedly different from the one reported by Johnson as fitting his and Hiteshue's data (30 minute residence times and pressures below 1000 psig).

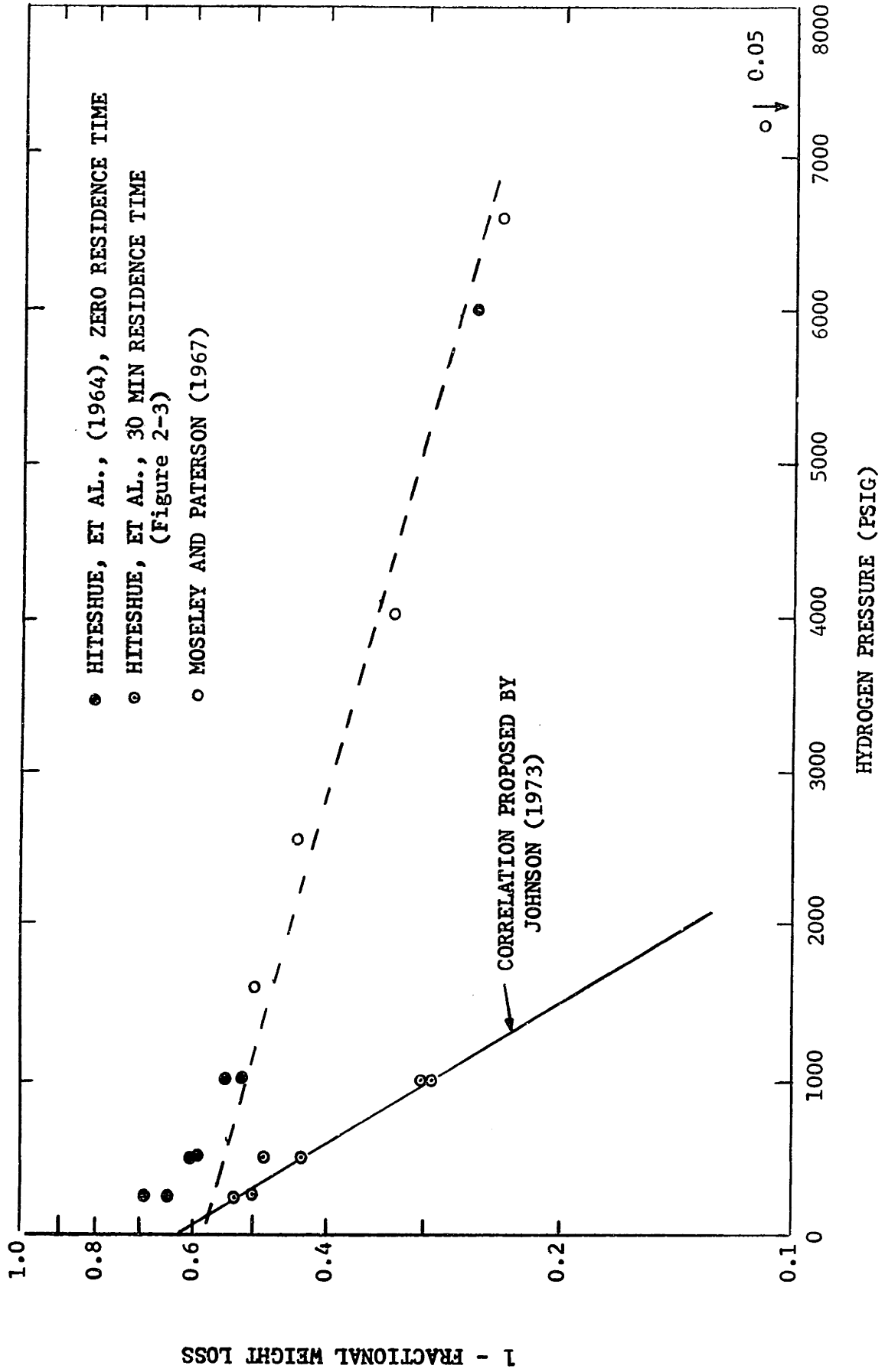


FIGURE 6-12 TEST OF EQUATION 2-20 WITH EXPERIMENTAL DATA

Clearly, Johnson's slope is in error as evidenced by Hiteshue's yield of 74% at high pressure (6000 psig). The explanation is believed to be similar to the one just advanced as to why Hiteshue's yields decrease sharply near the axis, i.e. secondary reactions in the bed. Johnson's thermobalance also has a relatively large bed and a very slow heat-up (2 minutes to temperature) compared to the use of finely dispersed particles in the present experiments and the work of Moseley and Paterson; each of these contributes to the loss at low H_2 concentrations of reactive volatile species.

Zahradnik and Glenn have proposed a different modification in the Moseley and Paterson model by assuming the active species also to disappear by reaction with hydrogen. With this assumption the expression for yield at long times becomes

$$X = \frac{k_1 P_{H_2} C_o^*}{k_1 P_{H_2} + k_2} \quad (2-16)$$

Equation 2-16 is empirically attractive since it provides a very steep slope initially which diminishes to zero at high pressures. Zahradnik and Glenn showed that constants could be found such that Equation 2-16 agreed very well with the data by Moseley and Paterson. The basis for outright rejection of these simple competitive reaction models was established in the Results Section where it was shown that a low temperature hydrogenation char upon heating to a higher temperature gave the same overall yield. If in fact there existed only a single type of active species (as assumed in Equations 2-9 through 2-20) it would have been completely deactivated in the low

temperature run with no additional conversion possible in the second heating. However, as shown in the decomposition of coal a great many reactions are involved many of which will not occur at low temperatures. Moseley and Paterson recognized that C_o^* would have to be a function of temperature. Attempting to incorporate this temperature dependency Johnson replaced C_o^* in Equation 2-20 with an expression involving statistically distributed activation energies (Equation 2-21) virtually identical to the decomposition model proposed in this paper. Johnson further claimed that at all temperatures the effect of hydrogen could be observed with his bituminous coal char. However, in Figure 4-15 at temperatures below 600°C no difference in yields between hydrogen and helium was seen. The explanation of this apparent difference lies in recognizing the fact that Johnson developed his temperature dependency correlation from run times of one hour. In Figure 6-13, Johnson's original data at residence times of 3 minutes are replotted, and these show much better agreement with the temperature dependency of rapid-rate yields found in this study.

6.4 EFFECT OF PARTICLE SIZE

The last major finding of the study was the significant influence of particle size on hydrogasification yields. Previous investigators have used a wide range of particle sizes in accumulating the available body of information of reactions of coal with hydrogen without concern for the effect of particle size. Table 6-5 lists the cited workers in this section and the particle sizes used by each. Examination of

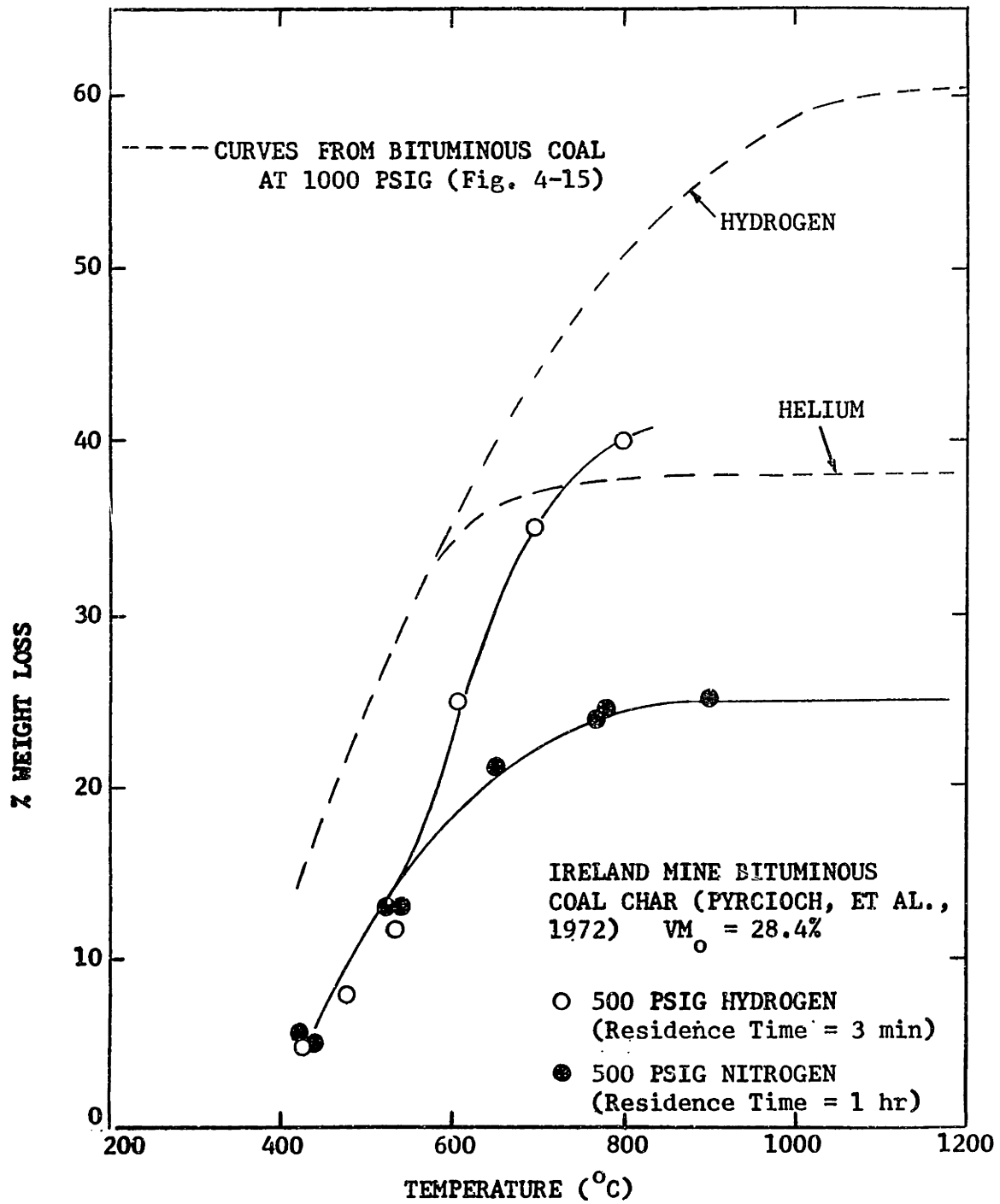


FIGURE 6-13 EFFECT OF TEMPERATURE ON HYDROGASIFICATION AND DEVOLATILIZATION YIELDS

TABLE 6-5
PARTICLE SIZES USED IN PREVIOUS INVESTIGATIONS

<u>Investigators</u>	<u>Particle Size (Dia.)</u>
Glenn, Donath and Grace (1967)	44 μ
Belt and Roder (1972)	70% < 74 μ
Moseley and Paterson (1967)	100-150 μ
Feldmann, <u>et al.</u> , (1970)	150-300 μ
Wiser, <u>et al.</u> , (1967)	246-417 μ
Hiteshue, <u>et al.</u> , (1964)	250-600 μ
Johnson (1973)	420-841 μ

the list, with reference to Figure 4-17, indicates that any conclusions drawn from such studies must be regarded with suspicion. Moseley and Paterson did attempt to study the particle size effect but found their apparatus unsuited for wide ranges of sizes. They did conclude that there seemed to be an effect, with smaller particles giving larger yields, certainly consistent with the findings of this study. Their data are compared with the present findings in Figure 6-14. Direct comparison is impossible because their data are reported in per cent carbon conversion rather than weight loss and the data were accumulated at 175 atm versus the 69 atm pressure used in this study. Nevertheless, the good agreement lends confidence to the data as well as the models.

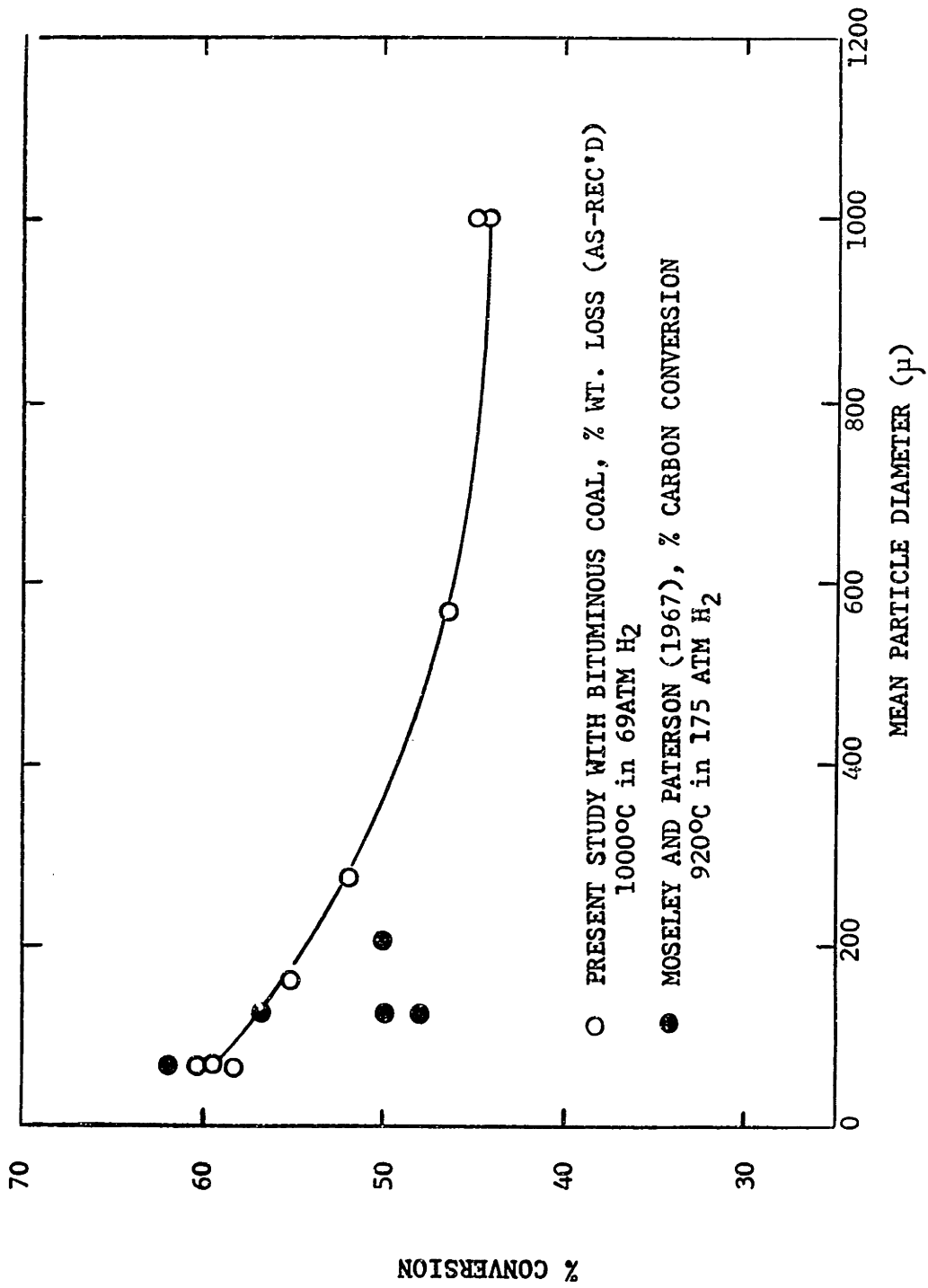


FIGURE 6-14 EFFECT OF PARTICLE SIZE ON YIELD

7. APPLICATION OF RESULTS

The following discussion addresses one of the major reasons for this investigation: provision of data useful in the design and scale-up of commercial systems. The present study was not undertaken with the intention of developing a data base unique to a specific process but rather to generate data of a more fundamental nature that hopefully would find widespread applications. Accordingly, models were constructed consistent with the findings in this laboratory as well as those reported in the literature. Key design parameters were isolated and the important mechanisms elucidated.

Among the present gasification schemes under serious consideration (Table 2-1), only the Bureau of Mines' Hydrane process envisions a hydrogen-rich conversion of fresh coal. The hydrogasifier portion of that process is sketched in Figure 7-1. Raw coal (150-300 μ) is to be fed into the top of a free-fall reactor (Stage 1) with a hot mixture of hydrogen (54%) and methane (46%)(Feldmann, et al., 1972). The resulting methane-rich gas (73%) is sent to the final clean-up stages while the partially converted char drops into a large fluidized bed (Stage 2) and further reacts with hydrogen producing more methane. The reaction heat from hydrogasification is transferred to the steam gasification system via superheated steam. Steam coils are situated in the fluidized bed to capitalize on its excellent heat transfer characteristics. Finally, the char (after approximately 50% conversion) is passed on to the synthesis gas generation system. One of the highly-touted advantages of the system is that only about 5% of the carbon in the off-gas is carbon monoxide thus requiring very little catalytic methanation.

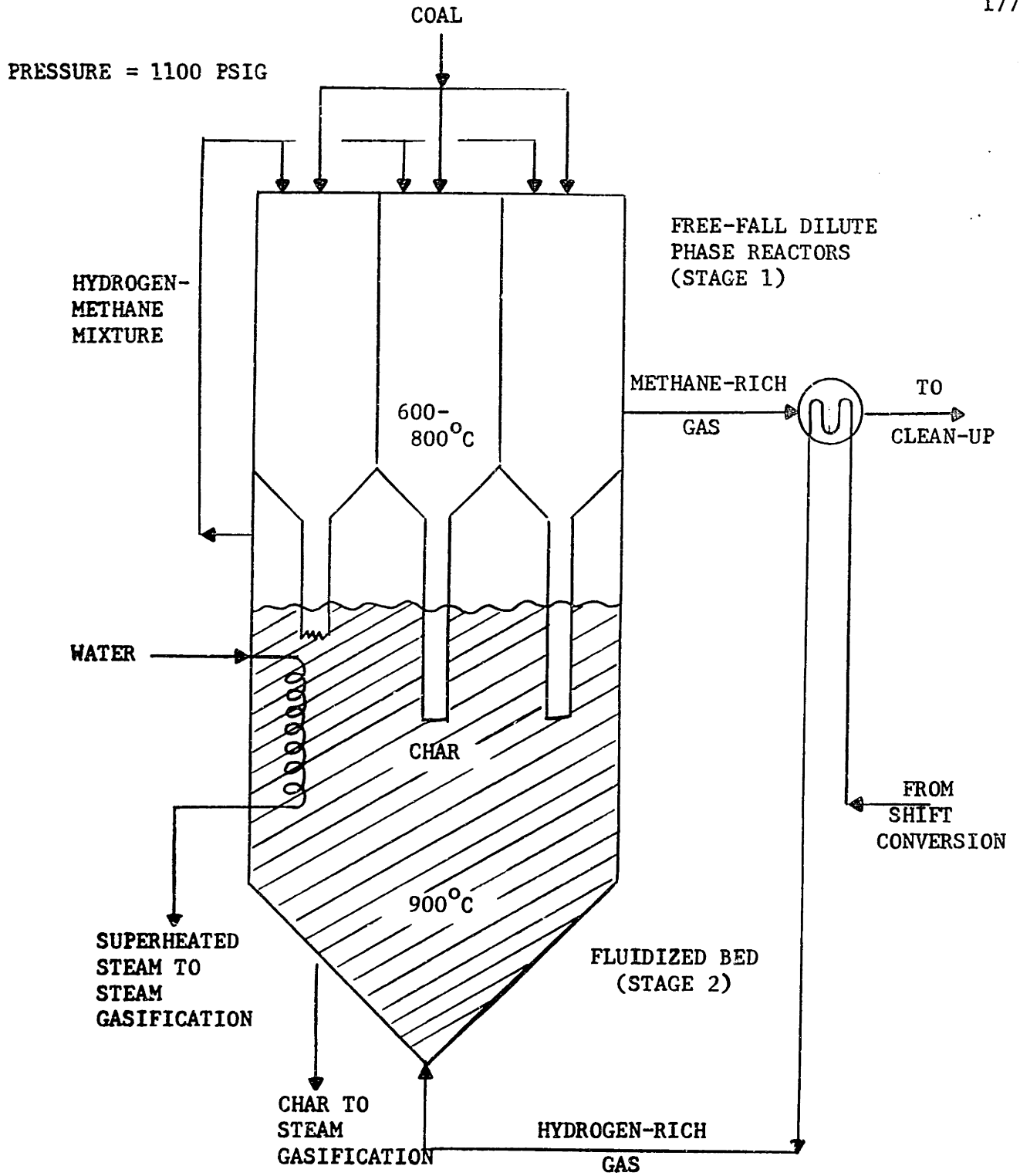


FIGURE 7-1 HYDRANE HYDROGASIFICATION SECTION

(FELDMANN, ET AL., 1972)

It is interesting to analyze this process and its anticipated performance in light of the experimental results presented previously. Perhaps, the most convenient forum would be to review each of the variables studied and reflect on how this study's findings might influence the design of Hydrane.

Residence Time -- The experimental evidence for both lignite and bituminous coal showed that residence times of a second or less at temperature were sufficient for near completion of the reactions. Feldmann, et al., (1972) calculated residence times in the free-fall section for 20% conversion in the range of 1/4 to 3/4 sec with heating rates of 3000°C/sec and 1000°C/sec, respectively. The data of the present study indicate conversions approximately twice as high suggesting that present design calculations for Hydrane are extremely conservative.

Temperature -- The maximum temperature reached in the free-fall reactors is expected to lie in the range of 600-800°C. This means, based upon the findings of the present study (see Figures 4-12 and 4-15), that as much as 40% of the potential rapid-rate material is unreacted. Since this portion of the rapid-rate material is the most reactive to hydrogen and due to the higher hydrogen pressures in the fluidized bed (600 versus 200 psig H₂), it appears desirable to maintain a low temperature (ca. 600°C) in the first stage for devolatilization and allow most of the hydrogasification to occur in the second stage. This 600°C is observed to be the point at which hydrogen begins to significantly attack the coal as established in Figure 4-15.

Heating Rate -- At 1000 psig, the data of the present study show no effect of heating rate on yield. In fact, the only consequence of increased heating rate will be decreased reaction time and vessel size.

It may, therefore, be of some advantage to permit higher wall temperatures in the first stage and shorten residence time. Heating rate should be no problem in the fluidized bed.

Pressure -- As mentioned before, hydrogen pressures are appreciably higher in the second stage. Bureau of Mines design calculations indicate that about 30% of the coal will be converted in the second stage with 20% in the first stage (the 50% total conversion is desired to maintain a char balance in the overall gasification system). However, if, as the data of the present study show, a 35% conversion is possible in the free-fall section (even at 600°C) only 15% conversion will be necessary in the fluidized bed leading to even higher hydrogen concentrations. Unfortunately, experiments by Feldmann, et al., (1970) show that the dilute phase section is essentially well-mixed with respect to the gas. This means that hydrogen pressures will be low and little hydrogenation of volatiles is expected. Every effort should be made to approach plug flow in order to preserve a maximum hydrogen concentration during devolatilization.

Particle Size -- Use of 150-300 μ particles may mean a loss of perhaps 10-11% of potential rapid-rate yield, relative to 70 μ particles, through secondary reactions. Finer particles would heat more quickly and fall more slowly thus significantly reducing the height required in the first stage reactors. The main problem with finer particles will be the difficulties of disengaging them from the gas stream at the bottom of the reactor.

In terms of overall process economics, the loss of yield from increasing particle size may be related directly to thermal efficiency loss by increased catalytic methanation requirements. This energy loss, in turn, is then compared to the gain in energy from reduced grinding

demands. A calculation based on a comparison between 70μ particles and 1000μ particles in 1000 psig H_2 indicates, however, that within the accuracy of the numbers the energy gain and loss are roughly equivalent, about 1000 BTU/lb coal. From this it may be concluded, for the time being, that particle size selection will be based on other criteria such as the additional residence time needed to heat up larger particles.

This brief overview strongly supports the general principles of the Hydrane process. The new results, in fact, are indicative of even greater potential than previously expected. The initial stage should be operated in near plug flow at a temperature around $600^\circ C$. The fluidized bed should complete the rapid hydrogasification and serve as a useful heat transfer medium. Residence time in this bed can be reduced substantially since little if any slow hydrogasification will be required. Current opinion at the Bureau of Mines contemplates much reduced rates of reaction in this stage, but evidence from this thesis establishes that potential rapid-rate yield at $900-1000^\circ C$ will be unaffected by the initial $600^\circ C$ stage. Furthermore, rapid-rate yields may well exceed the 50% conversion figure chosen for system balance. However, it may be more advantageous to permit an imbalance in favor of higher rapid-rate yields and make up carbon deficiencies by pumping a water slurry of raw coal directly into the steam gasifier.

The preceding analysis solely on the Hydrane system was not intended to mean that this is the only process where results are applicable, but rather that this process is unique in the sense that it closely conforms to general directions taken in this study. The devolatilization kinetics will be of general value to all processes in which coal is heated rapidly including pulverized coal burners, entrained flow carbonization systems as well as gasification plants.

8. CONCLUSIONS

1. The electrical strip furnace has been demonstrated to be an effective tool for study of extremely fast reactions in coal at high temperatures and pressures. In those few instances where comparisons are possible, data from this apparatus agrees quite well with results from continuous coal flow techniques designed to simulate full-scale systems. Thus, the data are believed to be very useful for future commercial design considerations.
2. The specific experimental conclusions are as follows:
 - a. The rate of coal conversion by devolatilization and hydrogasification is very fast with weight loss virtually ceasing within a second after reaching final temperature. Even with initial heating rates of 10-12,000°C/sec it is impossible to avoid significant reaction before reaching the desired temperature.
 - b. Yields in both hydrogen and helium increase with increasing temperature until approximately 900-1000°C after which further temperature increases resulted in essentially no further yield.
 - c. Heating rate has no discernible effect upon lignite yields regardless of conditions. However, at intermediate pressure levels (0.1 - 10 atm) increasing the rate of heating from 600 to 10,000°C/sec increases bituminous coal yield by approximately 2 percentage points. This effect is not observed at high pressures (1000 psig) for bituminous coal.
 - d. Total inert pressure has no effect on yields from lignite but increasing pressure from 0 to 1000 psig does reduce bituminous coal yields from 49% to about 37%. Increasing hydrogen

concentration at a fixed total pressure increases yields, but yields for bituminous coal in pure hydrogen show a minimum value ($\sim 50\%$) somewhere in the vicinity of 1-10 atm.

- e. Particle size has a small effect on yield for bituminous coal under 1.0 atm He, 48% yield for 70μ particles versus 44% for 1000μ particles. The effect on yields in hydrogen (1000 psig) is considerably greater with 60% yield for 70μ particles and 44% for 1000μ particles
 - f. In general, two quite different coals, Montana lignite and Pittsburgh Seam bituminous coal, have similar characteristics in terms of overall yields, rates, and trend with temperature. Bituminous coal yields are also affected by heating rate, total inert gas pressure, and particle size.
3. The general reaction scheme for coal is concluded to consist of a primary thermal decomposition forming volatiles and initiating a sequence of secondary reactions leading to char. Unique in the case of bituminous coal, intermediates in this char-forming sequence can volatilize as tar if the residence times are short enough (as in the case of low pressures, small sample sizes, and high heating rates). Primary decomposition is modelled as though it is an infinite set of first order decomposition reactions with a statistical distribution of activation energies.
- a. A Gaussian distribution of activation energies accurately accounts for the effects of residence time (0-20 secs), temperature ($400-1100^{\circ}\text{C}$), and heating rate ($65-10,000^{\circ}\text{C}/\text{sec}$) in the devolatilization of lignite. Estimated activation energies are in the range of 30-67 kcal/mole.

- b. A range of activation energies from 29-45 kcal/mole successfully correlates rate and yield data for bituminous coal at 1000 psig (no contribution from secondary reactions).
 - c. The increasing yields with decreasing pressure for bituminous coal is correlated by a selectivity expression derived from a secondary reaction model hypothesizing a competition between a char formation reaction and diffusional escape of intermediate species.
 - d. It was further concluded from the secondary reactions model that large coal beds, large particle sizes, and low heating rates would all promote the formation of char and diminish yield.
4. Hydrogen is also believed to interrupt the char-forming reaction sequence thus increasing the volatile yield. Further support of this argument is the observation that the additional conversion obtained in hydrogen atmospheres occurs at a slower rate than devolatilization.
- a. Susceptibility to hydrogen attack is observed to last for times approaching one second at 1000°C as shown in rapid heating experiments with lignite.
 - b. The yield from bituminous coal heated in pure hydrogen exhibits a minimum (around 50% weight loss) with respect to pressure occurring at 1-10 atm. This unique behavior was predicted qualitatively from the secondary reaction model assuming that reactive intermediates become non-reactive upon hydrogenation.
 - c. The secondary reaction model is inadequate in that parameters determined for conversion at low hydrogen partial pressures (constant total pressure) underpredicted yields at high hydrogen

partial pressures and in pure hydrogen. Two factors are believed responsible for this discrepancy: 1) hydrogenation of portions of the coal which are not volatile in inert atmospheres and 2) diffusional limitations on hydrogen at high total pressures.

- d. The importance of hydrogen diffusion to the coal particle is substantiated by the increasing hydrogenation yield with decreasing particle size. "Effective" hydrogen pressure was shown to be roughly proportional to the reciprocal of mean particle diameter.
5. The data agreed well with previously reported experimental trends and the model offered reasonable explanations for some of the observed "anomalies".

Devolatilization

- a. While rejected as mechanistically insufficient, the simple first order decomposition model does correlate the results over narrow ranges of experimental conditions and the estimated rate constants fall in the middle of a broad range of literature values. Activation energies around 10 kcal/mole are observed, consistent with many past studies, and these are shown to be the mathematical consequence of an inadequate model rather than an observation of mechanistic significance.
- b. Results from a number of different experimental techniques were collated and used to establish the existence of two broad rate regimes, a rapid devolatilization and a slow devolatilization, the latter being completely unimportant in the present study. While a few seconds at temperature are sufficient to bring an

end to the rapid devolatilization, it was impossible to devolatilize the char completely in times as long as 20 secs even at the highest temperatures with a residual volatile matter content of 4-7% of the original coal remaining.

- c. The interesting claim of rapid-heating induced excess yields was put into perspective in terms of secondary reactions. Bituminous coal yields 15 to 20% greater than proximate volatile content were observed and found to be in accord with other similar studies. Pressure and sample dimensions were found more useful than heating rate in illustrating the extent of these secondary reactions. It was emphasized, though, that "excess yields" depend on coal type with Montana Lignite giving yields approximately 90% of proximate volatile matter.
- d. From the results of this and several other studies, it is possible to conclude that the tarry species are centrally involved in the secondary reaction but exact identification of the nature of these reactions, polymerization or cracking, was not possible.

Hydrogasification

- a. For bituminous coal very close agreement is achieved between the estimated power-law rate constant of the present study and the work by Feldmann, et al., (1972). However, the simple model is rejected as inadequate to describe yield functionality with respect to pressure, temperature, and particle size.
- b. From the secondary reaction model it is possible in plots of yield versus P_{H_2} to explain the steep initial slope found by Hiteshue, et al., (1964) (secondary reactions in the bed)

as contrasted to the relatively flat curve of Moseley and Paterson (1967) (disperse phase heating with few secondary reactions).

- c. Use of the simple "active" species to explain temperature effects on yields suggested by Zahradnik and Glenn (1970) is dismissed based on experiments showing that hydrogenation yields are a state function of temperature. Data from Johnson's (1973) work are shown to be consistent with these findings.
 - d. The effect of particle size on yields is found to be important. Based on this result and the fact that a wide range of particle sizes were used in the various published studies, it is clear that intercomparisons of the literature results is difficult.
6. The correlation methods evolved in this work should prove valuable in future bench-scale and pilot-plant efforts with pulverized coal burners and entrained flow carbonization systems as well as with gasification plants. Specifically, the Bureau of Mines Hydrane process was analyzed and found to be well-suited for achieving significant rapid-rate yields. Higher conversions than previously anticipated are expected with further improvements possible from use of finer particles.

9. RECOMMENDATIONS

1. Since the primary impetus for this investigation was the need for data directed toward the commercialization of coal gasification, it is recommended that further work be done toward that specific goal.
 - a. A fairly detailed analysis of the specific products of gas, liquid and solid is deemed necessary to complement the overall conversion information obtained in this study. Since secondary reactions were shown to be important, it is emphasized that such work be designed to control carefully the residence time and to simulate the time-temperature history of the respective products as might be experienced in actual production.
 - b. To permit use in actual reactor design of these semi-fundamental kinetic data on conversion, further study of the actual solids residence time distribution in full-scale reactors is necessary.
 - c. In the present study particle size was shown to be a significant variable at high hydrogen pressures but the limitations of the apparatus prevented accurate identification of the particle size where the effectiveness factor is actually or very nearly unity. A study of very fine particles ($< 50\mu$) is recommended.
 - d. Study of the effect and mechanism of catalysts which have been used to obtain extremely high yields from low temperature short residence time experiments (Wiser et al., 1970) should provide useful commercial information as well as further enlightenment as to the nature of the rapid decomposition-

hydrogenation reactions of coal.

2. While the models advanced in this paper do represent a step toward more fundamental portrayal of rapid coal reactions more work on the improvement of these models is clearly justified.
 - a. The nature of the secondary reactions is not well-understood. Experiments directed specifically toward identifying the composition of the primary volatiles is probably the most advantageous aspect to pursue.
 - b. The assumption of a simple constant overall mass transfer coefficient in the secondary reaction model is probably not very good for a coal that simultaneously is undergoing major physical transformations (melting, swelling, etc.). An interesting study would focus on the relationship of these physical changes to the important diffusional processes occurring during the rapid-rate period.
3. Finally, it is recommended that the electrical strip furnace be utilized in studies of related interest. The apparatus worked well and proved extremely flexible in terms of performing unusual experiments.
 - a. Both oil shale and urban refuse have been suggested as sources of high heating value gas. This apparatus would provide a simple, quick and effective means of obtaining valuable devolatilization and hydrogasification data for design consideration.
 - b. In a more general sense, this apparatus could be quite useful in kinetic studies of a wide range of solid decompositions and various fast gas-solid reactions. For example, a study of

solid combustion would be interesting if a suitable support (non-oxidizing screen) could be found.

- c. It should not be forgotten, though, that only two types of coal were studied in this thesis and significant mechanistic information was acquired from their differences. Further clues would undoubtedly be forthcoming in studies of other types of coals (e.g. subbituminous, low-volatile bituminous and anthracitic coals).

10. APPENDIX

10.1 NOTES ON THERMODYNAMICS AND COAL

10.1.1 Thermodynamic Advantage of Fresh Coal

As a basis for analysis it is usually convenient to choose the carbon (β -graphite) and hydrogen reaction:



$$K_p = \frac{P_{CH_4}}{(P_{H_2})^2} \quad (10-1)$$

Values of K_p as a function of temperature are shown in Figure 10-1.

As usual with an exothermic reaction, increases in temperature (favorable to reaction kinetics) reduce attainable methane yields. Dent (1944) first suggested the possibility of attaining methane concentrations in excess of β -graphite equilibrium (illustrated in Figure 10-1) although this "activity" would decay with prolonged heating. Dent pictured the phenomenon as a thermal "graphitization" of the coal or coke's carbon. Squires (1961) compiled the data of numerous investigations (Figure 10-1) which also exhibited experimental achievements of "excess" methane. The "quasi-equilibrium" data suggest excess free energies of several kcal/mole. Squires further reviewed possible explanations for the phenomena

1. Hydrogen present in coal, although this was discounted as minor.
2. Structural differences, in particular surface area and crystallite size variations between the carbon in

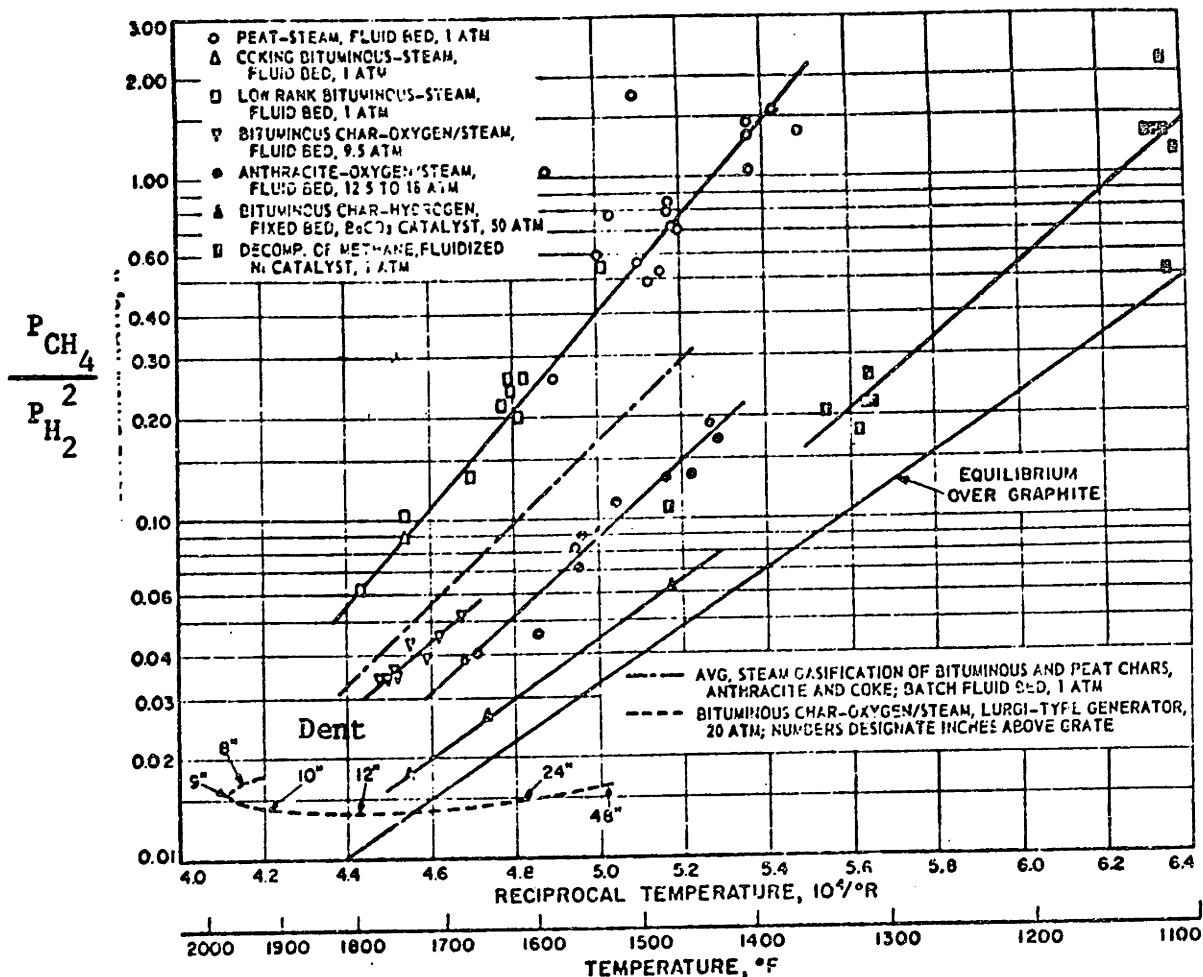


Figure 10-1 Methane Equilibrium in Gasification Systems
 (Squires, 1961; VonFredersdorff and Elliott, 1963)

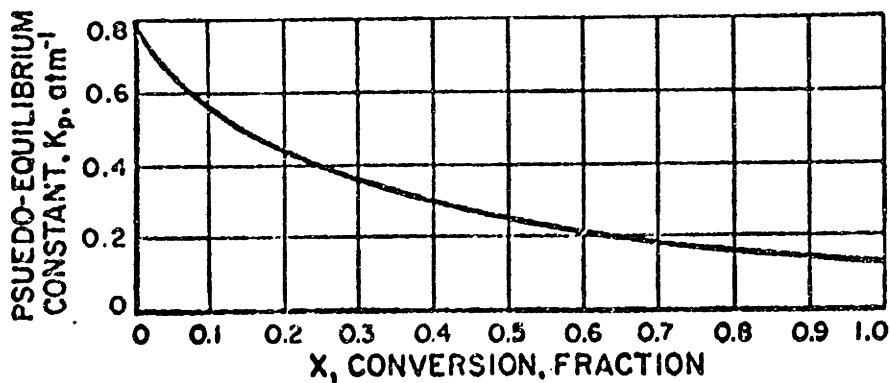


Figure 10-2 Equilibrium Constant as a Function of Conversion
 (Wen and Huebler, 1965)

char and graphite. Evidence from studies of various types of carbon were shown to favor this line of reasoning.

3. Methane from volatile decomposition; continuous gasification of raw coal will approach equilibrium "from above". That is, methane will be formed predominately by devolatilization in the presence of hydrogen with essentially none of the coal's fixed carbon reacting.

Wen and Huebler (1965) experimentally measured "equilibrium" methane-hydrogen concentrations over low temperature bituminous coal char and found K_p decreasing with conversion. This data is shown in Figure 10-2. A "zero" conversion K_p for char is 6.67 times greater than for graphite (or -3.7 kcal/mole excess free energy). As fractional conversion approached unity, K_p approached the value for equilibrium over graphite supporting to some extent Dent's original theory.

Feldmann, et al., (1970) argued that early methane formation from coal is a completely "irreversible" step ($C^* \rightarrow CH_4$) thereby invalidating equilibrium thermodynamics. The only effect of the methane present is to dilute the hydrogen since methane decomposition is slow.

10.1.2 Kinetics of Methane Cracking

Assuming that initial methane formation is completely irreversible, the only limitation on achievable methane concentrations is the rate of methane decomposition. Donath (Bituminous Coal Research, Inc., 1965) found no methane cracking for gas residence times of 5-10 secs at 1770°C

and 70 atm pressure, although heavier species were found to crack to methane. Zahradnik and Grace (1972), on the other hand, have published data for methane decomposition (1400-1600°C). The disappearance of methane is modeled as a first order decomposition (Data show approximately 50% decay in 7.5 secs at 1600°C. The rate constant is highly dependent on temperature, $E \approx 30$ kcal/mole). They believe the decomposition to be due to steam reforming ($\text{CH}_4 + \text{H}_2\text{O} = \text{CO} + 2\text{H}_2$) rather than cracking to carbon and hydrogen. This is consistent with Blackwood's (1962) findings that the rate of methane decomposition to graphite is of the same order of magnitude as methane formation rates from fixed carbon. Of course, these hydrogenation rates are several orders of magnitude slower than rapid-rate gasification.

10.1.3 Heat of Reaction for Hydrogasification of Fresh Coal

Heat effects associated with gasification reactions are of considerable importance in reactor design. Typically, coal gasification schemes have been based on the heat of reaction between graphite and hydrogen. Squires plot (Fig. 10-1), however, shows slopes for coal significantly greater than that for ξ -graphite, implying the molar enthalpy of reaction more exothermic for coal + hydrogen than ξ -graphite + hydrogen. (ΔH_{excess} as much as 15 kcal/mole). On the other hand, Lee, et al., (1968) published calorimetric values of the mass heat of reaction with hydrogen for the following:

Raw Coal	$\Delta H \sim$	-1.00 kcal/g at 704°C
Pretreated Coal		-1.09
Low-temperature Char		-1.35
High-temperature Char		-1.70
Graphite		-1.78

Moseley and Paterson (1967) calculated a heat of reaction for their coal-hydrogen reaction based on the heats of combustion for reactants and products. The reported value of -10.1 kcal/g-atom C at 298°K seems to support the trend identified by the IGT workers above. Birch (1969), though, computed a $\Delta H = -2.46$ kcal/g (at 298°K) also from an energy balance on reactants and products. This value, of course, is higher than graphite and supports the evidence of Squires. Experimental verification by the techniques of Moseley and Paterson and Birch is admittedly difficult since it involves subtracting two large numbers of roughly equal magnitude. In either case the dilemma is unresolved.

10.1.4 Thermodynamic Analysis of Coal Structure

It has long been empirically established that the heat of combustion of coal can be computed by simply summing up the heats of combustion of its constituent elements (ultimate analysis) (Perry, et al., 1963). This implies, however, that the heat of formation of the coal substance itself is identically zero. Since a number of structures for coal have been proposed in the literature, it was decided to apply this thermodynamic observation as a potential screening factor of coal structures. The heat of formation of the respective coal structures was estimated by the group contribution method of Franklin (Reid and

Sherwood, 1958). The analysis was completed for two example structures and the results are given in the accompanying illustration. As is apparent, the calculated heats of formation for both structures are very near zero, thus the method definitely lacks any discriminating potential.

10.1.5 Ultimate Analyses

The coals used in this investigation were not analyzed for their elemental composition, but the Institute of Gas Technology has worked with similar coals and reported their ultimate analyses as follows:

Lignite (North Dakota, Johnson 1973)

Ultimate Analysis		Proximate Analysis (Present Study Coals)		
C	66.4	FC	48.5	47.04
H	4.48	VCM	43.6	40.33
O	19.63	Ash	7.9	12.63
N	0.78			
S	0.79			
Ash	7.92			
$\text{CH}_{.81}\text{O}_{.22}\text{N}_{.01}\text{S}_{.0045}$				

Bituminous (Pittsburgh No. 8, Ireland Mine, Lee, et al., 1967)

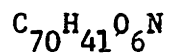
C	71.1	FC	51.8	46.34
H	4.95	VCM	35.9	39.81
O	7.35	Ash	11.3	12.20
N	1.18	Moisture	1.0	1.65
S	4.03			
Ash	11.39			
$\text{CH}_{.84}\text{O}_{.078}\text{N}_{.014}\text{S}_{.021}$				

Net H/C ratio (Neglecting N,S and assuming all O appears as H₂O)

Lignite CH_{0.37}

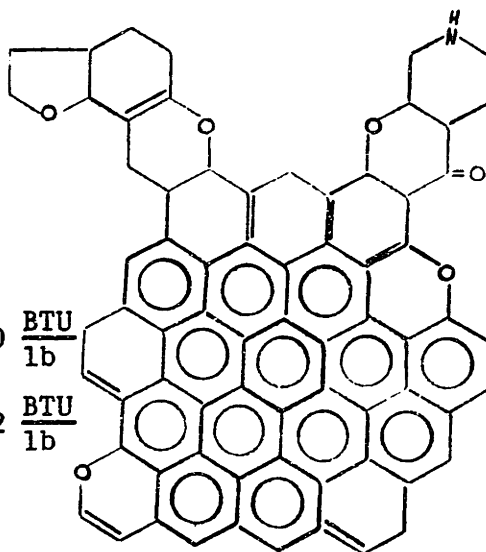
Bituminous CH_{0.68}

Factor of 1.85

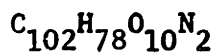


$$\text{Est. } \Delta H_{\text{comb}} = 13,710 \frac{\text{BTU}}{\text{lb}}$$

$$\text{Est. } \Delta H_f^\circ = 92 \frac{\text{BTU}}{\text{lb}}$$

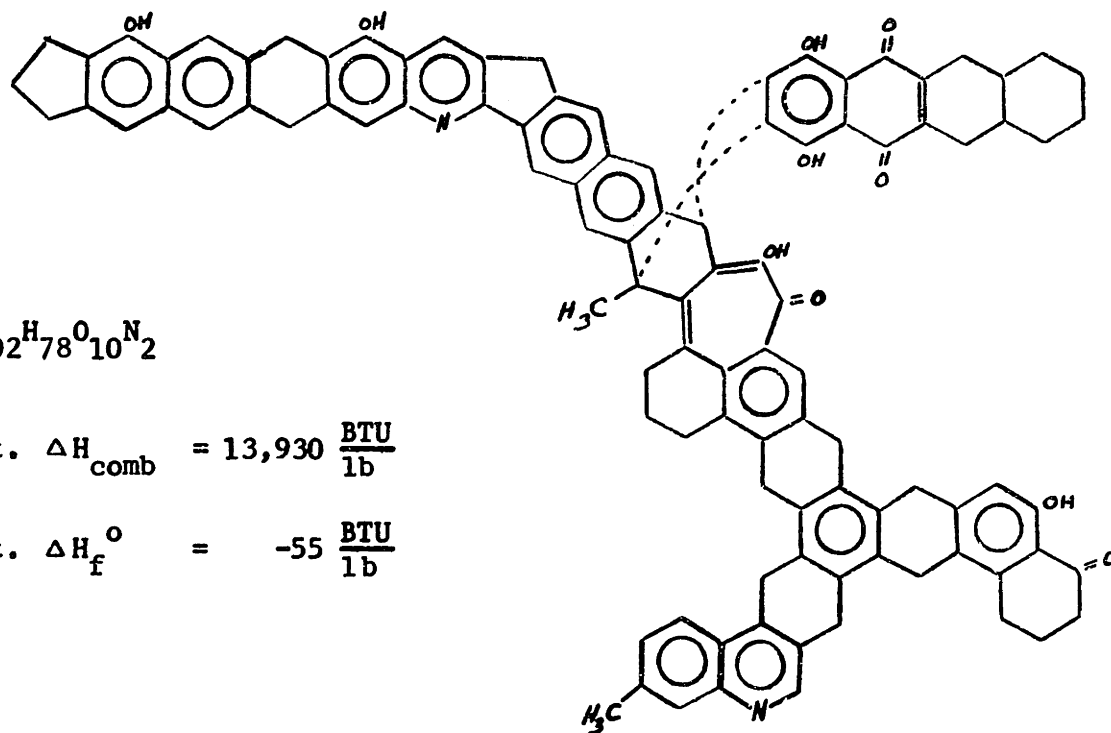


Fuchs and Sandhoff Model (1942)



$$\text{Est. } \Delta H_{\text{comb}} = 13,930 \frac{\text{BTU}}{\text{lb}}$$

$$\text{Est. } \Delta H_f^\circ = -55 \frac{\text{BTU}}{\text{lb}}$$



Given Model (1960)

10.2 SUMMARY OF EXPERIMENTAL DATA

The following listings were prepared from the experimental data decks used in the analysis of the respective models. The actual time-temperature histories are included (time in seconds and temperature in degrees Centigrade). Several additional listings of data not in the computer card files are included at the end of this section.

RUN NO. 69C2 WT. LOSS 0.1130

TIME	TEMP
0.00	25.
0.60	164.
1.20	291.
1.80	388.
2.40	443.
2.60	490.
3.20	436.
3.80	367.
4.40	322.
5.00	278.
5.60	252.
6.20	219.

RUN NO. 70A2 WT. LOSS 0.1507

TIME	TEMP
0.00	25.
0.60	172.
1.20	295.
1.80	396.
2.40	485.
2.70	515.
3.00	485.
3.60	419.
4.20	367.
4.80	319.
5.40	278.
6.00	244.

RUN NO. 69R2 WT. LOSS 0.1914

TIME	TEMP
0.00	25.
0.50	142.
1.00	247.
1.50	336.
2.00	415.
2.40	462.
2.80	513.
3.20	532.
3.60	504.
4.20	422.
5.20	329.
6.20	268.

RUN NO. 69A2 WT. LOSS 0.2360

TIME	TEMP
0.00	25.
1.00	222.
1.40	290.
2.00	381.
3.00	506.
3.60	560.
4.00	591.
4.20	600.
4.60	532.
5.20	445.
5.80	376.
6.80	298.
7.80	244.

RUN NO. 69E2 WT. LOSS 0.2539

TIME	TEMP
0.00	25.
0.80	219.
1.60	365.
2.40	481.
3.20	574.
4.00	631.
4.40	652.
4.80	588.
5.40	490.
6.00	419.
6.80	345.
7.60	293.
8.40	244.

RUN NO. 69D2 WT. LOSS 0.2586

TIME	TEMP
0.00	25.
0.60	144.
1.20	247.
1.80	341.
2.40	428.
3.00	509.
3.60	560.
4.10	603.
4.40	560.
5.00	485.
5.80	398.
6.60	333.
7.60	271.

RUN NO. 68E2 WT. LOSS 0.2752

TIME	TEMP
0.00	25.
1.00	222.
2.00	391.
3.00	516.
3.60	579.
4.00	607.
4.60	645.
5.00	657.
5.40	612.
6.00	514.
6.40	462.
7.40	355.
8.40	276.
9.40	222.

RUN NO. 68D2 WT. LOSS 0.3035

TIME	TEMP
0.00	25.
1.00	222.
2.00	389.
3.00	514.
4.00	603.
5.00	650.
6.00	671.
7.60	678.
8.20	579.
8.60	528.
9.60	398.
10.6	367.
11.6	252.

RUN NO. 31R2 WT. LOSS 0.0731

TIME	TEMP
0.00	25.
0.80	386.
1.20	367.
1.60	341.
2.00	314.
2.40	285.
2.80	258.
3.80	222.
4.80	177.
5.80	149.

RUN NO. 31C2 WT. LOSS 0.1177

TIME	TEMP
0.00	25.
1.00	481.
1.40	391.
1.80	372.
2.20	338.
2.60	314.
3.00	295.
3.80	251.
4.80	197.
6.40	174.

RUN NO. 30R2 WT. LOSS 0.1667

TIME	TEMP
0.00	25.
0.40	202.
0.80	379.
1.20	556.
1.60	554.
2.00	438.
2.40	393.
2.80	355.
3.20	321.
4.20	247.
5.20	209.
6.60	167.

RUN NO. 17C2 WT. LOSS 0.1701

TIME	TEMP
0.00	25.
0.30	172.
0.50	247.
1.40	532.
1.50	511.
1.70	473.
2.10	419.
2.50	379.
2.90	341.
3.50	295.
4.50	224.
5.50	174.

RUN NO. 30A2 WT. LOSS 0.2442

TIME	TEMP
0.00	25.
0.25	174.
0.50	294.
0.75	413.
1.00	533.
1.25	652.
1.65	579.
2.05	509.
2.45	450.
3.05	379.
3.85	314.
4.65	252.
5.85	197.
6.85	169.

RUN NO. 32B2 WT. LOSS 0.2709

TIME	TEMP
0.00	25.
1.50	702.
2.00	605.
2.40	532.
2.80	481.
3.20	431.
3.60	386.
4.60	298.
5.60	239.
6.60	194.

RUN NO. 17D2 WT. LOSS 0.2947

TIME	TEMP
0.00	25.
0.30	169.
0.70	343.
1.10	483.
1.50	605.
1.90	731.
2.10	697.
2.50	607.
2.90	539.
3.50	457.
4.10	391.
4.70	329.
5.70	259.
6.70	199.

RUN NO. 32C2 WT. LOSS 0.3352

TIME	TEMP
0.00	25.
1.00	485.
1.80	740.
2.20	818.
2.60	697.
3.00	606.
3.40	532.
3.80	462.
4.20	415.
5.20	317.
7.20	197.

RUN NO. 29B2 WT. LOSS 0.3416

TIME	TEMP
0.00	25.
0.40	295.
0.80	603.
1.20	738.
1.60	845.
2.00	895.
2.10	830.
2.40	723.
2.80	626.
3.20	553.
3.60	485.
4.00	436.
4.80	344.
5.80	276.
7.80	175.

RUN NO. 32A2 WT. LOSS 0.3421

TIME	TEMP
0.00	25.
1.20	579.
1.60	676.
2.20	774.
2.60	721.
3.00	652.
3.40	558.
3.80	488.
4.20	438.
5.20	353.
6.20	273.
7.20	222.

RUN NO. 71D2 WT. LOSS 0.1197

TIME	TEMP
0.00	25.
1.00	117.
2.00	184.
3.00	247.
4.00	295.
5.00	338.
6.00	365.
7.00	379.
8.00	393.
10.0	412.
12.0	417.
20.0	419.
21.0	343.
22.0	276.

RUN NO. 71C2 WT. LOSS 0.2398

TIME	TEMP
0.00	25.
0.50	096.
1.00	154.
1.50	217.
2.00	271.
2.50	320.
3.00	362.
4.00	417.
5.00	462.
6.00	490.
8.00	516.
11.0	530.
16.0	532.
17.0	414.
18.0	319.

RUN NO. 70B2 WT. LOSS 0.2744

TIME	TEMP
0.00	25.
0.50	122.
1.00	209.
1.50	283.
2.00	343.
2.50	391.
3.00	438.
4.00	522.
5.00	579.
6.00	603.
14.6	603.
15.6	485.
16.6	343.
17.6	271.

RUN NO. 68D2 WT. LOSS 0.3035

TIME	TEMP
0.00	25.
1.00	222.
2.00	389.
3.00	514.
4.00	603.
5.00	650.
6.00	671.
7.60	678.
8.20	579.
8.60	528.
9.60	398.
10.6	367.
11.6	252.

RUN NO. 68B2 WT. LOSS 0.3211

TIME	TEMP
0.00	25.
0.50	134.
1.00	247.
1.50	338.
2.00	415.
2.50	483.
3.00	537.
4.00	621.
5.00	671.
6.00	681.
7.40	697.
13.6	697.
14.2	579.
15.0	462.
16.0	353.

RUN NO. 71B2 WT. LOSS 0.3502

TIME	TEMP
0.00	25.
0.50	134.
1.00	247.
1.50	362.
2.00	462.
2.50	536.
3.00	607.
4.00	697.
5.00	721.
8.00	745.
11.0	762.
13.2	757.
14.2	532.
15.2	391.

RUN NO. 71A2 WT. LOSS 0.3892		RUN NO. 64A2 WT. LOSS 0.3977	
TIME	TEMP	TIME	TEMP
0.00	25.	0.00	25.
0.50	172.	0.70	295.
1.00	322.	1.50	581.
1.50	462.	2.00	762.
2.00	600.	2.50	872.
2.50	687.	3.00	937.
3.00	745.	3.50	968.
3.50	791.	4.00	991.
4.60	820.	8.80	995.
5.60	843.	9.50	759.
9.80	843.	10.5	567.
10.3	671.	11.5	438.
10.8	565.	12.5	345.
11.6	443.		

RUN NO. 70D2 WT. LOSS 0.4074		RUN NO. 29D2 WT. LOSS 0.4102	
TIME	TEMP	TIME	TEMP
0.00	25.	0.00	25.
0.50	261.	0.40	244.
1.00	487.	1.20	629.
1.50	692.	1.60	764.
2.00	820.	2.40	968.
2.50	920.	2.80	1040
3.00	945.	3.20	1068
3.50	978.	3.60	1050
4.00	990.	3.80	917.
6.00	971.	4.00	855.
9.40	943.	4.40	721.
9.90	769.	5.00	603.
10.6	624.	6.00	443.
11.6	438.	7.20	332.
12.6	366.	9.40	210.

RUN NO. 30D2 WT. LOSS 0.4105		RUN NO. 71E2 WT. LOSS 0.4189	
TIME	TEMP	TIME	TEMP
0.00	25.	0.00	25.
0.40	295.	0.50	276.
0.80	467.	1.00	494.
1.20	645.	1.50	695.
1.60	772.	2.00	843.
2.00	867.	2.50	924.
2.40	917.	3.00	968.
2.80	973.	3.50	993.
3.20	1009	4.00	1009
4.20	1021	11.4	1019
4.80	745.	11.9	828.
5.40	603.	12.4	673.
6.00	481.	12.9	574.
6.60	434.	13.4	490.
7.20	370.	14.4	381.

RUN NO. 29A2 WT. LOSS 0.4031

TIME	TEMP
0.00	25.
0.80	391.
5.00	919.
7.40	919.
8.00	678.

RUN NO. 29C2 WT. LOSS 0.4110

TIME	TEMP
0.00	25.
0.80	462.
2.40	979.
6.50	970.
7.00	764.

RUN NO. 29D2 WT. LOSS 0.4102

TIME	TEMP
0.00	25.
0.40	244.
1.20	629.
1.60	764.
2.40	968.
2.80	1040
3.20	1068
3.60	1050
3.80	917.
4.00	855.
4.40	721.
5.00	603.
6.00	443.
7.20	332.
9.40	210.

RUN NO. 30C2 WT. LOSS 0.4016

TIME	TEMP
0.00	25.
0.80	433.
3.00	994.
4.80	1021
5.40	818.

RUN NO. 30D2 WT. LOSS 0.4105

TIME	TEMP
0.00	25.
0.80	457.
3.00	978.
4.20	1021
5.00	695.

RUN NO. 35B2 WT. LOSS 0.1505

TIME	TEMP
0.00	25.
0.15	574.
0.30	556.
0.50	532.
0.75	511.
1.00	483.
1.25	459.
1.75	420.
2.25	367.
3.25	271.
4.25	242.

RUN NO. 36A2 WT. LOSS 0.2060

TIME	TEMP
0.00	25.
0.15	579.
0.20	565.
0.40	544.
0.90	504.
1.40	457.
2.40	367.
3.40	297.
4.40	241.

RUN NO. 35A2 WT. LOSS 0.2493

TIME	TEMP
0.00	25.
0.15	558.
0.20	647.
0.25	645.
0.40	636.
0.65	584.
0.90	556.
1.15	511.
1.65	459.
2.15	402.
3.15	319.
4.15	247.

RUN NO. 35C2 WT. LOSS 0.2897

TIME	TEMP
0.00	25.
0.15	536.
0.20	681.
0.25	697.
0.35	695.
0.50	678.
0.75	650.
1.25	560.
1.75	485.
2.25	433.
3.25	329.
4.25	259.

RUN NO. 36C2 WT. LOSS 0.2951

TIME	TEMP
0.00	25.
0.20	697.
0.25	750.
0.35	721.
0.50	676.
0.80	635.
1.30	574.
1.80	509.
2.80	393.
3.80	315.
4.80	247.

RUN NO. 34D2 WT. LOSS 0.3209

TIME	TEMP
0.00	25.
0.21	835.
0.30	797.
0.40	769.
0.55	723.
0.80	685.
1.05	638.
1.55	556.
2.05	485.
2.55	434.
3.55	338.
4.55	271.

RUN NO. 35D2 WT. LOSS 0.3608

TIME	TEMP
0.00	25.
0.24	967.
0.30	960.
0.35	942.
0.50	887.
0.75	793.
1.25	650.
1.75	553.
2.25	466.
3.25	362.
4.25	276.

RUN NO. 34C2 WT. LOSS 0.3650

TIME	TEMP
0.00	25.
0.25	1024.
0.35	993.
0.50	915.
0.75	815.
1.00	733.
1.25	661.
1.50	589.
2.00	511.
2.50	436.
3.00	372.
4.00	290.
5.00	222.

RUN NO. 36B2 WT. LOSS 0.4013

TIME	TEMP
0.00	25.
0.25	882.
0.40	955.
0.70	995.
0.90	917.
1.15	815.
1.40	721.
1.90	600.
2.40	506.
3.40	369.
4.40	293.
5.40	227.

RUN NO. 34B2 WT. LOSS 0.4098

TIME	TEMP
0.00	25.
0.25	993.
0.80	993.
1.15	843.
1.55	719.
1.90	628.
2.25	561.
2.65	490.
3.40	393.
4.15	315.

RUN NO. 36B2 WT. LOSS 0.4013

TIME	TEMP
0.00	25.
0.25	882.
0.40	955.
0.70	995.
0.90	917.
1.15	815.
1.40	721.
1.90	600.
2.40	506.
3.40	369.
4.40	293.
5.40	227.

RUN NO. 33C2 WT. LOSS 0.4039

TIME	TEMP
0.00	25.
0.10	307.
0.25	842.
0.50	892.
0.75	922.
1.00	945.
1.25	973.
1.50	993.
4.30	1019.
4.80	955.
5.30	697.
5.80	588.
6.30	508.

RUN NO. 33A2 WT. LOSS 0.4119

TIME	TEMP
0.00	25.
0.25	726.
2.00	1019
4.80	1019
5.25	798.

RUN NO. 34A2 WT. LOSS 0.4150

TIME	TEMP
0.00	25.
0.10	367.
0.25	867.
0.50	988.
0.75	1006
1.45	1006
1.60	940.
1.85	818.
2.10	736.
2.35	664.
2.60	603.
3.10	509.
3.60	438.

RUN NO. 41C2 WT. LOSS 0.1851

TIME	TEMP
0.00	25.
0.05	487.
0.10	532.
0.30	532.
0.45	530.
0.55	518.
0.80	497.
1.05	467.
1.55	415.
2.55	337.
3.55	266.

RUN NO. 41A2 WT. LOSS 0.1972

TIME	TEMP
0.00	25.
0.05	532.
0.10	602.
0.20	600.
0.45	562.
0.95	502.
1.45	445.
2.45	348.
3.45	271.

RUN NO. 41B2 WT. LOSS 0.3022

TIME	TEMP
0.00	25.
0.07	791.
0.17	776.
0.27	769.
0.42	757.
0.57	721.
0.82	662.
1.32	560.
1.82	485.
2.32	419.
3.32	327.
4.32	261.

RUN NO. 41D2 WT. LOSS 0.3111

TIME	TEMP
0.00	25.
0.06	757.
0.11	777.
0.16	769.
0.26	745.
0.51	676.
0.76	626.
1.01	581.
1.51	511.
2.51	391.
3.51	300.
4.51	244.

RUN NO. 40C2 WT. LOSS 0.3423

TIME	TEMP
0.00	25.
0.08	607.
0.13	733.
0.18	769.
0.23	774.
0.33	767.
0.43	745.
0.68	692.
0.93	640.
1.43	556.
1.93	485.
2.43	416.
3.43	324.
4.43	252.

RUN NO. 40D2 WT. LOSS 0.3547

TIME	TEMP
0.00	25.
0.20	843.
0.30	796.
0.45	759.
0.70	693.
0.95	631.
1.45	542.
2.45	415.
3.45	319.
4.45	252.

RUN NO. 40A2 WT. LOSS 0.3803

TIME	TEMP
0.00	25.
0.08	697.
0.13	845.
0.23	875.
0.33	865.
0.58	794.
1.08	671.
1.58	572.
2.08	488.
2.58	438.
3.58	346.
4.58	290.

RUN NO. 40B2 WT. LOSS 0.3812

TIME	TEMP
0.00	25.
0.10	892.
0.15	943.
0.20	943.
0.25	937.
0.50	837.
0.75	745.
1.00	674.
1.50	572.
2.00	490.
2.50	436.
3.50	343.
4.50	291.

RUN NO. 39D2 WT. LOSS 0.3824

TIME	TEMP
0.00	25.
0.05	806.
0.10	994.
0.15	990.
0.25	927.
0.50	843.
0.75	769.
1.25	650.
1.75	558.
2.25	483.
2.75	434.
3.75	343.
4.75	283.

RUN NO. 39C2 WT. LOSS 0.4030

TIME	TEMP
0.00	25.
0.10	1050
0.15	1111
0.20	1097
0.30	1050
0.65	907.
1.15	743.
1.65	621.
2.15	530.
2.65	457.
3.65	343.
4.65	271.

RUN NO. 39B2 WT. LOSS 0.4024

TIME	TEMP
0.00	25.
0.10	968.
3.70	922.
5.00	530.

RUN NO. 38C2 WT. LOSS 0.4139

TIME	TEMP
0.00	25.
0.10	1032
0.20	1045
1.00	1032
2.00	1019
4.35	1014
4.95	733.

RUN NO. 60B2 WT. LOSS 0.4158

TIME	TEMP
0.00	25.
0.05	719.
0.10	1047
0.15	1068
0.20	1071
1.70	1045
4.55	1022
5.55	669.

RUN NO. 39A2 WT. LOSS 0.4174

TIME	TEMP
0.00	25.
0.10	770.
0.20	945.
0.30	994.
0.80	991.
1.30	968.
4.35	940.
5.10	650.

RUN NO. 38B2 WT. LOSS 0.4189

TIME	TEMP
0.00	25.
0.10	855.
0.20	1004
0.30	1022
0.45	1032
1.05	1004
1.80	973.
4.25	963.
4.40	867.

RUN NO. 15D2 WT. LOSS 0.1129

TIME	TEMP
0.00	25.
0.70	320.
0.80	192.
1.00	127.
1.20	100.

RUN NO. 16B2 WT. LOSS 0.1813

TIME	TEMP
0.00	25.
0.40	331.
0.80	605.
1.00	542.
1.20	436.
1.60	314.
2.20	197.
3.00	120.

RUN NO. 17B2 WT. LOSS 0.1913

TIME	TEMP
0.00	25.
0.20	275.
0.40	478.
0.60	628.
0.80	529.
1.00	462.
1.40	367.
1.80	273.
2.20	222.
2.80	149.
3.20	122.

RUN NO. 15C2 WT. LOSS 0.1973

TIME	TEMP
0.00	25.
0.20	222.
0.40	386.
0.70	560.
0.75	584.
0.90	488.
1.10	380.
1.50	247.
2.30	142.
2.70	110.

RUN NO. 17A2 WT. LOSS 0.2972

TIME	TEMP
0.00	25.
0.20	135.
0.40	379.
0.60	532.
0.80	692.
1.00	842.
1.20	795.
1.40	609.
1.80	345.
2.20	234.
2.60	147.

RUN NO. 15A2 WT. LOSS 0.3097

TIME	TEMP
0.00	25.
0.30	341.
0.50	485.
0.80	769.
1.00	647.
1.30	464.
1.70	362.
2.10	242.
2.50	147.

RUN NO. 14C2 WT. LOSS 0.3540

TIME	TEMP
0.00	25.
0.30	249.
0.70	553.
1.10	769.
1.40	905.
1.60	943.
1.80	897.
2.20	609.
2.60	462.
3.00	362.
4.10	195.
5.10	122.

RUN NO. 15B2 WT. LOSS 0.3641

TIME	TEMP
0.00	25.
0.40	308.
0.80	649.
1.10	968.
1.20	892.
1.40	659.
1.80	419.
2.20	268.
3.20	122.

RUN NO. 14D2 WT. LOSS 0.4075

TIME	TEMP
0.00	25.
0.40	360.
0.80	650.
1.00	745.
1.20	801.
1.40	820.
1.80	943.
2.20	943.
2.40	920.
2.60	833.
3.00	497.
3.20	412.
3.40	338.
3.80	234.
4.80	103.

RUN NO. 16A2 WT. LOSS 0.4105

TIME	TEMP
0.00	25.
0.40	416.
0.80	687.
1.20	862.
1.40	867.
2.10	867.
2.40	574.
2.80	367.
3.20	242.
4.20	110.

RUN NO. 13B2 WT. LOSS 0.4040

TIME	TEMP
7.0	970

RUN NO. 13C2 WT. LOSS 0.4100

TIME	TEMP
4.7	1050

RUN NO. 14A2 WT. LOSS 0.4240

TIME

5.2

TEMP

1000

RUN NO. 14B2 WT. LOSS 0.4180

TIME

5.6

TEMP

1050

RUN NO. 49B2 WT. LOSS 0.0731		RUN NO. 49A2 WT. LOSS 0.2067	
TIME	TEMP	TIME	TEMP
0.00	25.	0.00	25.
0.05	450.	0.05	579.
0.10	445.	0.07	716.
0.20	417.	0.10	690.
0.30	389.	0.20	626.
0.50	334.	0.30	560.
0.75	272.	0.45	502.
1.00	227.	0.60	443.
		0.85	367.
		1.10	300.
		1.35	247.

RUN NO. 48E2 WT. LOSS 0.2305		RUN NO. 48D2 WT. LOSS 0.2488	
TIME	TEMP	TIME	TEMP
0.00	25.	0.00	25.
0.05	598.	0.07	674.
0.10	631.	0.12	668.
0.15	626.	0.17	626.
0.25	598.	0.27	560.
0.35	556.	0.37	514.
0.50	494.	0.52	457.
0.65	438.	0.77	396.
0.90	367.	1.02	343.
1.15	298.	1.27	293.
1.40	247.	1.52	244.

RUN NO. 50A2 WT. LOSS 0.2926		RUN NO. 49D2 WT. LOSS 0.3154	
TIME	TEMP	TIME	TEMP
0.00	25.	0.00	25.
0.04	462.	0.03	390.
0.09	842.	0.08	950.
0.14	818.	0.13	945.
0.24	697.	0.18	892.
0.34	626.	0.28	774.
0.44	539.	0.38	697.
0.59	485.	0.48	626.
0.74	415.	0.68	518.
0.99	345.	0.83	462.
1.24	295.	1.08	391.
1.49	247.	1.33	320.
		1.58	271.
		1.83	227.

RUN NO. 48A2 WT. LOSS 0.3277

TIME	TEMP
0.00	25.
0.07	796.
0.12	833.
0.17	820.
0.27	719.
0.37	626.
0.47	560.
0.57	506.
0.77	415.
1.02	341.
1.27	274.

RUN NO. 48B2 WT. LOSS 0.3413

TIME	TEMP
0.00	25.
0.05	723.
0.10	917.
0.20	819.
0.30	743.
0.40	697.
0.55	614.
0.70	567.
0.95	478.
1.20	369.
1.45	295.
1.70	242.

RUN NO. 48C2 WT. LOSS 0.3456

TIME	TEMP
0.00	25.
0.05	697.
0.10	1013.
0.20	867.
0.30	769.
0.40	685.
0.55	532.
0.70	485.
0.95	414.
1.20	348.
1.45	295.
1.70	247.

RUN NO. 49C2 WT. LOSS 0.3761

TIME	TEMP
0.00	25.
0.05	818.
0.10	1071.
0.20	917.
0.30	798.
0.40	721.
0.50	600.
0.65	541.
0.80	450.
1.05	367.
1.30	295.
1.55	244.

RUN NO. 51A2 WT. LOSS 0.3910

TIME	TEMP
0.00	25.
0.06	943.
0.11	1019.
0.21	1031.
0.31	1019.
0.41	1019.
0.46	855.
0.56	769.
0.71	671.
0.86	574.
1.01	494.
1.26	391.
1.51	315.
1.76	248.

RUN NO. 47B2 WT. LOSS 0.3890

TIME	TEMP
4.3	970

RUN NO. 47C2	WT. LOSS-0.4190	RUN NO. 47D2	WT. LOSS 0.3710
TIME	TEMP	TIME	TEMP
4.8	970	5.25	970

RUN NO. 50B2	WT. LOSS 0.3970	RUN NO. 65C2	WT. LOSS 0.4010
TIME	TEMP	TIME	TEMP
2.85	1100	4.05	840

RUN NO. 65D2	WT. LOSS 0.4070	RUN NO. 66A2	WT. LOSS 0.4350
TIME	TEMP	TIME	TEMP
4.05	1150	3.75	1100

RUN NO. 28-5 WT. LOSS 0.0979

TIME	TEMP
0.0	25
0.5	152
1.0	285
1.5	405
2.0	485
2.5	537
3.0	569
3.2	584
3.6	544
4.2	461

RUN NO. 28-6 WT. LOSS 0.1161

TIME	TEMP
0.0	25
0.5	212
1.0	367
1.5	485
2.0	579
2.5	645
3.0	680
3.4	702
4.0	579
4.5	499

RUN NO. 27-4 WT. LOSS 0.1220

TIME	TEMP
0.0	25
0.5	209
1.0	319
1.5	438
2.0	523
2.5	581
3.2	626
3.6	532
4.2	445

RUN NO. 28-3 WT. LOSS 0.2400

TIME	TEMP
0.0	25
0.8	315
1.6	520
2.0	600
2.4	650
2.8	685
3.6	715
4.0	720
4.5	590
5.0	505

RUN NO. 28-4 WT. LOSS 0.3490

TIME	TEMP
0.0	25
0.5	147
1.0	280
1.5	402
2.0	501
3.0	612
4.0	657
4.9	673
5.5	555
6.0	480

RUN NO. 27-2 WT. LOSS 0.3990

TIME	TEMP
0.0	25
0.5	259
1.0	461
1.5	595
2.0	685
3.0	747
4.0	764
4.8	767
5.5	591
6.0	508

RUN NO. 23-3 WT. LOSS 0.0530

TIME	TEMP
0.0	25
0.2	167
0.4	348
0.6	482
0.8	508
1.0	485
1.2	461
1.6	419

RUN NO. 26-5 WT. LOSS 0.0750

TIME	TEMP
0.0	25
0.2	222
0.4	414
0.6	555
0.8	649
1.0	614
1.2	588
1.4	521

RUN NO. 26-3 WT. LOSS 0.1370

TIME	TEMP
0.0	25
0.2	234
0.4	450
0.6	602
0.8	673
1.0	614
1.2	590
1.4	527

RUN NO. 24-1 WT. LOSS 0.2310

TIME	TEMP
0.0	25
0.2	167
0.4	367
0.6	508
0.8	649
1.0	740
1.2	697
1.4	642
1.6	602
1.8	560

RUN NO. 23-2 WT. LOSS 0.2850

TIME	TEMP
0.0	25
0.2	184
0.4	334
0.6	486
0.8	602
1.0	706
1.2	764
1.4	685
1.6	626
2.0	549

RUN NO. 23-4 WT. LOSS 0.2910

TIME	TEMP
0.0	25
0.4	285
0.8	508
1.0	602
1.2	661
1.4	706
1.6	704
1.8	649
2.0	602
2.4	532

RUN NO. 26-4 WT. LOSS 0.3630

TIME	TEMP
0.0	25
0.2	222
0.4	414
0.6	579
0.8	697
1.0	793
1.2	824
1.4	745
1.6	673
2.0	590

RUN NO. 24-2 WT. LOSS 0.4430

TIME	TEMP
0.0	25
0.4	390
0.8	697
1.0	786
1.2	861
1.4	916
1.6	928
2.0	941
2.4	946
2.8	745

RUN NO. 24-3 WT. LOSS 0.4450

TIME	TEMP
0.0	25
0.4	319
0.8	567
1.0	661
1.2	735
1.4	783
1.6	822
1.8	842
2.0	757
2.4	645

RUN NO. 23-1 WT. LOSS 0.4770

TIME	TEMP
0.0	25
0.4	234
0.8	567
1.2	793
1.6	842
2.0	866
2.4	869
2.8	876
3.2	673
3.6	555

RUN NO. 27-1 WT. LOSS 0.4780

TIME	TEMP
0.0	25
0.4	461
0.8	757
1.2	904
1.6	954
1.8	971
2.0	904
2.4	733
2.8	618
3.2	544

RUN NO. 28-2 WT. LOSS 0.4120

TIME	TEMP
0.00	25.
0.50	280.
1.00	535.
1.35	721.
12.0	721.
13.0	25.

RUN NO. 22-2 WT. LOSS 0.4200

TIME	TEMP
0.00	25.
0.50	280.
1.00	535.
1.40	709.
15.0	709.
16.0	25.

RUN NO. 28-1 WT. LOSS 0.4230

TIME	TEMP
0.00	25.
0.50	280.
1.00	535.
1.35	721.
12.0	721.
13.0	25.

RUN NO. 27-3 WT. LOSS 0.4370

TIME	TEMP
0.00	25.
0.50	280.
1.00	535.
1.50	745.
9.00	745.
10.	025.

RUN NO. 16-2 WT. LOSS 0.4610

TIME	TEMP
0.00	25.
0.50	280.
1.00	535.
1.50	750.
2.00	885.
2.20	927.
4.20	927.
5.20	25.

RUN NO. N 22 WT. LOSS 0.4730

TIME	TEMP
0.00	25.
0.50	280.
1.00	535.
1.50	750.
2.00	885.
2.75	993.
6.00	993.
7.00	25.

RUN NO. 24-4 WT. LOSS 0.4770

TIME	TEMP
0.00	25.
0.50	280.
1.00	535.
1.50	750.
2.00	867.
9.80	867.
10.8	25.

RUN NO. 13-1 WT. LOSS 0.5050

TIME	TEMP
0.00	25.
0.50	280.
1.00	535.
1.50	750.
2.00	885.
2.20	917.
4.00	917.
5.00	25.

RUN NO. 18-2 WT. LOSS 0.5070

TIME	TEMP
0.00	25.
0.50	280.
1.00	535.
1.50	750.
2.00	885.
2.20	917.
6.40	917.
7.40	25.

RUN NO. 18-1 WT. LOSS 0.5520

TIME	TEMP
0.00	25.
0.50	280.
1.00	535.
1.50	750.
2.00	885.
3.25	1000
3.30	1084
4.80	1084
5.80	25.

RUN NO. 46-5. WT. LOSS 0.1374

TIME	TEMP
0.0	25
0.4	246
0.6	355
0.8	443
0.9	485
1.0	485
1.5	414
2.0	343

RUN NO. 46-6 WT. LOSS 0.1490

TIME	TEMP
0.0	25
0.4	246
0.6	355
0.8	438
1.0	537
1.2	532
1.5	485
2.0	426

RUN NO. 46-7 WT. LOSS 0.1674

TIME	TEMP
0.0	25
0.4	295
0.6	414
0.8	532
1.0	609
1.2	579
1.5	508
2.0	414

RUN NO. 46-4 WT. LOSS 0.3811

TIME	TEMP
0.0	25
0.5	270
1.0	508
1.2	579
1.4	661
1.6	645
2.0	574
2.5	494
3.0	426

RUN NO. 46-3 WT. LOSS 0.4335

TIME	TEMP
0.0	25
0.5	270
1.0	485
1.2	555
1.5	661
1.7	702
2.0	638
2.5	532
3.0	450
3.5	381

RUN NO. 46-8 WT. LOSS 0.4453

TIME	TEMP
0.0	25
0.5	319
1.0	590
1.2	668
1.5	769
1.8	649
2.4	494
3.0	402

RUN NO. 46-2 WT. LOSS 0.4658

TIME	TEMP
0.0	25
0.5	246
1.0	508
1.5	769
1.8	842
2.0	793
2.5	649
3.0	590
3.5	480
4.0	414

RUN NO. 46-1 WT. LOSS 0.4774

TIME	TEMP
0.00	25.
0.50	280.
1.00	535.
1.50	750.
2.00	885.
2.70	968.
3.00	968.
4.00	25.

RUN NO. 38-4 WT. LOSS 0.4851

TIME	TEMP
0.00	25.
0.50	280.
1.00	535.
2.00	885.
2.50	942.
10.2	942.
11.2	25.

RUN NO. 48-2 WT. LOSS 0.0851

TIME	TEMP
0.00	25.
0.02	246.
0.04	504.
0.1	483.
0.2	464.
0.5	428.
1.0	390.

RUN NO. 47-2 WT. LOSS 0.1745

TIME	TEMP
0.00	25.
0.03	348.
0.05	555.
0.06	593.
0.2	560.
0.5	499.
1.0	428.

RUN NO. 47-3 WT. LOSS 0.2948

TIME	TEMP
0.00	25.
0.03	348.
0.05	555.
0.07	697.
0.08	749.
0.2	742.
0.5	664.
1.0	534.
1.5	443.

RUN NO. 48-1 WT. LOSS 0.4136

TIME	TEMP
0.00	25.
0.03	414.
0.05	625.
0.09	778.
0.15	756.
0.3	687.
0.5	621.
1.0	534.
1.5	480.

RUN NO. 47-1 WT. LOSS 0.4505

TIME	TEMP
0.00	25.
0.03	348.
0.05	555.
0.1	891.
0.2	842.
0.5	673.
1.0	527.
1.5	428.

RUN NO. 45-1 WT. LOSS 0.5020

TIME	TEMP
3.5	970

RUN NO. 48-3 WT. LOSS 0.4980

TIME	TEMP
5.5	1025

RUN NO. 44-5 WT. LOSS 0.1873

TIME	TEMP
0.0	25
0.2	270
0.4	462
0.6	640
0.8	532
1.0	438

RUN NO. 44-3 WT. LOSS 0.3177

TIME	TEMP
0.00	25.
0.05	590.
0.07	745.
0.09	625.
1.2	443.
2.0	216.

RUN NO. 44-2 WT. LOSS 0.3631

TIME	TEMP
0.0	25.
0.5	602.
0.8	790.
1.0	879.
1.2	745.
1.4	555.
2.0	295.

RUN NO. 44-1 WT. LOSS 0.3649

TIME	TEMP
0.0	25.
0.5	649.
0.8	879.
1.0	979.
1.1	992.
1.2	916.
1.4	720.
2.0	367.

RUN NO. 44-4 WT. LOSS 0.3693

TIME	TEMP
0.0	25.
0.5	649.
0.8	879.
1.0	979.
1.1	992.
1.2	916.
1.4	720.
2.0	367.

RUN NO. 54-2 WT. LOSS 0.0894

TIME	TEMP
0.0	25
4.0	367
24.	367

RUN NO. 54-3 WT. LOSS 0.2275

TIME	TEMP
0.0	25
3.0	485
14.	485

RUN NO. 54-1 WT. LOSS 0.2870

TIME	TEMP
0.0	25
3.0	544
11.6	544

RUN NO. 53-5 WT. LOSS 0.3547

TIME	TEMP
0.0	25
2.0	626
12.0	626

RUN NO. 53-6 WT. LOSS 0.3586

TIME	TEMP
0.0	25
2.2	626
15.	626

RUN NO. 53-4 WT. LOSS 0.3615

TIME	TEMP
0.0	25
2.0	650
10.	650

RUN NO. 53-1 WT. LOSS 0.3491

TIME	TEMP
0.0	25
1.5	673
8.0	672

RUN NO. 53-3 WT. LOSS 0.3709

TIME	TEMP
0.0	25
1.4	673
11.5	673

RUN NO. 53-2 WT. LOSS 0.3857

TIME	TEMP
0.0	25
1.2	818
7.0	818

RUN NO. 38-3 WT. LOSS 0.3820

TIME	TEMP
0.0	25
1.8	942
8.0	942

RUN NO. 38-2 WT. LOSS 0.3720

TIME	TEMP
0.0	25
1.5	980
5.5	980

RUN NO. 44-6 WT. LOSS 0.3810

TIME	TEMP
0.0	25
1.6	1045
6.4	1045

RUN NO. 38-1 WT. LOSS 0.3510

TIME	TEMP
0.0	25
1.6	1137
6.6	1137

RUN NO. 54-R WT. LOSS 0.3914

TIME	TEMP
0.0	25
1.0	1150
2.0	1150
3.0	400

RUN NO. 26A2 WT. LOSS 0.0731		RUN NO. 22E2 WT. LOSS 0.1035	
TIME	TEMP	TIME	TEMP
0.00	25.	0.00	25.
0.50	370.	0.50	532.
0.70	300.	0.60	485.
1.00	197.	0.80	395.
1.20	127.	1.20	273.
		1.60	202.
		2.00	159.
		2.60	107.

RUN NO. 22C2 WT. LOSS 0.2490		RUN NO. 25C2 WT. LOSS 0.2875	
TIME	TEMP	TIME	TEMP
0.00	25.	0.00	25.
0.30	334.	0.30	295.
0.80	631.	0.60	462.
1.10	471.	0.80	535.
1.50	324.	1.00	431.
1.90	222.	1.20	362.
2.30	152.	1.40	315.
2.70	120.	1.60	259.
		1.80	219.
		2.20	110.

RUN NO. 26B2 WT. LOSS 0.2969		RUN NO. 23B2 WT. LOSS 0.3155	
TIME	TEMP	TIME	TEMP
0.00	25.	0.00	25.
0.20	162.	0.40	459.
0.40	300.	0.80	676.
0.60	437.	1.00	518.
0.80	574.	1.20	407.
1.00	488.	1.60	331.
1.20	434.	2.00	222.
1.40	355.	2.40	167.
1.60	293.	2.80	122.
1.80	247.		
2.20	177.		
2.60	125.		

RUN NO. 22D2 WT. LOSS 0.3465

TIME	TEMP
0.00	25.
0.30	348.
0.70	704.
0.80	808.
1.00	699.
1.30	556.
1.70	376.
2.10	273.
2.50	202.
2.90	135.
3.30	117.

RUN NO. 22B2 WT. LOSS 0.4111

TIME	TEMP
0.00	25.
0.40	428.
0.80	723.
1.00	867.
1.20	894.
1.40	668.
1.60	553.
2.00	343.
2.40	222.
2.80	182.
3.40	98.

RUN NO. 23A2 WT. LOSS 0.5004

TIME	TEMP
0.00	25.
0.40	367.
0.80	574.
1.40	840.
1.70	968.
2.10	968.
2.40	733.
2.80	459.
3.20	271.
4.00	125.

RUN NO. 22A2 WT. LOSS 0.5076

TIME	TEMP
0.00	25.
0.30	331.
0.50	506.
1.10	702.
1.50	842.
1.80	905.
2.00	879.
2.20	842.
2.50	565.
2.90	379.
3.50	202.
4.10	137.

RUN NO. 25B2 WT. LOSS 0.5146

TIME	TEMP
0.00	25.
0.30	295.
0.70	588.
1.10	813.
1.50	940.
2.30	945.
2.50	838.
2.70	669.
3.10	448.
3.50	307.
3.90	219.
4.70	122.

RUN NO. 72E2 WT. LOSS 0.1310

TIME	TEMP
13.2	380

RUN NO. 72D2 WT. LOSS 0.2260
TIME TEMP
11.4 460

RUN NO. 73C2 WT. LOSS 0.2640
TIME TEMP
10.0 555

RUN NO. 73A2 WT. LOSS 0.3420
TIME TEMP
10.1 567

RUN NO. 73B2 WT. LOSS 0.4130
TIME TEMP
11.1 590

RUN NO. 72B2 WT. LOSS 0.4710
TIME TEMP
9.3 685

RUN NO. 73D2 WT. LOSS 0.4980
TIME TEMP
9.8 710

RUN NO. 23C2 WT. LOSS 0.5230
TIME TEMP
4.8 805

RUN NO. 21B2 WT. LOSS 0.5200
TIME TEMP
6.6 805

RUN NO. 23D2 WT. LOSS 0.5330
TIME TEMP
5.7 795

RUN NO. 66C2 WT. LOSS 0.5370
TIME TEMP
4.4 993

RUN NO. 67C2 WT. LOSS 0.5370
TIME TEMP
14.0 892

RUN NO. 72A2 WT. LOSS 0.5380
TIME TEMP
9.0 805

RUN NO. 25A2 WT. LOSS 0.5470

TIME	TEMP
6.6	1006

RUN NO. 72C2 WT. LOSS 0.5570

TIME	TEMP
9.2	843

RUN NO. 58C1 WT. LOSS 0.5650

TIME	TEMP
8.7	942

RUN NO. 67D2 WT. LOSS 0.5770

TIME	TEMP
12.7	1005

RUN NO. 1B2 WT. LOSS 0.5790

TIME	TEMP
4.6	1045

RUN NO. 66E2 WT. LOSS 0.5810

TIME	TEMP
17.3	1019

RUN NO. 21C2 WT. LOSS 0.5860
TIME TEMP
5.1 993

RUN NO. 25D WT. LOSS 0.6040
TIME TEMP
7.4 967

RUN NO. 58B1 WT. LOSS 0.6180
TIME TEMP
5.2 993

RUN NO. 66D2 WT. LOSS 0.6240
TIME TEMP
7.6 1019

RUN NO. 61A1 WT. LOSS 0.6320
TIME TEMP
9.2 967

RUN NO. 46B2 WT. LOSS 0.0997		RUN NO. 46A2 WT. LOSS 0.2240	
TIME	TEMP	TIME	TEMP
0.00	25.	0.00	25.
0.05	537.	0.06	598.
0.10	513.	0.11	622.
0.20	441.	0.16	614.
0.30	386.	0.26	565.
0.40	336.	0.36	513.
0.55	281.	0.46	438.
0.65	251.	0.61	395.
		0.86	320.
		1.11	247.

RUN NO. 46C2 WT. LOSS 0.2494		RUN NO. 45C2 WT. LOSS 0.2553	
TIME	TEMP	TIME	TEMP
0.00	25.	0.00	25.
0.03	443.	0.05	563.
0.08	631.	0.07	721.
0.13	631.	0.10	697.
0.18	605.	0.20	603.
0.28	532.	0.30	509.
0.38	464.	0.40	464.
0.63	365.	0.50	420.
0.78	320.	0.60	367.
0.93	268.	0.75	300.
		0.90	251.
		1.15	239.

RUN NO. 45D2 WT. LOSS 0.2630		RUN NO. 45E2 WT. LOSS 0.3213	
TIME	TEMP	TIME	TEMP
0.00	25.	0.00	25.
0.05	678.	0.05	647.
0.07	688.	0.10	697.
0.10	674.	0.15	676.
0.20	600.	0.25	622.
0.30	532.	0.35	541.
0.40	478.	0.45	493.
0.55	396.	0.70	386.
0.80	367.	0.95	291.
1.05	254.	1.20	222.

RUN NO. 46E2 WT. LOSS 0.3333

TIME	TEMP
0.00	25.
0.05	724.
0.10	791.
0.15	745.
0.25	654.
0.35	579.
0.45	514.
0.60	416.
0.75	338.
1.00	237.

RUN NO. 45B2 WT. LOSS 0.3830

TIME	TEMP
0.00	25.
0.05	631.
0.10	870.
0.20	723.
0.30	650.
0.40	623.
0.50	600.
0.75	490.
1.00	405.
1.25	353.
1.50	295.
1.75	247.

RUN NO. 44R2 WT. LOSS 0.4213

TIME	TEMP
0.00	25.
0.05	626.
0.10	968.
0.20	867.
0.30	754.
0.40	674.
0.50	603.
0.65	527.
0.90	431.
1.15	343.
1.40	251.
1.65	207.

RUN NO. 46D2 WT. LOSS 0.4216

TIME	TEMP
0.00	25.
0.05	726.
0.10	847.
0.15	818.
0.25	697.
0.35	609.
0.45	551.
0.55	506.
0.70	438.
0.85	374.
1.10	295.
1.35	224.

RUN NO. 45A2 WT. LOSS 0.4992

TIME	TEMP
0.00	25.
0.06	945.
0.11	988.
0.21	915.
0.36	892.
0.51	870.
0.66	917.
0.86	872.
1.11	889.
1.31	922.
1.46	769.
1.61	638.
1.86	457.
2.11	320.

RUN NO. 44A2 WT. LOSS 0.5023

TIME	TEMP
0.00	25.
0.05	721.
0.10	1045.
1.30	1045.
4.75	917.
5.05	650.

RUN NO. 44C2 WT. LOSS 0.5352

TIME	TEMP
0.00	25.
0.08	1019
1.00	880.
6.70	867.
7.00	603.

RUN NO. 44E2 WT. LOSS 0.5179

TIME	TEMP
0.00	25.
0.06	917.
0.66	1039
1.21	917.
4.46	917.
4.96	518.

RUN NO. 50C2 WT. LOSS 0.5258

TIME	TEMP
0.00	25.
0.06	988.
0.26	988.
0.56	1003
1.96	1006
3.96	993.
4.46	669.

RUN NO. 45A2 WT. LOSS 0.4990

TIME	TEMP
1.30	892

RUN NO. 47A2 WT. LOSS 0.5400

TIME	TEMP
1.15	1050

RUN NO. 54B2 WT. LOSS 0.1406		RUN NO. 54C2 WT. LOSS 0.1955	
TIME	TEMP	TIME	TEMP
0.00	25.	0.00	25.
0.06	582.	0.05	655.
0.10	553.	0.07	657.
0.20	447.	0.10	628.
0.35	362.	0.15	532.
0.50	317.	0.25	436.
0.65	274.	0.40	348.
0.80	247.	0.55	281.
0.95	202.	0.80	242.

RUN NO. 54A2 WT. LOSS 0.2803		RUN NO. 54E2 WT. LOSS 0.3721	
TIME	TEMP	TIME	TEMP
0.00	25.	0.00	25.
0.05	803.	0.08	968.
0.10	745.	0.13	892.
0.20	584.	0.18	774.
0.35	462.	0.28	654.
0.45	410.	0.43	556.
0.60	358.	0.58	459.
0.85	295.	0.83	348.
1.10	242.	1.08	276.
		1.33	231.

RUN NO. 53A2 WT. LOSS 0.3872		RUN NO. 54D2 WT. LOSS 0.4016	
TIME	TEMP	TIME	TEMP
0.00	25.	0.00	25.
0.05	721.	0.07	892.
0.08	960.	0.12	867.
0.10	917.	0.22	794.
0.20	745.	0.32	674.
0.30	626.	0.47	509.
0.45	513.	0.72	415.
0.70	440.	0.97	338.
0.95	343.	1.22	266.
1.45	217.	1.47	223.

RUN NO. 55A2 WT. LOSS 0.4727

TIME	TEMP
0.00	25.
0.05	750.
0.10	1019
0.20	889.
0.30	794.
0.45	638.
0.60	532.
0.85	433.
1.10	367.
1.35	315.
1.60	259.

RUN NO. 53C2 WT. LOSS 0.5006

TIME	TEMP
0.00	25.
0.05	726.
0.10	943.
0.20	950.
0.30	962.
0.40	867.
0.50	769.
0.65	650.
0.80	530.
0.90	462.
1.15	341.
1.40	247.

RUN NO. 53B2 WT. LOSS 0.5230

TIME	TEMP
0.00	25.
0.05	678.
0.10	890.
0.25	968.
0.35	1019
0.50	1097
0.55	1113
0.65	1113
0.80	902.
0.95	697.
1.05	607.
1.30	452.
1.55	319.
1.80	244.

RUN NO. 53D2 WT. LOSS 0.5314

TIME	TEMP
0.00	25.
0.05	721.
0.08	917.
0.10	943.
0.25	994.
0.40	1019
0.55	1019
0.70	1021
0.85	869.
1.00	745.
1.25	537.
1.50	391.
1.75	295.
2.00	227.

RUN NO. 52A2 WT. LOSS 0.5640

TIME	TEMP
4.9	850

RUN NO. 52B2 WT. LOSS 0.5830

TIME	TEMP
1.5	1050

RUN NO. 52C2 WT. LOSS 0.6000
TIME TEMP
3.9 1050

RUN NO. 52D2 WT. LOSS 0.5900
TIME TEMP
4.85 1050

RUN NO. 53E2 WT. LOSS 0.5390
TIME TEMP
0.60 967

RUN NO. 39-2 WT. LOSS 0.4750

TIME	TEMP
0.00	25.
0.40	485.
0.60	673.
0.80	861.
1.00	967.
1.20	1018.
1.40	757.
1.60	612.
1.80	496.
2.00	410.

RUN NO. 39-3 WT. LOSS 0.3590

TIME	TEMP
0.00	25.
0.20	246.
0.40	419.
0.60	574.
0.80	685.
0.90	721.
1.00	650.
1.20	497.
1.40	390.

RUN NO. 39-4 WT. LOSS 0.3080

TIME	TEMP
0.00	25.
0.20	222.
0.40	355.
0.60	462.
0.80	567.
0.90	625.
1.00	567.
1.20	450.
1.40	330.

RUN NO. 40-1 WT. LOSS 0.4370

TIME	TEMP
0.00	25.
0.40	443.
0.60	574.
0.80	696.
1.00	817.
1.20	940.
1.40	783.
1.60	697.
1.80	470.

RUN NO. 40-2 WT. LOSS 0.2160

TIME	TEMP
0.00	25.
0.20	302.
0.40	438.
0.60	556.
0.70	661.
0.80	614.
1.00	513.
1.20	455.

RUN NO. 40-3 WT. LOSS 0.1126

TIME	TEMP
0.00	25.
0.20	246.
0.40	438.
0.50	508.
0.60	508.
0.80	426.
1.00	355.

RUN NO. 41-3 WT. LOSS 0.1460
TIME TEMP
0.00 25.
0.20 391.
0.30 532.
0.40 446.
0.50 391.
0.60 331.

RUN NO. 39-1 WT. LOSS 0.5220
TIME TEMP
2.8 840

RUN NO. 62B1 WT. LOSS 0.5300
TIME TEMP
9.0 905

RUN NO. 50-1 WT. LOSS 0.4480
TIME TEMP
8.2 660

RUN NO. 50-2 WT. LOSS 0.2910
TIME TEMP
15.0 415

RUN NO. 50-3 WT. LOSS 0.5370
TIME TEMP
10.6 795

RUN NO. 0-4 WT. LOSS 0.5400

TIME
8.0TEMP
865

RUN NO. 0-5 WT. LOSS 0.4450

TIME
8.8TEMP
650

RUN NO. 50-6 WT. LOSS 0.3660

TIME
9.2TEMP
600

RUN NO. 51-1 WT. LOSS 0.5470

TIME
8.2TEMP
890

RUN NO. 51-2 WT. LOSS 0.5410

TIME
7.7TEMP
900

RUN NO. 51-3 WT. LOSS 0.5940

TIME
3.2TEMP
1150

RUN NO. 51-4 WT. LOSS 0.6030
TIME TEMP
6.0 1122

RUN NO. 51-5 WT. LOSS 0.3530
TIME TEMP
10.1 635

RUN NO. 51-6 WT. LOSS 0.1940
TIME TEMP
10.0 495

RUN NO. 51-7 WT. LOSS 0.3460
TIME TEMP
17.5 580

Bituminous Coal, Helium

<u>Run No.</u>	<u>Wt. Loss</u>	<u>Pressure</u>	<u>Heating Rate</u>
42-1	37.9	1500 psig	Low
42-2	40.0	500 psig	"
43-1	47.5	1 atm	"
43-2	52.4	5 mm Hg	"
43-3	52.7	0.5 mm Hg	"
43-4	49.9	25 "Hg	"
45-2	53.8	0.5 mm Hg	High
56-2	34.4	1000 psig	"
56-3	38.9	1000 psig	"
54-2A	39.1	1000 psig	Low

(Additional low pressure data on bituminous coal was taken by A. Cohen, 1973)

Lignite, Helium

28A2	40.8	1500 psig	Low
64B	40.2	0.5 mm Hg	"
64C	41.7	1 mm Hg	Med
64D	43.3	- 5 " Hg	High

Lignite, Hydrogen, Low Heating Rates

			<u>Time at Cutoff</u>	<u>Final Temp. °C</u>
6A2	41.2	0 psig(all)	7.5 sec	1000
6B2	27.7	0	9.6	757
6C2	36.0	0	13.0	820
6D2	40.8	0	6.5	993
5A2	47.8	200	7.0	1032
5B2	34.9	200	5.8	798
5C2	47.9	200	6.8	1113
7C2	48.2	200	7.0	1113
7D2	46.0	200	6.0	993
4A2	39.2	400	6.0	774
4B2	37.0	400	6.5	840
4C2	50.6	400	6.2	867+
4D2	43.2	400	8.4	867
7A2	52.6	400	6.8	1019
7B2	34.2	400	6.8	795
8A2	38.9	400	5.5	845
8D2	52.8	400	2.0	1145
3A2	48.3	600	5.0	917
3B2	51.3	600	6.0	917
3C2	49.7	600	6.4	917
19A2	51.1	600	4.9	1006
19B2	52.5	600	5.3	1019

Bituminous Coal, Helium

<u>Run No.</u>	<u>Wt. Loss</u>	<u>Pressure</u>	<u>Heating Rate</u>
42-1	37.9	1500 psig	Low
42-2	40.0	500 psig	"
43-1	47.5	1 atm	"
43-2	52.4	5 mm Hg	"
43-3	52.7	0.5 mm Hg	"
43-4	49.9	25 "Hg	"
45-2	53.8	0.5 mm Hg	High
56-2	34.4	1000 psig	"
56-3	38.9	1000 psig	"
54-2A	39.1	1000 psig	Low

(Additional low pressure data on bituminous coal was taken by A. Cohen, 1973)

Lignite, Helium

28A2	40.8	1500 psig	Low
64B	40.2	0.5 mm Hg	"
64C	41.7	1 mm Hg	Med
64D	43.3	- 5 " Hg	High

Lignite, Hydrogen, Low Heating Rates

			<u>Time at</u> <u>Cutoff</u>	<u>Final</u> <u>Temp.</u>
			7.5 sec	1000°C
6A2	41.2	0 psig(all)		
6B2	27.7	0	9.6	757
6C2	36.0	0	13.0	820
6D2	40.8	0	6.5	993
5A2	47.8	200	7.0	1032
5B2	34.9	200	5.8	798
5C2	47.9	200	6.8	1113
7C2	48.2	200	7.0	1113
7D2	46.0	200	6.0	993
4A2	39.2	400	6.0	774
4B2	37.0	400	6.5	840
4C2	50.6	400	6.2	867+
4D2	43.2	400	8.4	867
7A2	52.6	400	6.8	1019
7B2	34.2	400	6.8	795
8A2	38.9	400	5.5	845
8D2	52.8	400	2.0	1145
3A2	48.3	600	5.0	917
3B2	51.3	600	6.0	917
3C2	49.7	600	6.4	917
19A2	51.1	600	4.9	1006
19B2	52.5	600	5.3	1019

Lignite, Hydrogen, Low Heating Rates (Cont.)

Run No.	Wt. Loss	Pressure	Time at Cutoff	Final Temp.
2A2	56.8%	800 psig	6.2 sec	993 ^o C
2B2	53.2	800	2.0	1045
2C2	37.0	800	6.0	697
2D2	50.2	800	1.5	1045
59A1	57.0	900	5.3	945
20C	57.9	1300	4.7	993
20D	55.6	1300	5.5	967
18A2	57.1	1500	6.4	850
18B2	69.5	1500	6.9	1020
18C2	56.4	1500	7.4	915
19C2	54.9	1500	6.7	955
19D	53.5	1500	7.1	842
20A	56.6	1500	1.8	1150
20B	56.7	1500	1.6	1045
21A	60.6	1500	1.6	1007
24A	54.9	1500	7.0	1007
24B	60.2	1500	7.9	967
24C	60.0	1500	5.0	967
24D	62.2	1500	6.8	920

Bituminous, Low heating Rates, High Temperatures and Long Times

Constant $P_{tot} = 1000$ psigPH₂

57-1	58.19	1000
57-2	52.2	500
57-3	37.13	100
57-4	45.76	300
57-5	40.75	150
57-6	43.31	200
60-1	43.2	150
60-2	40.6	100
60-3	41.2	100
60-4	50.7	500
60-5	56.6	750

Pure H₂

60-6	50.9	100
60-7	49.5	100
61-1	50.4	200
61-2	49.2	200
61-3	54.1	500
61-4	55.9	750

(Other data from Lavery, 1973)

Bituminous, Low Heating Rates, High Temperatures and Long Times

1 atm Helium

<u>Run No.</u>	<u>Wt.Loss %</u>	<u>Particle Size</u>
55-1	44.72	991-1190u
55-2	47.24	250-297
55-3	46.68	149-177
55-7	48.07	53-88
30-4	44.1	991-1190

1000 psig Hydrogen

58-1	44.26	991-1190
58-2	44.66	991-1190
59-1	51.97	250-297
59-3	54.98	149-177
59-4	46.25	297-833

10.3 SAMPLE CALCULATIONS

10.3.1 Apparatus

Estimated Heating Rates -- Estimation of heating rates within an experimental system is important for two reasons: 1) to avoid improper isothermal treatment of data during a non-isothermal period and 2) to evaluate the influence of heating rate as an independent variable. The first problem is simply an error which may be readily remedied upon recognition. The second case poses the additional difficulty of requiring characterization of the heating rate. In order to establish a basis for such characterization several idealized situations for unsteady heat-up of spheres are outlined below:

1. Isothermal Sphere (i.e., $dT/dr = 0$)

- A. Constant heating rate or linear time-temperature profile such that

$$dT/dt = m \quad (10-3)$$

or
$$T = mt + T_0$$

This situation may be considered valid if:

1. $T_{\text{sphere}} = T_{\text{source}}$ (implies infinite heat transfer rate between source and sphere) and T_{source} is increased linearly with time.
2. $T_{\text{source}} \gg T_{\text{sphere}}$ such that the heating rate is given as

$$dT/dt = 3hT_{\text{source}}/(\rho C_p r) \quad (10-4)$$

(for transport by conduction-convection; when conduction predominates, $h = k/r$)

$$dT/dt = 3\sigma T_{\text{source}}^4/(\rho C_p r) \quad (10-5)$$

(for transport by radiation)

B. Exponential time-temperature behavior. If $T_{\text{source}} \gg$

$T_{\text{source}} - T_{\text{sphere}}$, Equation 10-4 is rewritten:

$$dT/dt = 3h(T_{\text{source}} - T)/\rho C_p r \quad (10-6)$$

$$T = T_{\text{source}}(1 - \exp(-3ht/\rho C_p r))$$

In the special case of conduction only, the heat-up time

($T = 0.95T_{\text{source}}$) is equal to $\rho C_p r^2/k$.

2. Non-Isothermal Sphere (gradients exist within the sphere)

The differential equation may be written

$$\frac{dT}{dt} = \frac{\alpha}{r^2} \frac{d}{dr} \left[r^2 \frac{dT}{dr} \right] \quad (10-7)$$

with typical boundary conditions:

$$\begin{aligned} t = 0 & \quad T = T_o \\ r = 0 & \quad dT/dr = 0 \\ r = r_s & \quad T = T_s \end{aligned}$$

Solutions may be found in Carslaw and Jaeger (1959), pp. 102 and 234. The criteria for selection of Case 2 over Case 1 may be obtained from the Biot number

$$N_{\text{Bi}} = hr/k_{\text{solid}} = \frac{\text{internal resistance}}{\text{external resistance}} \quad (10-8)$$

A large value for N_{Bi} would indicate preference for Case 2.

In the special case of pure conduction, $N_{\text{Bi}} = k_{\text{gas}}/k_{\text{solid}}$.

To illustrate typical results in two previously cited cases, property values from Badzioch (1967) have been used in the calculations.

Coal:

$$\rho = 1.0 \text{ g/cm}^3 \quad C_p = 0.4 \text{ cal/g } ^\circ\text{C} \quad k = 0.6 \times 10^{-3} \frac{\text{cal}}{\text{cm sec } ^\circ\text{C}}$$

Gas Medium:

$$k = 1.5 \times 10^{-4} \text{ cal/cm sec } ^\circ\text{C}$$

Example A -- 100 μ diameter particle heated by radiation from a source at 1200°C. This might simulate an entrained gas-coal mixture approaching or passing through a very hot chamber. Using Equation 10-5:

$$\frac{dT}{dt} = \frac{3(1.355 \times 10^{-12} \text{ cal/sec cm}^2 \text{ }^\circ\text{K}^4)(1473^\circ\text{K})^4}{(1.0 \text{ g/cc})(0.4 \text{ cal/g }^\circ\text{C})(0.005 \text{ cm})} = 9600^\circ\text{C/sec}$$

Example B -- 100 μ diameter particle suddenly immersed in a infinite stagnant medium at 1000°C. This might be comparable to the free-fall reactors used by several previous investigators. First, Equation 10-8

$$N_{Bi} = 1.5/6.0 = 0.25$$

suggests external resistance controlling (Eq. 10-6). The time required for 95% heat-up is

$$t_{0.95} = \rho C_p r^2 / k = (1.0)(0.4)(0.005)^2 / 1.5 \times 10^{-4} = 0.066 \text{ sec}$$

$$dT/dt = 950/0.066 = 14,400^\circ\text{C/sec}$$

These examples are illustrative of the general magnitude of heating rates and do not represent detailed analysis of the complex heat transfer problem that will undoubtedly accompany any actual design. Nevertheless, they are informative as to the needs of experimental data.

Sample Design Calculations --

1. Energy Requirements for Rapid Heat-Up (10^4 °C/sec)

$$\text{Accumulation} = \text{Generation} - \text{Heat Losses} \quad (10-9)$$

(assume heat losses negligible, this is confirmed in Part 3)

$$m_s C_p dT/dt = jE_v^2 / R_s \quad (10-10)$$

where m_s = mass of screens, 0.5 g

C_p = heat capacity, 0.12 cal/g °C

j = Joule's constant, 0.239 cal/sec watt

R_s = mean resistance of screen, 0.21 ohms

E_v = voltage drop, unknown

$$(0.5)(0.12)(10^4) = 360 \text{ cal/sec} = 0.239 E_v^2 / 0.21$$

$$E_v \approx 23 \text{ volts}$$

2. Response in Temperature Measurement

Of great importance in evaluating the experimental data is knowledge of the relationship between the temperature recorded by the thermocouple and the actual temperature of the coal. If the picture of the screen "sandwich" is idealized as two flat plates separated by a distance equal to particle diameter (the "bead" diameter of a thermocouple is roughly 3 times that of the wire, 0.001" TC has a "bead" = 75 μ), the time for the center of this "slab" to reach 95% of a step change in surface temperature is given by Carslaw and Jaeger as $N_{Fo} = \alpha t/r^2 = 1.5$. Approximate thermal diffusivities of the respective components of the slab are

$$\alpha_{\text{gas}} = (1.5 \times 10^{-4}) / (2.5 \times 10^{-4})(0.25) = 2.4 \text{ cm}^2/\text{sec}$$

$$\alpha_{\text{coal}} = (0.6 \times 10^{-3}) / (1.0)(0.4) = 1.5 \times 10^{-3} \text{ "}$$

$$\alpha_{\text{TC}} = (0.06) / (8.7)(0.11) = 6.3 \times 10^{-3} \text{ "}$$

Taking the worst case, coal, for 100 μ particles the time lag is

$$t = 1.5 (0.005)^2 / (1.5 \times 10^{-3}) = 0.025 \text{ sec}$$

This is an upper limit for several reasons; there is not a step change in the surface temperature but rather a linear increase reducing the time lag, also the surrounding gas will heat more rapidly (higher α) thus decreasing t_{lag} . With these considerations, the response is deemed quite good.

3. Steady-State Heat Transfer

An approximate solution of the energy balance at steady-state is possible given several simplifying assumptions. Let the energy generated by electrical current dissipation be transferred away from the screen by conduction to cold end terminals and by radiation to the surroundings. Furthermore, assume no gradients other than along the length of the strip. Writing the differential equation:

$$\frac{d^2T}{dx^2} - \sigma \epsilon p(T^4 - T_o^4)/kw + jE_v^2/kL^2q = 0 \quad (10-11)$$

with ϵ = emissivity of the screen, 0.5

p = perimeter of screen, 3.0 cm.

k = conductivity, 0.039 cal/cm sec $^{\circ}\text{C}$

w = effective cross-sectional area, $2.65 \times 10^{-3} \text{ cm}^2$

$2L$ = length of screen, 5 cm

$T_L = 923^{\circ}\text{C}$ $T_o = 27^{\circ}\text{C}$

q = resistivity, 142 $\mu\Omega\text{-cm}$

The equation is solved in terms of voltage (E_v) since it may be directly compared to experimental data. Solution is given in Carslaw and Jaeger (p. 154).

$$E_v = (\text{by trial and error}) \quad 5.0 \text{ volts}$$

which compares favorably to the 5-6 volts required experimentally.

Heat Losses = 23 cal/sec (justifying the assumption
in Part 1)

At 1000 psig the experimental voltage drop across the screen was estimated at 9 volts, a factor of 1.6 higher than at 1.0 atm. This means that power consumption was about 2.5 times as great requiring about 150% more power to maintain equal temperatures.

4. Pressure Tolerance of Vessel Components

A. Flanges --

1500 PSIG, Type 316SS, Pressure rating at -20 to 100°F equal to 3600 psig (tested hydrostaticly to 5400 psig)

B. Pipe Section

Pressure Tolerance for cylindrical vessel (Perry, et al., 1963)

$$P = \frac{2SEt}{D_o - 0.8t} \quad (10-12)$$

where S = allowable stress, 18,75 psi for TP316

E = weld factor, 1.0

t = thickness, 0.337" for Sch 80 pipe

D_o = outside diameter, 4.5"

$$P = 2987 \text{ psig}$$

C. Cap Section

Similar equation for an ellipsoidal closure, concave to pressure (Perry, et al.)

$$P = \frac{2SEt}{D_i + 0.2t} \quad (10-13)$$

$$P = 3246 \text{ psig}$$

10.3.2 Experimental Data

Secondary Reaction Model -- For bituminous coal, the yield of reactive species was represented by Equation 5-15

$$V_{\text{tot}} = 37.2 + \frac{V_R^*}{1 + \frac{k_4}{k^*} P_{\text{tot}}} \quad (5-15)$$

From the data, k_4/k^* was estimated to be 0.56 and V_R^* to be 17.0%.

Allowing for 3% average deposition on the screen in vacuum, the corrected value of V_R^* was 20.0%.

P_{tot} (atm)	$V_R^* = 17.0$		$V_R^* = 20.0$	
	V_R	V_{tot}	V_R	V_{tot}
0.01	16.9	54.1	19.9	57.1
0.1	--	--	18.9	56.1
1.0	10.9	48.1	12.8	50.0
10.0	2.6	39.8	3.0	40.2
100.0	--	--	0.4	37.6

Hydrogenation Model -- At a constant total pressure of 1000 psig, Equation 5-19 becomes

$$V_{\text{tot}} = 37.2 + 20.0 \left[\frac{1 + 69 \frac{k_5}{k^*} P_{\text{H}_2}}{1 + 38.6 + 69 \frac{k_5}{k^*} P_{\text{H}_2}} \right] \quad (5-19a)$$

Values of V_R and V_{tot} are calculated for three different values of k_5/k^* :

P_{H_2} (atm)	$k_5/k^* = 0.02$		0.05		0.1	
	V_R	V_{tot}	V_R	V_{tot}	V_R	V_{tot}
1	1.1	38.3	2.1	39.3	3.4	40.6
5	3.4	40.6	6.4	43.6	9.6	46.8
10	5.5	42.7	9.6	46.8	12.9	50.1
20	8.5	45.7	12.9	50.1	15.6	52.8
35	11.1	48.3	15.1	52.3	17.2	54.4
69	14.2	51.4	17.2	54.4	18.5	55.7

For conditions of pure hydrogen, Equation 5-19 is simplified to:

$$V_{\text{tot}} = 37.2 + 20.0 \left[\frac{1 + \frac{k_5}{k^*} P_{\text{H}_2}^2}{1 + 0.56 P_{\text{H}_2} + \frac{k_5}{k^*} P_{\text{H}_2}^2} \right] \quad (5-19b)$$

P_{H_2} (atm)	$k_5/k^* = 0.02$		0.05		0.1	
	V_R	V_{tot}	V_R	V_{tot}	V_R	V_{tot}
1	12.9	50.1	13.0	50.2	13.3	50.5
5	7.0	44.2	8.9	46.1	11.1	48.3
10	7.0	44.2	10.3	47.5	13.3	50.5
20	8.9	46.1	13.0	50.2	15.7	52.9
35	11.2	48.4	15.1	52.3	17.3	54.5
69	14.2	51.4	17.2	54.4	18.5	55.7

From Equation 5-20

P_{min} (atm)	7.1	4.5	3.2
V_{tot}	43.9	46.1	47.7

Corrected Hydrogenation Model -- Equation 5-19 was deemed inadequate for two reasons: 1) diffusional limitations at high pressures and 2) hydrogenation of non-volatile species. The first problem will manifest itself in a pressure-dependent k_5 while the second will simply appear as an underprediction of yields. Considering the diffusion problem, the rate of hydrogenation may be written as

$$k_5 P_{\text{H}_2}^{\text{eff}} C = K'' (P_{\text{H}_2} - P_{\text{H}_2}^{\text{eff}}) \quad (10-14)$$

where $P_{\text{H}_2}^{\text{eff}}$ = hydrogen pressure in the particle interior

K'' = overall mass transfer coefficient for hydrogen

Solving for "effective" hydrogen pressure:

$$P_{\text{H}_2}^{\text{eff}} = \frac{P_{\text{H}_2}}{1 + \frac{k_5 C}{K''}} \quad (10-15)$$

Since it is easier to adjust k_5 than P_{H_2} , an "effective" k_5 may be defined in the form of Equation 10-15:

$$k_5^{\text{eff}} = \frac{k_5}{1 + \frac{k_5 C}{K''}} = \frac{a}{1 + bP} \quad (10-16)$$

The final approximation assumes $K''/k_5 C$ inversely proportional to pressure.

The mechanism involved in solid phase hydrogenation, the second deficiency of Equation 5-19, is unknown so it is assumed that the Moseley and Paterson model is a reasonable approximation since temperatures are constant.

$$X = \frac{k_3 C_o^*}{k_2} P_{H_2} \quad (2-13)$$

With values of 0.106, 0.0625, and 0.116 for a , b , and $k_3 C_o^*/k_2$, the following yields were computed:

P_{H_2} (atm)	$P_{\text{tot}} = 1000$ psig V_{tot}	$P_{\text{tot}} = P_{H_2}$ V_{tot}
1	38.3	50.5
5	41.2	47.9
10	43.9	49.8
20	48.1	52.4
35	52.3	--
42	--	55.7
69	59.4	59.4

Grinding Costs Compared To Thermal Efficiency -- The experimental data show that, for example, 1000 μ will yield about 20% less weight loss than 88 μ in 1000 psig hydrogen. The energy lost in the catalytic methanation of this additional 20% is easily calculated to be about 1500 BTU per pound of original coal. Of course, this assumes no attempt to recover the heat. In reality, however, it would probably be desirable to recover at least some of this energy, so it should be interesting to compute the theoretical limit on this recovery. In simplified terms, heat is being generated at some intermediate temperature (T_2) while heat is needed at a higher temperature (T_1) elsewhere in the process (steam gasification). It is, therefore, desirable to know the amount of energy that can be raised to the higher temperature level and the amount that must be rejected to the ambient (T_o) and lost. The work required to move a unit of energy to T_1 is, based on Carnot efficiencies:

$$W/Q_1 = T_1 - T_2 / T_1 \quad (10-17)$$

while the amount of work produced by heat rejection is

$$W/Q_o = T_2 - T_o / T_o \quad (10-18)$$

Setting the two equations equal in terms of work, an efficiency

can be derived:

$$\frac{Q_2}{Q_1} = 1 + \frac{T_o(T_1 - T_2)}{T_1(T_2 - T_o)} \quad (10-19)$$

If reasonable values of temperature are selected ($T_o = 300^{\circ}\text{K}$, $T_1 = 1400$, $T_2 = 800$) it may be determined that about 20% of the energy produced is wasted. If one could achieve, in each step, say 50% of Carnot efficiency, a factor of 4 in temperature term of Equation 10-19, then

an overall efficiency of 50% is obtained. Compare now these losses with the energy consumption of grinding. Using the Bond Crushing Law and Work Index (Perry, et al., 1963):

$$\frac{P}{T} = 1.46 W_i \left(\frac{1}{D_{pb}} - \frac{1}{D_{pa}} \right) \quad (10-20)$$

where P is power in horsepower

T is Tons per minute

W_i is 13.00 for coal

D_{pb} is particle diameter (product) ft, based on 80% passage

D_{pa} is particle diameter (feed)

$$\frac{P}{T} = 785 \text{ hp-min/ton} \quad \text{or} \quad 1000 \text{ BTU/lb}$$

Within the accuracy of the numbers the two effects are roughly comparable.

10.3.3 Computer Routines

Listings of the programs used in the evaluation of kinetic models are provided on the next several pages. Following the program listings a sample print out has been included. The results of this particular run are plotted in Figures 6-2 and 6-3.


```

// FOP
*LIST ALL
*ONE WORD INTEGERS
*JOCS (CARD,1132 PRINTER,TYPEWRITER)
*NAME COAL }
C
C *****
C
C
C
C COAL 3, 5, AND 6 COMPRISE A NON-LINEAR LEAST SQUARES REGRESSION
C PROGRAM, WRITTEN BY P. C. LEWELLEN, FOR PARAMETER ESTIMATION IN
C SELECTED COAL DECOMPOSITION RATE MODELS
C
C COAL 3 READS DATA FROM CARD DECK AND PERFORMS AN OPTIONAL COARSE
C GRID SEARCH BASED ON USER SUPPLIED PARAMETER RANGES
C
C COAL 5 IS A MODIFIED VERSION OF CURFIT (BEVINGTON, 1969) AND
C UTILIZES A GRADIENT SEARCH TECHNIQUE
C
C COAL 6 IS USED TO PRINT OUT RESULTS
C
C SUBROUTINE INGR 3 IS REQUIRED FOR EVALUATION OF A FIRST ORDER
C DECOMPOSITION MODEL
C
C SUBROUTINE INGR 5 AND FUNCTION TRAPS ARE USED IN FITTING DATA TO
C THE STATISTICAL DISTRIBUTION MODEL
C
C THE OBJECTIVE FUNCTION TO BE MINIMIZED IS THE SUM OF THE SQUARES
C OF THE DIFFERENCE BETWEEN CALCULATED AND EXPERIMENTAL WEIGHT
C LOSSES
C
C NOMENCLATURE
C   BOTT(K)      LOWER VALUE OF INITIAL PARAMETER RANGE
C   ERROR       SUM OF THE SQUARES OF THE DIFFERENCE BETWEEN
C               FRAC AND V CALC
C   FRAC(I)     FRACTIONAL WEIGHT LOSS FOR EACH RUN
C   NPAM        NO. OF PARAMETERS TO BE ESTIMATED
C   NRFAD       I/O INDICATOR
C   NRUNZ       NO. OF RUNS IN DATA DECK
C   NUM(I)      NO. OF TIME-TEMPERATURE INTERVALS FOR EACH RUN
C   NWRIT       I/O INDICATOR
C   PARAM(K)    PARAMETER VALUES
C   RCODE(I)    RUN NUMBER
C   SAVE(K)     BEST PARAMETER VALUE
C   TEMP(I,J)   TEMPERATURE
C   TIME(I,J)   TIME
C   TOP(K)      UPPER VALUE OF INITIAL PARAMETER RANGE
C   TRY(K)      VALUE OF PARAMETERS USED IN COARSE GRID SEARCH
C   V CALC(I)   CALCULATED WEIGHT LOSS
C   VSTAR       EXPERIMENTAL YIELD
C   WATER       MOISTURE CONTENT
C
C *****

```

```
// FOR
*LIST ALL
*ONE I/O INTEGERS
*IOCS (CARD, 1132 PRINTER, TYPEWRITER)
*NAME COAL3
```

```
C
C *****
C
C
C
C COAL 3, 5, AND 6 COMPRISE A NON-LINEAR LEAST SQUARES REGRESSION
C PROGRAM, WRITTEN BY P. C. LEWELLEN, FOR PARAMETER ESTIMATION IN
C SELECTED COAL DECOMPOSITION RATE MODELS
C
C COAL 3 READS DATA FROM CARD DECK AND PERFORMS AN OPTIONAL COARSE
C GRID SEARCH BASED ON USER SUPPLIED PARAMETER RANGES
C
C COAL 5 IS A MODIFIED VERSION OF CURFIT (BEVINGTON, 1969) AND
C UTILIZES A GRADIENT SEARCH TECHNIQUE
C
C COAL 6 IS USED TO PRINT OUT RESULTS
C
C SUBROUTINE INGR 3 IS REQUIRED FOR EVALUATION OF A FIRST ORDER
C DECOMPOSITION MODEL
C
C SUBROUTINE INGR 5 AND FUNCTION TRAPS ARE USED IN FITTING DATA TO
C THE STATISTICAL DISTRIBUTION MODEL
C
C THE OBJECTIVE FUNCTION TO BE MINIMIZED IS THE SUM OF THE SQUARES
C OF THE DIFFERENCE BETWEEN CALCULATED AND EXPERIMENTAL WEIGHT
C LOSSES
C
C NOMENCLATURE
C   BOTT(K)      LOWER VALUE OF INITIAL PARAMETER RANGE
C   ERROR       SUM OF THE SQUARES OF THE DIFFERENCE BETWEEN
C               FRAC AND V CALC
C   FRAC(I)     FRACTIONAL WEIGHT LOSS FOR EACH RUN
C   NPAM        NO. OF PARAMETERS TO BE ESTIMATED
C   NREAD       I/O INDICATOR
C   NRUNZ       NO. OF RUNS IN DATA DECK
C   NUM(I)      NO. OF TIME-TEMPERATURE INTERVALS FOR EACH RUN
C   NWRIT       I/O INDICATOR
C   PARAM(K)    PARAMETER VALUES
C   RCODE(I)    RUN NUMBER
C   SAVE(K)     BEST PARAMETER VALUE
C   TEMP(I,J)   TEMPERATURE
C   TIME(I,J)   TIME
C   TOP(K)      UPPER VALUE OF INITIAL PARAMETER RANGE
C   TRY(K)      VALUE OF PARAMETERS USED IN COARSE GRID SEARCH
C   V CALC(I)   CALCULATED WEIGHT LOSS
C   VSTAR       EXPERIMENTAL YIELD
C   WATER       MOISTURE CONTENT
C
C *****
```

```

C
DIMENSION FRAC(50),NUM(50),TIME(50,15),TEMP(50,15),VCALC(50),
+ RCODE(50),PARAM(10),BOTT(10),TOP(10),TRY(10),SAVE(10)
COMMON NRUNZ,FRAC,NUM,TIME,TEMP,VCALC,VSTAR,WATER,RCODE,PARAM,
+ IFOO, NPAM, ERROR
EQUIVALENCE (BOTT(1),PARAM(1))
DATA NREAD,NWRIT,IX/2,3,127/
ERROR=1.E30

C
C READ DATA FROM CARD DECK
C
READ (NREAD,100) NRUNZ,VSTAR,WATER
100 FORMAT (20X,I5/20X,F5.0,F10.0)
WRITE (NWRIT,303) VSTAR,WATER
303 FORMAT (/35X,'ASSUMED VSTAR VALUE=',F6.4//35X,'ASSUMED H2O FRACTI
+ON=',F6.4)
WRITE (1,9999)

C
C DECISION TO INCLUDE COOLING CURVE
C
9999 FORMAT (' SET SWITCH 0 ON FOR HEATUP INTEGRATION ONLY')
CALL DATSW (0,LTEST)
DO 200 I=1,NRUNZ
TMAX=0.0
READ (NREAD,300) FRAC(I),RCODE(I),FOOZA
300 FORMAT (F10.0,8X,A4/F10.0)
READ (NREAD,400) (TIME(I,J),TEMP(I,J),J=1,15)
400 FORMAT (8(F4.0,F5.0))

C
C DETERMINE NUMBER OF TIME-TEMPERATURE INTERVALS FOR EACH RUN
C
DO 600 J=1,15
GO TO (498,499), LTEST
498 IF ((TEMP(I,J)-TMAX)+8.0) 500,500,600
499 IF (TEMP(I,J)-1.) 500,500,600
500 NUM(I)=J-1
GO TO 200
600 TMAX=TEMP(I,J)
NUM(I)=15
200 CONTINUE

C
C CONVERT TEMPERATURES TO DEGREES ABSOLUTE
C
DO 502 I=1,NRUNZ
DO 502 J=1,15
502 TEMP(I,J)=TEMP(I,J) + 273.15

C
C READ IN INITIAL ESTIMATES FOR PARAMETERS
C (EITHER SINGLE VALUE OR RANGE)
C
DO 702 NPAM=1,10
READ (NREAD,701) BOTT(NPAM),TOP(NPAM)
701 FORMAT (2E10.0)
IF (BOTT(NPAM)) 702,703,702

```

```

702 CONTINUE
    NPAM=11
703 IFOO=NPAM
    NPAM=NPAM-1
C
C   IF RANGE GIVEN DO COARSE GRID SEARCH FOR 20 RANDOM POINTS
C
    IF (TOP(1)) 731,732,731
731 DO 739 KNT=1,20
    DO 738 I=1,NPAM
    CALL RANDU (IX,IX,PARA)
738 TRY(I)=BOTT(I)+PARA*(TOP(I)-BOTT(I))
    CALL INGR3 (TRY,ERR2,0)
C
C   PRINT OUT BEST PARAMETER VALUES FROM GRID SEARCH AS STARTING
C   POINT FOR GRADIENT SEARCH
C
    WRITE (1,4001)(TRY(LEW),LEW=1,NPAM),ERR2
4001 FORMAT (6E20.5)
    IF (ERROR=ERR2) 739,740,740
    740 DO 741 K=1,NPAM
    741 SAVE(K)=TRY(K)
    ERROR=ERR2
    739 CONTINUE
    DO 744 K=1,NPAM
    744 PARAM(K)=SAVE(K)
    732 CALL INGR3 (PARAM,ERROR,0)
    WRITE (NWRT,750)
    750 FORMAT (// ' INITIAL PARAMETER VALUES=' )
    WRITE (NWRT,711) (I,PARAM(I),I=1,NPAM)
    711 FORMAT (/ ' (',I2,',')',E13.5)
    CALL LINK (COAL5)
    END
// DUP
*DELETE          COAL3
*STORE          WS  UA  COAL3

// FOR
*LIST ALL
*ONE WOPD INTEGERS
*IOCS (TYPEWRITER)
*NAME COAL5
C
C *****
C
C   COAL 5 IS A MODIFIED VERSION OF CURFIT (BEVINGTON, 1969) AND
C   UTILIZES A GRADIENT SEARCH TECHNIQUE
C
C   NOMENCLATURE

```

```

C      ALPHA(K,L)      CURVATURE MATRIX
C      ARRAY(K,L)      MODIFIED CURVATURE MATRIX
C      BETA(K)          ROW MATRIX
C      BPAM(K)          NO. OF PARAMETERS
C      DELTA            INCREMENTS FOR PARAMETERS
C      DERIV(K)         DERIVATIVE OF FUNCTION WITH RESPECT TO PARAMETER
C                       K
C      LAMDA            PROPORTION OF GRADIENT SEARCH INCLUDED
C      LDUMMY(K)        DUMMY VARIABLE FOR MATRIX INVERSION SUBROUTINE
C      MDUMMY(K)        DUMMY VARIABLE FOR MATRIX INVERSION SUBROUTINE
C      VECTO(M)         VECTOR EQUIVALENT TO THE ARRAY MATRIX

```

```

C      *****

```

```

C      REAL LAMDA
C      DIMENSION FRAC(50),NUM(50),TIME(50,15),TEMP(50,15),VCALC(50),
+ RCODE(50),PARAM(10),BPAM(10),DERIV(10),BETA(10),ALPHA(10,10),
+ ARRAY(10,10),LDUMMY(10),MDUMMY(10),VECTO(100)
C      COMMON NRUNZ,FRAC,NUM,TIME,TEMP,VCALC,VSTAR,WATER,RCODE,PARAM,
+ IFOO,NPAM,ERROR
C      EQUIVALENCE (ARRAY(1,1),VECTO(1))
C      DATA LAMDA/0.01/
99 LAMDA=0.1*LAMDA

```

```

C      EVALUATE ALPHA AND BETA MATRICES

```

```

C      DO 34 J=1,NPAM
C      BETA(J)=0.0
C      DO 34 K=1,J
34 ALPHA (J,K)=0.0

```

```

C      EVALUATE DERIVATIVES OF THE FITTING FUNCTION FOR THE ITH TERM
C      WITH RESPECT TO EACH PARAMETER

```

```

C      DO 50 I=1,NRUNZ
C      DO 98 JFOO=1,NPAM
C      PARA=PARAM(JFOO)
C      DELTA=0.01*PARA
C      PARAM(JFOO)=PARA+DELTA
C      CALL INGR3 (PARAM,VAL,I)
C      VAL2=VCALC(I)
C      PARAM(JFOO)=PARA
C      CALL INGR3 (PARAM,VAL,I)
98 DERIV(JFOO)=(VAL2-VCALC(I))/DELTA
C      DO 46 J=1,NPAM
C      BETA(J)=BETA(J)+(FRAC(I)-VCALC(I))*DERIV(J)
C      DO 46 K=1,J
46 ALPHA(J,K)=ALPHA(J,K)+DERIV(J)*DERIV(K)
50 CONTINUE
C      DO 53 J=1,NPAM
C      DO 53 K=1,J
53 ALPHA(K,J)=ALPHA(J,K)

```

```

C      INVERT MODIFIED CURVATURE MATRIX TO FIND NEW PARAMETERS

```

```

C
71 DO 74 J=1, NPAM
   DO 73 K=1, NPAM
73 ARRAY(J,K)=ALPHA(J,K)/SQRT(ALPHA(J,J)*ALPHA(K,K))
74 ARRAY(J,J)=ARRAY(J,J)*(1.+LAMDA)
   KNT=0
   DO 110 M=1, NPAM
   DO 110 N=1, NPAM
   KNT=KNT+1
110 VECTO(KNT)=ARRAY(N,M)
   CALL MINV (VECTO, NPAM, PARA, LDUMMY, MDUMMY)
   INT=NPAM*NPAM
   DO 120 M=1, NPAM
   MCOL=IFOO=M
   DO 120 N=1, NPAM
   NROW=IFOO=N
   ARRAY(NROW, MCOL)=VECTO(KNT)
120 KNT=KNT-1
   DO 84 J=1, NPAM
   BPAM(J)=PARAM(J)
   DO 84 K=1, NPAM
84 BPAM(J)=BPAM(J)+BETA(K)*ARRAY(J,K)/SQRT(ALPHA(J,J)*ALPHA(K,K))
   CALL INGR3 (BPAM, ERR2, 0)
   WRITE (1, 4001) (BPAM(LEW), LEW=1, NPAM) , ERR2
4001 FORMAT (6E20.5)
C
C   IF ERROR INCREASES, INCREASE LAMDA AND TRY AGAIN
C
   IF (ERROR-ERR2) 95, 101, 101
95 LAMDA=10.*LAMDA
   GO TO 71
101 DO 105 J=1, NPAM
   IF (ABS(BPAM(J)-PARAM(J))-0.005*ABS(PARAM(J))) 105, 105, 106
105 CONTINUE
   GO TO 700
C
C   EVALUATE PARAMETERS
C
106 DO 107 J=1, NPAM
107 PARAM(J)=BPAM(J)
   ERFOR=ERR2
   GO TO 99
700 ERROR=ERR2
   DO 707 J=1, NPAM
707 PARAM(J)=BPAM(J)
   CALL LINK (COAL6)
   END
// DUP
*DELETE          COAL5
*STORE           WS  UA  COAL5

```

```
// FOR
```

```
#LIST ALL
#ONE WORD INTEGERS
#IOCS (1132 PRINTER)
#NAME COAL6
```

```
C
C
C
C
C
C
C
C
C
C
```

```
*****
```

```
COAL 6 IS USED AS A PRINTING PROGRAM FOR RESULTS
```

```
*****
```

```
REAL NCALC(50),NFRAC(50)
DIMENSION FRAC(50),NUM(50),TIME(50,15),TEMP(50,15),VCALC(50),
+ RCODE(50),BPAM(10)
COMMON NRUNZ,FRAC,NUM,TIME,TEMP,VCALC,VSTAR,WATER,RCODE,BPAM,
+ IFOO,NPAM,ERR2
EQUIVALENCE (TIME(1,1),NCALC(1)),(TEMP(1,1),NFRAC(1))
DATA NWRIT/3/
DO 59 L=1,NRUNZ
NCALC(L)=VCALC(L)/VSTAR
59 NFRAC(L)=FRAC(L)/VSTAR
IRRN=ERR2/(VSTAR*VSTAR)
WRITE (NWRIT,501) (FRAC(I),VCALC(I),NFRAC(I),NCALC(I),RCODE(I),
+ I=1, NRUNZ)
501 FORMAT (' EXP. FRAC.=',F6.4,' AND CALC. FRAC.=',F6.4,9X,
+ 'NORMALIZED EXP. FRAC.=',F6.4,' AND NORMALIZED CALC. FRAC.=',
+ F6.4,2X,A4)
WRITE (NWRIT,710)
710 FORMAT (///' FINAL PARAMETER VALUES=' )
WRITE (NWRIT,711) (I,BPAM(I),I=1,NPAM)
711 FORMAT (' (' ,I2,')',E13.5)
WRITE (NWRIT,722) ERR2,ERRN
722 FORMAT (///' SUM OF SQUARED ERRORS=',E13.5,20X,'NORMALIZED ERROR S
+M=',E13.5)
CALL EXIT
END
```

```
// DUP
#DELETE COAL6
#STORE WS UA COAL6
```

```
// FOR
*LIST ALL
*ONE WORD INTEGERS
SUBROUTINE INGR3 (PAM,ERROR,ICODE)
```

C
C
C
C
C
C
C
C
C
C
C
C
C
C
C

INGR 3 USES THE TRAPEZOIDAL RULE TO NUMERICALLY INTEGRATE THE RATE CONSTANT OVER TIME FOR NON-ISOTHERMAL CONDITIONS

NOMENCLATURE

EA	ACTIVATION ENERGY
ICODE	USED IN DERIVATIVE DETERMINATIONS
KO	PRE-EXPONENTIAL FACTOR
PAM(K)	PARAMETERS

```
REAL KO
DIMENSION PAM(10)
COMMON NRUNZ,FRAC(50),NUM(50),TIME(50,15),TEMP(50,15),VCALC(50),
+ VSTAR,WATER
DATA R/1.9872/
EA=PAM(1)
KO=PAM(2)
ERROR=0.0
EB=-(EA/R)
IF (ICODE) 51,50,51
50 ILOW=1
   IHIGH=NRUNZ
   GO TO 52
51 ILOW=ICODE
   IHIGH=ICODE
52 ( ) 1 I=ILOW,IHIGH
   L=NUM(I)
   VCALC(I)=0.0
   DO 2 J=2,L
     K=J-1
     DELT=TIME(I,J)-TIME(I,K)
     ARGU=0.5*(EXP(EB/TEMP(I,J)) + EXP(EB/TEMP(I,K)))
2 VCALC(I)=VCALC(I) + ARGU*DELT
VCALC(I)=VSTAR+(WATER-VSTAR)*EXP(-KO*VCALC(I))
1 ERROR=ERROR+(VCALC(I)-FRAC(I))**2
RETURN
END
```

```
// DUP
*DELETE          INGR3
*STORE          WS UA INGR3
```

```
// FOR
```



```
#LIST ALL
#ONE WORD INTEGERS
FUNCTION TRAPS(I,E)
```

```
C
C
C
C
C
C
C
C
C
C
```

```
*****
```

```
TRAPS USES THE TRAPEZOIDAL RULE TO NUMERICALLY INTEGRATE THE RATE
CONSTANT OVER TIME FOR NON-ISOTHERMAL CONDITIONS
```

```
*****
```

```
COMMON NRUNZ,FRAC(50),NUM(50),TIME(50,15),TEMP(50,15),VCALC(50),
+ VSTAR,WATER,RCODE(50),PARAM(10),IFOO,NPAM,DUMMY
DATA R/1.9872/
EB=-E/R
L=NUM(I)
TRAPS=0.0
ALOW=EXP(EB/TEMP(I,1))
DO 1 J=2,L
DELT=TIME(I,J)-TIME(I,J-1)
AHIGH=EXP(EB/TEMP(I,J))
TRAPS=TRAPS+0.5*(ALOW+AHIGH)*DELT
1 ALOW=AHIGH
RETURN
END
```

```
// DUP
#DELETf          TRAPS
#STORE          WS UA TRAPS
```

```
// FOR
#LIST ALL
#ONE WORD INTEGERS
SUBROUTINE INGR5 (PAM,ERROR,ICODE)
```

```
C
C
C
C
C
C
C
C
C
C
C
C
C
C
```

```
*****
```

```
INGR 5 USES SIMPSONS RULE TO NUMERICALLY INTEGRATE THE EVALUATED
INTEGRAL FROM TRAPS OVER A DISTRIBUTION OF ACTIVATION ENERGIES
```

```
THIS SUBROUTINE REQUIRES FUNCTION TRAPS
```

```
NOMENCLATURE
```

```
    E0          MEAN ACTIVATION ENERGY
    SGMA        STD. DEVIATION OF EA DISTRIBUTION
```

```
*****
```

C

```
FEAL KO
DIMENSION PAM(10)
COMMON NRUNZ,FRAC(50),NUM(50),TIME(50,15),TEMP(50,15),VCALC(50),
+ VSTAR,WATER,RCODE(50),PARAM(10),IFOO,NPAM,DUMMY
EO=PAM(1)
KO=EXP(PAM(2))
SGMA=PAM(3)
VSTAR=PAM(4)
EMIN=EO-2.*SGMA
EMAX=EO+2.*SGMA
H=0.5*SGMA
SGMA2=0.5/(SGMA*SGMA)
ERROR=0.0
IF (ICODE) 51,50,51
50 ILOW=1
   IHIGH=NRUNZ
   GO TO 52
51 ILOW=ICODE
   IHIGH=ICODE
52 ( ) 1 I=ILOW,IHIGH
   VAL=EXP(-KO*TRAPS(I,EMIN)-(EMIN-EO)*(EMIN-EO)*SGMA2)
   VAL=VAL+EXP(-KO*TRAPS(I,EMAX)-(EMAX-EO)*(EMAX-EO)*SGMA2)
   JCODE=2
   E=EMIN
   DO 10 J=1,7
   E=E+H
   ARGU=EXP(-KO*TRAPS(I,E)-(E-EO)*(E-EO)*SGMA2)
   GO TO (2,4), JCODE
   2 VAL=VAL+2.*ARGU
   JCODE=2
   GO TO 10
   4 VAL=VAL+4.*ARGU
   JCODE=1
10 CONTINUE
   VAL=0.3333333*H*VAL
   VCALC(I)=VSTAR+(WATER-VSTAR)*(VAL/(SGMA*2.50663))
   1 EFROR=ERROR+(FRAC(I)-VCALC(I))**2
   RETURN
END
```

```
// DUP
*DELETE          INGR5
*STORE          WS UA INGR5
```

PAGE 6 PCLFWFLI.

// * THIS EXECUTION FOR 1 ATW HE H43 DATA SET

// XFO COAL3

ASSUMED VSTAR VALUE=0.4132

ASSUMED H2O FRACTION=0.0730

INITIAL PARAMETER VALUES=

(1) 0.10245E 05									
(2) 0.18303E 03									
EXP. FRAC.=0.1851 AND CALC. FRAC.=0.1784				NORMALIZED EXP. FRAC.=0.4479 AND NORMALIZED CALC. FRAC.=0.4319					41C2
EXP. FRAC.=0.1972 AND CALC. FRAC.=0.2063				NORMALIZED EXP. FRAC.=0.4772 AND NORMALIZED CALC. FRAC.=0.4994					41A2
EXP. FRAC.=0.3022 AND CALC. FRAC.=0.3334				NORMALIZED EXP. FRAC.=0.7313 AND NORMALIZED CALC. FRAC.=0.6069					41B2
EXP. FRAC.=0.3111 AND CALC. FRAC.=0.3093				NORMALIZED EXP. FRAC.=0.7529 AND NORMALIZED CALC. FRAC.=0.7487					41D2
EXP. FRAC.=0.3423 AND CALC. FRAC.=0.3285				NORMALIZED EXP. FRAC.=0.8284 AND NORMALIZED CALC. FRAC.=0.7951					40C2
EXP. FRAC.=0.3547 AND CALC. FRAC.=0.3372				NORMALIZED EXP. FRAC.=0.8584 AND NORMALIZED CALC. FRAC.=0.8161					40D2
EXP. FRAC.=0.3603 AND CALC. FRAC.=0.3730				NORMALIZED EXP. FRAC.=0.9203 AND NORMALIZED CALC. FRAC.=0.9027					40A2
EXP. FRAC.=0.3812 AND CALC. FRAC.=0.3801				NORMALIZED EXP. FRAC.=0.9225 AND NORMALIZED CALC. FRAC.=0.9199					4052
EXP. FRAC.=0.3824 AND CALC. FRAC.=0.3893				NORMALIZED EXP. FRAC.=0.9254 AND NORMALIZED CALC. FRAC.=0.9422					39D2
EXP. FRAC.=0.4030 AND CALC. FRAC.=0.4071				NORMALIZED EXP. FRAC.=0.9753 AND NORMALIZED CALC. FRAC.=0.9854					39C2

FINAL PARAMETER VALUES=

(1) 0.11099E 05
 (2) 0.28256E 03

SUM OF SQUARED ERRORS= 0.17218E-02
 // FJFCT
 NORMALIZED ERROR SUM= 0.10084E-01

10.4 NOMENCLATURE

<u>Symbol</u>	<u>Definition</u>	<u>Typical Units</u>	<u>Where Introduced</u>
A	Constant	--	2-27
a	"	--	2-7
B	"	--	2-27
b	"	--	2-7
b_1, b_2, b_3	"	--	Table 2-2
C	Conc. of Reactive Species	--	5-7
C^*, C_o^*	Fraction of Active Species	--	2-9
C_o	Residual Volatile Matter	--	2-24
d	Particle Diameter	mm	2-30
E	Activation Energy	kcal/mole	2-21
E_o	Mean Activation Energy	"	5-6
K^*	Mass Transfer Coefficient	--	5-7
K_v	Devolatilization Constant	sec/mm ²	2-31
k	Rate Parameter	sec ⁻¹	2-23
k_1	"	"	2-21
k_2	"	"	2-10
k_3	"	atm sec ⁻¹	2-7
k_4	"	--	5-7
k_5	"	--	5-16
k^*	Mass Transfer Coefficient	--	5-14
k^n	nth Order Rate Constant	sec ⁻¹	2-26
k''	Devolatilization Constant	--	2-31
k_o	Pre-Exponential Factor	sec ⁻¹	2-25
m	Heating Rate	°C/sec	2-28
n	Constant	--	2-26
P_{H_2}	Hydrogen Pressure	atm	2-7
$P_{H_2}^*$	Equilibrium H ₂ Pressure	atm	---
P_o	Permeability	mm ² /sec	2-31
Q	Constant	--	2-24
Q	Volatile Generation Rate	--	5-7
R	Gas Constant	cal/gmole °K	2-25
r	radius	cm	---
T	Temperature	°K or °C	2-25
T_A	Ambient Temperature	°C	2-30
t	time	sec	2-7
V	Volatiles (Fract.)	--	2-23
V^*	Volatile Yield	--	2-23
VM_o	Proximate Volatile Matter	--	2-24

<u>Symbol</u>	<u>Definition</u>	<u>Typical Units</u>	<u>Where Introduced</u>
V_R^*	Reactive Volatiles	--	5-10
V_{NR}	Non-Reactive Volatiles	--	5-15
V_{tot}	Total Volatiles	--	5-15
X^*	Fractional Carbon Yield	--	2-7
X	Fractional Carbon Conversion	--	2-7
α	Thermal Diffusivity	cm^2/sec	----
σ	Standard Deviation of $f(E)$	kcal/mole	5-6
S	Standard Deviation of Data	--	----
S'	Standard Deviation of Curves	--	----

10.5 LITERATURE CITATIONS

1. Badzioch, S., "Thermal Decomposition," BCURA Monthly Bulletin, 31 (4), 193 (1967).
2. Badzioch, S., and P.G.W. Hawksley, "Kinetics of Thermal Decomposition of Pulverized Coal Particles," Ind. Eng. Chem. Process Design Develop. 9, 521 (1970).
3. Belt, R.J., and M.M. Roder, "Low-Sulfur Fuel by Pressurized Entrainment Carbonization of Coal," Am. Chem. Soc., Div. of Fuel Chem. Preprints 17, No. 2, 82, August 1972.
4. Belt, R.J., J.S. Wilson and J.J.S. Sebastian, "Continuous Rapid Carbonization of Powdered Coal by Entrainment, and Response Surface Analysis of Data," Fuel, 50, 381 (1971).
5. Benson, S., "Thermochemical Kinetics," John Wiley and Sons, New York (1968).
6. Berkowitz, N., "Mechanism of Coal Pyrolysis, I," Fuel, 39, 47 (1960).
7. Berkowitz, N., and W. Den Hertog, "Mechanisms of Coal Pyrolysis V," Fuel, 41, 507 (1962).
8. Bevington, P.R., "Data Reduction and Error Analysis for the Physical Sciences," McGraw-Hill, New York (1969).
9. Birch, T.J., "Hydrogasification of Brown Coal, Parts 1 and 2," Div. of Chemical Engineering, C.S.R.I.O., Australia, Report No. CE/R25 (1969).
10. Birch, T.J., K.R. Hall and R.W. Urie, "Gasification of Brown Coal with Hydrogen in a Continuous Fluidized-bed Reactor," J. Inst. Fuel, 33, 422 (1960).
11. Bituminous Coal Research, Inc., "Gas Generator Research and Development-Survey and Evaluation," Government Printing Office, Washington D.C. (1965).
12. Blackwood, J.D., "The Kinetics of the System Carbon-Hydrogen-Methane," Australian J. Chem., 15, 397 (1962).
13. Bond, R.L., W.R. Ladner and R. Wheatley, "ESR of Rapidly Heated Coals," Fuel, 47, 213 (1968).
14. Boyer, M.S.F., Compt. Rend. Assoc. Tech. de l'Indus. du gaz en France Congres, 653 (1952) (as reported by Yellow, P.C., BCURA Monthly Bulletin, 29, 285 (1965).)

15. Carslaw, H.S., and J.C. Jaeger, "Conduction of Heat in Solids," 2nd Ed., Oxford University Press (1959).
16. Cech, R.E., "A High-Low Temperature Microscope Stage," Rev. Sci. Instr., 21, 747 (1950).
17. Chermin, H.A.G., and D.W. Van Krevelen, "Chemical Structure and Properties of Coal, XVII," Fuel, 36, 85 (1957).
18. Cohen, A., unpublished work at M.I.T., 1973.
19. Den Hertog, W., and N. Berkowitz, "Mechanisms of Coal Pyrolysis II," Fuel, 39, 125 (1960).
20. Dent, F.J. "The Production of Gaseous Hydrocarbons by the Hydrogenation of Coal," Gas J., 244, 502 (1944).
21. Dryden, I.G.C., "Chemistry of Coal and its Relation to Coal Carbonization," J. Inst. Fuel, 30, 193 (1957).
22. Eddinger, R.T., L.D. Friedman and E. Rau, "Devolatilization of Coal in a Transport Reactor," Fuel, 45, 245 (1966).
23. Essenhigh, R.H., "The Influence of Coal Rank on the Burning Times of Single Captive Particles," J. Eng. Power, 85, 183 (1963).
24. Feldkirchner, H.L., and J.L. Johnson, "High-Pressure Thermobalance," Rev. Sci. Instr., 39, 1227 (1968).
25. Feldkirchner, H.L., and H.R. Linden, "Reactivity of Coals in High-Pressure Gasification," Ind. Eng. Chem. Process Design Develop., 2, 153 (1963).
26. Feldmann, H.F., W.H. Simons, J.A. Mimm and R.W. Hiteshue, "Reaction Model for Bituminous Coal Hydrogasification in a Dilute Phase," Am. Chem. Soc., Div. of Fuel Chem. Preprints 14, No. 4, 1, Sept 1970.
27. Feldmann, H.F., C.Y. Wen, W.H. Simons and P.M. Yavorsky, "Supplemental Pipeline Gas from Coal by the Hydrane Process," 71st National AIChE Meeting, Dallas, Texas, Feb 20-23, 1972..
28. Finch, R.A., and R.E. Taylor, "Apparatus for Determining Thermophysical Properties of Solids by Direct Electrical Pulse Heating," Rev. Sci. Instr., 40, 1195 (1969).
29. Fischer, F., "The Conversions of Coal into Oils," D. Van Nostrand Company, New York (1925).
30. Fuchs W., and A.G. Sandhoff, "Theory of Coal Pyrolysis," Ind. Eng. Chem., 34, 587 (1942).

31. Furman, R.C., "Pipeline Gas from Coal--Comparisons and Technical Evaluations of Proposed Processes," S.M. Thesis, M.I.T., Cambridge, Mass. (1972).
32. Given, P.H., "The Distribution of Hydrogen in Coals and its Relation to Coal Structure," Fuel, 39, 147(1960).
33. Glenn, R.A., E.E. Donath and R.J. Grace, "Gasification of Coal under Conditions Simulating Stage 2 of the BCR Two-Stage Super Pressure Gasifier," Advan. Chem. Ser., 69, 253 (1967).
34. Graff, R.A. and A.M. Squires, "Innovation in Power Generation from Coal," National Commission on Materials Policy Forum on Technological Innovation in the Production and Utilization of Materials, June 18-21, 1972, Penn State Univ., Univ.Park, Pa.
35. Gray, D., J.G. Cogoli and R.H. Essenhigh, "Problems in Pulverized Coal and Char Combustion," Am. Chem. Soc., Div of Fuel Chem Preprints 18, No. 1, 135, April 1973.
36. Gregory, D.R. and R.F. Littlejohn, "A Survey of Numerical Data on the Thermal Decomposition of Coal," BCURA Monthly Bulletin, 29 (6), 173 (1965).
37. Hanbaba, P., H. Juntgen, and W. Peters, "Nicht-isotherme Reaktionskinetik der Kohlenpyrolyse, Teil II: Erweiterung der Theorie der Gasabspaltung und experimentelle Bestatigung an Steinkohlen," Brennstoff-Chem., 49, 368 (1968).
38. Henry, J.P., and B.M. Louks, "An Economic Study of Pipeline Gas Production from Coal," Chem Tech, p. 237-247 (April 1971).
39. Hiteshue, R.W., S. Friedman and R. Madden, "Hydrogenation of Coal to Gaseous Hydrocarbons," RI 6027, Bureau of Mines, Dept. of Interior (1962a).
40. Hiteshue, R.W., S. Friedman and R. Madden, "Hydrogasification of Bituminous Coals, Lignite, Anthracite, and Char," RI 6125, Bureau of Mines, Dept. of Interior (1962b).
41. Hiteshue, R.W., S. Friedman and R. Madden, "Hydrogasification of High-Volatile A Bituminous Coal," RI 6376, Bureau of Mines, Dept. of Interior (1964).
42. Hottel, H.C., and J.B. Howard, "New Energy Technology," M.I.T. Press, Cambridge, Mass. (1971).
43. Howard, J.B. and R.H. Essenhigh, "Pyrolysis of Coal Particles in Pulverized Fuel Flames," Ind. Eng. Chem. Process Design Develop., 6, 74 (1967).
44. Johnson, J.L., "Means of Relating Coal Characteristics to Chemical Engineering Data," Seminar on Characterization and Characteristics of U.S. Coals for Practical Use, Penn. State Univ., Univ. Park, Penn., October 25-28, 1971.

45. Johnson, J.L., "Kinetics of Bituminous Coal Char Gasification with Gases Containing Steam and Hydrogen," Am. Chem. Soc., Div. of Fuel Chem. Preprints 18, No. 1, 228, April 1973.
46. Jones, J.F., M.R. Schmid and R.T. Eddinger, "Fluidized Bed Pyrolysis of Coal," Chem. Eng. Progr., 60 (6), 69 (1964).
47. Juntgen, H., and K.H. Van Heek, "Gas Release from Coal as a Function of the Rate of Heating," Fuel, 47, 103 (1968).
48. Juntgen, H., and K.H. Van Heek, "Reaktionablaufe unter nicht-isothermen Bedingungen," "Fortschritte der chemischen Forschung," Vol. 13, pp. 601-699, Springer-Verlag, Berlin, 1970, translated by Belov and Assoc. Denver, Colo., APTIC-TR-0776.
49. Juntgen, H., K.H. Van Heek, and J. Klein, "Comparative Investigations into the Kinetics of Gasification with Steam or Hydrogen and Conclusions for Gasifier Design," paper presented at the Gordon Research Conference on Coal Science, July 2-6, 1973, New Hampton, New Hampshire.
50. Kimber, G.M. and M.D. Gray, "Rapid Devolatilization of Small Coal Particles," Combust. Flame, 11, 360 (1967a).
51. Kimber, G.M. and M.D. Gray, "Measurements of Thermal Decomposition of Low and High Rank Non-Swelling Coals at M.H.D. Temperatures," BCURA Document No. MHD 32, (January 1967b).
52. Koch, V., H. Juntgen, and W. Peters, "Nicht-Isotherme Reaktionskinetik der Kohlenpyrolyse, Teil III: Zum Reaktionsablauf bei hohen Aufheizgeschwindigkeiten," Brennstoff. Chem., 50, 369 (1969).
53. Koppers 1972, "Koppers Synthetic Methane Process (KSM Process) with Pulverized Coal Gasification Under Pressure," Heinrich Koppers GmbH, Essen, Germany, June 14 1972.
54. Lavery, H.P., "Effect of Hydrogen Pressure and Sample Temperature on the Gasification of Pittsburgh Bituminous Coal," S.B. Thesis, M.I.T., Cambridge, Mass, (1973).
55. Lee, A.L., H.L. Feldkirchner, F.C. Schora and J.J. Henry, "The Heat of Reaction of Hydrogen and Coal," Ind. Eng. Chem. Process Design Develop., 7, 244 (1968).
56. Lee, B.S., E.J. Pyrcioch and F.C. Schora, "Hydrogasification of Pretreated Coal for Pipeline Gas Production," Advan. Chem. Ser., 69, 50 (1967).
57. Linden, H.R., "New Policies Could Stimulate Gas Production But U.S. Gas Requirements May Not Be Met," Pipeline and Gas Journal, January 1973.

58. Loison, R., and F. Chauvin, "Pyrolyse Rapide Du Charbon," Chem. Ind. (Paris), 91, 269 (1964).
59. Mazumdar, B.K. and N.N. Chatterjee, "Mechanism of Coal Pyrolysis in Relation to Industrial Practice," Fuel, 52, 11 (1973).
60. Mentser, M., H.J. O'Donnell, S. Ergun, and R.A. Friedel, "Devolatilization of Coal by Rapid Heating," Am. Chem. Soc., Div. of Fuel Chem. Preprints 18, No. 1, 26, April 1973.
61. Mentser, M., J.J. O'Donnell and S. Ergun, "Rapid Thermal Decomposition of Bituminous Coals," Am. Chem. Soc., Div. of Fuel Chem. Preprints 14, No. 5, 94, Sept 1970.
62. Moseley, F., and D. Paterson, "Rapid High-Temperature Hydrogenation of Coal Chars, Part 1," J. Inst. Fuel, 38, 13 (1965a).
63. Moseley, F., and D. Paterson, "Rapid High-Temperature Hydrogenation of Coal Chars, Part 2," J. Inst. Fuel, 38, 378 (1965b).
64. Moseley, F., and D. Paterson, "Rapid High-Temperature High-Pressure Hydrogenation of Bituminous Coal," J. Inst. Fuel, 40, 523 (1967).
65. Perry, R.H., C.H. Chilton, and S.D. Kirkpatrick, "Perry's Chemical Engineers' Handbook," 4th Ed., McGraw-Hill, New York (1963).
66. Peters, W. "Stoff-und Wärmeübergang bei der Schnellentgasung feinkorniger Brennstoffe," Chem. Ing. Tech., 32, 178 (1960).
67. Peters, W. and H. Bertling, "Kinetics of the Rapid Degasification of Coals," Fuel, 44, 317 (1965).
68. Pitt, G.J., "The Kinetics of the Evolution of Volatile Products from Coal," Fuel, 41, 267 (1962).
69. Portal, C., and D. Tan, unpublished work at M.I.T., 1972.
70. Pyrcioch, E.J., H.L. Feldkirchner, C.L. Tsaros, J.L. Johnson, W.G. Blair, B.S. Lee, F.C. Schora, J. Huebler, H.R. Linden, "Production of Pipeline Gas by Hydrogasification of Coal," I.G.T. Research Bulletin No. 39, Vol. 1, December 1972.
71. Rau, E. and J.A. Robertson, "The Use of the Microsample Strip Furnace in Coal Research," Fuel, 45, 73 (1966).
72. Reid, R.C., and T.K. Sherwood, "The Properties of Gases and Liquids," 1st Ed., McGraw-Hill, New York (1958).
73. Sass, A., "The Garrett Research and Development Process for the Conversion of Coal into Liquid Fuels," 65th Annual AIChE Meeting, New York, New York, November 30 1972.

74. Schroeder, W.C., (to Fossil Fuels, Inc.), "Hydrogenation of Coal," U.S. Patent 3,030,297, April 17 1962.
75. Shapatina, E.A., V.V. Kalyuzhnyi, and Z.F. Chukhanov, Technological Utilization of Fuel for Energy, 1-Thermal Treatment of Fuels, 1960 (reviewed by Badzioch, S., BCURA Monthly Bulletin, 25, 285 (1961).).
76. Shreve, R.N., "Chemical Process Industries," 3rd Ed., McGraw-Hill Book Company (1967).
77. Skylar, M.G., V.I. Shustikov and I.V. Virozub, "Investigation of the Kinetics of Thermal Decomposition of Coals," Intern. Chem. Eng., 9, 595 (1969).
78. Squires, A.M., "Steam-Oxygen Gasification of Fine Sizes of Coal in a Fluidized Bed," Trans. Inst. Chem. Engrs. (London), 39, 3 (1961).
79. Stone, H.N., J.D. Batchelor, and H.F. Johnstone, "Low Temperature Carbonization Rates in a Fluidized Bed," Ind. Eng. Chem., 46, 274 (1954).
80. Vand, V., "A Theory of the Irreversible Electrical Resistance Changes of Metallic Films Evaporated in Vacuum," Proc. Phys. Soc. (London), A55, 222 (1943).
81. Van Krevelen, D.W., "Coal," Elsevier Publishing Co., Amsterdam (1961).
82. Van Krevelen, D.W., F.J. Huntjens, and J.N.M. Dormans, "Chemical Structure and Properties of Coal XVI," Fuel, 35, 462 (1956).
83. Van Krevelen, D.W., C. Van Heerden, and F.J. Huntjens, "Physicochemical Aspects of the Pyrolysis of Coal and Related Organic Compounds," Fuel, 30, 253 (1951).
(numerical results modified by Juntgen and Van Heek, 1970)
84. Von Fredersdorff, C.G. and M.S. Elliott, "Coal Gasification" in Chemistry of Coal Utilization," supplementary vol., H.H. Lowry, editor, John Wiley and Sons, New York (1963).
85. Wen, C.Y., "Optimization of Coal Gasification Processes," Research and Development Report No. 66, Interim Report No. 1, Office of Coal Research, U.S. Dept. of Interior (1972).
86. Wen, C.Y., O.C. Abraham and A.T. Talwalker, "Kinetic Study of the Reaction of Coal Char with Hydrogen-Steam Mixture," Advan. Chem. Ser., 69, 253 (1967).
87. Wen, C.Y., and J. Huebler, "Kinetic Study of Coal Char Hydrogasification," Ind. Eng. Chem. Process Design Develop., 4, 142 (1965).

88. Wen, C.Y., C.T. Li, S.H. Tscheng and W.S. O'Brien, "Comparison of Alternative Coal Gasification Processes," 65th Annual AIChE Meeting, New York, New York, Nov. 26-30, 1972.
89. West, J., "Higher Prices Trigger Increase in Gas Drilling," Oil Gas J., August 20, 1973.
90. Wisler, W.H., L.L. Anderson, S.A. Qader and G.R. Hill, "Kinetic Relationship of Coal Hydrogenation, Pyrolysis and Dissolution," J. Appl. Biotechnol., 21, 82 (1971).
91. Wisler, W.H., G.R. Hill and N.J. Kertamus, "Kinetic Study of the Pyrolysis of a High-Volatile Bituminous Coal," Ind. Eng. Chem. Process Design Develop., 6, 133 (1967).
92. Yellow, P.C., "Kinetics of the Thermal Decomposition of Coal," BCURA Monthly Bulletin, 29(9), 285 (1965).
93. Zahradnik, R.L., "Chemistry and Physics of Entrained Coal Gasification," Gordon Research Conf. on Coal Science, New Hampton, N.H. July 2-6, 1973.
94. Zahradnik, R.L., and R.A. Glenn, "Direct Methanation of Coal," Fuel, 50, 77 (1971).
95. Zahradnik, R.L., and R.J. Grace, "Chemistry and Physics of Entrained Coal Gasification," 71st National AIChE Meeting, Dallas, Texas, Feb. 20-23, 1972.
96. Zielinski, E., "The Evolution of Volatile Matter from Pulverized Coal Particles," Fuel, 46, 329 (1967).

10.6 BIOGRAPHICAL NOTE

The author, Donald Barrett Anthony, was born on January 28, 1948, in Kansas City, Kansas, the first of two children. He attended elementary and secondary schools in Kansas City, Kansas and Missouri, and Toledo, Ohio. He was graduated summa cum laude from the University of Toledo with a B. S. in Chemical Engineering in June 1970.

In September 1970, the author entered the Massachusetts Institute of Technology. He received his S. M. in Chemical Engineering Practice in June 1971. He returned in September 1971 to begin doctoral work.

The author has held various part-time and summer positions with Owens-Illinois, Inmont Corporation, Sun Oil Company and the University of Toledo. He is a member of Blue Key, Phi Kappa Phi, Tau Beta Pi and Sigma Xi.

In December 1972, he married the former Darla Sue Donovan of Toledo, Ohio.

At the present time, he has accepted an appointment as Assistant Professor and Director of the M.I.T. School of Chemical Engineering Practice Station at Bound Brook, New Jersey, to begin in August 1974.